DOC.20080107.0006

QA: QA

MDL-NBS-HS-000021 REV 03

August 2005

Saturated Zone Flow and Transport Model Abstraction

THIS DOCUMENT CONTAINS THE FOLLOWING, LOCATED AT THE BACK OF THE DOCUMENT:
1) ADDENDUM 001, DATED 09/07/2007
2) ADDENDUM 002, DATED 01/02/2008

Prepared for:
U.S. Department of Energy
Office of Civilian Radioactive Waste Management
Office of Repository Development
1551 Hillshire Drive
Las Vegas, Nevada 89134-6321

Prepared by:
Bechtel SAIC Company, LLC
1180 Town Center Drive
Las Vegas, Nevada 89144

Under Contract Number
DE-AC28-01RW12101

QA: QA

Saturated Zone Flow and Transport Model Abstraction

MDL-NBS-HS-000021 REV 03

August 2005

BSC	**Model Signature Page/Change History** *Complete only applicable items.*	Page ii 1. Total Pages: 298

2. Type of Mathematical Model

☐ Process Model ☒ Abstraction Model ☐ System Model

Describe Intended Use of Model

The purpose of the saturated zone flow and transport model abstraction is to provide radionuclide transport simulation results for use in the total system performance assessment calculations.

3. Title

Saturated Zone Flow and Transport Model Abstraction

4. DI (including Rev. No.):

MDL-NBS-HS-000021 REV 03

	Printed Name	Signature	Date
5. Originator	B.W. Arnold	Kenneth Rehfeldt for	8/1/05
6. Independent Technical Reviewer	R. Andrews	[signature]	8/2/05
7. Checker	S. James	Scott James	8/2/05
8. QER	K. McFall	Kenneth McFall	8/2/05
9. Responsible Manager/Lead	B.W. Arnold	Kenneth Rehfeldt for	8/2/05
10. Responsible Manager	M. Zhu	[signature]	8/2/05

11. Remarks

This report addresses comments from the Independent Verification and Review Team (IVRT) and comments from Safety Analysis Report (SAR). This report addresses the CR 5557 and contains additional analysis and results related to CR 4092. Limitations to the use of the models described in the report are described in Section 1.

Change History

12. Revision No.	13. Description of Change
REV 00	Initial issue.

REV 01	This report contains an analysis of the background gross alpha concentration in groundwater. This report also documents analyses with the SZ Transport Abstraction Model using updated uncertainty distributions for some sorption coefficients. This report also documents analyses with the SZ Transport Abstraction Model for a new radionuclide class defined as the fast fraction of radionuclides irreversibly attached to colloids.
REV 02	This report addresses comments from the Regulatory Integration Team. This report also contains additional analyses and results related to the impact analysis for CR 2222 (*Evaluate Revised LH Sampling Algorithm on the Results of ANL-EBS-PA-000009*). The entire model documentation was revised and sidebars were not used, per step 5.8 f) 1) of AP-SIII.10Q, REV 02, ICN 07, because the changes were too extensive to indicate individual changes.
REV 03	This report contains additional analysis of data on gross alpha concentration in groundwater, as related to issues in CR-4092 (Section 6.8). The report has also been revised to contain plots of radionuclide mass breakthrough curves for the SZ scaled for glacial-transition climatic conditions (Section 6.6). In addition, the report has been updated to cite current versions of other YMP reports and to remove TBV designators for references that are now verified.

CONTENTS

Page

CONTENTS (Continued)

Page

CONTENTS (Continued)

Page

INTENTIONALLY LEFT BLANK

FIGURES

Page

FIGURES (Continued)

Page

FIGURES (Continued)

Page

INTENTIONALLY LEFT BLANK

TABLES

Page

TABLES (Continued)

Page

ACRONYMS AND ABBREVIATIONS

1-D	one-dimensional
ACM	alternative conceptual model
ATC	Alluvial Tracer Complex
CDF	cumulative distribution function
CR	condition report
DOE	U.S. Department of Energy
ESF	Exploratory Studies Facility
FEHM	finite element heat and mass model
FEP	feature, event, and process
GWSPD	groundwater specific discharge factor
HFM	hydrogeologic framework model
LA	license application
NTS	Nevada Test Site
PDF	Probability Density Function
QA	Quality Assurance
RMEI	Reasonably Maximally Exposed Individual
SR	Site Recommendation
SZ	Saturated Zone
TBV	to be verified
TSPA	Total System Performance Assessment
TWP	Technical Work Plan
USGS	United States Geological Survey
UZ	Unsaturated Zone
YMP	Yucca Mountain Project
YMRP	Yucca Mountain Review Plan, Final Report

INTENTIONALLY LEFT BLANK

1. PURPOSE

The purpose of the saturated zone (SZ) flow and transport model abstraction task is to provide radionuclide-transport simulation results for use in the total system performance assessment (TSPA) for license application (LA) calculations. This task includes assessment of uncertainty in parameters that pertain to both groundwater flow and radionuclide transport in the models used for this purpose. This model report documents the following:

- The SZ transport abstraction model, which consists of a set of radionuclide breakthrough curves at the accessible environment for use in the TSPA-LA simulations of radionuclide releases into the biosphere. These radionuclide breakthrough curves contain information on radionuclide-transport times through the SZ.
- The SZ one-dimensional (1-D) transport model, which is incorporated in the TSPA-LA model to simulate the transport, decay, and ingrowth of radionuclide decay chains in the SZ.
- The analysis of uncertainty in groundwater-flow and radionuclide-transport input parameters for the SZ transport abstraction model and the SZ 1-D transport model.
- The analysis of the background concentration of alpha-emitting species in the groundwater of the SZ.

Figure 1-1 shows the relationship of this report to other model reports that also pertain to flow and transport in the SZ. Figure 1-1 also shows the flow of key information among the SZ reports. It should be noted that Figure 1-1 does not contain a complete representation of the data and parameter inputs and outputs of all SZ reports, nor does it show inputs external to this suite of SZ reports. The primary input model to this report is the SZ site-scale transport model, which forms the basis for the SZ transport abstraction model and the SZ 1-D transport model, as developed in this report. The output models from this report are direct feeds to the TSPA-LA model. Several other SZ reports provide information used to define the uncertainty distributions for groundwater flow and radionuclide transport parameters.

The following reports, through their output data tracking numbers (DTNs), provide direct input to this report:

- *Water-Level Data Analysis for the Saturated Zone Site-Scale Flow and Transport Model* (BSC 2004 [DIRS 170009])
- *Site-Scale Saturated Zone Transport* (BSC 2004 [DIRS 170036])
- *Probability Distributions for Flowing Interval Spacing* (BSC 2004 [DIRS 170014])
- *Saturated Zone Colloid Transport* (BSC 2004 [DIRS 170006])
- *Saturated Zone In-Situ Testing* (BSC 2004 [DIRS 170010])
- *Analysis of Hydrologic Properties Data* (BSC 2004 [DIRS 170038])

- *UZ Flow Models and Submodels* (BSC 2004 [DIRS 169861])
- *Rock Properties Model* (BSC 2004 [DIRS 170032])
- *Waste Form and In-Drift Colloids-Associated Radionuclide Concentrations: Abstraction and Summary* (BSC 2005 [DIRS 174290]).

The following reports use this report or its output DTNs as direct input:

- *Total System Performance Assessment (TSPA) Model/Analysis for the License Application*
- *Drift-Scale Radionuclide Transport*
- *Features, Events, and Processes in SZ Flow and Transport*
- *Features, Events, and Processes: Disruptive Events*.

Revision 03 of this report includes several changes relative to Revision 02 [*Saturated Zone Flow and Transport Model Abstraction* (BSC 2004 [DIRS 170042])]. This report contains additional analysis of data on gross alpha concentration in groundwater presented in Section 6.8, as related to issues in CR-4092, which is concerned with the negative concentrations in the data, the methods for analyzing background measurements, and the qualification of corroborative data. The report has also been revised to contain plots of radionuclide mass breakthrough curves for the SZ for glacial-transition climatic conditions in Section 6.6. In addition, the report has been updated to cite current versions of other Yucca Mountain Project (YMP) reports and to remove to-be-verified (TBV) designators for references that are now verified. This model report provides the technical basis for SZ-related features, events, and processes (FEPs) included in the TSPA-LA model, and contributes to the characterization of the SZ as part of the natural barrier below the repository. The natural-barrier characterization provides evidence pertaining to the capability of the SZ to delay movement of radionuclides through the SZ to the accessible environment. This report also contributes to the technical basis for the SZ transport-system description that is used in the LA, and provides evidence for the acceptance criteria specified in *Yucca Mountain Review Plan, Final Report* (YMRP) (NRC 2003 [DIRS 163274]) for flow paths and radionuclide transport in the SZ. The scope of this model report is limited to adaptation of an existing model (the SZ site-scale transport model) for the uncertainty analysis, as reflected in the SZ radionuclide breakthrough curves developed in this model report.

Use of the SZ transport abstraction model and the SZ 1-D transport model in this report and in the TSPA-LA is subject to the limitations imposed by the assumptions listed in Section 5 of this report. Limitations in knowledge of specific parameter values are addressed in this report in the analysis of parameter uncertainties in Section 6.5.2. The radionuclide breakthrough curves generated for the SZ transport abstraction model are limited to a simulation period of 100,000 years, for present-day climatic conditions. This limits the time period that can be simulated with the TSPA-LA model when using these breakthrough curves for the SZ. Because the SZ breakthrough curves are scaled for higher groundwater flow rates under future climatic conditions (i.e., the time scale of the breakthrough curve is divided by the multiplier of groundwater flux), the time period that can be simulated with the TSPA-LA model would be less than 100,000 years. If the glacial-transition climate state is applied for most of the simulation period in the TSPA-LA model, the SZ breakthrough curves would be scaled by a factor of approximately 3.9 (Section 6.5, Table 6-5), thereby limiting the TSPA-LA model simulation time to about 26,000 years.

Information on the correlation between distribution coefficients (K_ds) used in the sampling of uncertain parameters for the SZ transport abstraction model and for the SZ 1-D transport model is provided in Tables 4-3 and 6-8. The technical bases for correlations between distribution coefficients (or the lack thereof) are documented in *Site-Scale Saturated Zone Transport* (BSC 2004 [DIRS 170036], Section C1.2.1).

Evaluation of uncertainty in horizontal anisotropy in permeability is summarized in Section 6.5.2.10. Complete documentation of the technical basis for this evaluation of uncertainty is given in *Saturated Zone In-Situ Testing* (BSC 2004 [DIRS 170010], Section 6.2.6). Implementation of uncertainty in horizontal anisotropy in the SZ transport abstraction model and in the SZ 1-D transport model is discussed in Section 6.5.3.1 and Section 6.5.1.2, respectively.

The impacts of spatial variability of parameters that affect radionuclide transport in the alluvium are incorporated in the evaluation of uncertainties in model parameters in Section 6.5.2.3, Section 6.5.2.7, Section 6.5.2.8, Section 6.5.2.9, and Section 6.5.2.11. The technical bases for uncertainty in distribution coefficients are documented in *Site-Scale Saturated Zone Transport* (BSC 2004 [DIRS 170036], Appendix C).

Information on geological uncertainty in the location of the contact between tuff and alluvium, and the consequent uncertainty in flow-path lengths in the alluvium, are presented in Section 6.5.2.2. This evaluation of uncertainty includes information from the Nye County early warning drilling program.

The sensitivity analysis of matrix diffusion in the SZ transport abstraction model is presented in the assessment of alternative conceptual models (ACMs) in Section 6.4.

This model report is governed by *Technical Work Plan For: Natural System – Saturated Zone Analysis and Model Report Integration* (BSC 2005 [DIRS 173859], Work Package ARTM01). The work documented in this model report was conducted in accordance with the quality assurance (QA) procedure LP-SIII.10Q-BSC, *Models*.

In this report, a unique six-digit numerical identifier (the Document Input Reference System (DIRS) number) is placed in the text after the reference callout (e.g., BSC 2001 [DIRS 163566]). The DIRS numbers are provided to assist readers to locate specific references in the DIRS database.

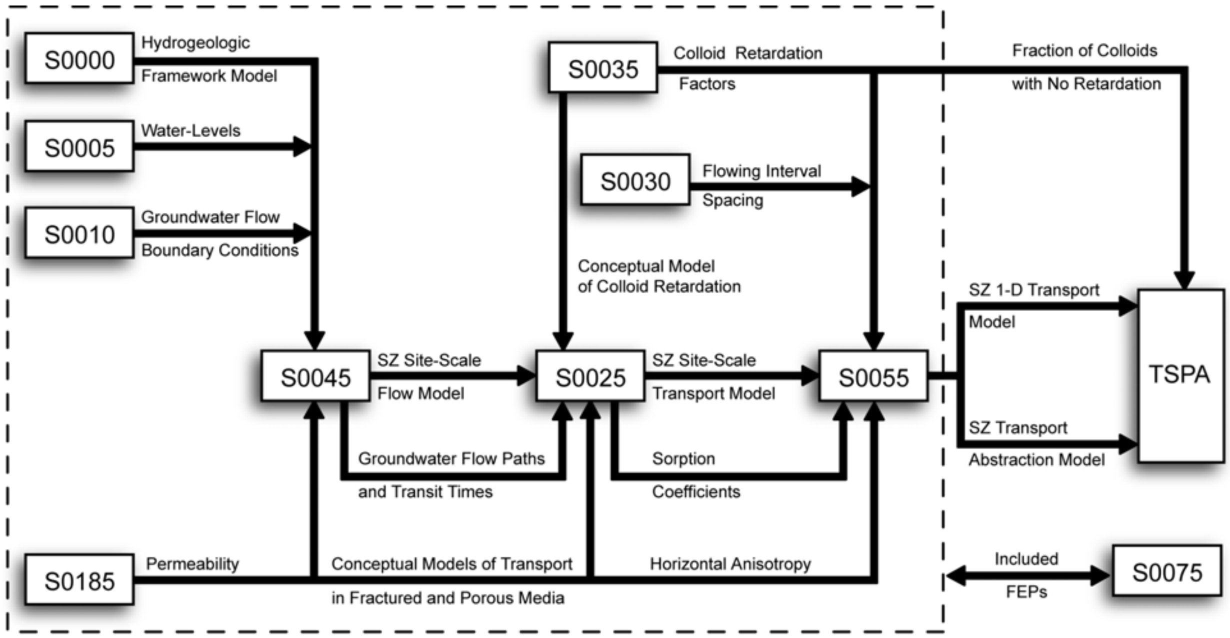

Legend

S0000 - Hydrogeologic Framework Model	MDL-NBS-HS-000024
S0005 - Water-Level Data Analysis	ANL-NBS-HS-000034
S0010 - Recharge and Lateral Groundwater Flow Boundary Conditions	ANL-NBS-MD-000010
S0025 - Site-Scale Saturated Zone Transport	MDL-NBS-HS-000010
S0030 - Probability Distribution for Flowing Interval Spacing	ANL-NBS-MD-000003
S0035 - Saturated Zone Colloid Transport	ANL-NBS-HS-000031
S0045 - Site-Scale Saturated Zone Flow Model	MDL-NBS-HS-000011
S0055 - Saturated Zone Flow and Transport Model Abstraction	MDL-NBS-HS-000021
S0075 - Features, Events, and Processes in SZ Flow and Transport	ANL-NBS-MD-000002
S0185 - Saturated Zone In-Situ Testing	ANL-NBS-HS-000039

00438DC_001c.ai

NOTE: This figure is a simplified representation of the flow of information among SZ reports. See the DIRS of each report for a complete listing of data and parameter inputs. This figure does not show inputs external to this suite of SZ reports.

Figure 1-1. Generalized Flow of Information Among Reports Pertaining to Flow and Transport in the SZ

2. QUALITY ASSURANCE

Development of this model report and the supporting modeling activities is subject to the Yucca Mountain Project (YMP) QA program (BSC 2005 [DIRS 173859], Section 8). Approved QA procedures identified in the technical work plan (BSC 2005 [DIRS 173859], Section 4) have been used to conduct and document the activities described in this model report. The technical work plan also identifies the methods used to control the electronic management of data (BSC 2005 [DIRS 173859], Section 8).

This model report provides values for hydrologic properties of the SZ as part of the natural barrier below the repository that is important to the demonstration of compliance with the postclosure performance objectives prescribed in 10 CFR 63.113 [DIRS 173273]. Therefore, it is classified in *Q-List* (BSC 2005 [DIRS 171190]) as "SC" (Safety Category), reflecting its importance to waste isolation, as defined in AP-2.22Q, *Classification Analyses and Maintenance of the Q-List*. The report contributes to the analysis and modeling data used to support postclosure performance assessment; the conclusions do not directly impact preclosure-engineered features important to safety, as defined in AP-2.22Q.

INTENTIONALLY LEFT BLANK

3. USE OF SOFTWARE

3.1 SOFTWARE TRACKED BY CONFIGURATION MANAGEMENT

The computer software codes used directly in this model report are listed in Table 3-1. The qualification status of the software is noted in the Software Configuration Management database. All software was obtained from Software Configuration Management and is appropriate for the application, considering the simulation capabilities of the software, the range of inputs, and the functionality required by the computational task. Qualified codes were used only within the range of validation as required by LP-SI.11Q-BSC, *Software Management*.

Table 3-1. Computer Software Used in This Model Report

Software Name and Version (V)	Software Tracking Number (STN)	Description	Computer Type, Platform, and Location	Date Baselined
FEHM (finite element heat and mass model) V2.20 [DIRS 161725]	10086-2.20-00	This code is a finite-element heat- and mass-transport code that simulates nonisothermal, multiphase, multicomponent flow, and solute transport in porous media.	Sun UltraSPARC - SunOS 5.7 Sandia National Laboratories	01/28/2003
GoldSim V7.50.100 [DIRS 161572]	10344-7.50.100-00	This code is the modeling software used in the TSPA-LA. Probabilistic simulations are represented graphically in GoldSim.	Dell OptiPlex GX260 Windows 2000 Professional 5.0.2195 Sandia National Laboratories	01/07/2003
GoldSim V8.01 SP4 [DIRS 169695]	10344-8.01SP4-00	GoldSim (GS) is a Windows-2000–based program that provides the following general capabilities: • Quantitatively address the inherent variability. • Superimposes the occurrence and consequences of discrete events onto continuously varying systems. • Builds top-down models, dynamically links external programs or spreadsheets directly to the GS model. • Directly exchanges data between any ODBC-compliant database to the GS model.	Computer: Master 06 Windows 2000 Advanced Server YMP Offices, Las Vegas, Building 3	04/01/2004
SZ_Pre V2.0 [DIRS 163281]	10914-2.0-00	This software is an automated method for preparing the FEHM input files for the SZ site-scale flow and transport model [a] for use in TSPA-LA analyses.	Sun UltraSPARC - SunOS 5.7 Sandia National Laboratories	04/28/2003

Table 3-1. Computer Software Used in This Model Report (Continued)

Software Name and Version (V)	Software Tracking Number (STN)	Description	Computer Type, Platform, and Location	Date Baselined
SZ_Post V3.0 [DIRS 163571]	10915-3.0-00	This software is used to translate the output files from the SZ site-scale model [b] into the format used by the SZ_Convolute software code. SZ_Post reads the output files from the FEHM software code and writes the breakthrough curve data for radionuclide transport in the SZ.	Sun UltraSPARC - SunOS 5.7, Solaris 2.7 Sandia National Laboratories	05/22/2003
CORPSCON V 5.11.08 [DIRS 155082]	10547-5.11.08 -00	This software is used to convert coordinate data to the Universal Transverse Mercator (UTM) coordinate system.	IBM Thinkpad 770Z - Windows NT 4.0 Sandia National Laboratories	08/27/2001
SZ_Convolute V2.2 [DIRS 163344]	10207-2.2-00	This software is used to calculate SZ response curves based on unsaturated zone (UZ) radionuclide source terms, generic SZ responses, and climate scenarios for the YMP.	Dell OptiPlex GX260 - Windows 2000 Professional 5.0.2195 Sandia National Laboratories	01/13/2003

[a]SZ site-scale flow and transport model refers to the SZ transport abstraction model.

[b]SZ site-scale model refers to the SZ transport abstraction model.

NOTE: The SZ_Convolute V2.2 software code (STN: 10207-2.2-00, SNL 2003 [DIRS 163344]) was used in the modeling and analyses in this report. SZ_Convolute V3.0 (STN: 10207-3.0-00, SNL 2003 [DIRS 164180]) will be used for implementation of the SZ transport abstraction model in TSPA-LA. The summary description of the changes in the SZ_Convolute software code in the software baseline report between versions 2.2 and 3.0 gives no indication that the changes in functionality would have any impact on the model validation performed in this report. Software descriptions are taken directly from the software baseline report.

FEHM = finite element heat and mass model; LA = license application; ODBC = Open Database Connectivity; STN = software tracking number; SZ = Saturated Zone; TSPA = Total System Performance Assessment; UTM = Universal Transverse Mercator; UZ = Unsaturated Zone; YMP = Yucca Mountain Project

3.2 EXEMPT SOFTWARE

The commercially available software cited in this section is appropriate for use in this application, considering the functionality required for the computational tasks. These software products were used primarily for plotting of graphs and the visualization of modeling results, and for simple spreadsheet operations. Different graphical software programs were used for different plotting requirements, as appropriate. The results were spot-checked by hand to ensure the results were correct. The computer that was used was a Dell OptiPlex GX1 with Pentium II processor, running Microsoft Windows 2000 Version 5.0.2195. The range of validation for Excel, Surfer, and Grapher is the set of real numbers.

Commercially available software:

- **Excel 2000**: Used for simple spreadsheet calculations in support of plotting and visualization. The formulas, listing of inputs, listing of outputs, and other required information can be found in the following spreadsheets: *Eff_MtrxDif_11.xls*, *bulkd_matr_eff_La.xls*, and *geonames.xls*. These spreadsheets can be found in DTN: SN0306T0502103.006.

- **Surfer 8.0**: Used for plotting and visualization.

- **Grapher 4.0**: Used for plotting graphs.

- **Igor 4.07**: Used for plotting graphs.

INTENTIONALLY LEFT BLANK

4. INPUTS

4.1 DIRECT INPUT

All data, parameters, and other model inputs documented in Section 4.1 are used as direct inputs to the analyses of parameter uncertainty and/or the SZ transport abstraction model and SZ 1-D transport model.

4.1.1 Data and Other Model Inputs

The data providing input for the development of parameters used in the models documented in this report are identified in Table 4-1.

These input data are considered appropriate for the development of uncertainty in parameters for the SZ transport abstraction model and the SZ 1-D transport model, considering the processes being simulated and the geological material in the model domain. The data that are used as direct input to the models developed in this report are the best relevant qualified data because they are taken from the Yucca Mountain site and region. Where available and appropriate, nonqualified data are used to corroborate those data that are used as direct input (see Section 6.5.2).

The data on effective porosity in alluvium from the Burbey and Wheatcraft report (1986 [DIRS 129679]) are obtained from an outside source and are not established fact. The suitability of these data is justified for this specific application, as outlined in LP-SIII.10Q-BSC, Section 5.2.1. U.S. Department of Energy (DOE) directed the collection of these data as part of the investigation of contaminant migration from underground nuclear testing at the Nevada Test Site (NTS). The porosity data in the alluvium were collected in Frenchman Flat from below the water table. That these data come from an area near Yucca Mountain and in a similar physiographic and hydrogeologic setting provides confidence that the data demonstrate the property of interest. The model of contaminant transport presented in the 1986 Burbey and Wheatcraft report was calibrated with measurements of contaminant concentrations during pumping near the Cambric nuclear test and no changes to the values of porosity were suggested as a result of the calibration process. This supports the values of porosity measured in the alluvium at the site. These porosity data generally are corroborated by comparison with other data sources, as discussed in Section 6.5.2.3, and fall within the total range of estimates from other sources.

Table 4-1. Direct Inputs

Data Name	Originating Report	DTN
Matrix Porosity in the Volcanic Units (HFM Units 15-8)	MDL-NBS-GS-000004 (HFM Units 15-13, 10-8) (BSC 2004 [DIRS 170032]) OFR 94-469 (Buesch et al. 1996 [DIRS 100106]); Flint 1998 [DIRS 100033]; OFR 94-460 (Moyer and Geslin 1995 [DIRS 101269]); (HFM Units 12 and 11) TDR-NBS-HS-000014 (BSC 2001 [DIRS 163566]) TDR-NBS-GS-000020, BSC 2001 [DIRS 163479] (HFM Units 12 and 11)	SN0004T0501399.003 [DIRS 155045] (HFM Units 15-13, 10-8) MO0109HYMXPROP.001 [DIRS 155989] (HFM Units 12 and 11) MO0010CPORGLOG.002 [DIRS 155229] (HFM Units 12 and 11)
Effective Porosity Alluvium	Bedinger, et al. 1989 [DIRS 129676], p. A18, Table 1 (HFM Units 19 and 7) EDCON 2000 [DIRS 154704] (HFM Units 19 and 7) Burbey and Wheatcraft 1986 [DIRS 129679] (HFM Units 19 and 7) DOE (U.S. Department of Energy) 1997 [DIRS 103021], Table 8-2, p. 8-6, Table 8-1 p. 8-5 (HFM Units 19 and 7)	MO0105HCONEPOR.000 [DIRS 155044] (HFM Units 19 and 7) MO0105GPLOG19D.000 [DIRS 163480] (HFM Units 19 and 7) Burbey and Wheatcraft 1986 [DIRS 129679] is an outside source of direct input (see text following table). (HFM Units 19 and 7) DOE 1997 [DIRS 103021] is an outside source of direct input (see text following table). (HFM Units 19 and 7)
Effective Porosity in the Other Units	Bedinger, et al. 1989 [DIRS 129676] (HFM Units, 18, 17, 16, 6-2, 1)	MO0105HCONEPOR.000 [DIRS 155044] (HFM Units, 18, 17, 16, 6-2, 1)
Bulk Density in the Volcanic Units	MDL-NBS-GS-000004 (HFM Units 15-13, 10-8) (BSC 2004 [DIRS 170032]) OFR 94-469 (Buesch et al. 1996 [DIRS 100106]); Flint 1998 [DIRS 100033]; OFR 94-460 (Moyer and Geslin 1995 [DIRS 101269]), (HFM Units 12, 11, and 9) TDR-NBS-HS-000014, (BSC 2001 [DIRS 163566]) TDR-NBS-GS-000020, BSC 2001 [DIRS 163479] (HFM Units 17, 12, 11, 6-2)	SN0004T0501399.002 [DIRS 155046] (HFM Units 15-13, 10, 8) SN0004T0501399.003 [DIRS 155045] (HFM Units 15-13, 10-8) MO0109HYMXPROP.001 [DIRS 155989] (HFM Units 12, 11, and 9) MO0010CPORGLOG.002 [DIRS 155229] (HFM Units 17, 12, and 11, 6-2)
Effective Diffusion Coefficient	BSC 2001 [DIRS 163566] (HFM Units 8-15)	MO0109HYMXPROP.001 [DIRS 155989] (HFM Units 8-15)
Bulk Density - Alluvium	EDCON 2000 [DIRS 154704] (HFM Units 19 and 7)	MO0105GPLOG19D.000 [DIRS 163480] (HFM Units 19 and 7)

Table 4-1. Direct Inputs (Continued)

Data Name	Originating Report	DTN
Flowing Interval Porosity in the Volcanic Units	BSC 2004 [DIRS 170038], Section 6.1.3 (HFM Units 8-15) BSC 2004 [DIRS 170010] DOE 1997 [DIRS 103021], p. 5-14 (HFM Units 8-15)	LB0205REVUZPRP.001 [DIRS 159525] (HFM Units 8-15) LA0303PR831231.005 [DIRS 166259] GS031008312315.002 [DIRS 166261] DOE 1997 [DIRS 103021] is an outside source of direct input (see text following table). (HFM Units 8-15)
Lithostratigraphy in Wells EWDP-10SA and EWDP-22SA	N/A	GS030108314211.001 [DIRS 163483]
Coordinates of Well Locations and Depth to Water Table	USGS 2001 [DIRS 157611]	GS010908312332.002 [DIRS 163555]
Uncertainty in Groundwater Specific Discharge	CRWMS M&O 1998 [DIRS 100353]	MO0003SZFWTEEP.000 [DIRS 148744]
Uncertainty in Groundwater Specific Discharge at the Alluvial Tracer Complex (ATC)	BSC 2004 [DIRS 170010]	LA0303PR831231.002 [DIRS 163561]
Site-Scale UZ Model Flow Fields – Infiltration for Nine Scenarios	BSC 2004 [DIRS 169861]	LB03023DSSCP9I.001 [DIRS 163044]

Table 4-1. Direct Inputs (Continued)

Data Name	Originating Report	DTN
Gross Alpha Concentrations in Groundwater	CRWMS M&O 1999 [DIRS 150420], Section 3.2.1, Table 3	MO9904RWSJJS98.000 [DIRS 165866]
	CRWMS M&O 1998 [DIRS 104963], Table E-1	CRWMS M&O 1998 [DIRS 104963], Table E-1 is a source of direct input that is qualified for intended use (see Appendix C).
	Townsend and Grossman 2001 [DIRS 156604], Table 8.3	Townsend and Grossman 2001 [DIRS 156604], Table 8.3 is an outside source of direct input (see Appendix C).
	Townsend and Grossman 2002 [DIRS 173960], Table 8.3	Townsend and Grossman 2002 [DIRS 173960], Table 8.3 is an outside source of direct input (see Appendix C).
	Townsend and Grossman 2003 [DIRS 168841], Table 8.3	Townsend and Grossman 2003 [DIRS 168841], Table 8.3 is an outside source of direct input (see Appendix C).
	Wills 2004 [DIRS 173956], Tables 3-1, 3-2, and 3-3	Wills 2004 [DIRS 173956], Tables 3-1, 3-2, and 3-3 is an outside source of direct input (see Appendix C).

NOTE: The column containing the originating report is provided for reference only. The direct source of the data used in this report is listed in the DTN column. The given HFM Unit numbers refer to the unit definitions in Table 6-9.

DTN = Data Tracking Number; HFM = hydrogeologic framework model; UZ = Unsaturated Zone

The data on effective porosity in alluvium from *Regional Groundwater Flow and Tritium Transport Modeling and Risk Assessment of the Underground Test Area, Nevada Test Site, Nevada* (DOE 1997 [DIRS 103021]) are obtained from an outside source and are not established fact. The suitability of these data is justified for this specific application, as outlined in LP-SIII.10Q-BSC. DOE directed the analyses of these data as part of a study of regional groundwater flow and tritium migration at the NTS. That these data come from an area near Yucca Mountain and in a similar hydrogeologic setting provides confidence that the data demonstrate the property of interest. The data on porosity in alluvium presented in the 1997 DOE report are based on a statistical analysis of measurements by several different methods and at different locations in the NTS. The average value of porosity is corroborated by comparison with another source in Table 8-2 of the 1997 DOE report, and the comparison for porosity in alluvium is very close. These porosity data generally are corroborated by comparison with other data sources, as discussed in Section 6.5.2.3, and fall within the total range of estimates from other sources.

The data on fracture spacing and aperture from *Regional Groundwater Flow and Tritium Transport Modeling and Risk Assessment of the Underground Test Area, Nevada Test Site,* *Nevada* (DOE 1997 [DIRS 103021]) used to estimate flowing interval porosity are obtained from an outside source and are not established fact. The suitability of these data is justified for this specific application, as outlined in LP-SIII.10Q-BSC. DOE directed the analyses of these data as part of a study of regional groundwater flow and tritium migration at the NTS. The data used in the 1997 DOE study were from seven cores from Pahute Mesa on the NTS, and were taken for volcanic rocks that are analogous to the volcanic units in the SZ at Yucca Mountain, providing confidence that the data demonstrate the property of interest. The resulting range of estimated fracture porosity is broad and generally is corroborated by comparison to other sources of information in Section 5.5.2.2 of the 1997 DOE report. These data also are corroborated by comparison to estimates of fracture porosity in *Total-System Performance Assessment for Yucca Mountain – SNL Second Iteration (TSPA-1993)* (Wilson et al. 1994 [DIRS 100191], Volume 1, Table 7-19), as described in Section 6.5.2.5 of this report.

Uncertainty associated with the model, including development of parameter values and their implementation in the SZ flow and transport abstraction model and the SZ 1-D transport model, is discussed in Sections 6.5.1 and 6.5.2. Parameter uncertainties are addressed by providing ranges, probability distributions, and bounding assumptions, as appropriate for each parameter.

Other model, analysis, design, and regulatory input information is listed in Table 4-2.

Table 4-2. Other Direct Inputs (Model, Analysis, Design, and Regulations)

Input Name	Input Description	DTN/IED
Site-Scale Saturated Zone Transport Model	The SZ site-scale model that forms the basis of the SZ flow and transport abstraction model.	LA0306SK831231.001 [DIRS 164362]
Matrix Diffusion Type Curves	The analytical solution type curves for matrix diffusion in fractured media. These type curves are used in the particle-tracking algorithm of the FEHM software to simulate radionuclide transport in fractured porous media.	LA0302RP831228.001 [DIRS 163557]
Repository Design	The coordinates of the outline of the repository design are used in defining the SZ source regions at the water table below the repository.	800-IED-WIS0-00101-000-00B (BSC 2004 [DIRS 172801])
Boundary of Accessible Environment	Latitude of the accessible environment, as defined by regulation.	10 CFR 63.302 [DIRS 173273] (regulatory input, technical information, no DTN)

DTN = Data Tracking Number; FEHM = finite element heat and mass model; IED = information exchange drawing; SZ = Saturated Zone

4.1.2 Parameters and Parameter Uncertainty

The parameters and parameter uncertainties from external sources used directly in the modeling documented in this report are shown in Table 4-3. Parameters are those variables that are used as direct inputs to the models documented in this report.

The input parameters are considered appropriate as direct input to the SZ flow and transport abstraction model and the SZ 1-D transport model. The data used in this report are appropriate for this study because they represent various parameter properties of the SZ at Yucca Mountain.

Table 4-3. Direct Input (Parameter Uncertainty)

Parameter Name	Parameter Source	DTN	Value(s)	Units	Parameter Type
KDNPVO (neptunium sorption coefficient in volcanic units)	BSC 2004 [DIRS 170036]	LA0310AM831341.002 [DIRS 165891]	CDF (cumulative distribution function): Probability Value 0.0 0.0 0.05 0.99 0.90 1.83 1.0 6.0	mL/g	Distribution
KDNPAL (neptunium sorption coefficient in alluvium)	BSC 2004 [DIRS 170036]	LA0310AM831341.002 [DIRS 165891]	CDF: Probability Value 0.0 1.8 0.05 4.0 0.95 8.7 1.0 13.0	mL/g	Distribution
KDSRVO (strontium sorption coefficient in volcanic units)	BSC 2004 [DIRS 170036]	LA0310AM831341.002 [DIRS 165891]	Uniform: Minimum 20. Maximum 400.	mL/g	Distribution
KDSRAL (strontium sorption coefficient in alluvium)	BSC 2004 [DIRS 170036]	LA0310AM831341.002 [DIRS 165891]	Uniform: Minimum 20. Maximum 400.	mL/g	Distribution
KDUVO (uranium sorption coefficient in volcanic units)	BSC 2004 [DIRS 170036]	LA0310AM831341.002 [DIRS 165891]	CDF: Probability Value 0.0 0.0 0.05 5.39 0.95 8.16 1.0 20.0	mL/g	Distribution
KDUAL (uranium sorption coefficient in alluvium)	BSC 2004 [DIRS 170036]	LA0310AM831341.002 [DIRS 165891]	CDF: Probability Value 0.0 1.7 0.05 2.9 0.95 6.3 1.0 8.9	mL/g	Distribution
KDRAVO (radium sorption coefficient in volcanic units)	BSC 2004 [DIRS 170036]	LA0310AM831341.002 [DIRS 165891]	Uniform: Minimum 100. Maximum 1000.	mL/g	Distribution
KDRAAL (radium sorption coefficient in alluvium)	BSC 2004 [DIRS 170036]	LA0310AM831341.002 [DIRS 165891]	Uniform: Minimum 100. Maximum 1000.	mL/g	Distribution

Table 4-3. Direct Input (Parameter Uncertainty) (Continued)

Parameter Name	Parameter Source	DTN	Value(s)	Units	Parameter Type
KD_Pu_Vo (plutonium sorption coefficient in volcanic units)	BSC 2004 [DIRS 170036]	LA0310AM831341.002 [DIRS 165891]	CDF: Probability Value 0.0 10. 0.25 89.9 0.95 129.87 1.0 300.	mL/g	Distribution
KD_Pu_Al (plutonium sorption coefficient in alluvium)	BSC 2004 [DIRS 170036]	LA0310AM831341.002 [DIRS 165891]	Beta: Mean 100. Standard Deviation 15. Minimum 50. Maximum 300.	mL/g	Distribution
KD_Am_Vo (americium sorption coefficient in volcanic units)	BSC 2004 [DIRS 170036]	LA0310AM831341.002 [DIRS 165891]	Truncated Normal: Mean 5500. Standard Deviation 1500. Minimum 1000. Maximum 10000.	mL/g	Distribution
KD_Am_Al (americium sorption coefficient in alluvium)	BSC 2004 [DIRS 170036]	LA0310AM831341.002 [DIRS 165891]	Truncated Normal: Mean 5500. Standard Deviation 1500. Minimum 1000. Maximum 10000.	mL/g	Distribution
KD_Cs_Vo (cesium sorption coefficient in volcanic units)	BSC 2004 [DIRS 170036]	LA0310AM831341.002 [DIRS 165891]	CDF: Probability Value 0.0 100. 0.05 3000.59 1.0 6782.92	mL/g	Distribution
KD_Cs_Al (cesium sorption coefficient in alluvium)	BSC 2004 [DIRS 170036]	LA0310AM831341.002 [DIRS 165891]	Truncated Normal: Mean 728. Standard Deviation 464. Minimum 100. Maximum 1000.	mL/g	Distribution
FISVO (flowing interval spacing in the volcanic units)	BSC 2004 [DIRS 170014]	SN9907T0571599.001 [DIRS 122261]	CDF: (Log_{10}-transformed) Probability Value 0.0 0.087 0.05 0.588 0.25 1.00 0.50 1.29 0.75 1.58 0.95 1.90 1.0 2.62	m	Distribution

Table 4-3. Direct Input (Parameter Uncertainty) (Continued)

Parameter Name	Parameter Source	DTN	Value(s)	Units	Parameter Type
CORAL (colloid retardation factor in the alluvium)	BSC 2004 [DIRS 170006]	LA0303HV831352.004 [DIRS 163559]	CDF : (Log_{10}-transformed) Probability Value 0.0 0.903 0.331 0.904 0.50 1.531 1.0 3.715	N/A	Distribution
CORVO (colloid retardation factor in the volcanic units)	BSC 2004 [DIRS 170006]	LA0303HV831352.002 [DIRS 163558]	CDF : (Log_{10}-transformed) Probability Value 0.0 0.778 0.15 0.779 0.25 1.010 0.50 1.415 0.80 1.778 1.0 2.903	N/A	Distribution
HAVO (ratio of horizontal anisotropy in permeability)	BSC 2004 [DIRS 170010]	SN0302T0502203.001 [DIRS 163563]	CDF : Probability Value 0.0 1.0 0.60 5. 1.0 20.	N/A	Distribution
LDISP (longitudinal dispersivity)	CRWMS M&O 1998 [DIRS 100353]	MO0003SZFWTEEP.000 [DIRS 148744]	Truncated Normal: Log_{10}-transformed) Mean 2.0 Standard Deviation 0.75	m	Distribution
Kd_Pu_Col (plutonium sorption coefficient onto colloids)	BSC 2005 [DIRS 174290]	SN0306T0504103.006 [DIRS 164131]	CDF: Probability Value 0.0 1.e3 0.04 5.e3 0.12 1.e4 0.37 5.e4 0.57 1.e5 0.92 5.e5 1.0 1.e6	mL/g	Distribution
Kd_Am_Col (americium sorption coefficient onto colloids)	BSC 2005 [DIRS 174290]	SN0306T0504103.006 [DIRS 164131]	CDF: Probability Value 0.0 1.e4 0.07 5.e4 0.17 1.e5 0.40 5.e5 0.60 1.e6 0.92 5.e6 1.0 1.e7	mL/g	Distribution

Table 4-3. Direct Input (Parameter Uncertainty) (Continued)

Parameter Name	Parameter Source	DTN	Value(s)	Units	Parameter Type
Kd_Cs_Col (cesium sorption coefficient onto colloids)	BSC 2005 [DIRS 174290]	SN0306T0504103.006 [DIRS 164131]	CDF: Probability / Value 0.0 1.e2 0.2 5.e2 0.45 1.e3 0.95 5.e3 1.0 1.e4	mL/g	Distribution
Conc_Col (groundwater concentration of colloids)	BSC 2005 [DIRS 174290]	SN0306T0504103.005 [DIRS 164132]	CDF: (Log_{10}-transformed) Probability / Value 0.0 -9.0 0.50 -7.0 0.75 -6.0 0.90 -5.0 0.98 -4.3 1.0 -3.7	g/mL	Distribution
Correlation coefficient for U K_d in volcanic units and alluvium	BSC 2004 [DIRS 170036]	LA0310AM831341.002 [DIRS 165891]	0.75	N/A	Single Value
Correlation coefficient for Np K_d in volcanic units and alluvium	BSC 2004 [DIRS 170036]	LA0310AM831341.002 [DIRS 165891]	0.75	N/A	Single Value
Correlation coefficient for Pu K_d in volcanic units and alluvium	BSC 2004 [DIRS 170036]	LA0310AM831341.002 [DIRS 165891]	0.50	N/A	Single Value
Correlation coefficient for U K_d and Np K_d	BSC 2004 [DIRS 170036]	LA0310AM831341.002 [DIRS 165891]	0.50	N/A	Single Value

NOTE: DTN: MO0003SZFWTEEP.000 [DIRS 148744] contains qualified data from an expert elicitation that was determined to comply with expert elicitation procedure LP-AC.1Q Rev 0, ICN 1, which is consistent with the branch technical position on expert elicitation, NUREG-1563 (Kotra et al. 1996 [DIRS 100909]).

CDF=cumulative distribution function

4.2 CRITERIA

The general requirements to be satisfied by the TSPA-LA are stated in 10 CFR 63.114 (10 CFR 63 [DIRS 173273]). Technical requirements to be satisfied by the TSPA-LA are identified in the Yucca Mountain *Project Requirements Document* (Canori and Leitner 2003 [DIRS 166275], Section 3). The acceptance criteria that will be used by the U.S. Nuclear Regulatory Commission (NRC) to determine whether the technical requirements have been met are identified in the *Yucca Mountain Review Plan, Final Report* (YMRP)

(NRC 2003 [DIRS 163274]). The pertinent requirements and criteria for this report are summarized in Table 4-4.

Table 4-4. Project Requirements for This Model Report

Requirement Number[a]	Requirement Title[a]	10 CFR 63 Link	YMRP Acceptance Criteria[b]
PRD -002/T-015	Requirements for Performance Assessment	10 CFR 63.114 [DIRS 173273]	2.2.1.3.8.3, criteria 1 to 5; 2.2.1.3.9.3, criteria 1 to 5

[a] Canori and Leitner 2003 [DIRS 166275].
[b] NRC 2003 [DIRS 163274].

YMRP = Yucca Mountain Review Plan

In this section, the acceptance criteria identified in Sections 2.2.1.3.8.3, and 2.2.1.3.9.3 of the YMRP (NRC 2003 [DIRS 163274]) are given below. In cases where subsidiary criteria are listed in the YMRP for a given criterion, only the subsidiary criteria addressed by this model report are listed below. Where a subcriterion includes several components, only some of those components may be addressed. How these components are addressed is summarized in Section 8.3 of this report.

Acceptance criteria from Section 2.2.1.3.8, Flow Paths in the Saturated Zone

Acceptance Criterion 1, System Description and Model Integration are Adequate:

(1) Total system performance assessment adequately incorporates important design features, physical phenomena, and couplings, and uses consistent and appropriate assumptions, throughout the flow paths in the SZ abstraction process.

(2) The description of the aspects of hydrology, geology, geochemistry, design features, physical phenomena, and couplings that may affect flow paths in the SZ is adequate. Conditions and assumptions in the abstraction of flow paths in the SZ are readily identified and consistent with the body of data presented in the description.

(3) The abstraction of flow paths in the SZ uses assumptions, technical bases, data, and models that are appropriate and consistent with other related DOE abstractions. For example, the assumptions used for flow paths in the SZ are consistent with the total system performance assessment abstraction of representative volume (Section 2.2.1.3.12 of NRC 2003 [DIRS 163274]). The descriptions and technical bases provide transparent and traceable support for the abstraction of flow paths in the SZ.

(4) Boundary and initial conditions used in the total system performance assessment abstraction of flow paths in the SZ are propagated throughout its abstraction approaches. For example, abstractions are based on initial and boundary conditions consistent with site-scale modeling and regional models of the Death Valley groundwater flow system.

(5) Sufficient data and technical bases to assess the extent to which features, events, and processes have been included in this abstraction are provided.

(7) Long-term climate change, based on known patterns of climatic cycles during the Quaternary period, particularly the last 500,000 years, and other paleoclimate data, are adequately evaluated.

(9) The impact of the expected water table rise on potentiometric heads and flow directions, and consequently on repository performance, is adequately considered.

(10) Guidance in NUREG-1297 (Altman et al. 1988 [DIRS 103597]) and NUREG-1298 (Altman et al. 1988 [DIRS 103750]) or other acceptable approaches for peer review and data qualification is followed.

Acceptance Criterion 2, Data are Sufficient for Model Justification:

(1) Geological, hydrological, and geochemical values used in the license application to evaluate flow paths in the SZ are adequately justified. Adequate descriptions of how the data were used, interpreted, and appropriately synthesized into the parameters are provided.

(3) Data on the geology, hydrology, and geochemistry of the SZ used in the total system performance assessment abstraction are based on appropriate techniques. These techniques may include laboratory experiments, site-specific field measurements, natural analogue research, and process-level modeling studies. As appropriate, sensitivity or uncertainty analyses used to support the U.S. Department of Energy total system performance assessment abstraction are adequate to determine the possible need for additional data.

Acceptance Criterion 3, Data Uncertainty is Characterized and Propagated Through the Model Abstraction:

(1) Models use parameter values, assumed ranges, probability distributions, and/or bounding assumptions that are technically defensible, and reasonably account for uncertainties and variabilities, and do not result in an under-representation of the risk estimate.

(2) Uncertainty is appropriately incorporated in model abstractions of hydrologic effects of climate change, based on a reasonably complete search of paleoclimate data.

(3) Uncertainty is adequately represented in parameter development for conceptual models, process-level models, and ACMs considered in developing the abstraction of flow paths in the SZ. This may be done either through sensitivity analyses or use of conservative limits. For example, sensitivity analyses and/or similar analyses are sufficient to identify

saturated zone flow parameters that are expected to significantly affect the abstraction model outcome.

(4) Where sufficient data do not exist, the definition of parameter values and conceptual models is based on appropriate use of expert elicitation, conducted in accordance with NUREG-1563 (Kotra et al. 1996 [DIRS 100909]). If other approaches are used, the U.S. Department of Energy adequately justifies their uses.

Acceptance Criterion 4, Model Uncertainty is Characterized and Propagated Through the Model Abstraction:

(1) Alternative modeling approaches of features, events, and processes are considered and are consistent with available data and current scientific understanding, and the results and limitations are appropriately considered in the abstraction.

(2) Conceptual model uncertainties are adequately defined and documented, and effects on conclusions regarding performance are properly assessed. For example, uncertainty in data interpretations is considered by analyzing reasonable conceptual flow models that are supported by site data, or by demonstrating through sensitivity studies that the uncertainties have little impact on repository performance.

(3) Consideration of conceptual model uncertainty is consistent with available site characterization data, laboratory experiments, field measurements, natural analog information and process-level modeling studies; and the treatment of conceptual model uncertainty does not result in an under-representation of the risk estimate; and

(4) Appropriate alternative modeling approaches are consistent with available data and current scientific knowledge and appropriately consider their results and limitations, using tests and analyses that are sensitive to the processes modeled.

Acceptance Criterion 5, Model Abstraction Output Is Supported by Objective Comparisons:

(1) The models implemented in this total system performance assessment abstraction provide results consistent with output from detailed process-level models and/or empirical observations (laboratory and field testing and/or natural analogues).

(2) Outputs of flow paths in the SZ abstractions reasonably produce or bound the results of corresponding process-level models, empirical observations, or both.

(3) Well-documented procedures that have been accepted by the scientific community for the construction and testing of the mathematical and numerical models are used to simulate flow paths in the SZ.

(4) Sensitivity analyses or bounding analyses are provided to support the abstraction of flow paths in the saturated zone that cover ranges consistent with site data, field or laboratory experiments and tests, and natural analog research.

Acceptance criteria from Section 2.2.1.3.9, Radionuclide Transport in the Saturated Zone

Acceptance Criterion 1, System Description and Model Integration are Adequate:

(1) Total system performance assessment adequately incorporates important design features, physical phenomena, and couplings, and uses consistent and appropriate assumptions throughout the radionuclide transport in the saturated zone abstraction process.

(2) The description of the aspects of hydrology, geology, geochemistry, design features, physical phenomena, and couplings that may affect radionuclide transport in the SZ is adequate. For example, the description includes changes into transport properties in the saturated zone, from water-rock interaction. Conditions and assumptions in the abstraction of radionuclide transport in the saturated zone are readily identified, and consistent with the body of data presented in the description.

(3) The abstraction of radionuclide transport in the SZ uses assumptions, technical bases, data, and models that are appropriate and consistent with other related DOE abstractions. For example, assumptions used for radionuclide transport in the saturated zone are consistent with the total system performance assessment abstractions of radionuclide release rates and solubility limits, and flow paths in the saturated zone (Sections 2.2.1.3.4 and 2.2.1.3.8 of the Yucca Mountain Review Plan, respectively). The descriptions and technical bases provide transparent and traceable support for the abstraction of radionuclide transport in the saturated zone.

(4) Boundary and initial conditions used in the abstraction of radionuclide transport in the SZ are propagated throughout its abstraction approaches. For example, the conditions and assumptions used to generate transport parameter values are consistent with other geological, hydrological, and geochemical conditions in the total system performance assessment abstraction of the saturated zone.

(5) Sufficient data and technical bases for the inclusion of features, events, and processes related to radionuclide transport in the SZ in the total system performance assessment abstraction are provided.

(6) Guidance in NUREG-1297 (Altman et al. 1988 [DIRS 103597]) and NUREG-1298 (Altman et al. 1988 [DIRS 103750]) or other acceptable approaches for peer review and data qualification is followed.

Acceptance Criterion 2, Data are Sufficient for Model Justification:

(1) Geological, hydrological, and geochemical values used in the license application are adequately justified (e.g., flow path lengths, sorption coefficients, retardation factors, colloid concentrations, etc.). Adequate descriptions of how the data were used, interpreted, and appropriately synthesized into the parameters are provided

(2) Sufficient data have been collected on the characteristics of the natural system to establish initial and boundary conditions for the total system performance assessment abstraction of radionuclide transport in the saturated zone

Acceptance Criterion 3, Data Uncertainty is Characterized and Propagated Through the Model Abstraction:

(1) Models use parameter values, assumed ranges, probability distributions, and/or bounding assumptions that are technically defensible, and reasonably account for uncertainties and variabilities, and do not result in an under-representation of the risk estimate.

(4) Parameter values for processes, such as matrix diffusion, dispersion, and groundwater mixing, are based on reasonable assumptions about climate, aquifer properties, and groundwater volumetric fluxes (Section 2.2.1.3.8 of NRC 2003 [DIRS 163274]).

(5) Uncertainty is adequately represented in parameter development for conceptual models, process-level models, and ACMs considered in developing the abstraction of radionuclide transport in the SZ. This may be done either through sensitivity analyses or use of conservative limits.

(6) Where sufficient data do not exist, the definition of parameter values and conceptual models is based on appropriate use of expert elicitation, conducted in accordance with NUREG-1563 (Kotra et al. 1996 [DIRS 100909]). If other approaches are used, the U.S. Department of Energy adequately justifies their use.

Acceptance Criterion 4, Model Uncertainty is Characterized and Propagated Through the Model Abstraction:

(1) Alternative modeling approaches of features, events, and processes are considered and are consistent with available data and current scientific understanding, and the results and limitations are appropriately considered in the abstraction.

(2) Conceptual model uncertainties are adequately defined and documented, and effects on conclusions regarding performance are properly assessed.

(3) Consideration of conceptual model uncertainty is consistent with available site characterization data, laboratory experiments, field measurements, natural analog information and process-level modeling studies; and the treatment of conceptual model uncertainty does not result in an under-representation of the risk estimate; and

(4) Appropriate alternative modeling approaches are consistent with available data and current scientific knowledge and appropriately consider their results and limitations, using tests and analyses that are sensitive to the processes modeled. For example, for radionuclide transport through fractures, the U.S. Department of Energy adequately considers alternative modeling approaches to develop its understanding of fracture distributions and ranges of fracture flow and transport properties in the saturated zone.

Acceptance Criterion 5, Model Abstraction Output is Supported by Objective Comparisons:

(1) The models implemented in this total system performance assessment abstraction provide results consistent with output from detailed process-level models and/or empirical observations (laboratory and field testing and/or natural analogs);

(2) Outputs of radionuclide transport in the SZ abstractions reasonably produce or bound the results of corresponding process-level models, empirical observations, or both. The U.S. Department of Energy-abstracted models for radionuclide transport in the saturated zone are based on the same hydrological, geological, and geochemical assumptions and approximations shown to be appropriate for closely analogous natural systems or laboratory experimental systems.

(3) Well-documented procedures that have been accepted by the scientific community for the construction and testing of the mathematical and numerical models are used to simulate radionuclide transport through the SZ.

(4) Sensitivity analyses or bounding analyses are provided, to support the total system performance assessment abstraction of radionuclide transport in the SZ, that cover ranges consistent with site data, field or laboratory experiments and tests, and natural analogue research.

4.3 CODES, STANDARDS, AND REGULATIONS

No codes, standards, or regulations other than those identified in the *Project Requirements Document* (Canori and Leitner 2003 [DIRS 166275], Table 2-3) and determined to be applicable (Table 4-4) were used in this analysis.

INTENTIONALLY LEFT BLANK

5. ASSUMPTIONS

Several types of assumptions pertain to model development. The assumptions listed in this section of the report are restricted to those that meet the definition given in the QA procedure LP-SIII.10Q-BSC, *Models*. This definition states that an assumption is "a statement or proposition that is taken to be true or representative in the absence of direct confirming data or evidence." Additional technical modeling bases (assumptions) pertaining to the modeling framework are documented in Section 6 of this report (primarily in Section 6.3).

1. For the transport of radionuclides irreversibly attached to colloids in the SZ, it is assumed that radionuclides will not desorb from colloids. This assumption is carried forward from the scientific analysis report *Saturated Zone Colloid Transport* (BSC 2004 [DIRS 170006], Section 6.3) and is consistent with the mineralogic characteristics of colloids from the degradation of the glass waste form. This assumption is also conservative with regard to repository performance due to the comparatively high mobility of colloids in the SZ relative to the sorptive characteristics of the radionuclides (plutonium and americium) that are subject to colloid-facilitated transport. This assumption is used in Sections 6.3.1, 6.3.2, 6.5.1, and 6.5.2.11. This assumption needs no further confirmation, given that it is a bounding assumption that maximizes the rate of radionuclide migration in the SZ.

2. Colloids with irreversibly attached radionuclides are assumed to be subject to attachment and detachment to mineral grains in the aquifer, but not to be subject to permanent filtration from the groundwater of the SZ. This assumption is carried forward from the scientific analysis report *Saturated Zone Colloid Transport* (BSC 2004 [DIRS 170006], Section 6.3). The kinetically controlled attachment and detachment of colloids in the aquifer is consistent with tracer testing in the SZ using microspheres. The permanent filtration of colloids in the SZ has not been demonstrated by field-testing, although this process can occur. This assumption's alternative, in which permanent filtration were simulated to occur, would lead to significant attenuation of the migration of radionuclides irreversibly attached to colloids. This assumption is used in Sections 6.3.1, 6.3.2, 6.5.1, and 6.5.2.11. This assumption needs no further confirmation, given that it is a bounding assumption that maximizes the migration of radionuclides in the SZ.

3. The assumption is made that the average concentration of radionuclides in the groundwater supply of the hypothetical community in which the reasonably maximally exposed individual (RMEI) resides is an appropriate estimate of radionuclide concentration for the calculation of radiological dose. This assumption applies to the calculation of radionuclide concentrations for evaluation of compliance with 10 CFR 63.332 (10 CFR 63 [DIRS 173273]) and with groundwater protection in 10 CFR 63.331. Realistically, the concentrations of radionuclides encountered by wells in the hypothetical community in which the RMEI resides would vary from location to location within the contaminant plume in the SZ. However, radionuclide transfer processes within the biosphere (e.g., redistribution of agricultural products, communal water supplies, etc.) would tend to average the overall dose received by the population of the community in which the RMEI resides. This assumption is used in

Section 6.3.3. This assumption needs no further confirmation, given that there is a regulatory basis for this approach to calculating average concentrations of radionuclides and radiological dose in 10 CFR 63.332 (10 CFR 63 [DIRS 173273]).

4. The assumption is made that the horizontal anisotropy in permeability applies to the fractured and faulted volcanic units of the SZ system along the groundwater flow path from the repository to the south and east of Yucca Mountain. This assumption is carried forward from the scientific analysis report *Saturated Zone In-Situ Testing* (BSC 2004 [DIRS 170010], Section 6.2.6). The inferred flow path from beneath the repository extends to the south and east. This is the area in which pumping tests were conducted at the C-holes well complex (BSC 2004 [DIRS 170010]), from which horizontal anisotropy was inferred. Given the conceptual basis for the anisotropy model, it is appropriate to apply anisotropy only to those hydrogeologic units that are dominated by groundwater flow in fractures because it is the preferential orientations of open fractures that impart anisotropy in the system. This assumption is used in Section 6.5.2.10. This assumption needs no further confirmation, given the wide range of uncertainty in horizontal anisotropy used in the SZ flow and transport abstraction model.

5. It is assumed that the change in groundwater flow in the SZ from one climatic state to another occurs rapidly and is approximated by an instantaneous shift from one steady-state flow condition to another steady-state flow condition. In actuality, even an extremely rapid shift in climatic conditions would result in a transient response of the SZ flow system because of changes in groundwater storage associated with water table rise or fall and because of the response time in the unsaturated zone (UZ) flow system. The assumption of instantaneous shifts to new steady-state conditions would tend to overestimate the rate of radionuclide transport in the TSPA-LA calculations. The progression of climate states in the 10,000 years following repository closure is anticipated to be from drier to wetter climatic conditions and thus from slower to more rapid groundwater flow in the SZ. By assuming an instantaneous shift to higher groundwater flux in the SZ, the simulations tend to overestimate the radionuclide transport velocities during the period of transition from drier conditions to wetter conditions. This assumption is used in Section 6.5. This assumption needs no further confirmation, given that this simplified approach underestimates the transport times for radionuclides in the SZ and is thus pessimistic with regard to repository performance.

6. Groundwater flow pathways in the SZ from beneath the repository to the accessible environment are assumed not to be significantly altered for wetter climatic states. Scaling of present-day groundwater flux and radionuclide mass breakthrough curves by a proportionality factor implies that only the groundwater velocities are changed in the SZ system in response to climate change. This assumption is supported by the observation that the shape of the simulated potentiometric surface downgradient from Yucca Mountain remains essentially the same under glacial-transition climatic conditions in simulations using the Death Valley regional groundwater flow model (D'Agnese et al. 1999 [DIRS 120425], p. 30). Water table rise directly beneath the repository under wetter climatic conditions would tend to place volcanic units higher

in the stratigraphic sequence at or just below the water table. These higher volcanic units (Prow Pass Tuff and Calico Hills Formation) have lower values of permeability than the underlying Bullfrog Tuff. This approximation of climate change with unaltered SZ flow paths is shown to underestimate radionuclide transport times in sensitivity studies documented in *Site-Scale Saturated Zone Transport* (BSC 2004 [DIRS 170036], Appendix E). This assumption is used in Section 6.5. This assumption needs no further confirmation, given that this simplified approach tends to underestimate the transport times for radionuclides in the SZ.

INTENTIONALLY LEFT BLANK

6. MODEL DISCUSSION

6.1 MODELING OBJECTIVES

The primary objective of the SZ flow and transport abstraction model and the SZ 1-D transport model is to provide a method of simulating radionuclide transport in the SZ for use in the TSPA-LA model of repository performance. Analyses of parameter uncertainty and multiple realizations of the SZ system using the SZ flow and transport abstraction model constitute an assessment of uncertainty in the SZ system for direct implementation in the TSPA-LA model. Model uncertainty is addressed by generating a suite of radionuclide breakthrough curves based on the multiple realizations of the SZ system. The general approach to modeling radionuclide migration and the assessment of uncertainty in the SZ is also described by Arnold et al. in "Radionuclide Transport Simulation and Uncertainty Analyses with the Saturated-Zone Site-Scale Model at Yucca Mountain, Nevada" (2003 [DIRS 163857]). The objective of the SZ 1-D transport model is to provide a simplified, yet accurate, representation of SZ flow and transport for the simulation of four radionuclide decay chains for implementation with the TSPA-LA model. Figure 1-1 shows the flow of information among the SZ reports used in the development of the SZ flow and transport abstraction model and the SZ 1-D transport model as outputs from this report.

In the TSPA-LA analyses, the convolution integral method is used by the SZ flow and transport abstraction model to determine the radionuclide mass flux at the SZ/biosphere interface, 18 km downgradient of the repository at 36°40'13.6661" north latitude (10 CFR 63.302 [DIRS 173273]) as a function of the transient radionuclide mass flux at the water table beneath the repository. This computationally efficient method combines information about the unit response of the system, as simulated by the SZ flow and transport abstraction model, with the radionuclide source history from the UZ, to calculate transient system behavior. The fundamental concepts of the convolution integral method, as applied to solute transport in groundwater, are presented by Jury et al. (1986 [DIRS 164314]), in which the method is called the transfer function model. The most important assumptions of the convolution method are linear system behavior and steady-state flow conditions in the SZ.

The SZ 1-D transport model is used in the TSPA-LA analyses for the purpose of simulating radioactive decay and ingrowth for four decay chains. This simplified model is required because the radionuclide transport methodology used in the SZ flow and transport abstraction model is not capable of simulating ingrowth by radioactive decay. Although it is not anticipated that the decay products generated from these radioactive decay chains during transport in the SZ are significant contributors to the total radiological dose, regulations concerning groundwater protection contained in 10 CFR 63.331 (10 CFR 63 [DIRS 173273]) require explicit analysis of the total concentrations of ^{226}Ra plus ^{228}Ra, gross alpha emitters, and beta plus photon emitters in the water supply of the RMEI. Consequently, only the results for decay product-radionuclides from the SZ 1-D transport model are input to the TSPA-LA simulations. Although transport of the parent radionuclides is also included in the SZ 1-D transport model, the results for parent-radionuclides input to the TSPA-LA simulations are those derived from the SZ flow and transport abstraction model. The SZ 1-D transport model for TSPA-LA differs in implementation from the SZ flow and transport abstraction model in that it is constructed directly within the GoldSim V7.50.100 software code (GoldSim V7.50.100, STN: 10344-7.50.100-00

[DIRS 161572]) in the TSPA-LA model. It should be noted that transport of the first-generation decay products in the four decay chains is simulated with the SZ flow and transport abstraction model using a simplified method of inventory boosting, as described in Section 6.3.1.

6.2 FEATURES, EVENTS, AND PROCESSES FOR THIS MODEL REPORT

As stipulated in *Technical Work Plan For: Natural System - Saturated Zone Analysis Model Report Integration* (BSC 2004 [DIRS 171421], Section 2.1.5) this model report addresses the SZ FEPs pertaining to the abstraction of SZ flow and transport that are included in the TSPA-LA model (Table 6-1). Table 6-1 provides a list of FEPs that are relevant to the models documented in this report, in accordance with their assignment in the LA FEP list (DTN: MO0501SEPFEPLA.001 ([DIRS 172601]). Specific reference to the various sections within this document where issues related to each FEP are addressed is provided in Table 6-1. The detailed discussions of these FEPs and their implementation in TSPA-LA are documented in the *Features, Events, and Processes in SZ Flow and Transport* (BSC 2005 [DIRS 174190]) report. Saturated zone FEPs that were excluded from the TSPA-LA modeling are also described in *Features, Events, and Processes in SZ Flow and Transport*.

Table 6-1. Features, Events, and Processes Included in TSPA-LA and Relevant to This Model Report

FEP No.	FEP Name	Sections Where Disposition is Supported	FEP Topic Addressed in Other SZ Analysis or Model Reports
1.2.02.01.0A	Fractures	6.5.2.1, 6.5.2.4, 6.5.2.5, 6.5.2.9, 6.5.2.10, 6.5.2.11, 6.5.2.12, 6.5.2.15	Upstream Feeds[a]—BSC 2004 [DIRS 170036] Expanded Discussion[c]—BSC 2004 [DIRS 170014] Corroborating[b]—BSC 2004 [DIRS 170010]
1.2.02.02.0A	Faults	6.3.1, 6.5.2.1, 6.5.2.10	Upstream Feeds[a]—BSC 2004 [DIRS 170036] Expanded Discussion[c]—BSC 2004 [DIRS 170037], BSC 2004 [DIRS 170008] Corroborating[b]—BSC 2004 [DIRS 170010]
1.3.07.02.0A	Water table rise affects SZ	5	Upstream Feeds[a]—BSC 2004 [DIRS 170036] Expanded Discussion[c]—BSC 2004 [DIRS 170009]
1.4.07.01.0A	Water management activities	6.3.3, 6.7.2	Upstream Feeds[a]—BSC 2004 [DIRS 170009]
1.4.07.02.0A	Wells	6.3.3	Upstream Feeds[a]—BSC 2004 [DIRS 170009]
2.2.03.01.0A	Stratigraphy	6.5.2, 6.5.2.1, 6.5.2.2, 6.5.2.3, 6.5.2.6, 6.5.2.18, 6.5.2.19	Upstream Feeds[a]—BSC 2004 [DIRS 170036] Expanded Discussion[c]—BSC 2004 [DIRS 170008], BSC 2004 [DIRS 170037] Corroborating[b]—BSC 2004 [DIRS 170010], BSC 2004 [DIRS 170014]
2.2.03.02.0A	Rock properties of host rock and other units	6.5.2.1, 6.5.2.2, 6.5.2.3, 6.5.2.4, 6.5.2.5, 6.5.2.7, 6.5.2.8, 6.5.2.9, 6.5.2.10, 6.5.2.14, 6.5.2.15, 6.5.2.16, 6.5.2.17, 6.5.2.18, 6.5.2.19, 6.5.2.20	Upstream Feeds[a]—BSC 2004 [DIRS 170036] Corroborating[b]—BSC 2004 [DIRS 170010], BSC 2004 [DIRS 170014], BSC 2004 [DIRS 170008]

Table 6-1. Features, Events, and Processes Included in TSPA-LA and Relevant to This Model Report (Continued)

FEP No.	FEP Name	Sections Where Disposition is Supported	FEP Topic Addressed in Other SZ Analysis or Model Reports
2.2.07.12.0A	Saturated groundwater flow in the geosphere	6.3, 6.5, 6.5.2.1, 6.5.2.10	Upstream Feeds[a]—BSC 2004 [DIRS 170036] Expanded Discussion[c]—BSC 2004 [DIRS 170037] Corroborating[b]—BSC 2004 [DIRS 170010], BSC 2004 [DIRS 170037], BSC 2004 [DIRS 170014]
2.2.07.13.0A	Water-conducting features in the SZ	6.5.2.1, 6.5.2.4, 6.5.2.5, 6.5.2.9, 6.5.2.10	Upstream Feeds[a]—BSC 2004 [DIRS 170036] Expanded Discussion[c]—BSC 2004 [DIRS 170037] Corroborating[b]—BSC 2004 [DIRS 170014], BSC 2004 [DIRS 170010]
2.2.07.15.0A	Advection and dispersion in the SZ	6.3, 6.5.2.1, 6.5.2.9, 6.5.2.10	Upstream Feeds[a]—BSC 2004 [DIRS 170036] Corroborating[b]—BSC 2004 [DIRS 170010]
2.2.07.16.0A	Dilution of radionuclides in groundwater	6.5.2.9, 6.7.2	Upstream Feeds[a]—BSC 2004 [DIRS 170036]
2.2.07.17.0A	Diffusion in the SZ	6.3, 6.5.2.6	Upstream Feeds[a]—BSC 2004 [DIRS 170036] Corroborating[b]—BSC 2004 [DIRS 170010], BSC 2004 [DIRS 170006]
2.2.08.01.0A	Chemical characteristics of groundwater in the SZ	6.5.2.8, 6.5.2.11, 6.5.2.12	Upstream Feeds[a]—BSC 2004 [DIRS 170036] Corroborating[b]—BSC 2004 [DIRS 170037]
2.2.08.06.0A	Complexation in the SZ	6.5.2.8, 6.5.2.11, 6.5.2.12	Upstream Feeds[a]—BSC 2004 [DIRS 170036]
2.2.08.08.0A	Matrix diffusion in the SZ	6.3, 6.5.2.4, 6.5.2.5, 6.5.2.6	Upstream Feeds[a]—BSC 2004 [DIRS 170036] Corroborating[b]—BSC 2004 [DIRS 170010], BSC 2004 [DIRS 170014], BSC 2004 [DIRS 170006]
2.2.08.09.0A	Sorption in the SZ	6.3, 6.5.2.8, 6.5.2.11, 6.5.2.12	Upstream Feeds[a]—BSC 2004 [DIRS 170036]
2.2.08.10.0A	Colloidal transport in the SZ	6.3.1, 6.5.1, 6.5.2.11, 6.5.2.12	Upstream Feeds[a]—BSC 2004 [DIRS 170036], BSC 2004 [DIRS 170006]
2.2.10.03.0A	Natural geothermal effects on flow in the SZ	6.5.2.6	Upstream Feeds[a]—BSC 2004 [DIRS 170036] Expanded Discussion[c]—BSC 2004 [DIRS 170037]
2.2.12.00.0B	Undetected features in the SZ	6.5.2.1, 6.5.2.3, 6.5.2.4, 6.5.2.10	Upstream Feeds[a]—BSC 2004 [DIRS 170036], BSC 2004 [DIRS 170014] Corroborating[b]—BSC 2004 [DIRS 170010], BSC 2004 [DIRS 170037]
3.1.01.01.0A	Radioactive decay and in-growth	6.3.1, 6.5, 6.5.1	Upstream Feeds[a]—N/A

[a]Upstream Feeds – Aspects of the SZ FEP discussion adopted in this report are a result of SZ analyses performed in a directly upstream SZ model or analyses.

[b]Corroborating – Corroborative aspect(s) of the FEP topic is (are) discussed in a SZ analysis report.

[c] Expanded Discussion – The primary discussion of the FEP topic is discussed in the referenced SZ report.

NOTE: See Table 6-2 for key to SZ Analysis and Model Reports (e.g., BSC 2004 [DIRS 170036])

FEP = feature, event, or process; SZ = saturated zone

Table 6-2 provides a key to the SZ analysis and model reports listed in Table 6-1. SZ FEPs that are excluded from the models in the SZ are listed in Table 6-3. Screening arguments for the exclusion of the excluded FEPs are provided in *Features, Events, and Processes in SZ Flow and Transport* (BSC 2005 [DIRS 174190].

Table 6-2. SZ Analysis and Model Reports

SZ Analysis or Model Report Number	Report Title	Document Identification Number
BSC 2004 [DIRS 170008]	Hydrogeologic Framework Model for the Saturated Zone Site Scale Flow and Transport Model	MDL-NBS-HS-000024
BSC 2004 [DIRS 170009]	Water-Level Data Analysis for the Saturated Zone Site-Scale Flow and Transport Model	ANL-NBS-HS-000034
BSC 2004 [DIRS 170015]	Recharge and Lateral Groundwater Flow Boundary Conditions for the Saturated Zone Site-Scale Flow and Transport Model	ANL-NBS-MD-000010
BSC 2004 [DIRS 170036]	Site-Scale Saturated Zone Transport	MDL-NBS-HS-000010
BSC 2004 [DIRS 170014]	Probability Distribution for Flowing Interval Spacing	ANL-NBS-MD-000003
BSC 2004 [DIRS 170006]	Saturated Zone Colloid Transport	ANL-NBS-HS-000003
BSC 2004 [DIRS 170037]	Saturated Zone Site-Scale Flow Model	MDL-NBS-HS-000011
This report	Saturated Zone Flow and Transport Model Abstraction	MDL-NBS-HS-000021
BSC 2005 [DIRS 174190]	Features, Events, and Processes in SZ Flow and Transport	ANL-NBS-MD-000002
BSC 2004 [DIRS 170010]	Saturated Zone In-Situ Testing	ANL-NBS-HS-000039

SZ = saturated zone

Table 6-3. SZ Excluded FEPs

FEP Number	FEP Name
1.2.04.02.0A	Igneous activity changes rock properties
1.2.04.07.0B	Ash redistribution in groundwater
1.2.06.00.0A	Hydrothermal activity
1.2.09.02.0A	Large-scale dissolution
1.2.10.01.0A	Hydrologic response to seismic activity
1.2.10.02.0A	Hydrologic response to igneous activity
1.3.07.01.0A	Water table decline
1.4.07.03.0A	Recycling of accumulated radionuclides from soils to groundwater
2.1.09.21.0B	Transport of particles larger than colloids in the SZ
2.2.06.01.0A	Seismic activity changes porosity and permeability of rock
2.2.06.02.0A	Seismic activity changes porosity and permeability of faults
2.2.06.02.0B	Seismic activity changes porosity and permeability of fractures
2.2.07.14.0A	Chemically-induced density effects on groundwater flow
2.2.08.03.0A	Geochemical interactions and evolution in the SZ
2.2.08.07.0A	Radionuclide solubility limits in the SZ
2.2.08.11.0A	Groundwater discharge to surface within the reference biosphere
2.2.09.01.0A	Microbial activity in the SZ
2.2.10.02.0A	Thermal convection cell develops in SZ
2.2.10.04.0A	Thermo-mechanical stresses alter characteristics of fractures near repository

Table 6-3. SZ Excluded FEPs (Continued)

FEP Number	FEP Name
2.2.10.04.0B	Thermo-mechanical stresses alter characteristics of faults near repository
2.2.10.05.0A	Thermo-mechanical stresses alter characteristics of rocks above and below repository
2.2.10.08.0A	Thermo-chemical alteration in the SZ (solubility, speciation, phase changes, precipitation/dissolution)
2.2.10.13.0A	Repository-induced thermal effects on flow in the SZ
2.2.11.01.0A	Gas effects in the SZ
2.3.11.04.0A	Groundwater discharge to surface outside the reference biosphere
3.2.07.01.0A	Isotopic dilution

FEP = feature, event, or process; SZ = saturated zone

Screening arguments for the exclusion of the excluded FEPs are provided in Features, Events, and Processes in SZ Flow and Transport (BSC 2005 [DIRS 174190], Section 6.2).

6.3 BASE-CASE CONCEPTUAL MODEL

The base-case conceptual model for radionuclide transport, as implemented in the SZ flow and transport abstraction model, implicitly includes the conceptual models of groundwater flow and transport incorporated in the SZ site-scale flow model (BSC 2004 [DIRS 170037], Section 6.3) and the SZ site-scale transport model (BSC 2004 [DIRS 170036], Sections 6.3). The SZ site-scale flow model and alternative conceptualizations of groundwater flow are also described by Zyvoloski et al. (2003 [DIRS 163341]). The base-case conceptual model for the SZ 1-D transport model also implicitly includes the conceptual models in these same underlying models, with the conceptual simplifications in flow associated with representation by 1-D groundwater flow. The SZ flow and transport abstraction model and the SZ 1-D transport model also include the concept of uncertainty in key model parameters. The probabilistic analysis of uncertainty is implemented through Monte Carlo realizations of the SZ flow and transport system, in a manner consistent with the TSPA-LA simulations.

6.3.1 SZ Flow and Transport Abstraction Model

The conceptual model of groundwater flow in the SZ includes steady-state flow conditions in a three-dimensional (3-D) flow system (BSC 2004 [DIRS 170037], Section 6.3.3). Groundwater flow occurs in a continuum fracture network in the fractured volcanic rocks beneath the repository site, at the scale of individual grid blocks in the SZ flow and transport abstraction model. The effective continuum conceptual model is appropriate, given the relatively large horizontal scale (500 m by 500 m) of the grid in the model. Grid resolution studies with the SZ site-scale flow model indicate that the 500 m grid resolution and the effective continuum conceptual model are adequate to capture the flow behavior of the SZ system and to calibrate the model (Bower et al. 2000 [DIRS 149161]). Groundwater flow is conceptualized to occur in a continuum porous medium in the alluvium and valley-fill units of the SZ flow and transport abstraction model. Contrasting values of average permeability among hydrogeologic units influence the patterns of groundwater flow in the SZ (BSC 2004 [DIRS 170037], Sections 6.3 and 6.6).

Some of the major faults and other discrete geological features are conceptualized to impact the groundwater flow due to contrasts in permeability with surrounding hydrogeologic units. In addition, the prevailing structural fabric in the volcanic hydrogeologic units near Yucca Mountain can possibly impart horizontal anisotropy in the permeability between the major faults in this area of the SZ system. Significant variations in the hydraulic gradient near Yucca Mountain occur to the north of Yucca Mountain at the Large Hydraulic Gradient and to the west of Yucca Mountain at the Moderate Hydraulic Gradient, corresponding to the Solitario Canyon fault (Luckey et al. 1996 [DIRS 100465], pp. 21 to 26). Analysis of the different conceptualizations of the Large Hydraulic Gradient showed that the specific discharge was only mildly sensitive to choice of conceptual model if the hydraulic head measurements along the flow path were reasonably well matched by the numerical model (BSC 2004 [DIRS 170037], Section 6.4.1).

Groundwater flow enters the SZ site-scale flow system primarily as underflow at the lateral boundaries of the model domain (BSC 2004 [DIRS 170037], Section 6.3.2). The conceptual model of recharge to the SZ includes distributed recharge, primarily in the northern part of the model domain, and focused recharge along the Fortymile Wash channel (BSC 2004 [DIRS 170037], Section 6.3.2). Recharge within the area of the SZ flow and transport abstraction model domain constitutes a small fraction of the entire groundwater budget of the site-scale flow system. Groundwater flow paths from beneath Yucca Mountain to the south are conceptualized to occur near the water table, due to the generally small amount of recharge in this area.

The conceptual model of the SZ flow system for future climatic conditions includes significant changes in the groundwater flow rates for potential wetter, cooler climate states. Increases in recharge at both the local and regional scales for monsoonal and glacial-transition climatic conditions would increase the specific discharge of groundwater in the SZ. Given the inferred climatic variations within the 10,000-year period of regulatory concern, the conceptual model of SZ flow includes higher groundwater fluxes for the future.

The conceptual model of radionuclide transport in the SZ includes the processes of advection, dispersion, matrix diffusion in fractured volcanic units, sorption, and colloid-facilitated transport (BSC 2004 [DIRS 170036], Section 6.3). In addition, radionuclides are subject to radioactive decay and ingrowth during migration in the SZ in the TSPA-LA analyses. These processes are illustrated in Figures 6-1 and 6-2.

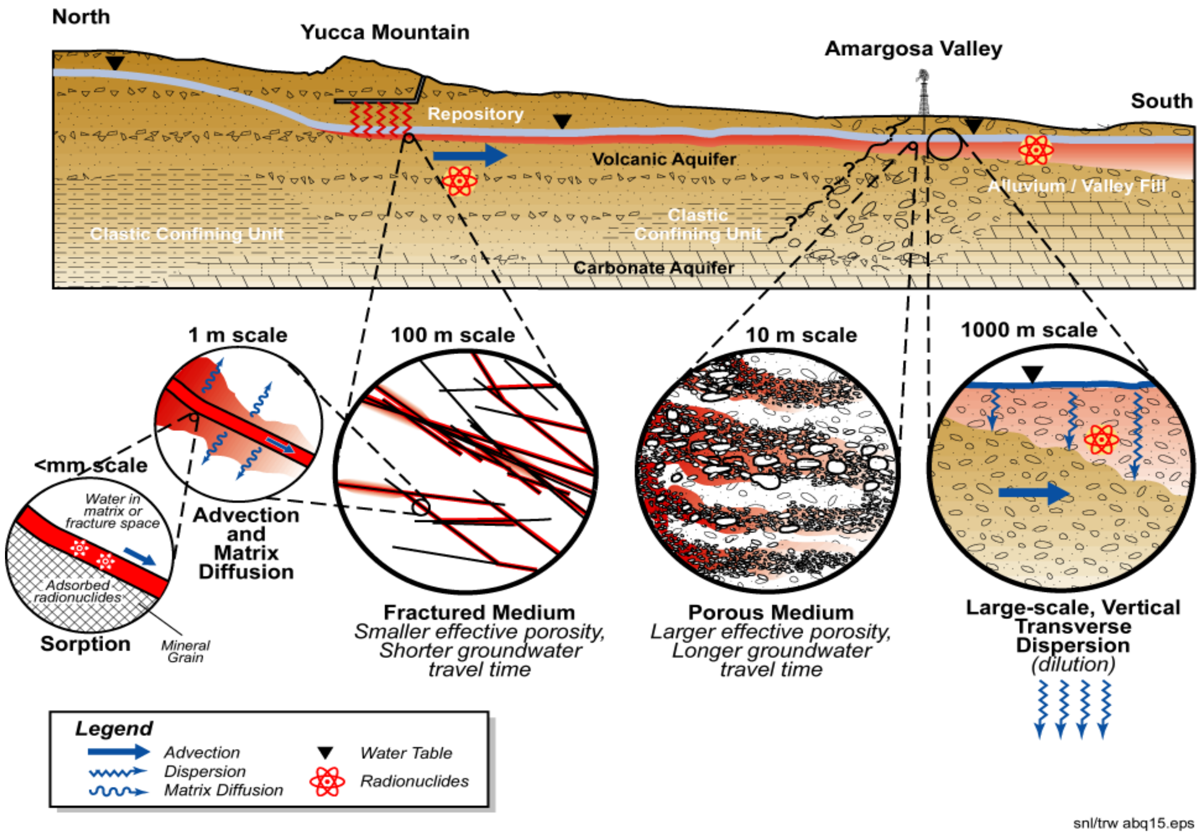

Figure 6-1. Illustration of the Conceptual Model of Radionuclide Transport Processes in the SZ

Groundwater advection is the primary mechanism to drive the migration of contaminants from the SZ beneath the repository to the accessible environment. Advective transport of radionuclides is conceptualized to occur primarily within the fracture network of the volcanic hydrogeologic units (BSC 2004 [DIRS 170036], Section 6.3) due to the very high contrast in permeability between the fractures and the rock matrix. The conceptual model of advection within the porous medium of the alluvium units envisions the flow of groundwater to be much more widely distributed, but excludes groundwater flow from zones or sedimentary facies of lower permeability material within the alluvium.

Dispersion of contaminant mass during transport in the SZ is conceptualized to occur because of hydrodynamic dispersion and molecular diffusion. Hydrodynamic dispersion is the result of variations in groundwater flow rates induced by heterogeneities within the aquifer, both in fractured and porous media. The conceptual model of hydrodynamic dispersion distinguishes between longitudinal dispersion, which occurs in the direction of groundwater flow, and transverse dispersion, which occurs perpendicular to the direction of groundwater flow. Longitudinal dispersion is typically much greater than transverse dispersion (see Section 6.5.2.9). Molecular diffusion also contributes to dispersion in radionuclide transport in the advective domain, but to a much lesser degree than hydrodynamic dispersion.

The dual-porosity conceptual model of matrix diffusion in fractured media describes the transfer of radionuclide mass from the flowing groundwater within the fractures to the relatively stagnant groundwater contained in the pores of the rock matrix. This mass transfer, either into or out of the rock matrix, occurs by molecular diffusion, which is driven by differences in the concentration of the contaminant in the fractures and matrix. The simplified conceptual model of the spatial distribution of groundwater-conducting fractures and matrix is a set of parallel, uniformly spaced fractures, separated by blocks of porous matrix (BSC 2004 [DIRS 170036], Section 6.4.2.4.1). This conceptual model considers that groundwater flow occurs only in the fractures and that the groundwater in the rock matrix has no advective groundwater movement. Although this aspect of the dual-porosity conceptual model is difficult to confirm, the contrast in permeability between the rock matrix and the fracture network in fractured tuff supports this approach. Groundwater flow is conceptualized to not necessarily occur in all fractures of the system, but is limited to those fractures that are interconnected in the through-going fracture network. The matrix diffusion process is controlled primarily by the effective diffusion coefficient in the rock matrix, the spacing between fractures carrying flowing groundwater, and the aperture of the fractures.

The conceptual model of matrix diffusion also recognizes the possibility of groundwater flow in fracture zones, in which numerous, closely spaced fractures can possibly transmit groundwater. Such fracture zones could exist along faults, which have experienced multiple episodes of displacement and potentially contain zones of rubblized bedrock. Diffusion of contaminants into the relatively small blocks of matrix within a fracture zone would be rapid in comparison to the matrix diffusion that would occur into the large blocks that exist between such zones. The contaminant storage capacity of the small blocks within such a fracture zone would be the total matrix porosity (and sorption capacity of mineral grains) of the blocks, corresponding to essentially complete matrix diffusion within the small matrix blocks.

The conceptual model of radionuclide sorption in the SZ is local equilibrium distribution of radionuclide mass between the aqueous phase and the mineral grains of the aquifer. This equilibrium distribution of contaminant mass is defined by the linear sorption coefficient relationship (BSC 2004 [DIRS 170036], Section 6.4.2.5). In fractured media, sorption is conceptualized to occur in the rock matrix; no sorption of solutes is conceptualized to occur on the fracture surfaces or coatings. Although sorption can possibly occur on fracture surfaces or coatings, there are no definitive measurements of this process. Discounting possible sorption on fracture surfaces in the conceptual model results in more rapid radionuclide migration in numerical simulations of transport in the SZ. In the porous media of the alluvium, sorption is conceptualized to occur in that portion of the aquifer corresponding to the effective porosity of the alluvium. In other words, sorption can occur in that part of the alluvium through which significant groundwater flow occurs; zones or layers of low permeability are effectively excluded from the sorption process.

In the conceptual model of colloid-facilitated transport radionuclide migration associated with colloids can occur by two modes (BSC 2004 [DIRS 170006], Section 6.3), as illustrated in Figure 6-2. In the first mode, radionuclides that are reversibly attached to colloids are in equilibrium with the aqueous phase and the aquifer material. In this mode of transport, the effective retardation of these radionuclides during transport in the SZ is dependent on the sorption coefficient of the radionuclide onto colloids, the concentration of colloids in the groundwater, and the sorption coefficient of the radionuclide onto the aquifer material. In the second mode, radionuclides that are irreversibly attached to colloids are transported at the same rate as the colloids. The colloids with the irreversibly attached radionuclides are themselves retarded by interaction (attachment and detachment) with the aquifer material. Specifically, the colloids undergo reversible filtration, which is represented by a retardation factor in the model. This conceptual model also recognizes that a small fraction of colloids with irreversibly attached radionuclides could be transported through the SZ with no retardation, due to kinetic effects of colloid attachment and detachment. This fast fraction of the colloids with irreversibly attached radionuclides is transported with no retardation in the SZ (similar to nonsorbing solutes), but without diffusion into the matrix of the volcanic units.

The conceptual model of radioactive decay in the SZ flow and transport abstraction model is that radionuclides experience a decrease in mass during transport time using the first-order decay constant for that radionuclide. Because the ingrowth of radionuclides is not explicitly included in the SZ flow and transport abstraction model, a simplified approach is used to account for this process for some of the radionuclides that have parent radionuclides. In this simplified approach, the mass of the decay product-radionuclide is boosted by the maximum mass of the parent radionuclide that would decay over the remaining TSPA-LA simulation time (BSC 2005 [DIRS 174227], Section 6.3.10). The boosting of the decay product-radionuclide mass occurs for the input to the SZ flow and transport abstraction model (i.e., at the UZ-SZ interface). The decay product-radionuclides that are boosted in this manner are ^{239}Pu (from ^{243}Am), ^{237}Np (from ^{241}Am), ^{236}U (from ^{240}Pu), ^{238}U (from ^{242}Pu), and ^{234}U (from ^{238}U and ^{238}Pu). It should be noted that the parent radionuclides of these boosted decay products are not diminished and that, consequently, this approach overestimates the mass of radionuclides being transported in the SZ. Transport of subsequent decay products in the four decay chains is explicitly simulated using the SZ 1-D transport model, as described in Section 6.3.2.

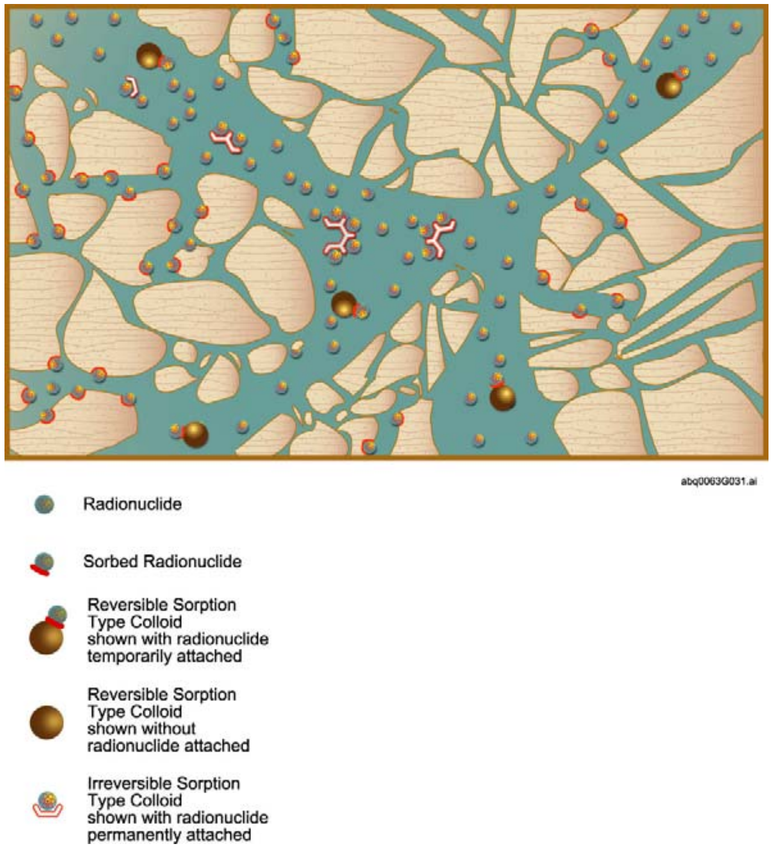

Figure 6-2. Illustration of the Conceptual Model of Colloid-Facilitated Radionuclide Transport in Fractured Tuff in the SZ

Homogeneous material properties are assigned to individual hydrogeologic units. The assumption of intra-unit homogeneity is justified primarily on the basis of scale in the SZ flow and transport abstraction model. The horizontal grid resolution of 500 m implies averaging of spatially variable properties over a very large volume. In addition, variations among realizations for stochastic parameters in the analysis encompass probable spatial variations in material properties within the model domain.

The groundwater flow conditions in the SZ system are also assumed to be in steady state. This approach is carried forward from the SZ site-scale flow model (BSC 2004 [DIRS 170037], Section 5). The site-scale SZ flow model is a steady-state model of the flow conditions, reflecting the conclusion that a steady-state representation of the SZ system is accurate. This conclusion is supported by the lack of consistent, large-magnitude variations in water levels observed in wells near Yucca Mountain (Luckey et al. 1996 [DIRS 100465], pp. 29 to 32). The convolution integral method has been extended to incorporate multiple steady-state flow conditions for future climate states in the TSPA-LA analyses.

The conceptual model of matrix diffusion in the fractured volcanic units of the SZ assumes groundwater flow in evenly spaced, parallel-walled fractures separated by impermeable matrix (BSC 2004 [DIRS 170036], Section 6.4.2.4). Although this dual-porosity conceptual model of radionuclide transport represents a significant simplification of the complex fracture network observed in fractured volcanic rocks at the site, it is an acceptable approximation at the scale of individual grid blocks in the SZ flow and transport abstraction model. Individual grid blocks in the transport model have horizontal dimensions of 500 m by 500 m, in comparison to a geometric mean flowing interval spacing of approximately 21 m. This comparison indicates that the grid blocks in the numerical model are more than an order of magnitude larger than the expected spacing between fracture zones that contain flowing groundwater. In addition, the relatively broad range of uncertainty in the flowing interval spacing used in this analysis encompasses the variability in spacing of the actual fracture network. Thus, the variability in flowing interval spacing among stochastic realizations in the TSPA-LA simulations captures the impact of variable spacing between fractures in an ensemble fashion.

For transport of radionuclides reversibly attached to colloids in the SZ, it is assumed that equilibrium conditions exist among radionuclides sorbed onto colloids, the aqueous phase concentration, and those sorbed onto the aquifer material. This approach is carried forward from the SZ site-scale transport model (BSC 2004 [DIRS 170036], Section 6.3) and is related to the general assumption regarding linear, equilibrium sorption presented in Section 5. This approach is consistent with laboratory observations of sorption onto colloids, particularly given the time scales of transport in the SZ. This modeling approach is appropriate, given the broad ranges of uncertainty applied to parameters underlying the simulated transport of radionuclides reversibly attached to colloids in the SZ.

Pumping of groundwater by the hypothetical community in which the RMEI resides is assumed not to alter significantly the groundwater pathways or radionuclide travel times in the SZ. Calibration of the SZ site-scale flow model is based on the present-day potentiometric surface observed in the model domain. Whereas the SZ site-scale model does not explicitly include the withdrawal of groundwater by pumping at the location of the hypothetical community in which the RMEI resides, the model does implicitly account for the drawdown of water levels associated with pumping at the southern boundary of the model domain. The values of specified head along the western part of the southern boundary reflect the lower water levels resulting from pumping in the Amargosa Farms region. Consequently, the model does implicitly include the influence of pumping in terms of increased hydraulic head gradients.

6.3.2 SZ 1-D Transport Model

Many components of the conceptual model for the SZ flow and transport abstraction model also apply to the SZ 1-D transport model. Representation of the groundwater flow processes in the 3-D SZ flow and transport abstraction model is simplified to 1-D streamtubes in the SZ 1-D transport model. However, characteristics of the conceptual model of groundwater flow in the SZ flow and transport abstraction model are implicitly included in the SZ 1-D transport model because the average values of groundwater flow rate used in the SZ 1-D transport model are extracted from the three dimensional (3-D) flow model. The conceptual model of aquifer properties has also been simplified in the SZ 1-D transport model, relative to the SZ flow and transport abstraction model. Material properties in the SZ 1-D transport model streamtubes are for average fractured tuff or for alluvium; no distinctions among volcanic hydrogeologic units are made.

The conceptual model of radionuclide transport in the SZ 1-D transport model includes the same processes of advection, dispersion, matrix diffusion in fractured volcanic units, sorption, and colloid-facilitated transport described in the previous section. The conceptualization of dispersion in the SZ 1-D transport model is simplified to the extent that transverse dispersion is precluded in the streamtube representation of the SZ system. The conceptual model of radionuclide decay in the SZ 1-D transport model includes both decay and ingrowth of radionuclides in decay chains.

The final radionuclide decay product in three of the radionuclide decay chains simulated in the 1-D radionuclide transport model is calculated to be in secular equilibrium with its parent radionuclide (see Section 6.5.1.2). This is a reasonable approach because it simplifies the analysis and the final decay product-radionuclides have relatively short half-lives (less than 25 years). This approach overestimates the concentration of decay products because it implies an instantaneous increase in the mass of the final decay product to be in equilibrium with the mass of parent radionuclide present.

The groundwater flux within each 1-D "pipe" segment used in the model is assumed to be constant along the length of the pipe. Each pipe segment used in the model consists of homogenous material properties, for which the radionuclide transport process is simulated. This constitutes a reasonable approach because the average groundwater flux along that portion of the radionuclide flow path is derived from the corresponding region of the 3-D SZ flow and transport abstraction model.

6.3.3 Interfaces with the UZ and the Biosphere

The source of radionuclides in the SZ flow and transport abstraction model is conceptualized to be a point source from the UZ transport model. The location of this source is treated as uncertain and constant for a given realization of the system. This conceptual model is consistent with a contaminant source to the SZ resulting from a single leaking waste package, focused groundwater flow in the UZ, or the human intrusion scenario in which a borehole intersects a waste package and extends to the water table (CRWMS M&O 2000 [DIRS 153246], Section 4.4).

The conceptual model of radionuclide releases from the SZ to the biosphere includes discharge of groundwater from wells to the hypothetical community in which the RMEI resides. The extent of the controlled area is specified in the regulations for the Yucca Mountain site (10 CFR 63.302 (10 CFR 63 [DIRS 173273])) and the location of the hypothetical community in which the RMEI resides is taken to be adjacent to the controlled area. In addition, the quantity of groundwater in the representative volume from which contaminated water is withdrawn by the RMEI is specified by the regulations to be 3,000 acre-ft/year (10 CFR 63.332 (10 CFR 63 [DIRS 173273])). The conceptualization of the SZ system is that the entire mass flux of radionuclides that crosses the regulatory boundary in the SZ would be contained in the representative volume of groundwater from which the RMEI obtains water and that these contaminants would be homogeneously distributed in the specified volume of groundwater.

The interface between radionuclide transport in the UZ and the SZ is assumed to be a point source near the water table. This approach is physically consistent with a single leaking waste package and highly focused transport of radionuclides in the UZ flow system, as can possibly occur early in the history of the repository. This approach is also consistent with the human intrusion scenario, in which a borehole penetrates a waste package and provides a direct pathway for radionuclide migration to the SZ. The approach of a point source for radionuclides in the SZ flow and transport simulations, while not physically realistic for the situation in which multiple, dispersed leaking waste packages exist, provides a generally conservative approximation of the source term to the SZ. This approximation results in less dispersion of the radionuclide transport times through the SZ and thus to less attenuation of peaks in radionuclide discharge. Although in situ concentrations of radionuclides are not utilized in the analysis of SZ flow and transport, a point source maximizes the simulated concentrations of radionuclides at the outlet to the accessible environment.

The location of the point source of radionuclides for transport in the SZ site-scale flow and transport model is assumed to be randomly located within the four source regions defined at the water table (Section 6.5.2.13). This approach implies that there are no consistent spatial patterns of waste package failure or delivery of radionuclides at the water table within each of the four source regions. Many of the processes that may lead to waste package failure are spatially random (e.g., manufacturing defects, seepage onto waste packages, etc.). The spatial pattern of preferential groundwater flow pathways in the UZ flow model is represented in a general sense by the locations of the four source regions (e.g., the southeastern source region corresponds to focused vertical groundwater flow along the Ghost Dance fault).

An assumption inherent to the convolution integral method is that the system being simulated exhibits a linear response to the input function. In the case of solute transport in the SZ system, this approach implies, for example, that a doubling of the input mass flux results in a doubling of the output mass flux. This approach is valid for the SZ flow and transport abstraction model because the underlying transport processes (e.g., advection and sorption) are all linear with respect to solute mass (BSC 2004 [DIRS 170036], Section 6.3). The processes of colloid filtration and sorption are both represented as equilibrium retardation processes. Simple retardation affects the timing of the release of radionuclides from the SZ, but still constitutes a linear relationship between mass input and mass output to the SZ.

It is assumed that all radionuclide mass crossing the regulatory boundary at approximately 18 km distance from the repository at the boundary of the controlled area (10 CFR 63.302 (10 CFR 63 [DIRS 173273])) in the SZ is contained in the representative volume of groundwater, which serves as a source of water to the RMEI, based on 10 CFR 63.332 (10 CFR 63 [DIRS 173273]). This approach implies that the representative volume of groundwater is large relative to the volumetric flow in the plume of contaminated groundwater in the SZ. This approach is justified on the basis of conservatism with respect to the analysis of repository performance. The total mass of radionuclides released to the biosphere for a given time period cannot be larger than the amount of radionuclide mass delivered by groundwater flow (for the nominal case).

6.4 CONSIDERATION OF ALTERNATIVE CONCEPTUAL MODELS

Two significant ACMs regarding groundwater flow and radionuclide transport in the SZ have been considered in this report. Both of these ACMs are encompassed in the range of uncertainty evaluated in the SZ flow and transport abstraction model and the SZ 1-D Transport model and are thus implicitly carried forward to the TSPA-LA modeling analyses. Consequently, these

ACMs need not be separately evaluated from the base case. Information on ACMs is summarized in Table 6-4. The ACMs are consistent with available data and current scientific knowledge and appropriately consider their results and limitations.

Table 6-4. ACMs Considered

ACM	Key Assumptions	Screening Assessment and Basis
Minimal Matrix Diffusion	Diffusion of radionuclides into the pore space of the rock matrix in the fractured volcanic units is extremely limited due to highly channelized groundwater flow, fracture coatings, or other factors.	This ACM is implicitly included in the SZ flow and transport abstraction model and in the SZ 1-D transport model through the range of uncertainty in key input parameters. The uncertain input parameters influencing matrix diffusion include effective diffusion coefficient (DCVO), flowing interval spacing (FISVO), and flowing interval porosity (FPVO).
Horizontal Anisotropy in Permeability	Alternative interpretations of pump test results in the fractured volcanic units indicate preferential permeability along structural features oriented in the NNE-SSW direction or in the WNW-ESE direction.	This ACM is implicitly included in the SZ flow and transport abstraction model and in the SZ 1-D transport model through the range of uncertainty in an input parameter. The uncertain input parameter influencing horizontal anisotropy in permeability in the volcanic units near Yucca Mountain is the ratio of N-S to E-W permeability (HAVO, see Section 6.5.2.10). This continuously distributed parameter varies from less than one to greater than one with most of the realizations greater than one.

ACM = alternative conceptual model; SZ = saturated zone

A sensitivity analysis using the SZ flow and transport abstraction model was conducted to show that the minimal matrix diffusion ACM is included within the range of parameter uncertainties considered. Figure 6-3 shows the solute mass breakthrough curves for a nonsorbing tracer, using the expected values of flow and transport parameters. The short-dashed line shows the simulated breakthrough curve for transport with no diffusion into the matrix of the fractured volcanic units, and the long-dashed line shows the breakthrough curve for maximum matrix diffusion. The solid line shows the simulated breakthrough curve using the 95th percentile value for flowing interval spacing (79.4 m) from the uncertainty distribution in this parameter. These results indicate that the breakthrough curve using the 95th percentile value of flowing interval spacing is very near the bounding case of no matrix diffusion. Similarly, low values of effective diffusion coefficient and low values of flowing interval porosity would produce breakthrough curves tending toward the no-matrix-diffusion case. This sensitivity analysis demonstrates that the minimal matrix diffusion ACM is captured within the range of uncertainty used in the model.

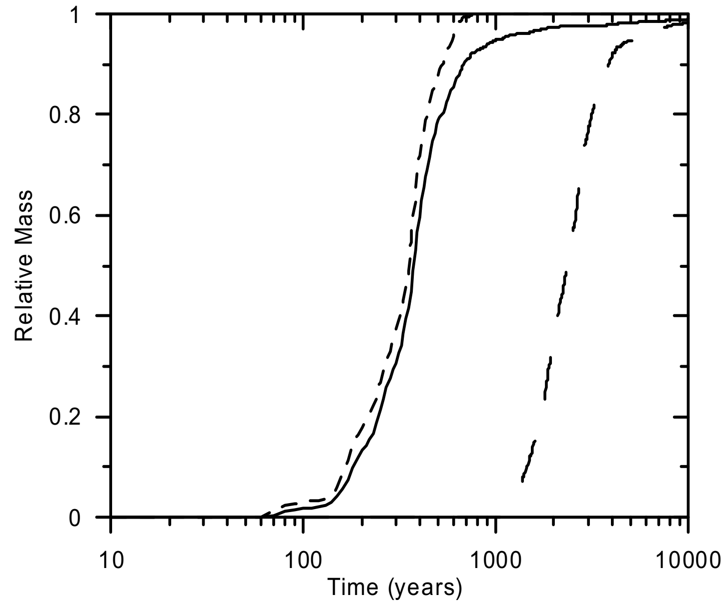

NOTE: The case of no matrix diffusion is shown with the short-dashed line. The case of maximum matrix diffusion is shown with the long-dashed line. The case for which flowing interval spacing is set to its 95th percentile value (79.4 m) is shown with the solid line. Mass breakthrough curves are for present climate and do not include radionuclide decay.

Figure 6-3. Mass Breakthrough Curves at 18-km Distance Showing Sensitivity to Matrix Diffusion for a Non-Sorbing Radionuclide

The incorporation of the horizontal anisotropy ACM into the SZ flow and transport abstraction model is inherent in the range of parameter values used for the parameter HAVO in the analyses. A complete discussion of uncertainty in horizontal anisotropy of permeability and the basis for the uncertainty distribution are provided in the *Saturated Zone In Situ Testing* scientific analysis report (BSC 2004 [DIRS 170010], Section 6.2.6). The uncertainty distribution for HAVO indicates that there is a 10 percent probability that the direction of maximum horizontal permeability is east-west with a ratio between 1 and 20. The uncertainty distribution also indicates that there is a 90 percent probability that the direction of maximum horizontal permeability is north-south with a ratio between 1 and 20. The isotropic case, corresponding to a horizontal permeability ratio of one, is included in this continuous uncertainty distribution for the parameter HAVO.

6.5 MODEL FORMULATION FOR BASE-CASE MODELS

<u>SZ Transport Abstraction Model</u>

The SZ site-scale flow model (BSC 2004 [DIRS 170037]) and the SZ site-scale transport model (BSC 2004 [DIRS 170036]) form the bases for the SZ flow and transport abstraction model. The progression in the development of models is from the SZ site-scale flow model to the SZ site-scale transport model to the SZ flow and transport abstraction model. The SZ site-scale flow model includes the implementation of the hydrogeologic framework, the numerical grid, and the boundary conditions for steady-state groundwater flow. The SZ site-scale flow model is calibrated to water-level measurements in wells and estimates of groundwater flow rates at the lateral boundaries. The SZ site-scale transport model begins with the SZ site-scale flow model and adds the model input files required for the simulation of radionuclide transport using the particle-tracking method. A set of representative parameter values for radionuclide transport is included in the SZ site-scale transport model and the range of behavior associated with parameter uncertainty is examined. Finally, the SZ flow and transport abstraction model begins with the SZ site-scale transport model and adds the capability to perform probabilistic uncertainty analyses using multiple Monte Carlo realizations of the SZ flow and transport system. The resulting radionuclide breakthrough curves are then used in the convolution integral method to couple the SZ flow and transport abstraction model with the TSPA-LA model.

The SZ site-scale flow model, the SZ site-scale transport model, and the SZ flow and transport abstraction model share a common model domain, hydrogeologic framework, numerical grid, and groundwater flow boundary conditions. The model domain is shown in Figure 6-4 with the blue dashed line overlain on a shaded relief map of the surface topography. The nodes that constitute the model grid form an orthogonal mesh with 500-m spacing in the north-south and east-west directions. The repository outline is shown with the bold blue line and the nodes that occur along the regulatory boundary of the accessible environment are shown as overlapping red crosses.

The groundwater flow boundary conditions for the SZ site-scale flow model, the SZ site-scale transport model, and the SZ flow and transport abstraction model are specified head at the lateral boundaries and specified groundwater flux for recharge at the upper boundary. These boundary conditions are described in detail in *Site-Scale Saturated Zone Flow Model* (BSC 2004 [DIRS 170037], Section 6.3.2) and are the same for all three models with the following exception: for the SZ flow and transport abstraction model, the specified flux for recharge is scaled in proportion to the uncertainty in groundwater specific discharge (see Section 6.5.2.1). Scaling the recharge flux and the values of permeability in proportion to the groundwater specific discharge uncertainty factor maintains the calibration of the flow model with regard to water-level measurements.

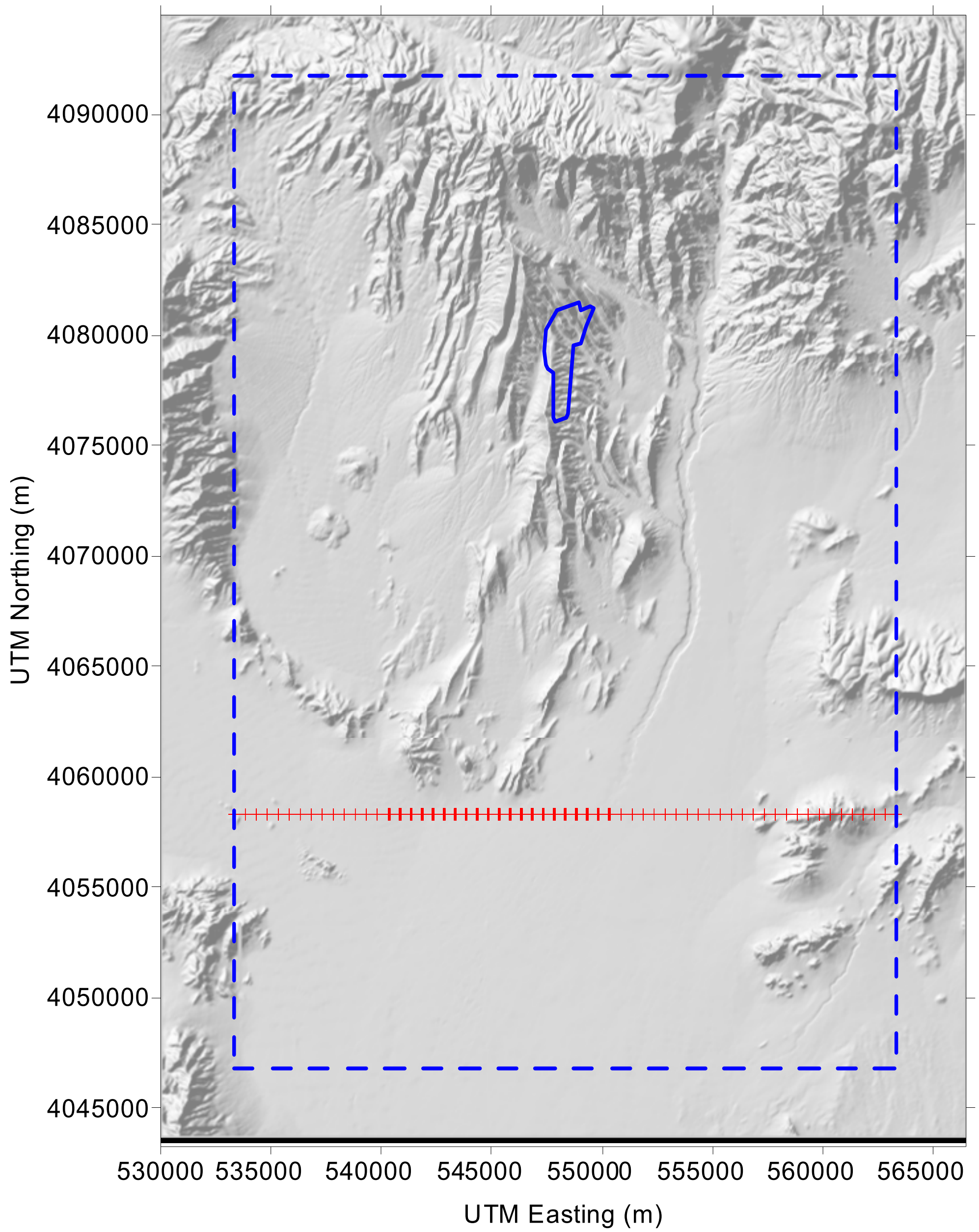

Source: Repository outline is from 800-IED-WIS0-00101-000-00B (BSC 2004 [DIRS 172801]).

NOTE: The dashed blue line indicates the boundaries of the SZ flow and transport abstraction model, the solid blue line shows the outline of the repository, and the red crosses indicate the latitude of the accessible environment (10 CFR 63.302 [DIRS 173273]) for radionuclide transport in the SZ.

Figure 6-4. Model Domain of the SZ Site-Scale Flow Model, SZ Site-Scale Transport Model, and the SZ Flow and Transport Abstraction Model

Radionuclide transport is simulated in the SZ flow and transport abstraction model using a particle tracking method. This method, as implemented by the FEHM (finite element heat and mass model) V2.20 software code (FEHM V2.20 STN: 10086-2.20-00 [DIRS 161725]), simulates advection along groundwater streamlines, random-walk dispersion, retardation due to sorption, and matrix diffusion. Each simulation uses 500 particles, which results in a continuous, generally smooth cumulative mass breakthrough curve at the boundary of the accessible environment. The time-step size that determines output intervals varies from 10 years to 100 years, depending on the radionuclide. Internally, the simulation uses local flow conditions to determine time steps for dispersion and matrix diffusion calculations. This internal time step is controlled such that the particles take approximately 20 internal time steps to traverse each cell in the model.

The convolution integral method used in the SZ flow and transport abstraction model for the TSPA-LA analyses provides an approximation of the transient radionuclide mass flux at a specific point downgradient in the SZ in response to the transient radionuclide mass flux from transport in the UZ. This coupling method makes full use of detailed SZ flow and transport simulations for a given realization of the system, without requiring complete numerical simulation of the SZ for the duration of each TSPA-LA realization. The two input functions to the convolution integral method are:

1. A unit radionuclide mass breakthrough curve in response to a step-function mass flux source as simulated by the SZ flow and transport abstraction model.

2. The radionuclide mass flux history as simulated for transport in the UZ. The output function is the radionuclide mass flux history downgradient in the SZ.

There are several important assumptions in the use of the convolution integral method. Groundwater flow in the SZ is assumed to be steady state. The transport processes in the SZ must be linear with respect to the solute source term (i.e., a doubling of the solute mass source results in a doubling of mass flux). In addition, the flow and transport processes in the UZ and the SZ must be independent of one another.

Radioactive decay is also applied to radionuclide mass flux calculated with the convolution integral computer code SZ_Convolute V3.0 software code (STN: 10207-3.0-00, SNL 2003 [DIRS 164180]) in the TSPA-LA analyses. The convolution integral method consists of numerical integration that accounts for the contributions to the outlet radionuclide mass flux from a series of time intervals. Because the travel time for each contribution to radionuclide mass flux is known, the loss of radionuclide mass (and consequent decrease in mass flux) during transport is calculated by first-order decay for that time interval.

The effects of climate change on radionuclide transport in the SZ are incorporated into the convolution integral analysis in the TSPA-LA by assuming instantaneous change from one steady-state flow condition to another steady-state condition in the SZ. A description of the mathematical and numerical implementation of multiple steady-state flow conditions is given in DOE 2003 [DIRS 167588], Equation 3. Changes in climate state are assumed to affect the magnitude of groundwater flux through the SZ system but have a negligible impact on flow paths. The effect of changes in groundwater flux is incorporated into the convolution method by scaling the timing of radionuclide mass breakthrough curves proportionally to the change in SZ-specific discharge.

For the base-case TSPA-LA analyses, present-day climatic conditions are modeled to occur from the time of repository closure and to be followed by monsoonal conditions and glacial-transition climatic conditions. The monsoonal climatic state is wetter than present-day conditions and the glacial-transition state is conceptualized to be wetter and cooler than present-day conditions (BSC 2004 [DIRS 170002], Section 6.6). Note that the glacial-transition climate state is approximately equivalent to the long-term average climate state, as referenced in *Total System Performance Assessment-Viability Assessment (TSPA-VA) Analyses Technical Basis Document* (CRWMS M&O 1998 [DIRS 100365], Table 8-16, p. T8-20).

Estimates of the scaling factors for groundwater flux in the SZ under alternative climatic conditions are based on simulations using the Death Valley regional groundwater flow model (D'Agnese et al., 1999 [DIRS 120425]; CRWMS M&O 1998 [DIRS 100365]) and on the infiltration for the site-scale UZ flow model (BSC 2004 [DIRS 169861], Section 6.1.4). Simulations using the Death Valley regional groundwater flow model were conducted for the past-climate state that likely existed about 21,000 years ago (D'Agnese et al., 1999 [DIRS 120425]). This climatic state approximately corresponds to the glacial-transition state, as defined for TSPA-LA calculations. A comparison of the groundwater flux in the SZ near Yucca Mountain under past-climate conditions (i.e., 21,000 years ago) using the Death Valley regional groundwater flow model indicates that the simulated flux under the past-climate conditions was approximately 3.9 times the flux of present-day simulations, as shown in Table 6-5.

Simulations of SZ flow under monsoonal climatic conditions have not been performed using the Death Valley regional groundwater flow model. Information on the increased infiltration through the site-scale UZ flow model is used as the basis for estimating flux increases in the SZ for monsoonal conditions (DTN: LB03023DSSCP9I.001 [DIRS 163044]) (see also *UZ Flow Models and Submodels* (BSC 2004 [DIRS 169861], Table 6.1-2)). Values of average infiltration in the model domain of the site-scale UZ flow model (second column of Table 6-5) are taken from the "GENER" card of the TOUGH2 input files "*preq_mA.dat*", "*glaq_mA.dat*", and "*monq_mA.dat*". This value of average infiltration is the mean groundwater flux at the upper boundary of the site-scale UZ flow model, as stated in the three input files named above. Similarly, the total infiltration through the site-scale UZ flow model for present and glacial-transition climatic conditions is calculated (DTN: LB03023DSSCP9I.001 [DIRS 163044]). Note in Table 6-5 that the ratio of glacial-transition infiltration in the UZ model to the present-day infiltration (a factor of 3.8) is approximately the same value as the estimate of increased SZ groundwater flux from the Death Valley regional groundwater flow model (i.e., 3.9). This correspondence suggests that the UZ infiltration ratio provides a reasonable estimate of the flux ratio for the SZ. Thus, the values of the SZ groundwater flux ratio for TSPA-LA simulations of future climatic states are derived from the estimates of increased UZ infiltration at Yucca Mountain. For monsoonal climatic conditions, the ratio of UZ infiltration to the infiltration for present-day conditions is 2.7 (see Table 6-5) and this value is applied to the SZ flux as well. The values of flux ratio used as scaling factors of SZ flow and transport for alternative climate states are given in the last column of Table 6-5.

Table 6-5. Groundwater Flow Scaling Factors for Climate Change

Climate State	Average Infiltration, UZ Model (Mean Case) (mm/year) [a]	Ratio to Present Climate, UZ Model	SZ Groundwater Flux Ratio from Death Valley Regional Groundwater Flow Model	SZ Groundwater Flux Ratio for TSPA-LA Simulations
Present-Day	4.43	1.0	1.0	1.0
Glacial-Transiti on	17.0	3.8	3.9 [b]	3.9
Monsoonal	11.8	2.7	N/A	2.7

[a] Source: DTN: LB03023DSSCP9I.001 [DIRS 163044].
[b] *Total System Performance Assessment-Viability Assessment (TSPA-VA) Analyses Technical Basis Document* (CRWMS M&O 1998 [DIRS 100365], Table 8-16, p. T8-20).

Output DTN: MO0506SPAINPUT.001

LA = license application; SZ = saturated zone; TSPA = total system performance assessment; UZ = unsaturated zone

Uncertainty exists in the groundwater flow scaling factors for climate change in the SZ. The uncertainty in groundwater flux estimates under alternative climatic conditions has not been explicitly evaluated with the Death Valley regional groundwater flow model, but lower and upper bounds of infiltration over the site-scale UZ flow model domain have been estimated for the present-day, monsoonal, and glacial-transition climatic conditions. These bounding estimates can be used as an indication of the uncertainty in groundwater flux in the SZ. These bounding estimates differ from the mean infiltration case by a factor of about 3.5 lower to about 2.4 higher for present-day conditions (BSC 2004 [DIRS 169861], Table 6.1-2). The bounding estimates for the glacial-transition climatic state span a greater overall uncertainty, differing from the mean infiltration case by a factor of about 7.2 lower to about 1.9 higher (BSC 2004 [DIRS 169861], Table 6.1-2). These ranges of uncertainty in the scaling factors for climate change in the SZ fall within the range of overall uncertainty in groundwater specific discharge, which varies from a factor of 30 lower to a factor of 10 higher than the expected value (Section 6.5.2.1). The uncertainty in the groundwater specific discharge multiplier (parameter GWSPD) is applied to all of the climate states in the simulations with the SZ flow and transport abstraction model. Consequently, uncertainty in the groundwater flow scaling factors for climate change in the SZ is implicitly contained within the range of uncertainty in the specific discharge multiplier.

SZ 1-D Transport Model

The SZ 1-D transport model is a simplified model of radionuclide transport for the purpose of simulating decay chains and is implemented with the GoldSim V7.50.100 software code in the TSPA-LA simulator as a series of "pipes." The same radionuclide transport processes that are simulated in the 3-D SZ flow and transport abstraction model (e.g., sorption, matrix diffusion in fractured units, and colloid-facilitated transport) are analyzed in the "pipe" segments, with the exception of transverse dispersion. Transverse dispersion is not very important to the modeling results, given the assumption that all radionuclide mass is captured by the wells of the receptor group. Although strict consistency between the SZ 1-D transport model and the 3-D SZ flow and transport abstraction model is not possible, average groundwater flow and transport characteristics of the SZ flow and transport abstraction model are used to define flow and transport properties within the “pipe” segments of the 1-D model. Average specific discharge along different segments of the flow path is estimated using the 3-D SZ flow and transport abstraction model. The resulting values of average specific discharge are applied to the individual “pipe” segments in the 1-D transport model.

6.5.1 Mathematical Description of Base-Case Conceptual Model

6.5.1.1 SZ Flow and Transport Abstraction Model

The mathematical descriptions of the processes of groundwater flow and radionuclide transport in the SZ site-scale flow model (BSC 2004 [DIRS 170037], Section 6.5) and the SZ site-scale transport model (BSC 2004 [DIRS 170036], Section 6.4.2) are presented in the corresponding reports for these models. The SZ site-scale flow model forms the direct basis for the SZ site-scale transport model, which forms the direct basis for the SZ flow and transport abstraction model. Therefore, the mathematical bases for those models, as implemented by the FEHM V2.20 software code [DIRS 161725], apply to the SZ flow and transport abstraction model and are not reproduced here.

The particle tracking method is used to simulate radionuclide transport in the SZ flow and transport abstraction model (see *Site-Scale Saturated Zone Transport* (BSC 2004 [DIRS 170036], Section 6.4.2) for a description of the particle tracking method). This method exhibits very limited numerical dispersion relative to standard finite-difference and finite-element methods of solute transport simulation. Consequently, particle tracking is appropriate for use in the SZ flow and transport abstraction model, in which the spatial discretization (500 m) exceeds the values of dispersivity being simulated for many of the model realizations.

<u>Convolution Integral</u>

The convolution integral method is used to couple the radionuclide transport in the UZ with the simulations of mass transport in the SZ in the TSPA-LA analyses. The convolution integral method takes the radionuclide mass breakthrough curve for a continuous, unitary mass source (step function input of mass) from the SZ and the time-varying radionuclide mass from the UZ as inputs. The output is the time-varying radionuclide mass exiting the SZ.

The mathematical expression for the convolution integral method is written as:

$$M_{sz}(t) = \int_0^t \dot{m}_{uz}(t-t') \frac{\overline{M}_{sz}(t')}{m_p} dt' \qquad \text{(Eq. 6-1)}$$

where

$M_{sz}(t)$ = radionuclide mass rate output downstream in the SZ [M/T]
t = time [T],
$\dot{m}_{UZ}(t)$ = time dependent radionuclide mass rate entering the SZ from the UZ [M/T]
t' = time lag [T]
$\overline{M}_{SZ}(t')$ = derivative of the downstream radionuclide mass-time response curve [M/T] to a step input of mass m_p [M]

Note that symbols in brackets are generalized dimensions with T denoting time and M denoting mass.

This expression is taken from the convolution integral for concentration (CRWMS M&O 1998 [DIRS 100365], p. 8-39) and rewritten in terms of radionuclide mass. A description of the mathematical implementation of multiple steady-state flow conditions for alternative climate states is given in DOE 2003 [DIRS 167588], Equation 3.

Correction of Retardation

The retardation factor for linear sorption of radionuclides during transport in porous media is defined (Freeze and Cherry 1979 [DIRS 101173], p. 404) as:

$$R_f = 1 + \frac{\rho_b}{\phi} K_d \qquad \text{(Eq. 6-2)}$$

where R_f is the retardation factor in the porous media [-] (the symbol - denotes a dimensionless parameter), ρ_b is the bulk density [M/L^3], ϕ is the porosity of the porous media [-], and K_d is the distribution coefficient [L^3/M]. The FEHM V2.20 software code [DIRS 161725] to be used in the SZ flow and transport abstraction model automatically calculates R_f based on input values of ρ_b, ϕ, and K_d.

Effective porosity (ϕ_e) [-] is a macroscopic parameter that helps account for discrete flow paths and channelized flow in the porous medium of the alluvium (see Section 6.5.2.3). The effective porosity is defined as the fraction of the total volume of the medium through which significant groundwater flow occurs. The effective porosity parameter in the alluvium is used to correctly calculate the pore velocity of groundwater. Effective porosity is not intended to be used to estimate surface areas in Equation 6-2. Therefore, it is necessary to adjust another parameter in the equation to compensate for the lower effective porosity that is entered. If this were not done, then the calculated values of R_f would be overestimated, given that values of K_d used in Equation 6-2 are based on laboratory-scale measurements. For the SZ flow and transport abstraction model and the SZ 1-D transport model, the K_d values for the alluvium are adjusted according to the following relationship (CRWMS M&O 1998 [DIRS 100365], Equation 8-4, p. 8-55):

$$K_d^{new} = K_d \cdot \frac{\phi_e}{\phi_T} \qquad \text{(Eq. 6-3)}$$

where K_d^{new} is the adjusted distribution coefficient [L^3/M] and ϕ_T is the total porosity [-]. The total porosity is 0.30, which is the upper bound of the effective porosity uncertainty distribution and also documented in Section 6.5.2.14.

Colloid-Facilitated Transport

For colloid-facilitated radionuclide transport in which radionuclides are reversibly attached to colloids, a partition coefficient is defined to represent the potential for enhanced migration of radionuclides in association with colloids. This unitless constant, K_c, is defined as:

$$K_c = K_d^{coll} C_{coll} \qquad \text{(Eq. 6-4)}$$

where K_d^{coll} is the sorption coefficient for the radionuclide onto colloids [L^3/M] and C_{coll} is the concentration of colloids in the groundwater [M/L^3]. The conceptual model of colloid-facilitated transport of reversibly sorbed radionuclides is described in Section 6.3, and the underlying theoretical derivation of the model is presented in *The Site-Scale Unsaturated Zone Transport Model of Yucca Mountain* (CRWMS M&O 1997 [DIRS 124052], pp. 8-32 to 8-36).

For equilibrium conditions in a porous medium, the effective sorptive capacity of the aquifer is reduced when the groundwater colloids carry a significant fraction of radionuclide mass in the system. The values of the sorption coefficient in the alluvium and undifferentiated valley fill hydrogeologic units for the colloid-facilitated transport of radionuclides with the K_c model are modified by the value of K_c, according to the relationship:

$$K_d^{adjusted} = \frac{K_d^{new}}{(1+K_c)} \qquad \text{(Eq. 6-5)}$$

as derived from Equation 6-2 and *Total System Performance Assessment-Viability Assessment (TSPA-VA) Analyses Technical Basis Document* (CRWMS M&O 1998 [DIRS 100365], Equation 8-8, pp. 8-54 and 8-56), and assigning the retardation factor for colloids with reversibly attached radionuclides a value of one. $K_d^{adjusted}$ is the adjusted distribution coefficient [L^3/M] to account for reversible sorption onto colloids.

For transport in fractured media, the effective diffusion coefficient into the rock matrix is reduced due to the affinity of radionuclides for sorption onto colloids in the fractures. To evaluate this effect with constant velocity and dispersion, consider the 1-D advection-dispersion equation for a solute in the fractures (BSC 2004 [DIRS 170036], Section 6.4.2) with a term for retardation and a final term added for diffusion into the matrix:

$$R_{f,f}\frac{\partial C}{\partial t} = D\frac{\partial^2 C}{\partial x^2} - v\frac{\partial C}{\partial x} - \frac{q}{b} \qquad \text{(Eq. 6-6)}$$

where $R_{f,f}$ is the retardation factor in the fractures [-], D is the dispersion coefficient in the fracture [L^2/T], C is aqueous concentration of the solute [M/L^3], t is time [T], x is distance [L], v is groundwater velocity in the fractures [L/T], q is the diffusive flux into the rock matrix

[M/L^{2}T], and b is the half-aperture of the fracture [L]. For that part of the solute mass that is sorbed onto colloids the advection-dispersion equation is:

$$R_{col}\ \frac{\partial C^{coll}}{\partial t} = D\frac{\partial^2 C^{coll}}{\partial x^2} - v\frac{\partial C^{coll}}{\partial x} \qquad \text{(Eq. 6-7)}$$

where R_{col} is the retardation factor of the colloids in the fractures [-] and C^{coll} is the concentration of the solute in the groundwater [M/L^3]. Adding the two advection dispersion equations and using the relationship that K_c = C^{coll}/C, the combined advection-dispersion equation for colloid-facilitated transport of radionuclides reversibly sorbed onto colloids can be written as:

$$\left(\frac{R_{f,f} + K_c R_{col}}{1 + K_c}\right)\frac{\partial C}{\partial t} = D\frac{\partial^2 C}{\partial x^2} - v\frac{\partial C}{\partial x} - \frac{q}{b(1 + K_c)} \qquad \text{(Eq. 6-8)}$$

As seen by comparing this equation with Equation 6-6, the term for diffusive mass flux into the rock matrix is modified by dividing by the factor (1 + K_c) to account for the equilibrium colloid-facilitated transport. One approach would be to adjust the value of fracture half-aperture by multiplying by the factor (1 + K_c). An alternative approach is possible based on examination of the ω term in the analytical solution for transport in fractures with matrix diffusion by Sudicky and Frind (1982 [DIRS 105043], Equation 34, p. 1638). In the ω term, adjusting the value of b by multiplying it by the factor (1 + K_c) is equivalent to dividing the effective diffusion coefficient in the matrix by the factor (1 + K_c)^2. In the SZ flow and transport abstraction model and the SZ 1-D transport model, the values of effective diffusion coefficient for radionuclides subject to the K_c model of colloid-facilitated transport are adjusted according to the relationship:

$$D_e^{adjusted} = \frac{D_e}{(1 + K_c)^2} \qquad \text{(Eq. 6-9)}$$

where $D_e^{adjusted}$ is the adjusted effective diffusion coefficient in the rock matrix [L^2/T], and D_e is the effective diffusion coefficient in the rock matrix [L^2/T]. It should be noted that this approach to adjusting the effective diffusion coefficient to account for colloid-facilitated transport in fractured media is not exact. The σ term of the Sudicky and Frind analytical solution also contains the variable b and the adjustment to the effective diffusion coefficient does not scale the variable b in the same manner as in the ω term. However, the variable b is a minor contributor in the expression for the σ term (i.e., value of b is much smaller than the value of B, which is the half fracture spacing). In addition, the adjusted diffusion coefficient, as applied in the σ term, is equivalent to increasing the value of B and a higher value of B underestimates the mass transfer to the matrix and overestimates the rate of migration of radionuclides through the SZ. The approach of adjusting the effective diffusion coefficient is thus an acceptable approximation for use in the SZ flow and transport simulations.

For colloid-facilitated radionuclide transport in which radionuclides are irreversibly attached to colloids, most of the colloids (and attached radionuclides) are delayed during transport in the SZ by a retardation factor. A small fraction of colloids with irreversibly attached radionuclides is subject to rapid transport without retardation, as described in *Saturated Zone Colloid Transport*

(BSC 2004 [DIRS 170006], Section 6.6). In fractured volcanic units, the retardation factor for the majority of colloids is applied directly in the SZ flow and transport abstraction model input files as an input parameter. In porous media, it is not possible to directly specify a retardation factor in the SZ flow and transport abstraction model; therefore, an effective sorption coefficient is specified that results in the sampled value of the retardation factor. In the porous medium of the alluvium, the colloid retardation factor in the alluvium units is converted to a value of effective sorption coefficient according to the relationship:

$$K_d^{eff} = \frac{(R_f - 1)\phi_e}{\rho_b} \qquad \text{(Eq. 6-10)}$$

where K_d^{eff} is the effective K_d in the porous media [L^3/M].

<u>Retardation in Fracture Zones</u>

As described in the conceptual model of transport in fractured media of the SZ (Section 6.3.1), relatively small blocks of rock matrix or rubblized material in fracture zones may participate in radionuclide transport via diffusion on a short time scale. The impact of rapid diffusion into small matrix blocks on the calculation of average linear velocity of groundwater is captured with a correspondingly larger value of flowing interval porosity for the volcanic units. In this conceptualization, the flowing interval porosity includes the fracture porosity with flowing groundwater plus it may include the matrix porosity of the small matrix blocks within the fracture zones. The possibility of small matrix blocks within fracture zones is encompassed within a range of uncertainty in transport behavior in fractured tuff. If this process of rapid diffusion occurs, the sorptive capacity of the small matrix blocks would also be important to the transport of sorbing radionuclides. This is handled in the following way: if the flowing interval porosity (ϕ_f) [-] is less than the average fracture porosity (ϕ_f^{avg}) [-], then groundwater flow is conceptualized to occur only in fractures, and no retardation due to sorption within small matrix blocks occurs. If the flowing interval porosity is greater than the average fracture porosity, then the portion of the flowing interval porosity in excess of the average fracture porosity corresponds to the matrix porosity of the small matrix blocks within the fracture zones. If the flowing interval porosity is greater than the average fracture porosity, then the retardation factor within the fracture domain due to sorption within small matrix blocks (R'_f) is calculated as:

$$R'_f = 1 + \frac{(fraction * \rho_b K_{dm})}{\phi_m} \qquad \text{(Eq. 6-11)}$$

where K_{dm} is the sorption coefficient in the rock matrix [L^3/M], ϕ_m is the rock matrix porosity [-], and *fraction* is calculated as:

$$fraction = \frac{(\phi_f - \phi_f^{avg})}{(\phi_m - \phi_f^{avg})} \qquad \text{(Eq. 6-12)}$$

The term *fraction* [-] describes the fraction of the entire rock matrix that is accessible to rapid matrix diffusion within the small matrix blocks of the fracture zone. Typically, the value of *fraction* would be small for the range of uncertainty in flowing interval porosity. For example, if the flowing interval porosity is 0.01 (80th percentile from Figure 6-13), the rock matrix porosity is 0.20, and the average fracture porosity is 0.001, then the value of *fraction* is 0.045. This means that 4.5 percent of the total rock matrix is available for direct interaction with radionuclide advection and sorption.

6.5.1.2 SZ 1-D Transport Model

The SZ 1-D transport model provides simulation results for several radionuclide chains that are not simulated in the SZ flow and transport abstraction model. The simplified decay chains considered (CRWMS M&O 2000 [DIRS 153246], Figure 3.5-5, p. F3-67) consist of the following.

1. Actinium series:

$$^{243}Am \rightarrow {}^{239}Pu \rightarrow {}^{235}U \rightarrow {}^{231}Pa$$

2. Neptunium Series:

$$^{241}Am \rightarrow {}^{237}Np \rightarrow {}^{233}U \rightarrow {}^{229}Th$$

3. Thorium Series:

$$^{240}Pu \rightarrow {}^{236}U \rightarrow {}^{232}Th$$

4. Uranium Series:

$$\left.\begin{matrix} ^{242}Pu \rightarrow {}^{238}U \\ ^{238}Pu \end{matrix}\right\} \rightarrow {}^{234}U \rightarrow {}^{230}Th \rightarrow {}^{226}Ra$$

The radionuclide decay chain analysis is simplified in a manner that overestimates the concentration of decay product-radionuclides by calculating secular equilibrium between the final decay products and their parents in three of these chains. ^{227}Ac is in secular equilibrium with ^{231}Pa in the actinium chain at the downstream end of the SZ analysis. Radium-228 is in secular equilibrium with ^{232}Th in the thorium series. ^{210}Lead is in secular equilibrium with ^{226}Ra in the uranium series. The mass of the final daughter in the neptunium series is explicitly simulated. In the model setup, radioisotopes of americium and plutonium are subject to transport as irreversibly attached to colloids; and radioisotopes of americium, plutonium, thorium, protactinium, and cesium are subject to the equilibrium colloid-facilitated transport mode. The 1-D model is set up using the Pathway Component of the Contaminant Transport Module in the GoldSim V7.50.100 Graphical Simulation Environment. The pipe component is able to simulate advection, longitudinal dispersion, retardation, decay and ingrowth, and matrix diffusion (Figure 6-5) (Miller and Kossik 1998 [DIRS 100449]).

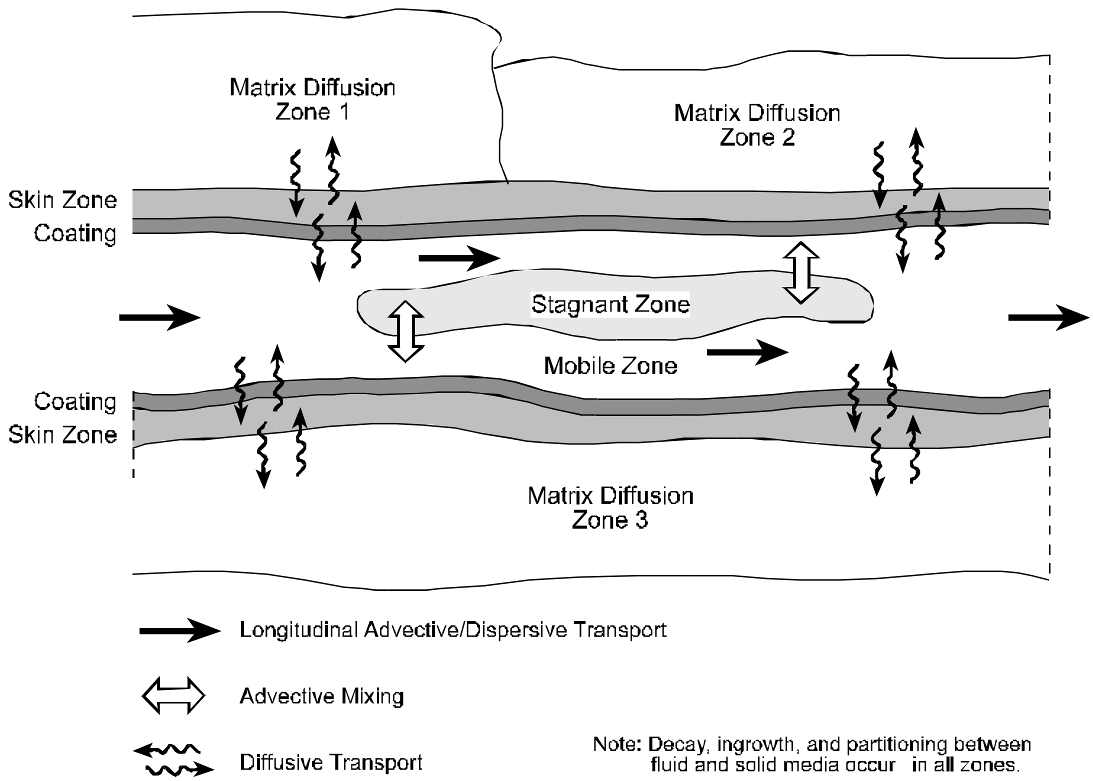

Sources: GoldSim V7.50.100; figure from Miller and Kossik 1998 [DIRS 100449].

Figure 6-5. Transport Processes Simulated in 1-D Pipe Pathways in the GoldSim V7.50.100 Software Code

Each pipe in the GoldSim V7.50.100 software code represents a 1-D mass transport model with uniform properties, as illustrated conceptually in Figure 6-5. The ratio of the volumetric outflow rate to the cross-sectional area of each pipe pathway represents the specific discharge in the pipe. A mass flux loading at the beginning of the first pipe is the source of the radionuclides that are transported along the connected pipes. The GoldSim V7.50.100 software code also provides a graphical "container" that isolates all of the model components in one compartment, to better organize the model components graphically on screen.

Transport from the four source regions in the SZ is represented by four sets of connected pipes in the SZ 1-D transport model. Each set of pipes consists of three pipe segments. The first segment extends from the center of the corresponding source region beneath the repository to a distance of 5 km. The second pipe segment extends from 5 km to the contact between the volcanic aquifer and the alluvium. The third pipe segment extends from the contact between the volcanic aquifer and the alluvium to the regulatory boundary with the accessible environment.

The input parameters used in GoldSim V7.50.100 to define flow properties in the pipe pathway are: pipe cross-sectional area, pipe perimeter, and volumetric flow in and out of the pipe.

The volumetric flow is specified first as outflow from the first pipe (pipe a) and it is held constant for each successive pipe. This is implemented in GoldSim V7.50.100 using parameter *Flow*. *Flow* is calculated as the product of the specific discharge in the first pipe (pipe a) and flow cross-sectional area, which is equal to 10^{FISVO}(FISVO is log-transformed) multiplied by unit thickness. Note that the flow cross-sectional area of the 1-D flow path consists of the fracture itself and associated matrix slabs on each side of the fracture. Because the specific discharge in the pathway applies to both fracture and matrix, the corresponding cross-sectional area consists of both fracture and matrix. Consequently, the cross-sectional area is equal to unit thickness multiplied by 10^{FISVO}.

The pipe cross-sectional area and perimeter are specified differently depending on whether the pipe represents the volcanics or the alluvium. The pipe representing volcanics is modeled as a fracture with the cross-sectional area equal to the product of the fracture aperture and the fracture thickness. Unit thickness is assumed for the fracture. The aperture is calculated as a product of the flowing interval spacing 10^{FISVO} and flowing interval porosity 10^{FPVO}(*FISVO* and *FPVO* are log-transformed). The fracture porosity, φ_p, is equal to one because fractures are assumed to have no filling medium. Two of three pipes along a pathway represent the volcanics in the SZ 1-D transport model. The cross-sectional areas of the first pipes are defined in the GoldSim V7.50.100 model using parameter *Volcanic_Fracture_Area_Pipe_a.* The cross-sectional area of the second pipe *(Volcanic_Fracture_Area_Pipe_b*) is calculated as the product of the cross-sectional area of the first pipe *(Volcanic_Fracture_Area_Pipe_a)* and the ratio of the specific discharge in the first and in the second pipes. This is done to maintain the same volumetric flow rate (specific discharge multiplied by cross-sectional area) through both pipes. The fracture perimeter (pipe a and pipe b) is 2 m because the fracture is assumed to have unit thickness and a single fracture within the pipe has two faces and thus a perimeter of 2 m (output [DTN: MO0506SPAINPUT.001]).

The pipe representing the alluvium, pipe c, consists of the porous medium and has cross-sectional area equal to the ratio of groundwater volumetric flow defined above by parameter *Flow* and the specific discharge in the pipe c. This is implemented in GoldSim V7.50.100 using parameter *SZ_Alluvium_Area*. The pipe perimeter is defined as the sum of all the pipe sides. This includes two unit thicknesses and two pipe widths. The pipe width is calculated as the pipe area (*SZ_Alluvium_Area)* divided by the unit thickness. The pipe perimeter is implemented in GoldSim V7.50.100 using the parameter *SZ_Alluvium_Perimeter*. The pipe perimeter in the alluvium is not used in the transport simulations because there is no matrix diffusion in the alluvium. The mathematical representation of radionuclide transport in the SZ 1-D transport model is the same as that in the SZ flow and transport abstraction model, as presented in Equation 6-2 to Equation 6-5 and Equation 6-9. There are some differences in the mathematical implementation between the models with regard to retardation in fractures, as described below.

In the GoldSim V7.50.100 SZ 1-D transport model, the retardation factor for colloids with irreversibly attached radionuclides in the volcanics cannot be specified directly. Rather, it is calculated internally as a function of system properties and the sorption coefficient on fracture coatings according to (GoldSim V7.50.100 [DIRS 161572]):

$$R_{m,s} = 1 + \frac{PT}{A_m \phi_p}(\rho_c K_{c,s} + \phi_c) \quad \text{(Eq. 6-13)}$$

where $R_{m,s}$ is the retardation factor due to the coating [-], P is the perimeter of the fracture pathway [L], T is the thickness of the coating (equal to 0.0001 m) [L], A_m is the cross-sectional area of the mobile zone (equal to the fracture cross-sectional area because there are no stagnant zones in the fracture) [L^2], ϕ_p is the porosity in the pipe (equal to 1.0 for fractures) [-], ρ_c is the dry bulk density of the coating material (assumed equal to the dry bulk density of the volcanic matrix) [M/L^3], $K_{c,s}$ is the sorption coefficient of the coating [L^3/M], and ϕ_c is the porosity of the coating material (equal to 0.01) [-]. Because $R_{m,s}$ is specified based on the known selection from CORVO ($R_{m,s} = 10^{CORVO}$), but is internally calculated in the GoldSim V7.50.100 software, the value of the sorption coefficient must be specified to ensure congruence. Specifically, $R_{m,s}$ is used to calculate $K_{c,s}$ after Equation 6-13 has been rearranged as:

$$K_{c,s} = \frac{1}{\rho_c}\left[\frac{A_m \phi_p}{PT}\left(R_{m,s} - 1\right) - \phi_c\right] \qquad \text{(Eq. 6-14)}$$

Substituting $R_{m,s}$ with its values calculated from the given selection from the uncertainty distribution yields the appropriate value for $K_{c,s}$ that must be supplied to the GoldSim V7.50.100 software to ensure that the proper retardation value is used in the SZ 1-D transport calculations. It should be noted that the parameters T and ϕ_c (Output DTN: MO0506SPAINPUT.001) are chosen to be realistic, but are essentially irrelevant because they are only used to calculate $K_{c,s}$, which the GoldSim V7.50.100 software requires to calculate $R_{m,s}$. These parameters, T and ϕ_c, are not used elsewhere.

The representation of retardation in the fractures using the coating option in the GoldSim V7.50.100 software code described above is for mathematical convenience only. This does not constitute an inconsistency in the conceptual model between the SZ 1-D transport model and the SZ flow and transport abstraction model.

The coating option in GoldSim V7.50.100 is also used to simulate the retardation of aqueous radionuclides due to rapid diffusion into matrix blocks and sorption in the matrix as described by Equation 6-11. Rapid diffusion is only assumed to occur for realizations in which the flowing interval porosity (10^{FPVO}) is greater than the expected value of 0.001. In this situation, the retardation of an aqueous radionuclide in the fracture is calculated using Equation 6-11. The corresponding $K_{c,s}$ is back calculated in the same way as described above using Equation 6-14. The only difference is that the value of $R_{m,s}$ in Equation 6-14 is equal to R_f', as defined by Equation 6-11. Thus, substituting $K_{c,s}$ in Equation 6-13 with the value calculated with Equation 6-14 results in $R_{m,s} = R_f'$. This is done because GoldSim V7.50.100 requires $K_{c,s}$ as an input and does not allow for inputting $R_{m,s}$.

The governing equation for the concentration of a species in a matrix diffusion zone of a pipe pathway is implemented in GoldSim V7.50.100 using available porosity of the porous medium in the matrix diffusion zone for this species. The available porosity in the matrix diffusion zone is defined as the product of the actual porosity in the matrix diffusion zone and the fraction representing the porosity of the matrix diffusion zone available to the species in consideration.

In the case of the aqueous radionuclides that are not subject to colloid-facilitated transport, the available porosity in the matrix diffusion zone is equal to the actual porosity. This is achieved by specifying the fraction of the available porosity being equal to one for these radionuclides.

In the SZ flow and transport abstraction model and the SZ 1-D transport model, there is no matrix diffusion in fractured media for colloids with irreversibly attached radionuclides. Consequently, there is no sorption in the matrix for radionuclides irreversibly attached onto colloids. This is simulated by specifying an arbitrarily small value of the available porosity fraction (approximately 10^{-10}) and zero sorption coefficients for these species in the volcanic matrix. Available porosity fraction is the GoldSim V7.50.100 input parameter and must be greater than zero. It is defined arbitrarily small even though no sorption in the matrix is achieved by specifying zero sorption coefficients.

The fraction of the porosity available to each radionuclide reversibly attached onto colloids (americium, cesium, and plutonium) is calculated in the same way as the adjusted sorption coefficient in Equation 6-5 by substituting K_d with the actual matrix porosity, substituting $K_d^{adjusted}$ with the available matrix porosity, and by defining the available porosity fraction as the ratio of available matrix porosity to actual matrix porosity. This fraction is implemented in the SZ 1-D transport model using parameters *Volc_Porosity_Avail_Am* for Am, *Volc_Porosity_Avail_Cs* for Cs, and *Volc_Porosity_Avail_Pu for Pu*.

GoldSim V7.50.100 allows up to three matrix diffusion zones to be specified in addition to the "skin" zone. As shown in Figure 6-5, the three matrix zones exist in parallel and the skin zone is located in front of all matrix diffusion zones. Only the skin option is used in the SZ 1-D transport model and it represents the matrix diffusion zone in volcanic units. The outer boundary condition for the matrix diffusion zone in this case is defined at a distance equal to the skin thickness, which represents the distance from the pipe surface to the outer boundary of the skin. Skin thickness specified in the base SZ 1-D transport model, using parameter *Volcanic_Matrix_Skin_Thickness,* is equal to flowing interval spacing (10^{FISVO}) divided by 4. The thickness of the skin was decreased based on a comparison of 1-D and 3-D models. Thick skin (1/2 of the flowing interval spacing) resulted in concentrations less than those obtained with the 3-D model due to greater radionuclide masses diffused into the skin. A skin thickness equal to 1/4 of the flowing interval spacing yields a significantly better match for the validation test cases defined in Section 7.1. Corrections to this approach and the impacts on the results of the SZ 1-D transport model are described in Section 7.5.

The matrix diffusion coefficient for those radionuclides that do experience matrix diffusion is implemented by calculating an effective tortuosity, based on the sampled value of effective diffusion coefficient and the free water diffusion coefficient. The free water diffusion coefficient is adjusted by a factor approximately equivalent to the volcanic matrix porosity, using the parameter "Adjusted_Diffusion_Free" to match results from the 3-D SZ site-scale transport model.

Values of specific discharge for segments represented by pipe pathways in the SZ 1-D transport model vary along the flow path from the repository. A plot of the particle paths in the SZ flow and transport abstraction model indicates that the flow path length through the alluvium varies, depending on uncertainty in the SZ flow field (see Figure 6-6). This uncertainty is represented by variation in the geometry of the alluvial uncertainty zone in the SZ flow and transport abstraction model. Specifically, the lengths of the flow paths in the volcanic units and the alluvium are functions of the western boundary of the alluvial uncertainty zone (as controlled by the FPLAW stochastic parameter). Secondarily, this variability is the result of different flow paths (i.e., width of the plume). The lengths of the flow paths are also functions of the anisotropy ratio in horizontal permeability of the volcanic units (as controlled by the HAVO stochastic parameter) (see Figure 6-6). In the 1-D radionuclide transport model, the length of the alluvium (out to an 18-km distance) is varied from 2 km to 10 km as functions of the FPLAW and HAVO parameter values and the source region beneath the repository (see Table 6-7 and supporting text).

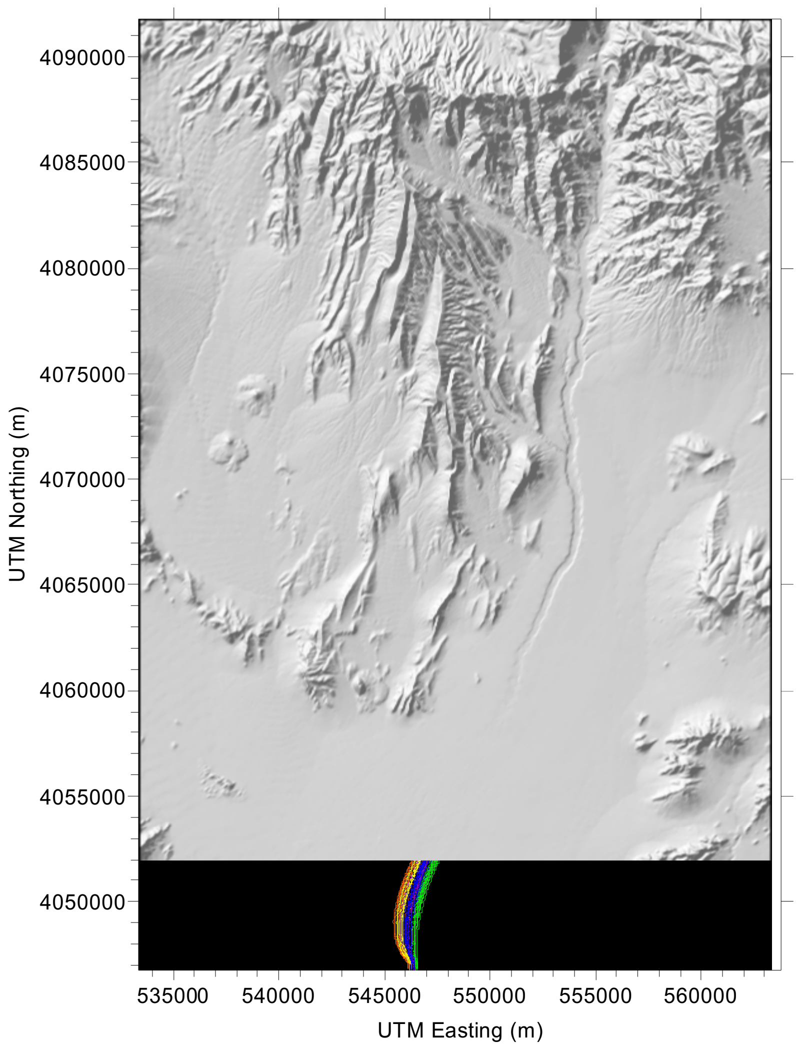

Source: Repository outline is from 800-IED- WIS0-00101-000-00B (BSC 2004 [DIRS 172801]).

NOTE: Green lines, purple lines, blue lines, yellow lines, and red lines show simulated particle paths for horizontal anisotropy values of 0.05, 0.20, 1.0, 5.0, and 20.0, respectively.

Figure 6-6. Simulated Particle Paths for Different Values of Horizontal Anisotropy in Permeability

The SZ 1-D transport model represents a significant simplification of the 3-D groundwater flow system, relative to the SZ flow and transport abstraction model. To accurately capture the 3-D characteristics of the SZ flow and transport system in this 1-D model, the SZ 1-D transport model is divided into three sets of "pipe" segments. The lengths and groundwater flow rates of these "pipe" segments are estimated from the SZ flow and transport abstraction model.

Average specific discharge along different segments of the flow path is estimated using the SZ flow and transport abstraction model in the following way: 1,000 particles are released from a point beneath the repository (as shown in Figure 6-6) in the simulation, matrix diffusion is not used, and all porosities are assigned a value of 1.0 for the assessment of average specific discharge. The average specific discharge is calculated by dividing the flow path length by the 50th percentile of travel times among the particles, for that flow path segment. The average specific discharge also varies as a function of the horizontal anisotropy (parameter HAVO). The resulting values of average specific discharge, as used in the SZ 1-D transport model, are shown in Table 6-6. The values in Table 6-6 are input as a GoldSim V7.50.100 software code look-up table in the SZ 1-D transport model. Note that the values of specific discharge scale linearly with the groundwater specific discharge-scaling factor (parameter GWSPD) for the consideration of uncertainty in specific discharge. The values of specific discharge within the three pipe segments are calculated within the model by interpolating between the values of HAVO and scaling by the value of GWSPD. The volumetric flow rate is the same for all segments in the SZ 1-D transport model, and the variations in specific discharge along the flow path are incorporated by varying the cross-sectional areas of the pipe segments.

Table 6-6. Average Specific Discharge in Flow Path Segments

HAVO	Average Specific Discharge (m/year)		
	0-5 km	5-13 km	13-18 km
0.05	0.312	7.50	1.936
1.00	0.536	1.824	2.357
5.00	0.722	2.694	2.793
20.00	0.870	4.465	3.183

Output DTN: MO0506SPAINPUT.001

The impacts of different climate states are implemented in the SZ 1-D transport model in a manner similar to the SZ flow and transport abstraction model. The specific discharge within all pipe segments of the SZ 1-D transport model is scaled by the groundwater flow factors given in Table 6-5 for the monsoonal and glacial-transition climate states. Application of this scaling begins at the time of climate change. However, an important limitation of the Laplace transform solution used for radionuclide transport simulation within the pipe segments in the SZ 1-D transport model should be noted. Radionuclide mass already within a given pipe segment of the SZ 1-D transport model does not increase in velocity in response to increased specific discharge resulting from climate change. Radionuclide mass introduced after the change in specific discharge is transported at the proper, correspondingly faster rate. The impacts of this limitation to calculations of peak dose in the TSPA-LA model are not large due to the following considerations: the SZ 1-D transport model results are used only for the daughter products of the decay chains in the TSPA-LA calculations and these daughter products are only minor contributors to total simulated dose. This limitation applies only to radionuclide mass that enters a given pipe segment prior to 2,000 years, after which glacial-transition climatic conditions continue unchanged. In addition, only radionuclide mass that enters the SZ 1-D transport model prior to 600 years, at the time of change from present to monsoonal conditions, would experience this limitation to a large extent. Finally, this limitation applies only to an individual pipe segment, and the entire SZ 1-D transport model is composed of three pipe segments. This computational limitation thus applies only to a part of the total transport pathway in the SZ for any given unit of radionuclide mass.

The flow path length of each pipe segment in the SZ 1-D transport model varies as a function of FPLAW, HAVO, and the source region from which the radionuclide source originates beneath the repository. The first pipe segment is 5 km in length for all cases [DTN: MO0506SPAINPUT.001]. The second pipe segment represents that portion of the flow path from the 5-km distance to the contact between the volcanic units and the alluvium in the SZ. The third pipe segment represents the portion of the flow path from the contact between the volcanic units and the alluvium out to the regulatory boundary to the accessible environment. The lengths of the second and third pipe segments were estimated from the particle tracking results of the 3-D SZ flow and transport abstraction model, as shown in Figure 6-6 and as summarized in Table 6-7. The estimated pipe segment lengths are shown in Table 6-7 for differing values of HAVO and for the four source regions. Each entry in the table contains a range of values in length, where the minimum value shown for the 5-to-13-km pipe segment (second pipe segment) corresponds to FPLAW equal to 1.0 and the maximum value corresponds to FPLAW equal to 0.0. By contrast, the minimum value of length for the 13- to 18-km-pipe segment (third pipe segment) corresponds to FPLAW equal to 0.0 and the maximum value corresponds to FPLAW equal to 1.0. In other words, the maximum length of the flow path in the alluvium corresponds to the maximum westerly extent of the alluvium uncertainty zone, and the minimum length of the flow path in the alluvium corresponds to the minimum westerly extent of the alluvium uncertainty zone. The values in Table 6-7 are input as a GoldSim V7.50.100 software code look-up table in the SZ 1-D transport model.

Table 6-7. Flow Path Lengths of Pipe Segments

	Minimum and Maximum Flow Path Lengths of Pipe Segments (km)							
	Source Region 1		Source Region 2		Source Region 3		Source Region 4	
HAVO	5 – 13 km	13 – 18 km	5 – 13 km	13 – 18 km	5 – 13 km	13 – 18 km	5 – 13 km	13 – 18 km
0.05	12.0 – 14.5	7.5 – 10.0	12.0 – 14.0	7.0 – 9.0	13.0 – 16.0	3.0 – 6.0	12.5 – 15.0	3.5 – 6.0
1.00	12.0 – 14.0	5.5 – 7.5	12.0 – 14.5	4.5 – 7.0	10.0 – 13.5	2.0 – 5.5	10.0 – 12.0	3.0 – 5.0
5.00	12.5 – 14.5	3.0 – 5.0	11.5 – 14.0	3.0 – 5.5	10.5 – 14.0	1.0 – 4.5	10.5 – 12.5	2.0 – 4.0
20.00	12.5 – 14.5	2.5 – 4.5	11.5 – 14.0	3.0 – 5.5	10.5 – 14.0	1.0 – 4.5	10.5 – 12.5	2.0 – 4.0

HAVO = horizontal anisotropy

Output DTN: MO0506SPAINPUT.001

The SZ 1-D transport model is not strictly consistent with the 3-D SZ flow and transport abstraction model for several reasons. Average, homogeneous material properties are specified within each pipe segment of the SZ 1-D transport model, whereas material properties are specified on a node-by-node basis in the SZ flow and transport abstraction model. The specified value of groundwater specific discharge is constant within each pipe segment of the SZ 1-D transport model, whereas simulated specific discharge is continuously variable within the SZ flow and transport abstraction model. In addition, transverse dispersion leads to divergence of flow paths and variations in flow path lengths in the SZ flow and transport abstraction model, which is not possible with the pipe segment representation in the SZ 1-D transport model. Model validation activities for the SZ 1-D transport model (Section 7) indicate acceptable agreement with the SZ site-scale transport model in spite of the inconsistencies discussed above. Although differences in transport simulation results between the SZ 1-D transport model and the 3-D SZ flow and transport abstraction model exist for a given realization, the average results are similar (Section 7.3.2). The adequacy of the SZ 1-D transport model for its intended purpose is also supported by the fact that it is used only to simulate the ingrowth of decay products, which are not anticipated to be major contributors to total radiological dose. Estimates of concentrations of some decay products are used for comparison to groundwater protection standards (10 CFR 63 [DIRS 173273], Section 63.331).

6.5.2 Base-Case Model Inputs

The SZ flow and transport abstraction model and the SZ 1-D transport model include uncertainty through stochastic simulations of uncertain parameters. Parameter uncertainties are quantified through uncertainty distributions, which numerically represent our state of knowledge about a particular parameter on a scale of the model domain. The uncertainty distribution (either cumulative distribution function (CDF) or probability density function (PDF)) of a parameter, represents what is known and what is unknown about the parameter, and reflects the current knowledge of the range and likelihood of the appropriate parameter values when used in these models (BSC 2002 [DIRS 158794], p. 45). The uncertainty distributions incorporate uncertainties associated with field or laboratory data, knowledge of how the parameter will be used in the model, and theoretical considerations. Geologic uncertainty is incorporated with regard to the location of the contact between the tuff and alluvium at the water table (see Section 6.5.2.2). In some cases, parameters are assigned constant values because radionuclide transport is relatively insensitive to the parameter, or the uncertainty is relatively small. Constant parameters are defined to vary from one hydrogeologic unit to another, but for a given hydrogeologic unit, the parameter remains constant for all realizations. The development and justification for the parameter uncertainty distributions are discussed below. See Table 6-8 for a comprehensive list of the models/analyses inputs used in the SZ flow and transport abstraction model and the SZ 1-D transport model. The unit numbers given in Table 6-8 are defined by hydrogeologic unit in Table 6-9. Please note that parameter values are developed for the 19 hydrogeologic units in Table 6-9 for completeness; however, 18 units are included in the SZ site-scale flow model, the SZ site-scale transport model, and the SZ flow and transport abstraction model. The valley-fill confining unit has a very small volume relative to other units in the model domain, and there are no occurrences of this unit along the flow path from the repository. Consequently, it is not included in the models as a separate unit.

Table 6-8. Models/Analyses Inputs Used in the SZ Flow and Transport Abstraction Model and the SZ 1-D Transport Model

Input Name	Input Description	Input Source (DTN, if applicable)	Value or Distribution	Units	Type of Uncertainty
KDNPVO	Neptunium sorption coefficient in volcanic units	LA0310AM831341.002 [DIRS 165891]	CDF: Probability Value 0.0 0.0 0.05 0.99 0.90 1.83 1.0 6.0	mL/g	Epistemic
KDNPAL	Neptunium sorption coefficient in alluvium	LA0310AM831341.002 [DIRS 165891]	CDF: Probability Value 0.0 1.8 0.05 4.0 0.95 8.7 1.0 13.0	mL/g	Epistemic
KDSRVO	Strontium sorption coefficient in volcanic units	LA0310AM831341.002 [DIRS 165891]	Uniform: Minimum 20. Maximum 400.	mL/g	Epistemic
KDSRAL	Strontium sorption coefficient in alluvium	LA0310AM831341.002 [DIRS 165891]	Uniform: Minimum 20. Maximum 400.	mL/g	Epistemic
KDUVO	Uranium sorption coefficient in volcanic units	LA0310AM831341.002 [DIRS 165891]	CDF: Probability Value 0.0 0.0 0.05 5.39 0.95 8.16 1.0 20.0	mL/g	Epistemic
KDUAL	Uranium sorption coefficient in alluvium	LA0310AM831341.002 [DIRS 165891]	CDF: Probability Value 0.0 1.7 0.05 2.9 0.95 6.3 1.0 8.9	mL/g	Epistemic
KDRAVO	Radium sorption coefficient in volcanic units	LA0310AM831341.002 [DIRS 165891]	Uniform: Minimum 100. Maximum 1000.	mL/g	Epistemic
KDRAAL	Radium sorption coefficient in alluvium	LA0310AM831341.002 [DIRS 165891]	Uniform: Minimum 100. Maximum 1000.	mL/g	Epistemic
KD_Pu_Vo	Plutonium sorption coefficient in volcanic units	LA0310AM831341.002 [DIRS 165891]	CDF: Probability Value 0. 10. 0.25 89.9 0.95 129.87 1.0 300.	mL/g	Epistemic

Table 6-8. Models/Analyses Inputs Used in the SZ Flow and Transport Abstraction Model and the SZ 1-D Transport Model (Continued)

Input Name	Input Description	Input Source (DTN, if applicable)	Value or Distribution	Units	Type of Uncertainty
KD_Pu_Al	Plutonium sorption coefficient in alluvium	LA0310AM831341.002 [DIRS 165891]	Beta: Mean 100. Standard Deviation 15. Minimum 50. Maximum 300.	mL/g	Epistemic
KD_Am_Vo	Americium sorption coefficient in volcanic units	LA0310AM831341.002 [DIRS 165891]	Truncated Normal: Mean 5500. Standard Deviation 1500. Minimum 1000. Maximum 10000.	mL/g	Epistemic
KD_Am_Al	Americium sorption coefficient in alluvium	LA0310AM831341.002 [DIRS 165891]	Truncated Normal: Mean 5500. Standard Deviation 1500. Minimum 1000. Maximum 10000.	mL/g	Epistemic
KD_Cs_Vo	Cesium sorption coefficient in volcanic units	LA0310AM831341.002 [DIRS 165891]	CDF: Probability Value 0.0 100. 0.05 3000.59 1.0 6782.92	mL/g	Epistemic
KD_Cs_Al	Cesium sorption coefficient in alluvium	LA0310AM831341.002 [DIRS 165891]	Truncated Normal: Mean 728. Standard Deviation 464. Minimum 100. Maximum 1000.	mL/g	Epistemic
FISVO	Flowing interval spacing in volcanic units	SN9907T0571599.001 [DIRS 122261]	CDF : (Log_{10}-transformed) Probability Value 0.0 0.087 0.05 0.588 0.25 1.00 0.50 1.29 0.75 1.58 0.95 1.90 1.0 2.62	m	Epistemic
CORAL	Colloid retardation factor in alluvium	LA0303HV831352.004 [DIRS 163559]	CDF : (Log_{10}-transformed) Probability Value 0.0 0.903 0.331 0.904 0.50 1.531 1.0 3.715	N/A	Epistemic

Table 6-8. Models/Analyses Inputs Used in the SZ Flow and Transport Abstraction Model and the SZ 1-D Transport Model (Continued)

Input Name	Input Description	Input Source (DTN, if applicable)	Value or Distribution	Units	Type of Uncertainty
CORVO	Colloid retardation factor in volcanic units	LA0303HV831352.002 [DIRS 163558]	CDF : (Log_{10}-transformed) Probability Value 0.0 0.778 0.15 0.779 0.25 1.010 0.50 1.415 0.80 1.778 1.0 2.903	N/A	Epistemic
HAVO	Ratio of horizontal anisotropy in permeability	SN0302T0502203.001 [DIRS 163563]	CDF: Probability Value 0.0 0.05 0.0042 0.2 0.0168 0.4 0.0379 0.6 0.0674 0.8 0.10 1.0 0.60 5. 0.744 8. 0.856 11. 0.936 14. 0.984 17. 1.0 20.	N/A	Epistemic
LDISP	Longitudinal dispersivity	MO0003SZFWTEEP.000 [DIRS 148744]	Truncated Normal: (Log_{10}-transformed) Mean 2.0 Standard Deviation 0.75	m	Epistemic
Kd_Pu_Col	Plutonium sorption coefficient onto colloids	SN0306T0504103.006 [DIRS 164131]	CDF: Probability Value 0.0 1.e3 0.04 5.e3 0.12 1.e4 0.37 5.e4 0.57 1.e5 0.92 5.e5 1.0 1.e6	mL/g	Epistemic
Kd_Am_Col	Americium sorption coefficient onto colloids	SN0306T0504103.006 [DIRS 164131]	CDF: Probability Value 0.0 1.e4 0.07 5.e4 0.17 1.e5 0.40 5.e5 0.60 1.e6 0.92 5.e6 1.0 1.e7	mL/g	Epistemic

Table 6-8. Models/Analyses Inputs Used in the SZ Flow and Transport Abstraction Model and the SZ 1-D Transport Model (Continued)

Input Name	Input Description	Input Source (DTN, if applicable)	Value or Distribution	Units	Type of Uncertainty
Kd_Cs_Col	Cesium sorption coefficient onto colloids	SN0306T0504103.006 [DIRS 164131]	CDF: Probability / Value 0.0 / 1.e2 0.2 / 5.e2 0.45 / 1.e3 0.95 / 5.e3 1.0 / 1.e4	mL/g	Epistemic
Conc_Col	Groundwater concentration of colloids	SN0306T0504103.005 [DIRS 164132]	CDF : (Log_{10}-transformed) Probability / Value 0.0 / -9.0 0.50 / -7.0 0.75 / -6.0 0.90 / -5.0 0.98 / -4.3 1.0 / -3.7	g/mL	Epistemic
R_U_Kd	Correlation coefficient for U K_d in volcanic units and alluvium	LA0310AM831341.002 [DIRS 165891]	0.75	N/A	N/A
R_Np_Kd	Correlation coefficient for Np K_d in volcanic units and alluvium	LA0310AM831341.002 [DIRS 165891]	0.75	N/A	N/A
R_Pu_Kd	Correlation coefficient for Pu K_d in volcanic units and alluvium	LA0310AM831341.002 [DIRS 165891]	0.50	N/A	N/A
R_U_Np	Correlation coefficient for U K_d and Np K_d	LA0310AM831341.002 [DIRS 165891]	0.50	N/A	N/A
FPLAW	Western boundary of alluvial uncertainty zone	Internal to this report	Uniform: Minimum 0.0 Maximum 1.0	N/A	Epistemic
FPLAN	Northern boundary of alluvial uncertainty zone	Internal to this report	Uniform: Minimum 0.0 Maximum 1.0	N/A	Epistemic
NVF19	Effective porosity in shallow alluvium	Internal to this report	Truncated Normal: Mean 0.18 Standard Deviation 0.051 Minimum 0.00 Maximum 0.30	N/A	Epistemic
NVF7	Effective porosity in undifferentiated valley fill	Internal to this report	Truncated Normal: Mean 0.18 Standard Deviation 0.051 Minimum 0.00 Maximum 0.30	N/A	Epistemic

Table 6-8. Models/Analyses Inputs Used in the SZ Flow and Transport Abstraction Model and the SZ 1-D Transport Model (Continued)

Input Name	Input Description	Input Source (DTN, if applicable)	Value or Distribution	Units	Type of Uncertainty
FPVO	Fracture porosity in volcanic units	Internal to this report	CDF: (Log_{10}-transformed) Probability Value 0.0 -5.0 0.05 -4.0 0.50 -3.0 0.80 -2.0 1.0 -1.0	N/A	Epistemic
DCVO	Effective diffusion coefficient in volcanic units	Internal to this report	CDF: (Log_{10}-transformed) Probability Value 0.0 -11.3 0.08 -10.7 0.50 -10.3 0.83 -9.9 1.0 -9.3	m^2/s	Epistemic
GWSPD	Groundwater specific discharge multiplier	Internal to this report	CDF: (Log_{10}-transformed) Probability Value 0.0 -1.477 0.10 -0.477 0.50 0.0 0.90 0.477 1.0 1.0	N/A	Epistemic
bulkdensity	Bulk density of alluvium	Internal to this report	Normal: Mean 1910 Standard Deviation 78	kg/m^3	Epistemic
SRC1X SRC1Y SRC2X SRC2Y SRC3X SRC3Y SRC4X SRC4Y	Source regions beneath the repository	Internal to this report	Uniform: Minimum 0.0 Maximum 1.0	N/A	Epistemic and Aleatory
Alluv_xmin1	UTM minimum easting, SW corner alluvial uncertainty zone	Internal to this report	548285.	m	N/A
Alluv_xmax1	UTM maximum easting, SW corner alluvial uncertainty zone	Internal to this report	546669.	m	N/A
Alluv_ymin1	UTM minimum northing, SW corner alluvial uncertainty zone	Internal to this report	4057240.	m	N/A
Alluv_ymax1	UTM maximum northing, SW corner alluvial uncertainty zone	Internal to this report	4057620.	m	N/A

Table 6-8. Models/Analyses Inputs Used in the SZ Flow and Transport Abstraction Model and the SZ 1-D Transport Model (Continued)

Input Name	Input Description	Input Source (DTN, if applicable)	Value or Distribution	Units	Type of Uncertainty
Alluv_xmin2	UTM minimum easting, SE corner alluvial uncertainty zone	Internal to this report	555550.	m	N/A
Alluv_xmax2	UTM maximum easting, SE corner alluvial uncertainty zone	Internal to this report	555550.	m	N/A
Alluv_ymin2	UTM minimum northing, SE corner alluvial uncertainty zone	Internal to this report	4055400.	m	N/A
Alluv_ymax2	UTM maximum northing, SE corner alluvial uncertainty zone	Internal to this report	4055400.	m	N/A
Alluv_xmin3	UTM minimum easting, NE corner alluvial uncertainty zone	Internal to this report	557424.	m	N/A
Alluv_xmax3	UTM maximum easting, NE corner alluvial uncertainty zone	Internal to this report	557758.	m	N/A
Alluv_ymin3	UTM minimum northing, NE corner alluvial uncertainty zone	Internal to this report	4065430.	m	N/A
Alluv_ymax3	UTM maximum northing, NE corner alluvial uncertainty zone	Internal to this report	4067430.	m	N/A
Alluv_xmin4	UTM minimum easting, NW corner alluvial uncertainty zone	Internal to this report	554192.	m	N/A
Alluv_xmax4	UTM maximum easting, NW corner alluvial uncertainty zone	Internal to this report	553579.	m	N/A
Alluv_ymin4	UTM minimum northing, NW corner alluvial uncertainty zone	Internal to this report	4065430.	m	N/A
Alluv_ymax4	UTM maximum northing, NW corner alluvial uncertainty zone	Internal to this report	4067430.	m	N/A
A1_1_x	UTM easting, SW corner source zone 1	Internal to this report	547570.	m	N/A

Table 6-8. Models/Analyses Inputs Used in the SZ Flow and Transport Abstraction Model and the SZ 1-D Transport Model (Continued)

Input Name	Input Description	Input Source (DTN, if applicable)	Value or Distribution	Units	Type of Uncertainty
A1_1_y	UTM northing, SW corner source zone 1	Internal to this report	4078630.	m	N/A
A1_2_x	UTM easting, SE corner source zone 1	Internal to this report	548500.	m	N/A
A1_2_y	UTM northing, SE corner source zone 1	Internal to this report	4078630.	m	N/A
A1_3_x	UTM easting, NE corner source zone 1	Internal to this report	548500.	m	N/A
A1_3_y	UTM northing, NE corner source zone 1	Internal to this report	4081090.	m	N/A
A1_4_x	UTM easting, NW corner source zone 1	Internal to this report	547570.	m	N/A
A1_4_y	UTM northing, NW corner source zone 1	Internal to this report	4081090.	m	N/A
A2_1_x	UTM easting, SW corner source zone 2	Internal to this report	548500.	m	N/A
A2_1_y	UTM northing, SW corner source zone 2	Internal to this report	4078630.	m	N/A
A2_2_x	UTM easting, SE corner source zone 2	Internal to this report	549320.	m	N/A
A2_2_y	UTM northing, SE corner source zone 2	Internal to this report	4078630.	m	N/A
A2_3_x	UTM easting, NE corner source zone 2	Internal to this report	549320.	m	N/A
A2_3_y	UTM northing, NE corner source zone 2	Internal to this report	4081210	m	N/A
A2_4_x	UTM easting, NW corner source zone 2	Internal to this report	548500.	m	N/A
A2_4_y	UTM northing, NW corner source zone 2	Internal to this report	4081210.	m	N/A
A3_1_x	UTM easting, SW corner source zone 3	Internal to this report	547720.	m	N/A
A3_1_y	UTM northing, SW corner source zone 3	Internal to this report	4076170.	m	N/A

Table 6-8. Models/Analyses Inputs Used in the SZ Flow and Transport Abstraction Model and the SZ 1-D Transport Model (Continued)

Input Name	Input Description	Input Source (DTN, if applicable)	Value or Distribution	Units	Type of Uncertainty
A3_2_x	UTM easting, SE corner source zone 3	Internal to this report	548500.	m	N/A
A3_2_y	UTM northing, SE corner source zone 3	Internal to this report	4076170.	m	N/A
A3_3_x	UTM easting, NE corner source zone 3	Internal to this report	548500.	m	N/A
A3_3_y	UTM northing, NE corner source zone 3	Internal to this report	4078630.	m	N/A
A3_4_x	UTM easting, NW corner source zone 3	Internal to this report	547720.	m	N/A
A3_4_y	UTM northing, NW corner source zone 3	Internal to this report	4078630.	m	N/A
A4_1_x	UTM easting, SW corner source zone 4	Internal to this report	548500.	m	N/A
A4_1_y	UTM northing, SW corner source zone 4	Internal to this report	4076170.	m	N/A
A4_2_x	UTM easting, SE corner source zone 4	Internal to this report	548890.	m	N/A
A4_2_y	UTM northing, SE corner source zone 4	Internal to this report	4076170.	m	N/A
A4_3_x	UTM easting, NE corner source zone 4	Internal to this report	548890.	m	N/A
A4_3_y	UTM northing, NE corner source zone 4	Internal to this report	4078630.	m	N/A
A4_4_x	UTM easting, NW corner source zone 4	Internal to this report	548500.	m	N/A
A4_4_y	UTM northing, NW corner source zone 4	Internal to this report	4078630.	m	N/A
Max_al_por	Total alluvium porosity	Internal to this report	0.30	N/A	N/A
Fpor	Average fracture porosity in volcanic units	Internal to this report	0.001	N/A	N/A
Mpor	Average matrix porosity in volcanic units	Internal to this report	0.22	N/A	N/A

Table 6-8. Models/Analyses Inputs Used in the SZ Flow and Transport Abstraction Model and the SZ 1-D Transport Model (Continued)

Input Name	Input Description	Input Source (DTN, if applicable)	Value or Distribution	Units	Type of Uncertainty
Bdens	Average bulk density in volcanic units	Internal to this report	1.88	g/mL	N/A
Matrix porosity	Expected values for matrix porosity per volcanic unit	SN0004T0501399.003 [DIRS 155045] Units 15-13, 10 and 8 Units 12, 11, and 9 are internal to this report	Unit 15: 0.15 Unit 14, 10, and 8: 0.25 Unit 13: 0.23 Unit 12: 0.18 Unit 11: 0.21 Unit 9: 0.21	N/A	N/A
Bulk Density	Expected bulk density values per volcanic unit	Units 15-13, 10, 8; DTN: SN0004T0501399.002 [DIRS 155046] and SN0004T0501399.003 [DIRS 155045] Units 17, 12, 11, 9, and 6-2 are internal to this report	Unit 18: 2.50 Unit 17, 6, 5, and 3: 2.77 Unit 16: 2.44 Unit 15: 2.08 Unit 14, 10 and 8: 1.77 Unit 13: 1.84 Unit 12: 2.19 Unit 11: 2.11 Unit 9: 2.05 Unit 4 and 2: 2.55 Unit 1: 2.65	g/cm^3	N/A
Effective Porosity	Expected effective porosity values for other units (see Section 6.5.2.20)	Units 18-16 and 1: DTN: MO0105HCONEPOR.000 [DIRS 155044] Units 6-2 Internal to this report	Unit 18: 0.32 Unit 17: 0.01 Unit 16: 0.08 Unit 6,5 and 3: 0.01 Unit 4: 0.18 Unit 2: 0.18 Unit 1: 0.0001	N/A	N/A

CDF = cumulative distribution function; UTM = Universal Transverse Mercator

NOTE: Unit numbers refer to hydrogeologic units in Table 6-9

Table 6-9. Hydrogeologic Unit Definition

Hydrogeologic Unit	Hydrogeologic Unit Identification Number
Valley Fill	19
Valley Fill Confining Unit	18
Cenozoic Limestones	17
Lava Flows	16
Upper Volcanic Aquifer	15
Upper Volcanic Confining Unit	14

Table 6-9. Hydrogeologic Unit Definition (Continued)

Hydrogeologic Unit	Hydrogeologic Unit Identification Number
Lower Volcanic Aquifer Prow Pass	13
Lower Volcanic Aquifer Bullfrog	12
Lower Volcanic Aquifer Tram	11
Lower Volcanic Confining Unit	10
Older Volcanic Aquifer	9
Older Volcanic Confining Unit	8
Undifferentiated Valley Fill	7
Upper Carbonate Aquifer	6
Lower Carbonate Aquifer Thrust	5
Upper Clastic Confining Unit	4
Lower Carbonate Aquifer	3
Lower Clastic Confining Unit	2
Granites	1

NOTE: Hydrogeologic Units adapted from *Hydrogeologic Framework Model for the Saturated-Zone Site-Scale Flow and Transport Model* (BSC 2004 [DIRS 170008], Table 6-1).

6.5.2.1 Groundwater Specific Discharge

Uncertainty exists in the groundwater specific discharge in the SZ along the flow path from beneath the repository to the hypothetical point of release into the biosphere. This uncertainty was quantified as a distribution of specific discharge in the volcanic aquifer near Yucca Mountain by the SZ expert elicitation (CRWMS M&O 1998 [DIRS 100353], p. 3-43). This expert elicitation was conducted in a manner consistent with *Branch Technical Position on the Use of Expert Elicitation in the High-Level Radioactive Waste Program* (NUREG-1563) (Kotra et al. 1996 [DIRS 100909]). Conclusions regarding the uncertainty in specific discharge by the expert elicitation panel primarily were based on single- and multi-well hydraulic testing of wells in the fractured volcanic units near Yucca Mountain. The aggregate uncertainty distribution of specific discharge in the SZ from the expert elicitation had a median value of about 0.6 m/year, with a range of values from less than 0.01 m/year to about 10 m/year (CRWMS M&O 1998 [DIRS 100353], p. 3-43). It should be noted that the experts in the SZ expert elicitation were only elicited regarding uncertainty in specific discharge within about 5 km of the repository.

More recently, estimates of groundwater specific discharge in the SZ have been obtained at another location in the SZ system: from field-testing at the alluvial tracer complex (ATC) (BSC 2004 [DIRS 170010], Section 6.5.4.3). The ATC is approximately located at the boundary of the accessible environment, as specified in regulations for the Yucca Mountain project, 10 CFR 63.302 (10 CFR 63 [DIRS 173273]). The location of the ATC is approximately 18 km from Yucca Mountain, and testing was performed in the alluvium aquifer. Estimates of groundwater specific discharge at the ATC range from 1.2 m/year to 9.4 m/year (DTN: LA0303PR831231.002, [DIRS 163561]), using alternative means of analyzing the single-well tracer testing results. The simulated average specific discharge in this region of the SZ system using the SZ flow and transport abstraction model ranges from 1.9 m/year to 3.2 m/year for differing values of horizontal anisotropy in permeability, as shown in Table 6-6. Correspondingly, the simulated average specific discharge in the volcanic aquifer near Yucca Mountain using the SZ flow and transport abstraction model ranges from 0.31 m/year to 0.87 m/year for differing values of horizontal anisotropy in permeability. These results show that the average groundwater specific discharge tends to increase along the flow path from beneath Yucca Mountain to the south. This increase in the specific discharge is due to convergent groundwater flow in this region of the SZ system. These results also indicate that there is general consistency between the simulated specific discharge and the median values of uncertainty ranges estimated for the volcanic aquifer and the alluvial aquifer along the flow path.

The additional data from the ATC constitutes new information on the specific discharge in the SZ, and significantly reduces uncertainty in the specific discharge relative to the assessment by the expert elicitation panel. Estimates of specific discharge at the ATC range from 1.2 m/year to 9.4 m/year; the upper end of the range is 7.8 times the lower end of the range. This range of uncertainty in specific discharge is somewhat less than one order of magnitude, which is considerably less than the degree of uncertainty from the SZ expert elicitation project (CRWMS M&O 1998 [DIRS 100353]). Consequently, the uncertainty distribution for the groundwater specific discharge factor (GWSPD) is reevaluated to reflect the reduced uncertainty. From this information, a discrete CDF of uncertainty in specific discharge is constructed, in which 80 percent of the probability is between 1/3 and 3 times the best estimate of specific discharge. The lower tail of the uncertainty distribution extends to 1/30 of the expected value and 10 percent of the probability is assigned to this lower tail. The upper tail of the uncertainty distribution extends to ten times the expected value and ten percent of the probability is assigned to this upper tail. The lower and upper tails of the uncertainty distribution approximately correspond to the greater uncertainty reflected in the SZ expert elicitation results. The resulting wide total range of uncertainty in specific discharge implicitly includes the potential existence of undetected features in the SZ, such as fault and fracture zones that could significantly impact groundwater flow.

Uncertainty in the groundwater specific discharge is incorporated into the SZ flow and transport abstraction model using the continuously distributed GWSPD parameter. This parameter is a multiplication factor that is applied to all values of permeability and values of specified boundary fluxes in the SZ flow and transport abstraction model to effectively scale the simulated specific discharge in the model. Note that a separate steady-state groundwater flow field is simulated for each realization of the system, using the value of GWSPD (and the value of HAVO, for horizontal anisotropy). The sampling of GWSPD is performed on the log-transformed values of the specific discharge multiplication factor, as indicated in Table 6-8. The CDF of uncertainty in the groundwater specific discharge multiplier is shown in Figure 6-7.

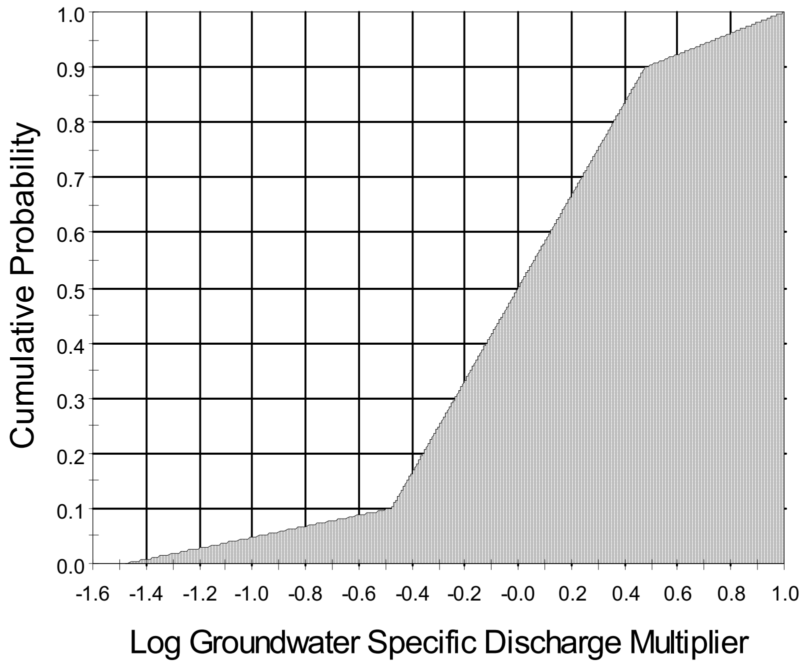

Output DTN: SN0310T0502103.009.

Figure 6-7. CDF of Uncertainty in Groundwater Specific Discharge Multiplier

6.5.2.2 Alluvium Uncertainty Zone

Uncertainty exists in the geology below the water table, along the inferred flow path from the repository at distances of approximately 10 km to 20 km downgradient of the repository. The uncertainty in flow path lengths between the repository and the contact with the alluvium is a function of the uncertainty in groundwater flow pathways from beneath the repository in the SZ and geologic uncertainty in the subsurface location of the contact between the tuff and the alluvium. Most of the uncertainty in 10 to 20 km flow path length in the tuff cited above is related to uncertainty in groundwater flow pathways, with geologic uncertainty in the location of the contact between the tuff and alluvium contributing to overall uncertainty to a lesser degree. The location at which groundwater flow moves from fractured volcanic rocks to alluvium is of particular significance from the perspective of repository performance assessment. This is because of contrasts between the fractured volcanic units and the alluvium in terms of groundwater flow (fracture-dominated flow versus porous medium flow) and in terms of sorptive properties of the media for some radionuclides.

The uncertainty in the northerly extent of the alluvium in the SZ of the site-scale flow and transport simulations is abstracted as a polygonal region that is assigned radionuclide transport properties representative of the valley-fill aquifer hydrogeologic unit (Table 6-9). The dimensions of the polygonal region are randomly varied in the SZ flow and transport abstraction model for the multiple realizations. The northern boundary of the uncertainty zone is varied between the dashed lines at the northern end of the polygonal area shown in Figure 6-8. The western boundary of the uncertainty zone is varied between the dashed lines along the western side of the polygonal area shown in the figure.

The uncertainty in the contact between volcanic rocks and alluvium at the water table along the northern part of the uncertainty zone is approximately bounded by the location of well UE-25 JF#3, in which the water table is below the contact between the volcanic rocks and the overlying alluvium, and by the location of well EWDP-10S, in which the water table is above the contact between the volcanic rocks and the alluvium. The uncertainty in the contact along the western part of the uncertainty zone is defined by the locations of wells EWDP-10S, EWDP-22S, and EWDP-19D1, in which the water table is above the contact between volcanic rocks and the overlying alluvium, and outcrops of volcanic bedrock to the west.

The lower boundary of the alluvium uncertainty zone varies from an elevation of 670 m in the northwestern corner of the uncertainty zone to 400 m along the southern edge of the uncertainty zone. This corresponds to a saturated alluvium thickness of approximately 50 m in the northwestern corner varying to about 300 m along the southern boundary of the uncertainty zone.

The boundaries of the alluvium uncertainty zone are determined for a particular realization by the parameters FPLAW and FPLAN. These parameters have uniform distributions from 0.0 to 1.0, where a value of 0.0 corresponds to the minimum extent of the uncertainty zone, and 1.0 corresponds to the maximum extent of the uncertainty zone in a westerly direction and northerly direction, respectively. A uniform distribution is appropriate for these uncertainty distributions because only the bounding values are known. A uniform distribution is the best statistically unbiased choice in this situation. These parameters are used to independently and uniformly vary the northern and western contacts of the volcanic rocks and alluvium at the water table. The maximum and minimum coordinates of the alluvium uncertainty zone, corresponding to the plot shown in Figure 6-8, are given in Table 6-8 (Alluv_xmin1 to Alluv_ymax4).

6.5.2.3 Effective Porosity of Alluvium

For the TSPA Site Recommendation (SR) calculations, effective porosity in the alluvium was a truncated normal distribution with a mean of 0.18, a standard deviation of 0.051, a lower bound of 0, and an upper bound of 0.35 (CRWMS M&O 2000 [DIRS 153246], Table 3.8-3). The basis for this parameter is from Bedinger et al. (1989 [DIRS 129676], p. A18, Table 1). There were no site-specific data for effective porosity in the alluvium at the time of the TSPA-SR. Bedinger et al. (1989 [DIRS 129676]) include a study of hydraulic characteristics of alluvium within the Basin and Range Province of the Southwestern U.S. This study is relevant to the local basin fill conditions, and provides values for effective porosity as a stochastic parameter. Since the TSPA-SR, a site-specific value was determined for effective (or flow) porosity from well EWDP-19D1 at the ATC, based on a single-well pumping test (BSC 2004 [DIRS 170010], Section 6.5.4.2.4). There are also total porosity values from the same well based on borehole gravimeter surveys, which are used in developing the upper bound of the effective porosity in the alluvium uncertainty distribution.

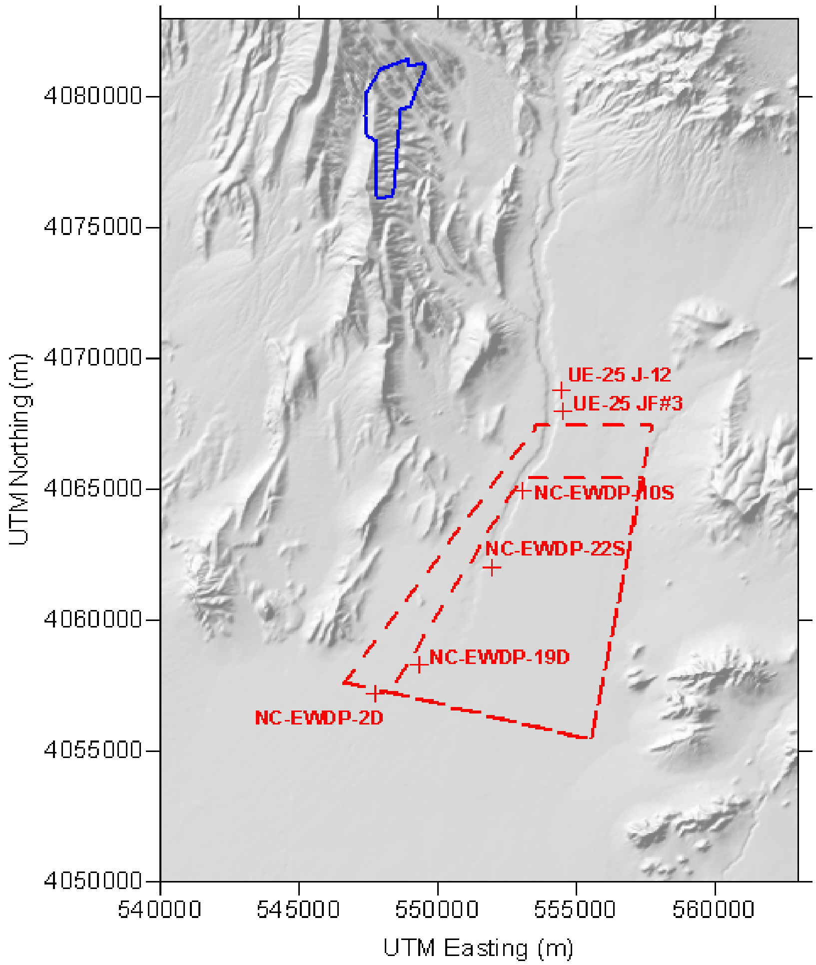

Sources: Repository outline is from 800-IED-WIS0-00101-000-00B (BSC 2004 [DIRS 172801]); well locations are from DTNs: GS010908312332.002 [DIRS 163555]; GS030108314211.001 [DIRS 163483].

NOTE: The repository outline is shown by the solid line, and the minimum and maximum boundaries of the alluvium uncertainty zone are shown by the dashed lines. Key well locations and well numbers are shown with the cross symbols.

Figure 6-8. Minimum and Maximum Extent of the Alluvium Uncertainty Zone

Effective porosity is important for determining the average linear groundwater velocities used in the simulation of radionuclide transport. They are customarily calculated by dividing the specific discharge of groundwater through a model grid cell by the porosity, ϕ_e. Groundwater velocities are rendered more accurate when dead-end pores are eliminated from consideration because they do not transmit water. The effective porosity results from that elimination. As a result ϕ_e will always be less than or equal to total porosity, ϕ_T. The retardation coefficient, R_f, is also a function of porosity. Reducing total porosity to ϕ_e can erroneously raise the magnitude of this value within the model. The correction for this is detailed in the Equation 6-3 discussion in Section 6.5.1.

Effective porosity is treated as an uncertain parameter for the two alluvium units (19 and 7) of the nineteen SZ model hydrogeologic units. Uncertain, in this sense, means that ϕ_e will be constant spatially for each unit for any particular model realization, but that value will vary from one realization to the next. In comparison, constant parameters are constant spatially and do not change from realization to realization.

The parameter input sources used in this analysis are described in Table 4-1, and corroborative data are discussed in this section. The uncertainty distribution used for the analysis is the distribution used for TSPA-SR, with a change to the upper bound. The effective porosity uncertainty distribution is shown in Figure 6-9. Figure 6-9 compares the distribution of Bedinger et al. (1989 [DIRS 129676]) (DTN: MO0105HCONEPOR.000 [DIRS 155044]) to distributions, ranges, and values from the other sources that were considered to develop the uncertainty distribution. The site-specific effective porosity data point of 0.1 from well EWDP-19D1 (BSC 2004 [DIRS 170010], Section 6.5) is shown on Figure 6-9. This is considered a corroborative data point, and falls within the uncertainty distribution.

The upper bound of the uncertainty distribution for effective porosity is re-evaluated because of new site-specific data obtained after TSPA-SR. The new upper bound is based on the total porosity values from well EWDP-19D1 and the average of the total porosity values from the Cambric study (Burbey and Wheatcraft 1986 [DIRS 129679], pp. 23 and 24) within the NTS, but several kilometers to the east, in Frenchman Flat; and total porosity shown in Tables 8-1 and 8-2 of *Regional Groundwater Flow and Tritium Transport Modeling and Risk Assessment of the Underground Test Area, Nevada Test Site, Nevada* (DOE 1997 [DIRS 103021], pp. 8-5 and 8-6, see Table 6-10). The computed total porosity values from EWDP-19D1 are shown in Table 6-11, and have an average value of 0.24.

The average of the total porosity values in Table 6-10 and the average of the site-specific data from well EWDP-19D1 were used to develop the upper bound of the effective porosity uncertainty distribution. Although there is considerable variability in measured total porosity within alluvial strata (see Table 6-11), an average value to define the upper bound of the uncertainty distribution is appropriate because of scaling considerations. The grid cells in the SZ site-scale transport model are 500 m by 500 m and smaller scale variations in total porosity would be averaged over this large volume of alluvium. The average total porosity value of 0.35 and the average value from EWDP-19D1 of 0.24 result in a mean of 0.30. Figure 6-10 shows the truncated normal distribution developed in this analysis for effective porosity in the alluvium (parameter NVF19 and NVF7) with a mean of 0.18, standard deviation of 0.051, a lower bound of 0, and an upper bound of 0.30. Note that parameter NVF7 has the same distribution as NVF19, and is sampled independently. The hydrogeologic units corresponding to the parameters NVF19 and NVF7 (Units 19 and 7) developed at different geologic times and under potentially differing tectonic conditions. Consequently, they may have different characteristics with regard to effective porosity and the parameters are not correlated in the sampling process. The resulting range of uncertainty in effective porosity of the alluvium implicitly accounts for the potential existence of undetected stratigraphic and sedimentological features, such as fine-grained, low-permeability facies, that could exclude groundwater flow through the alluvium aquifer.

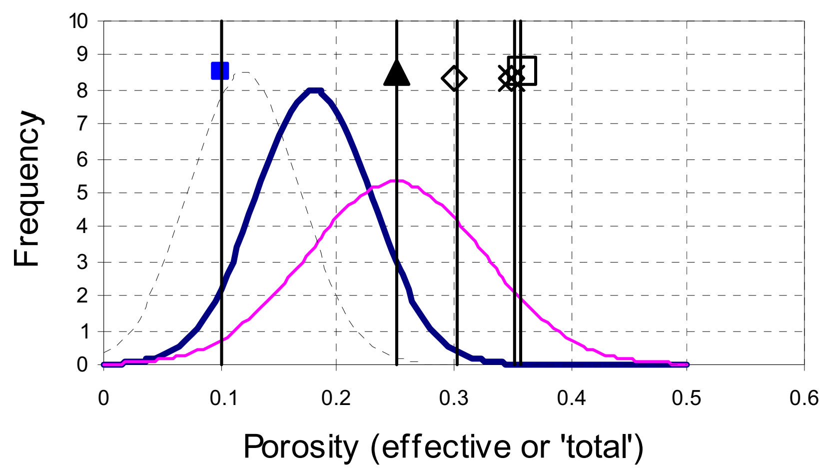

Sources: DTN: MO0003SZFWTEEP.000 [DIRS 148744]; BSC 2004 [DIRS 170010], Section 6.5; Burbey and Wheatcraft 1986 [DIRS 129679], pp. 23 to 24; DOE 1997 [DIRS 103021], Table 8-1, p. 8-5, and Table 8-2, p. 8-6.

NOTE: The dashed black line is Neuman (MO0003SZFWTEEP.000 [DIRS 148744]); the solid heavy blue line is DTN: MO0105HCONEPOR.000 [DIRS 155044]; the solid pink line is Gelhar (DTN: MO0003SZFWTEEP.000 [DIRS 148744]); the solid blue block is the effective porosity value calculated from EWDP-19D1 (BSC 2004 [DIRS 170010], Section 6.5).

The single value data points do not have a y-scale value, but do correspond to the x-axis. These points are shown for comparison purposes only.

The solid black triangle is DOE 1997 [DIRS 103021], Table 8-1, mean matrix porosity; the diamond outlined shapes are Burbey and Wheatcraft 1986 [DIRS 129679] total porosity; the X is DOE 1997 [DIRS 103021], Table 8-2, total porosity; and the square outlined shape is DOE 1997 [DIRS 103021], Table 8-1, mean bulk porosity.

Figure 6-9. Effective Porosity Distributions and Values for Alluvium Compared

Table 6-10. Total Porosity Summary (ϕ_T) for Alluvium

Reference	Total Porosity	Comments
DOE 1997 [DIRS 103021], Table 8-1, p. 8-5	0.36	Mean bulk porosity
DOE 1997 [DIRS 103021], Table 8-2, p. 8-6	0.35	Total porosity
Burbey and Wheatcraft 1986 [DIRS 129679], pp. 23 to 24	0.34	Average of porosity values from Table 3 of that study
Average of above	0.35	N/A

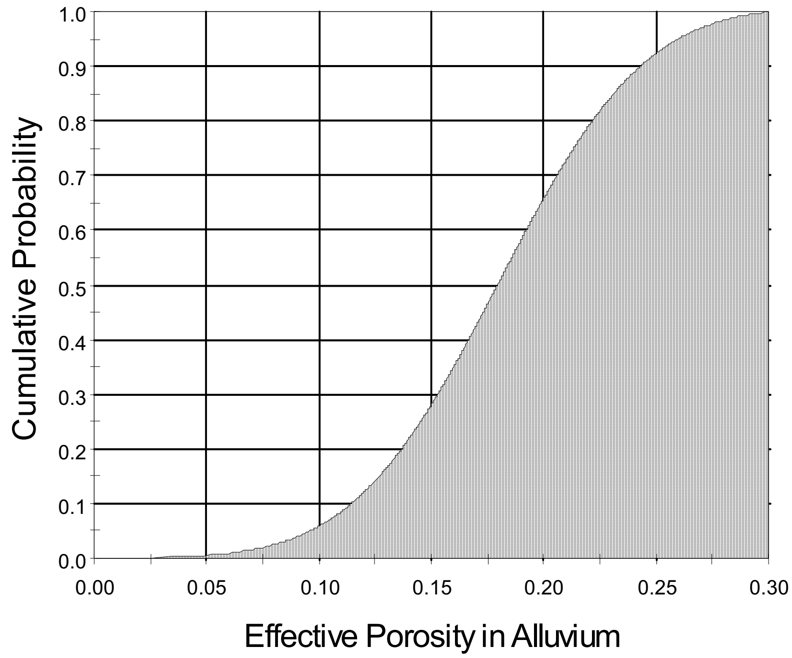

Output DTN: SN0310T0502103.009.

Figure 6-10. CDF of Uncertainty in Effective Porosity in Alluvium

6.5.2.4 Flowing Interval Spacing

The flowing interval spacing is a key parameter in the dual porosity model that is included in the SZ flow and transport abstraction model. A flowing interval is defined as a fractured zone that transmits fluid in the SZ, as identified through borehole flow meter surveys (see Figure 6-11). This figure shows a borehole that is intersected by multiple, irregularly spaced fractures. The figure also shows several black bands, labeled as flowing intervals, in which a flow meter survey has detected groundwater flow into (or out of) the borehole. The analysis uses the term "flowing interval spacing" as opposed to "fracture spacing," which is typically used in the literature. Fracture spacing was not used because field data identified zones (or flowing intervals) that contain fluid-conducting fractures but do not distinguish how many or which fractures comprise the flowing interval. These data also indicate that numerous fractures between flowing intervals do not transmit significant amounts of groundwater. The flowing interval spacing is the distance between the midpoints of each flowing interval. The flowing interval approach and the resulting uncertainty distribution implicitly accounts for the potential existence of undetected features, such as fracture zones through which groundwater flow is channeled, in the fractured volcanic units of the SZ.

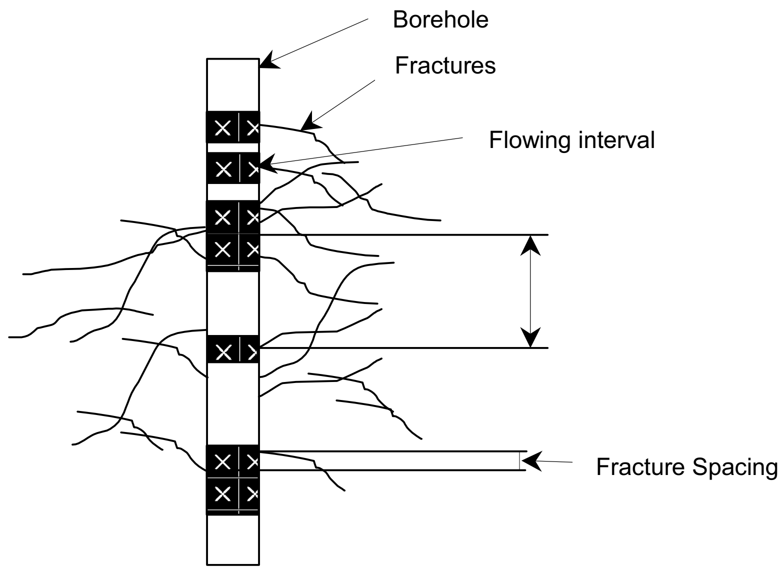

Source: BSC 2004 [DIRS 170014], Figure 6-1.

Figure 6-11. Example of Flowing Interval Spacing for a Typical Borehole

There is considerable uncertainty regarding the flowing interval spacing parameter due to the limited number of data points available. The data set used for the analysis consisted of borehole flow meter survey data. This analysis is described in detail in *Probability Distributions for Flowing Interval Spacing* (BSC 2004 [DIRS 170014]).

There are no new data available to reevaluate the uncertainty distribution for this parameter; therefore, a CDF based on the lognormal distribution (BSC 2004 [DIRS 170014], Section 7) that was used in TSPA-SR is used as input to the TSPA-LA model. A simplified piecewise CDF is defined for sampling of the flowing interval spacing parameter for TSPA-LA. This CDF is shown as the red line in Figure 6-12 and is plotted for comparison to the Monte Carlo analysis results from *Probability Distribution for Flowing Interval Spacing* (BSC 2004 [DIRS 170014], Section 7) as the solid black line. The flowing interval spacing parameter is specified for a particular realization by the parameter FISVO. See Table 6-8 for the associated probabilities for the flowing interval spacing CDF.

6.5.2.5 Flowing Interval Porosity

The flowing interval porosity is defined as the volume of the pore space through which significant groundwater flow occurs, relative to the total volume. At Yucca Mountain, rather than attempt to define the porosity within all fractures, a flowing interval is defined as the region in which significant groundwater flow occurs at a well. The fracture porosity then characterizes these flowing intervals rather than all fractures. The advantage to this definition of fracture porosity is that in situ well data may be used to characterize the parameter. The flowing interval porosity may also include the matrix porosity of small matrix blocks within fracture zones that potentially experience rapid matrix diffusion.

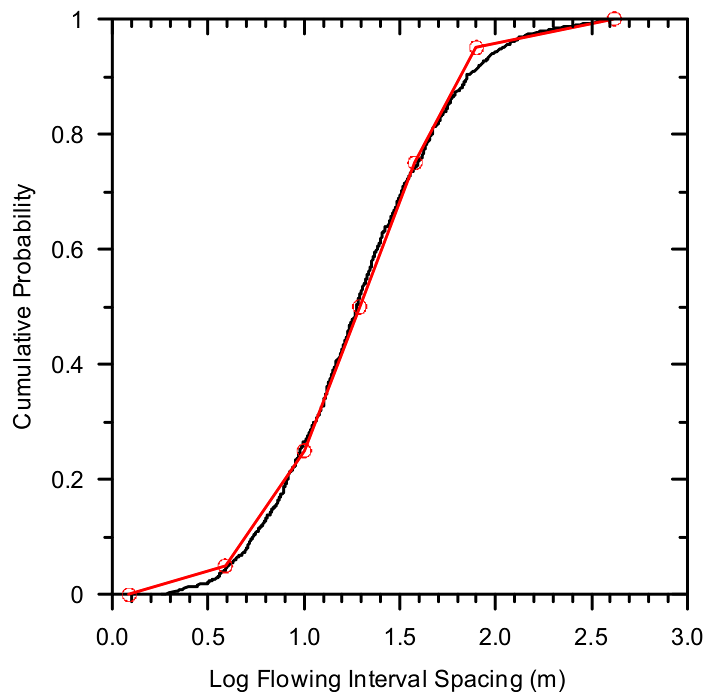

Source: DTN: SN9907T0571599.001 [DIRS 122261], File: *resul_fis2.xls* (solid black line)

Output DTN: SN0310T0502103.009 (solid red line).

Figure 6-12. CDF of Uncertainty in Flowing Interval Spacing

For the TSPA-SR calculations, the flowing interval (fracture) porosity probability distribution was a uniform distribution with an upper bound of $\log_{10}$ (flowing interval porosity) of −1.0 and a lower bound of $\log_{10}$ (flowing interval porosity) of −5.0 (CRWMS M&O 2000 [DIRS 147972], Section 6.7). The basis for this uncertainty distribution includes estimates of fracture porosity in intact cores of volcanic rock, and the results of pumping tests and tracer tests in the Bullfrog Tuff at the C-wells complex (CRWMS M&O 2000 [DIRS 147972], Section 6.7).

The TSPA-SR probability distribution for the flowing interval porosity has been modified based on new sources of information pertaining to flowing interval porosity. New information has been derived from tests in unsaturated tuff in the Exploratory Studies Facility (ESF). Fracture porosity has been estimated in unsaturated volcanic tuff in the ESF for the middle nonlithophysal welded tuff (UZ model layer tsw34) using gas tracer testing. The assumptions used in obtaining the fracture porosity from gas tracer tests are that the diffusion of gas into the rock matrix is negligible compared to the flow through the fractures, that the fracture network is well connected, and that the gas flow is approximately radial toward the pumped borehole. This calculation of fracture porosity is documented in the *Analysis of Hydrologic Properties Data* report (BSC 2004 [DIRS 170038], Section 6.1.3) and estimates of fracture porosity in other volcanic subunits have been based on these testing results. The estimated average value of fracture porosity is on the order of 0.01.

Fracture porosity has also been estimated using the residence time of conservative tracers during cross-hole tracer tests at the C-wells complex (CRWMS M&O 1997 [DIRS 100328], pp. 2 to 4; BSC 2004 [DIRS 170010]). This method assumes that the mean tracer arrival time is equal to the time required to drain a homogenous, fractured cylinder of rock with a radius equal to the distance between the pumping well and the tracer-injection well. A large range in estimated fracture porosity for the saturated Bullfrog Tuff resulted from this method because the tracers were interpreted to have traveled along two paths with different travel times. The path with the longer travel time resulted in a larger estimate of fracture porosity. The resulting lower and upper bounds of fracture porosity were 0.003 and 0.10, respectively (DTNs: LA0303PR831231.005 [DIRS 166259] and GS031008312315.002 [DIRS 166261]).

The Department of Energy Nevada Site Office Underground Test Area Project (DOE 1997 [DIRS 103021]) evaluated the fracture spacing and apertures in seven cores from wells in volcanic rocks at Pahute Mesa. The estimated open fracture porosities based on the assumption of parallel plates range from 2.6×10^{-6} to 4.7×10^{-4} in these cores (DOE 1997 [DIRS 103021], p. 5-14). Information compiled for *Total-System Performance Assessment for Yucca Mountain – SNL Second Iteration (TSPA-1993)* (Wilson et al. 1994 [DIRS 100191], Volume 1, Chapter 7, Table 7-19, p. 7-30) indicates expected values of fracture porosities ranging from 8.1×10^{-5} to 2.8×10^{-3} in core from USW G-1, USW GU-3, USW G-4, and UE25a#1, when parallel plate fracture geometry is assumed. This information generally corroborates the estimates of fracture porosity from DOE (1997 [DIRS 103021]). There is large uncertainty in the flowing interval porosity parameter.

Given the estimates of this parameter from values based on theoretical models, pumping tests, and tracer data, the parameter uncertainty ranges over four orders of magnitude. To estimate the lower bound of flowing interval porosity, the estimates of fracture porosity of intact cores of volcanic rock were used. The upper bound of uncertainty in the flowing interval porosity is based on interpretations of pumping test and tracer data. The new data from the ESF provide an estimate of flowing interval porosity that falls in the upper half of the distribution used for this parameter (CRWMS M&O 2000 [DIRS 147972], Section 6.7) in the TSPA-SR.

For the TSPA-LA calculations, a cumulative distribution with a lower bound of $\log_{10}$ (flowing interval porosity) equal to −5.0, and an upper bound of $\log_{10}$ (flowing interval porosity) equal to −1.0 is selected for this parameter, as shown in Figure 6-13. This distribution places more weight in the middle of the distribution range in comparison to the TSPA-SR uniform distribution (CRWMS M&O 2000 [DIRS 147972], Section 6.7) that results in equal probabilities for the given range. The 0.5 probability value of −3.0 is representative of the smallest values of fracture porosity estimated from the new data from the ESF and previous field tests. See Table 6-8 for the associated probabilities for the flowing interval porosity CDF. The flowing interval porosity parameter is specified for a particular realization by the parameter FPVO.

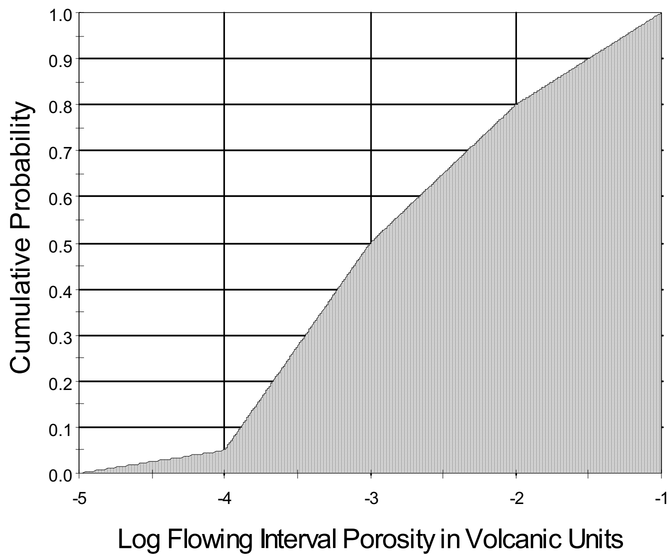

Output DTN: SN0310T0502103.009.

Figure 6-13. CDF of Uncertainty in Flowing Interval Porosity

6.5.2.6 Effective Diffusion Coefficient

Matrix diffusion is a process in which diffusing particles move, via Brownian motion, through both mobile and immobile fluids. Diffusion is a Fickian process; that is, diffusing species move from high to low concentrations. It is dependent on the free water molecular diffusion coefficient for individual constituents and the characteristics of the flow path in which the diffusing species passes. Because diffusion through porous media is less than free water molecular diffusion, it is quantitatively defined as the effective diffusion coefficient, D_e.

Matrix diffusion has been demonstrated to occur in the volcanic rocks within the vicinity of Yucca Mountain (Reimus et al. 2002 [DIRS 162956]; Reimus et al. 2002 [DIRS 163008]). Thus, it is modeled in the volcanic units of the SZ flow and transport abstraction model and the SZ 1-D transport model for TSPA-LA. It is the transport mechanism that occurs in the rock matrix portion of the volcanic units. Consequently, it can be an important process that physically retards net radionuclide transport in fractured media (Section 6.7). As a conservative approach, no credit is taken for matrix diffusion that could potentially occur into the low-permeability regions of the alluvium. No credit is taken for matrix diffusion of colloids in either the volcanic units or the alluvium, because the effects would be small and would only retard transport.

The variability in D_e in saturated media is caused by the variability in:

1. The individual constituents' size (atom, ion, or molecule) and charge
2. Fluid temperature
3. The unique properties of a porous media's lithology at a microscopic scale.

The contribution of these uncertainties and variabilities to deriving a value of D_e is evaluated in the following subsections.

Variability between Lithologic Units

There are several derived 'lumped' parameters, used as adjustments to the free water molecular diffusion, to account for the impact of lithology on molecular diffusion. Tortuosity, formation, and constrictivity factors are common adjustment parameters. These lumped parameters are based on various linear regression models, fit to field and laboratory experimental results and measured properties of the host rock, such as porosity, permeability, and formation electrical resistivity (from geophysical logs).

Diffusion cell experiments have demonstrated that D_e is affected more by the structural properties of the porous medium, such as permeability, porosity, pore size distribution, and pore geometry, than by the mineralogy or geochemistry (Skagius and Neretnieks 1986 [DIRS 156862], pp. 389 to 398). Specific to Yucca Mountain, diffusion cell experiments documented in *Saturated Zone In-Situ Testing* (BSC 2004 [DIRS 170010], Section E.2) on dilute bromide solutions diffusing through Yucca Mountain tuff samples demonstrated D_e was directly proportional to the variability in permeability. Buchholtz ten Brink et al. (1991 [DIRS 162954]) found D_e for ^{238}U on various Yucca Mountain tuff samples to be dependent on the pore size distribution of the hydrostratigraphic units.

Many mathematical models have been formulated to derive a value of D_e. Most, if not all, rely on porosity, with some adding other "lumped" parameters. For example, *Dynamics of Fluids in Porous Media* (Bear 1972 [DIRS 156269], Sections 4.8.2 and 4.8.3) relates effective matrix diffusion to porosity, formation factor (derived from geophysical logs), and the free water molecular diffusion coefficient as follows:

$$D_e = \frac{D_0}{\phi F} \qquad \text{(Eq. 6-15)}$$

where D_e is the effective diffusion coefficient in a porous medium [L^2/T], D_0 is the diffusion coefficient in water [L^2/T], and F is the formation factor [-]. The formation factor is defined by the electrical resistivity of the porous medium saturated with electrolyte divided by the resistivity of the electrolyte. This method has limitations, in that it relies on formation factor measurements.

Domenico and Schwartz (1990 [DIRS 100569], p. 368) document the relationship between porosity and effective diffusion with the following:

$$D_m = (\phi / \tau) D_0 \qquad \text{(Eq. 6-16)}$$

where τ (= L_e/L) is the tortuosity [-], L_e is the length of the channel for the fluid particle [L], and L is the length of the porous media channel [L]. This method has limitations, in that it relies on multiple diffusion cell measurements on a wide variety of rock samples to derive a global value for τ.

Domenico and Schwartz (1990 [DIRS 100569], p. 368) define a range for D_m with the following empirical equation:

$$D_m = \frac{\phi D_0}{2} \quad \text{to} \quad D_0\left(\frac{\phi}{2-\phi}\right)^2 \qquad \text{(Eq. 6-17)}$$

Bound 1 Bound 2

This relationship captures the uncertainty and range of D_m in a heterogeneous system. It is dependent only on porosity and, because there are many matrix porosity measurements on Yucca Mountain tuffs, site-specific data can be used as input.

Using Equation 6-17 and site-specific porosity data, a range in the effective diffusion coefficient in the volcanic rock matrix (D_e) can be calculated. Mean porosity values were calculated using the relative-humidity porosities found in DTN: MO0109HYMXPROP.001 [DIRS 155989] for the SZ hydrostratigraphic units defined in *Characterization of Hydrogeologic Units Using Matrix Properties, Yucca Mountain, Nevada* (Flint 1998 [DIRS 100033]) as input. Relative-humidity porosity is measured by drying the sample in an oven for 48 hours at 60°C and 65 percent relative humidity. (Note: Flint's hydrostratigraphic units are subunits of the SZ hydrogeologic framework models (HFM) units adopted in TSPA-LA.) Using Flint's hydrostratigraphic units to represent a mean porosity is appropriate for this exercise because Flint's basis for categorizing the units is heavily based on matrix rather than fracture properties, and it is the matrix properties that are important to diffusion in the SZ.

Using relative-humidity porosity values in DTN: MO0109HYMXPROP.001 [DIRS 155989], the minimum average porosity is 0.042, and is located in the Calico Hills-vitric unit (a subunit of the SZ's Upper Volcanic Confining, Unit 14); the maximum average is 0.321, and is located in unit TC (Tiva Canyon Tuff, a subunit of the SZ Upper Volcanic Aquifer, Unit 15). For this exercise, D_0 is that of ^{3}HHO (tritiated water), 2.44×10^{-5} cm^2/s. The resulting range in D_e is between 3.92×10^{-6} and 1.12×10^{-8} cm^2/s when the largest porosity is used as input in bound 1, and the smallest porosity is used as input to bound 2. The variability in D_e is a factor of:

$$\frac{3.92 \times 10^{-6} cm^2/s}{1.12 \times 10^{-8} cm^2/s} = 350 \qquad \text{(Eq. 6-18)}$$

Reimus et al. (2002 [DIRS 163008]) have developed an empirical relationship between D_e and porosity and permeability measurements based on diffusion cell experiments on rock samples from the Yucca Mountain area. Diffusing species used in the experiments are ^{99}Tc (as TcO_4^-), ^{14}C (as HCO_3^-) and ^{3}HHO, as well as Br^- and I^-. Rock samples used were taken from within the vicinity of Yucca Mountain, under Pahute Mesa and Area 25 of the NTS. Based on these experiments, Reimus et al. (2002 [DIRS 163008]) describe three different approaches to deriving D_e. Two are dependent on linear regression relationships fitting the experimental results to diffusion cell measurements for:

1. Both matrix porosity and permeability
2. Only matrix porosity measurements.

The third approach is simply compiling a CDF based on their numerous diffusion cell results. Reimus et al. (2002 [DIRS 163008], Section 4) found that differences in rock type account for the largest variability in the effective diffusion coefficients, rather than variability between diffusing species, size, and charge. The highest predictability in determining a value of D_e occurs when both matrix porosity and log permeability are known, with log permeability the most important predictive variable.

The following equation defines their linear regression relationship based on porosity and permeability values and diffusion cell results (Reimus et al. 2002 [DIRS 163008], p. 2.25):

$$\log_{10}(D_e) = -3.49 + 1.38\phi_m + 0.165(\log_{10} k_m) \quad \text{(Eq. 6-19)}$$

where D_e is in units of cm^2/s and k_m is matrix permeability [L^2] in units of m^2.

Again, using matrix properties based on Flint's hydrostratigraphic subdivisions (denoted as hydrogeologic units in this report), the variability in D_e can be calculated using Equation 6-19 and the following inputs:

- Find the maximum and minimum geometric mean permeability in DTN: MO0109HYMXPROP.001 [DIRS 155989] within the Flint-defined set of hydrostratigraphic units (listed as hydraulic conductivities in DTN: MO0109HYMXPROP.001 [DIRS 155989], then converted to permeability).

- Determine the maximum and minimum average porosity within the Flint-defined set of hydrostratigraphic units (listed as relative-humidity porosities in DTN: MO0109HYMXPROP.001 [DIRS 155989]).

The highest mean log permeability is −13.25, and is located in the Calico Hill-vitric unit (a subunit of the SZ HFM Unit 14), the lowest mean log permeability is −19.39, and is located in unit TLL (a subunit of SZ HFM Unit 15). The largest porosity, 0.321, is located in the Calico Hill-vitric unit; the smallest porosity, 0.042, is located in unit TC (Tiva Canyon Tuff).

The variation in D_e, using Equation 6-19 and average maximum and minimum permeabilities and porosities values, expressed as a ratio of maximum to minimum estimated D_e, is as:

$$\frac{5.84\times10^{-6} cm^2/s}{2.34\times10^{-7} cm^2/s} = 25 \quad \text{(Eq. 6-20)}$$

Variability from Ionic Radius and Charge

Empirical correlations exist in the literature to adjust free diffusion coefficients dependent on species size and charge. For this analysis, general guidance provided by Newman (1973 [DIRS 148719], Table 75-1, p. 230), which lists diffusion coefficients for ions and cations of varying charges and size, is adopted in the scaling of radionuclide diffusion coefficients.

Diffusion coefficients listed for the simple monovalent ions Br^- and I^- are the largest values listed by Newman. Consequently, diffusion coefficient scaling factors for all other ions and cations are relative to those listed for Br^- and I^-. The rationale for specific scaling factors is given below.

1. Simple monovalent cations tend to be more hydrated than anions, resulting in larger effective radii than anions, and concomitantly, diffusion coefficients are about 0.90 and 0.95 times that of simple monovalent anions such as Br^- and I^-. PuO_2^+ and NpO_2^+ would fall into this category, since they both have relatively low charge-to-mass ratios and should not be highly hydrated.

2. Cations, such as Na^+ and Li^+, with high charge-to-mass ratios have a diffusion coefficient between 0.65 and 0.5 times that of Br^- and I^-.

3. Multivalent anions (which are generally multiatom species) tend to have diffusion coefficients of 0.4 to 0.6 times that of Br^- and I^-.

4. Multivalent cations have diffusion coefficients between 0.3 to 0.4 times that of Br^- and I^-.

5. Diffusion coefficients of organic molecules can be considered reasonable lower bounds for diffusion coefficients of large anionic radionuclide complexes. An example is the large monovalent anions, such as pentafluorobenzoate, which have diffusion coefficients about 0.33 times that of Br^- and I^- (Callahan et al. 2000 [DIRS 156648], Tables 5 and 6, p. 3553).

6. Cations with charges of +3 typically hydrolyze or form complexes in solution, resulting in a lower charge and higher mass species (e.g., hydroxyl or carbonate complexes). Consequently, the multivalent and complexed species could diffuse between 0.3 and 0.25 times that of Br^- and I^-.

Concluding from the above, the variation between the diffusion coefficients for simple and relatively small monovalent ions and the larger multivalent complexed cations can be as much as:

$$\frac{1}{0.25} = 4.0 \qquad \text{(Eq. 6-21)}$$

The variability in D_e due to ionic charge and species size can be as much as a factor of 4.0.

Variability from Temperature

The uncertainty and variability in diffusion due solely to temperature variations (over space and time) will affect all contaminants equally. Hence, the uncertainty in temperature will not affect the decision to use a single diffusion coefficient. The Stokes-Einstein relationship can be used to approximate the molecular diffusion of ions in water with concentrations of ions as high as seawater and with temperatures ranging from 0°C to 100°C (Li and Gregory 1974 [DIRS 129827], p. 704; (Simpson and Carr 1958 [DIRS 139449], p. 1201). Using the Stokes-Einstein relationship, the molecular diffusion coefficient for a given temperature can be estimated as a function of the diffusion coefficient at a reference absolute temperature (T_0) and the relative change in temperature and water viscosity, (η) [M/(LT)] (Li and Gregory 1974 [DIRS 129827], p. 704):

$$D_0(T_1) = \frac{T_1}{T_0}\frac{\eta_0}{\eta_1}D_0(T_0) \qquad \text{(Eq. 6-22)}$$

Given the maximum potential range in temperature for the Yucca Mountain groundwater along the transport pathway of 20°C to 50°C (293.15 K to 323.15 K), based on the ambient geothermal gradient and range in depth to the shallow SZ and the viscosity of water at those temperatures (Viswanath and Natarajan 1989 [DIRS 129867], p. 714), Equation 6-22 can be rewritten and solved as follows:

$$\frac{D_0(T_1)}{D_0(T_0)} = \frac{T_1}{T_0}\frac{\eta_0}{\eta_1} = \frac{323.15K}{293.15K}\frac{1.007Ns/m^2}{0.516Ns/m^2} = 2.15 \qquad \text{(Eq. 6-23)}$$

Thus, D_0 can vary by a factor of about 2.2 due to changes in water temperature.

<u>Effective Diffusion Coefficients for Yucca Mountain Volcanic Units</u>

Given the above arguments, it is demonstrated that the largest variability in D_e is due to differences in lithology. The variability in D_e using Equation 6-19 is not as high as that derived using Equation 6-17. However, Equation 6-19 will be adopted in deriving the uncertainty distribution of D_e for the following reasons:

1. Because Equation 6-19 is derived based on site-specific data, it is more appropriate in determining the range of D_e due to lithology specific to Yucca Mountain.

2. A large number of permeability and porosity measurements are taken from the SZ hydrogeologic units where flow is expected to take place. Averages of these measurements can be used as input to Equation 6-19.

3. Using maximum and minimum averages from matrix porosity and permeability as input yields a range in D_e that approaches that of the few laboratory-derived D_e measurements specific to Yucca Mountain tuffs for TcO_4^- (1.0×10^{-7} to 2.0×10^{-6}) and HTO^- (1.2×10^{-7} to 3.5×10^{-6}) (see Triay et al. 1993 [DIRS 145123]); Rundberg et al. 1987 [DIRS 106481]) as indicated on the "Flint_Reim_TrRnd" spreadsheet in the EXCEL workbook *Eff_MtrxDif_11.xls* file (DTN: SN0306T0502103.006).

The CDF for uncertainty in the effective diffusion coefficient used in this analysis is derived as follows:

1. Mean porosity and permeability values (calculated from values found in DTN: MO0109HYMXPROP.001 [DIRS 155989]) were calculated for the volcanic hydrostratigraphic units TC, TR, TUL, TMN, TLL, TM2, TM1, CHV, CHZ, PP4, PP3, PP2, PP1, BF3, and BF2, defined by Flint (1998 [DIRS 100033]). These are

subunits of the more broadly defined SZ HFM Units 11, 12, 13, 14, and 15, and are units where flow and transport are expected to take place. Mean porosity and permeability values are given on the spreadsheets "LVA (12 &11)", "LVA (13)", "UVC (14)", and "UVA (15)" in the EXCEL file *Eff_MtrxDf_11.xls* (DTN: SN0306T0502103.006).

2. A CDF for D_e was calculated with Equation 6-19, using the mean permeability and porosity values for the above hydrostratigraphic units as input. These values are given on the spreadsheet "drns_all_straight", (Column AG, Rows 34 through 49) in the EXCEL file *Eff_MtrxDf_11.xls* (DTN: SN0306T0502103.006).

3. The derived CDF was then scaled down to account for the variability in D_e (to account for ionic charge and size). The scaling factors used are: 1) 0.9, to represent diffusion of simple monovalent cations, 2) 0.65 and 0.50, to represent cations with a high charge-to-mass ratios, 3) 0.3, to represent large monovalent anions, and 4) 0.25, to represent multivalent and complexed cations (Figure 6-14). Note the rationale for the above scaling factors is discussed in the subsection "Variability from Ionic Radius and Charge". These values are given on the spreadsheet "drns_all_straight" in the EXCEL file *Eff_MtrxDf_11.xls* (Column AG, Rows 50 through 109) (DTN: SN0306T0502103.006). The resulting CDF yields a distribution given in Figure 6-14, with a range in log space of –5.3 to –7.12 cm^2/s. The range captures laboratory ^3HHO and TcO_4^- measured values of D_e on Yucca Mountain tuffs reported by Triay et al. (1993 [DIRS 145123]) and Rundberg et al. (1987 [DIRS 106481]) and ^3HHO, TcO_4, and ^{14}C D_e reported by Reimus et al. (2002 [DIRS 163008]) and Reimus et al. (2003 [DIRS 162950]). Additionally, this range incorporates the interpreted diffusion coefficients (6.0×10^{-6} cm^2/s and 1.3×10^{-7} cm^2/s) derived from field tests using Br^-, PFBA (a fluorinated organic acid) as the diffusing species (Reimus et al. 2003 [DIRS 162950]).

The distribution for the derived values of effective diffusion coefficient using Equation 6-19 is about half an order of magnitude lower than the distribution of values from laboratory and field results. This is because the derived distribution scales the effective diffusion coefficient to take into account species not measured in laboratory or field experiments, as described in step 3, above. The lowest values of effective diffusion coefficient are those for hydrolyzed or complexed ions having a low charge and high mass, which would have diffusion coefficients about 0.25 times the values for Br^- and I^- ions.

To account for uncertainties in D_e at the lower end, the uncertainty range is expanded to span a full 2 orders of magnitude (log D_e –5.3 to –7.3 with D_e in units of cm^2/s), with the 50-percentile log D_e set at –6.3. When converted to m^2/s, it results in a log D_e (m^2/s) range of –9.3 to –11.3, with the 50-percentile log D_e set at –10.3 (see Figure 6-15). The effective matrix diffusion coefficient is determined for a particular realization by the parameter DCVO. See Table 6-8 for the associated probabilities for the effective matrix diffusion coefficient CDF.

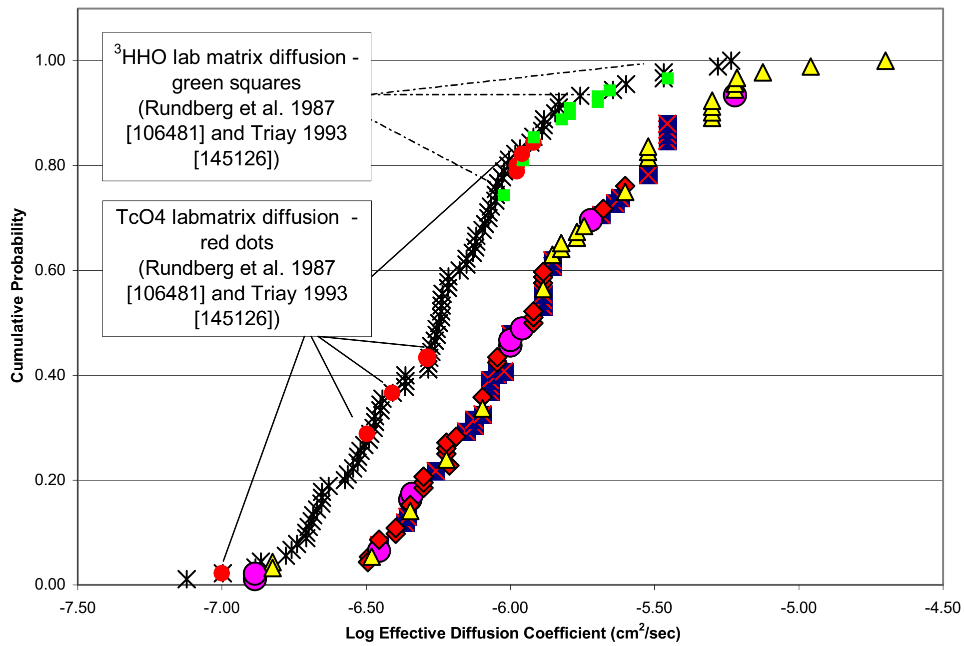

Output DTN: SN0306T0502103.006.

NOTE: The CDF to the left represents values of effective diffusion coefficient derived using Equation 6-19 (black asterisks). Included in the plot are laboratory measurements of effective diffusion coefficient from Triay 1993 [DIRS 145123] and Rundberg et al. 1987 [DIRS 106481] to demonstrate the reasonableness of the derived values of effective diffusion coefficient. The CDF to the right represents laboratory and field-derived values.
Yellow Triangles – ^{14}C laboratory values;
Blue Squares – ^{3}HHO laboratory values;
Red Diamonds – TcO_4 laboratory values;
Purple Circles – Br^- and PFBA field values
(Reimus et al. 2002 [DIRS 163008]; Reimus et al. 2003 [DIRS 162950]).

Figure 6-14. CDFs of Data Used in the Assessment of Uncertainty in Effective Diffusion Coefficient

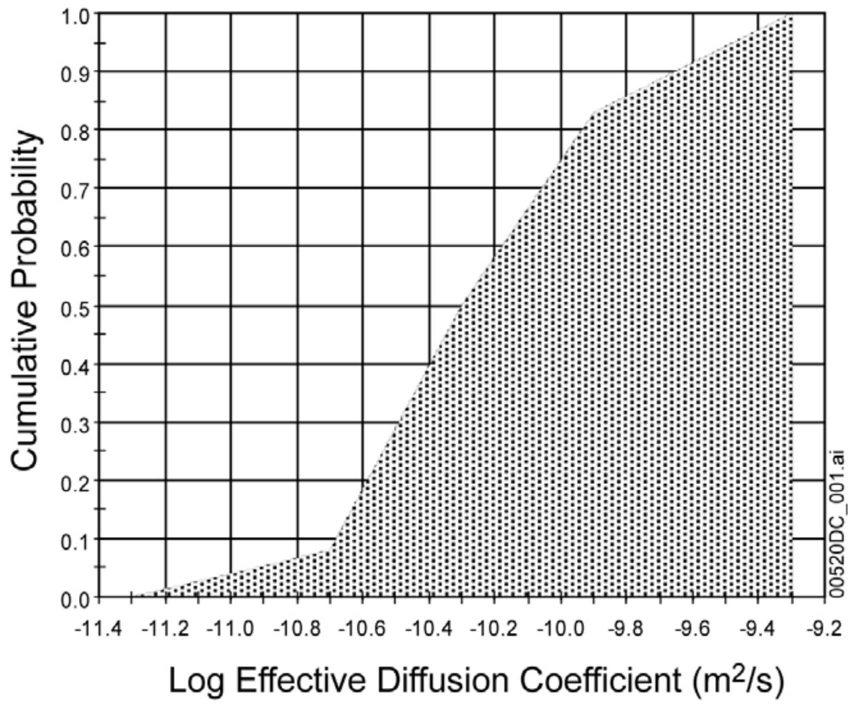

Output DTN: SN0310T0502103.009.

Figure 6-15. CDF of Uncertainty in Effective Diffusion Coefficient

6.5.2.7 Bulk Density of Alluvium

For the TSPA-SR, the dry bulk density was considered to be a constant, and set to 1.27 g/cm^3 (CRWMS M&O 2000 [DIRS 147972], Section 6.9). The basis for this parameter value is a set of tests performed on four five-foot alluvial intervals from each of the EWDP Boreholes 2D, 9S, and 3S, at depths of 395 to 415 feet, 145 to 165 feet, and 60 to 80 feet, respectively (DTN: LA0002JC831341.001 [DIRS 147081]). These samples were drill cuttings and thus highly disturbed from their condition in the aquifer. The range of the dry bulk density values in laboratory columns packed with alluvium from these wells was 1.2 to 1.3 g/cm^3. The data are presented in *Unsaturated Zone and Saturated Zone Transport Properties (U0100)* (CRWMS M&O 2000 [DIRS 152773], p. 86) with a note stating that densities were measured in the laboratory and do not represent in situ conditions.

The values used in the TSPA-SR were low compared to dry bulk densities measured in alluvium at Frenchman Flat and the NTS near Yucca Mountain (Howard 1985 [DIRS 153266], Table 3, p. 31, and Table A-1, p. 38). Similarly, a comparison to the range of dry bulk densities of alluvial material in general (Manger 1963 [DIRS 154474], pp. E41 to E42) led to the conclusion that the values used in the TSPA-SR were likely an underestimate of the true bulk density. Consequently, bulk density in the alluvium and its uncertainty has been reevaluated using data from the Yucca Mountain area that have been measured at a larger, more representative scale.

The dry bulk density of the alluvium is used in the computation of the retardation of sorbing radionuclides. The dry bulk density is related to the matrix retardation coefficient as indicated in Equation 6-2.

Borehole gravimeter surveys were conducted by EDCON (2000 [DIRS 154704], pp. 1 to 23) at well EWDP-19D1 directly south of Yucca Mountain near U.S. Highway 95. A total of 36 values of saturated bulk density were estimated, based on the geophysical measurements taken from this well (EDCON 2000 [DIRS 154704], p. 3). Seventeen measurements were taken from a depth corresponding to the inferred depth of the flow path through the alluvium near Yucca Mountain (401.5 to 776 feet). The wet bulk density computed from gravimeter measurements is presented in Table 6-11, and also includes the porosity and dry bulk density computed from Freeze and Cherry (1979 [DIRS 101173], p. 337):

$$\phi_T = \frac{\rho_{\text{sat}} - \rho_{\text{grain}}}{\rho_{\text{w}} - \rho_{\text{grain}}} \qquad \text{(Eq. 6-24)}$$

$$\rho_{\text{b}} = \rho_{\text{grain}}(1 - \phi_T) \qquad \text{(Eq. 6-25)}$$

where ρ_{sat} is the saturated bulk density [M/L^3], ρ_{grain} is the average grain density for these samples [M/L^3] (2.52 g/cm^3), and ρ_{w} is the density of water (1.0 g/cm^3).

The average grain density was computed to be 2.52 g/cm^3 (2520 kg/m^3) from alluvial samples from other boreholes in the vicinity of Yucca Mountain (USGS n.d. [DIRS 154495], pp. 3 to 4). The grain density varied little (2.49 to 2.55 g/cm^3), and so the average was used in the computation of the porosity and dry bulk density.

The mean dry bulk density for this set of measurements was 1.91 g/cm^3 (1910 kg/m^3). This value is close to dry bulk density values previously measured at Frenchman Flat and the NTS in similar material at similar depth (Howard 1985 [DIRS 153266], Table 3, p. 31, and Table A-1, p. 38), and it is the value used as the mean in the uncertainty distribution. The computed standard deviation for these measurements is 0.078 g/cm^3. A normal distribution was selected to characterize the uncertainty in the dry bulk density based on the frequency plot shown in Figure 6-16. The relatively large volume of the medium interrogated by the borehole gravimeter method suggests that the variability observed is appropriate for the uncertainty in this parameter at the scale of individual grid cells in the SZ flow and transport abstraction model. The CDF of uncertainty in bulk density of the alluvium is shown in Figure 6-17. The bulk density in the alluvium is specified for a particular realization by the parameter bulk density.

Table 6-11. Measured Saturated Density, Computed Porosity, and Computed Dry Bulk Density for Depths from 402 to 776 Feet Below the Surface at the Nye County Well EWDP-19D1

Sample Depth (ft)	Drift-Corrected Saturated Bulk Density, ρ_{sat} (g/cm^3)	Computed Total Porosity, ϕ_T	Computed Dry Bulk Density, ρ_b (g/cm^3)
402	2.231	0.190	2.04
422	2.156	0.239	1.92
442	2.180	0.224	1.96
485	2.163	0.235	1.93
505	2.174	0.228	1.95
525	2.214	0.201	2.01
569.95	2.148	0.245	1.90
589.9	2.142	0.249	1.89
610	2.105	0.273	1.83
630	2.079	0.290	1.79
649.95	2.077	0.291	1.79
669.95	2.133	0.255	1.88
690	2.121	0.262	1.86
715.95	2.158	0.238	1.92
736	2.143	0.248	1.90
756	2.105	0.273	1.83
776	2.239	0.185	2.05

Source: DTN: MO0105GPLOG19D.000 [DIRS 163480].

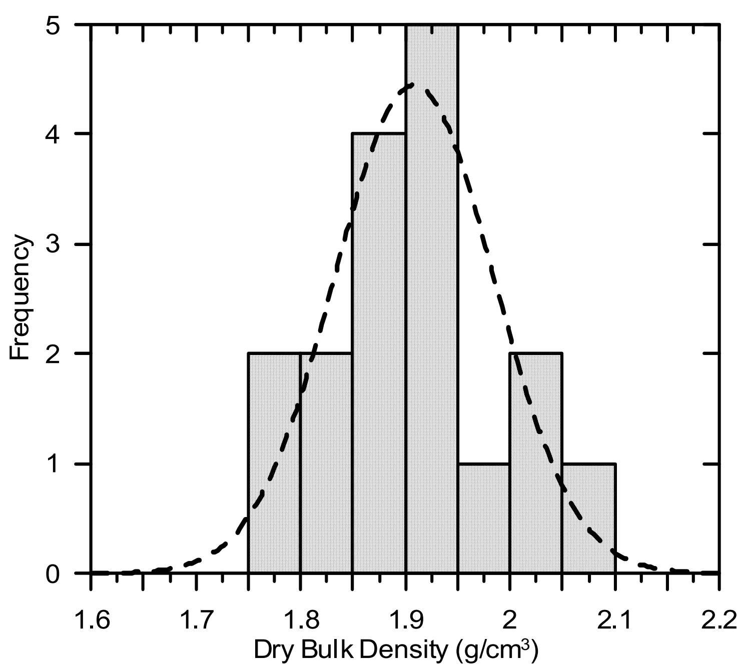

NOTE: Normal distribution fit to the data shown with the dashed line.

Figure 6-16. Histogram of Dry Bulk Density from Borehole Gravimeter Data

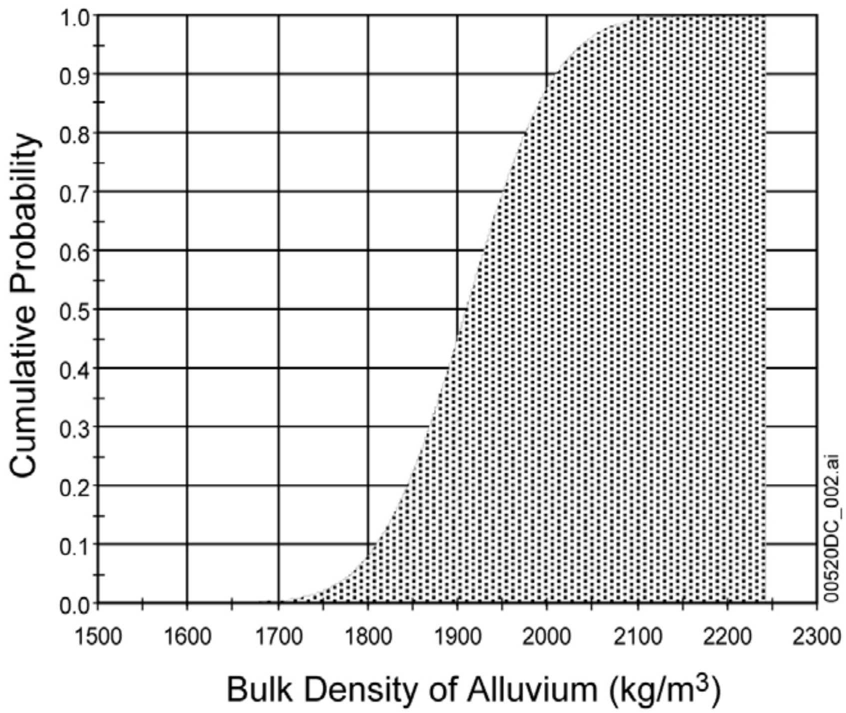

Output DTN: SN0310T0502103.009.

Figure 6-17. CDF of Uncertainty in Bulk Density of Alluvium

6.5.2.8 Sorption Coefficients

Sorption, or adsorption, is the process by which dissolved radionuclides temporarily adhere or bond to rock and alluvial substrate along a transport path. Sorption occurs because of the electrochemical affinity between the dissolved species and the substrate. The significance of sorption to the SZ flow and transport abstraction model and the SZ 1-D transport model is that sorption results in a retardation of the radionuclide because part of the radionuclide transport time is spent on an immobile surface.

A linear, equilibrium, sorption coefficient, K_d, is considered appropriate for the radionuclides that exhibit sorption during transport because of experimental observations that establish the adequacy of this approach. The K_d model also depends on chemical equilibrium between the aqueous phase and sorbed phase of a given species.

The K_d relationship is defined as follows (Domenico and Schwartz 1990 [DIRS 100569], p. 441):

$$S = K_d C \qquad \text{(Eq. 6-26)}$$

where S [moles/M] is the mass sorbed on the surface of the substrate, and C [moles/L^3] is the concentration of the dissolved mass. The K_d model determines transport retardation as described earlier per Equation 6-2.

A detailed discussion of the uncertainty distributions for sorption coefficients used in the SZ flow and transport abstraction model and the SZ 1-D transport model is given in *Site-Scale*

Saturated Zone Transport (BSC 2004 [DIRS 170036], Appendix A). The documentation provided by *Site-Scale Saturated Zone Transport* (BSC 2004 [DIRS 170036], Appendix A) includes the technical bases for the values of sorption coefficient for the relevant radionuclides in volcanic units and alluvium at Yucca Mountain.

6.5.2.9 Dispersivity

Longitudinal dispersion is the mixing of a solute in groundwater that occurs along the direction of flow. This mixing is a function of many factors, including the relative concentrations of the solute, the velocity pattern within the flow field, and the host rock properties. An important component of this dispersion is the dispersivity, a coarse measure of solute (mechanical) spreading properties of the rock. The dispersion process causes spreading of the solute in directions transverse to the flow path, as well as in the longitudinal flow direction (Freeze and Cherry 1979 [DIRS 101173], p. 394). Longitudinal dispersivity will be important only at the leading edge of the advancing plume; transverse dispersivity (horizontal transverse and vertical transverse) is the strongest control on plume spreading and possible dilution within the aquifer (CRWMS M&O 1998 [DIRS 100353], p. LG-12).

Temporal changes in the groundwater flow field can significantly increase the apparent dispersivity displayed by a contaminant plume, particularly with regard to transverse dispersion. However, observations of water levels in wells at Yucca Mountain have not indicated large or consistent variations (Luckey et al. 1996 [DIRS 100465], pp. 29 to 32), suggesting that transience in the SZ flow system would not lead to much greater dispersion. The thick UZ in the area of Yucca Mountain likely dampens the response of the SZ flow system to seasonal variations or transience in infiltration on time scales of less than centuries.

These dispersivities (longitudinal, vertical transverse, and horizontal transverse) are used in the advection-dispersion equation governing solute transport, and are implemented into the SZ flow and transport abstraction model as stochastic parameters. Recommendations from the SZ expert elicitation were used as the basis for determining the distribution for longitudinal and transverse dispersivity. This expert elicitation was conducted in a manner consistent with *Branch Technical Position on the Use of Expert Elicitation in the High-Level Radioactive Waste Program* (Kotra et al. 1996 [DIRS 100909]). As part of the expert elicitation, Dr. Lynn Gelhar provided statistical distributions for longitudinal dispersivity at 5 km and 30 km (CRWMS M&O 1998 [DIRS 100353], p. 3-21). These distributions for longitudinal dispersivity are consistent with his previous work (Gelhar 1986 [DIRS 101131], pp. 135s to 145s). *Modeling Sub Gridblock Scale Dispersion in Three-Dimensional Heterogeneous Fractured Media* (CRWMS M&O 2000 [DIRS 152259], p. 53) provided estimates of the transverse and longitudinal dispersion that can occur at the subgridblock scale within the SZ site-scale model. The estimation of dispersivity using subgridblock scale modeling is also described by McKenna et al. (2003 [DIRS 163578]). The results from the subgridblock scale modeling (CRWMS M&O 2000 [DIRS 152259], p. 55) are in general agreement with the estimates by the expert elicitation panel (CRWMS M&O 1998 [DIRS 100353], p. 3-21). However, there is a significant difference in the spatial scale at which the analyses in *Modeling Sub Gridblock Scale Dispersion in Three-Dimensional Heterogeneous Fractured Media* (CRWMS M&O 2000 [DIRS 152259]) were conducted (500 m) and the scales at which the expert elicitation (CRWMS M&O 1998 [DIRS 100353]) estimates were made

(5 km and 30 km). Nonetheless, both sources of information on dispersivity are mutually supportive.

In the SZ flow and transport abstraction model, the longitudinal dispersivity parameter is sampled as a log-transformed parameter, and the transverse dispersivities are then calculated as indicated by *Saturated Zone Flow and Transport Expert Elicitation Project* (CRWMS M&O 1998 [DIRS 100353], p. 3-21), according to the following relationships:

$$\alpha_h = \frac{\alpha_L}{200} \qquad \text{(Eq. 6-27)}$$

$$\alpha_v = \frac{\alpha_L}{20000} \qquad \text{(Eq. 6-28)}$$

where α_L is the longitudinal dispersivity [L], α_h is the transverse horizontal dispersivity [L], and α_v is transverse vertical dispersivity [L].

The longitudinal dispersivity is specified for a particular realization by the parameter LDISP. The statistical distribution is a lognormal distribution: E[$\log_{10}(\alpha_L)$]: 2.0 and S.D.[$\log_{10}(\alpha_L)$]: 0.75. The CDF of uncertainty in longitudinal dispersivity is shown in Figure 6-18.

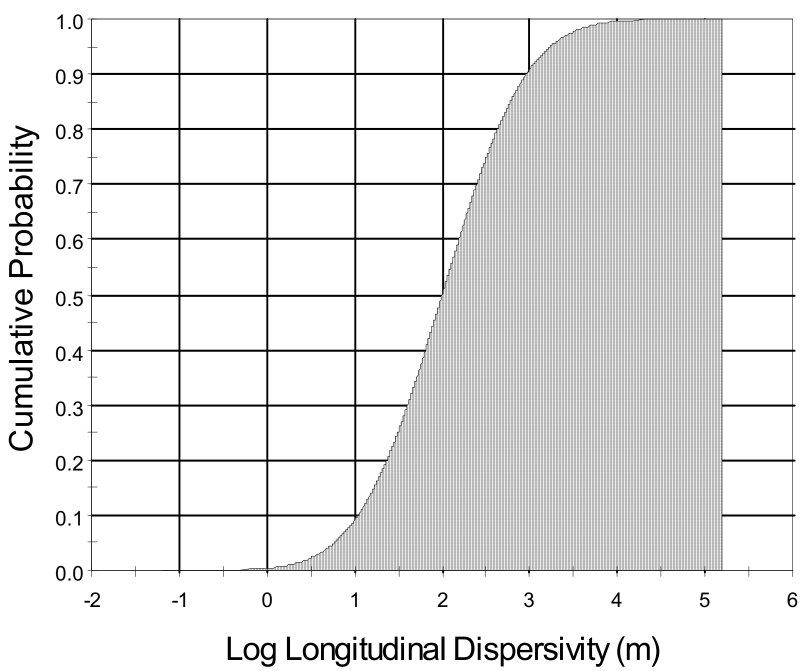

Output DTN: SN0310T0502103.009.

Figure 6-18. CDF of Uncertainty in Longitudinal Dispersivity

Effective Longitudinal Dispersivity in the SZ Flow and Transport Abstraction Model

Longitudinal dispersivity for radionuclide transport simulations in the SZ flow and transport abstraction model is specified as a transport parameter. The dispersion process is simulated by the random-walk displacement algorithm on the local scale for each time step in the transport simulation. In addition, the spatial distribution of hydrogeologic units of contrasting permeability within the model imparts additional dispersion to the simulated transport of particles as the flow paths diverge to adjacent grid cells of contrasting permeability during transport. The effective longitudinal dispersivity simulated by the SZ flow and transport abstraction model can be significantly larger than the specified value due to the additive effects of these two processes.

The effective longitudinal dispersivity in the SZ flow and transport abstraction model is analyzed for a range of values of specified longitudinal dispersivity to evaluate this effect. A point source beneath the repository is used for the analysis. Neither sorption nor matrix diffusion is included in the simulations. Effective longitudinal dispersivity is estimated using the relationship from Kreft and Zuber (1978 [DIRS 107306]):

$$\alpha_L = \frac{L_f}{2}\left(\frac{\sigma_t}{m_t}\right)^2 \qquad \text{(Eq. 6-29)}$$

where L_f is the flow path length [L], σ_t is the standard deviation in travel time [T], and m_t is the mean travel time [T]. The standard deviation is estimated from the particle mass breakthrough curve at an 18-km distance by taking the difference in time between the arrival of 0.159 fraction of the mass (the mean minus one standard deviation for a Gaussian distribution) and the arrival of 0.841 fraction of the mass (the mean plus one standard deviation for a Gaussian distribution), and dividing by 2. The mean travel time is estimated using the arrival time of 0.500 fraction of the mass.

The results of this analysis are shown in Figure 6-19, with the plotted open circles. The effective simulated longitudinal dispersivity is consistently about one order of magnitude higher (bold red dashed line) than the specified longitudinal dispersivity (for values of specified longitudinal dispersivity of less than 1,000 m). These results indicate that the heterogeneous distribution of permeability in the SZ flow and transport abstraction model in the region along the flow path is contributing approximately one order of magnitude of dispersivity relative to the specified value.

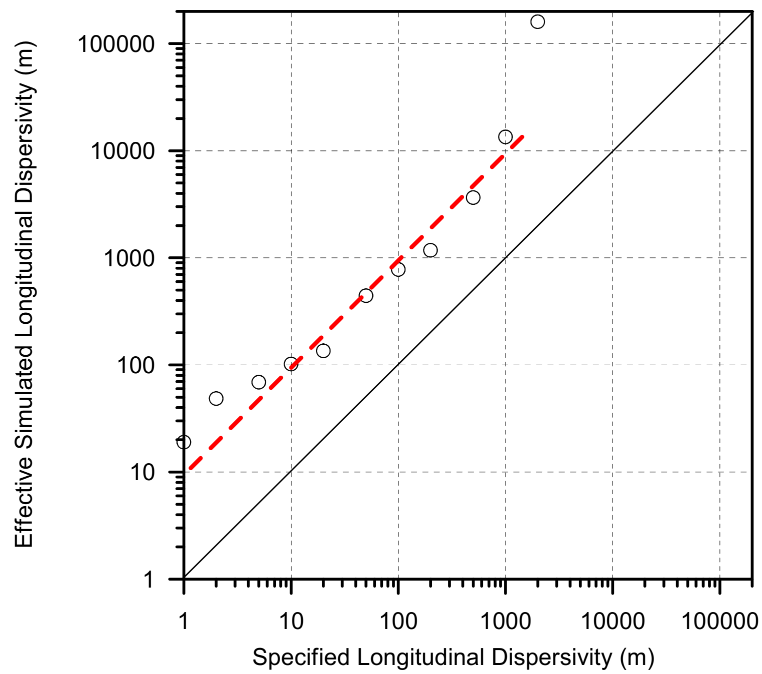

Figure 6-19. Effective Simulated Longitudinal Dispersivity Versus the Specified Longitudinal Dispersivity in the SZ Flow and Transport Abstraction Model

These results indicate that the effective longitudinal dispersivity in the SZ flow and transport abstraction model is significantly higher than the value input to the model. In order to avoid the excessive effective dispersion in the SZ flow and transport abstraction model, the input value of longitudinal dispersivity can be reduced. Based on these results, the value of specified longitudinal dispersivity used in the SZ flow and transport abstraction model for the TSPA-LA abstraction simulations is adjusted to yield the correct value of effective simulated longitudinal dispersivity. This is accomplished by scaling the input value of longitudinal dispersivity down by one order of magnitude (i.e., dividing the longitudinal dispersivity by 10) in the input files for each realization.

6.5.2.10 Horizontal Anisotropy in Permeability

Although a detailed description of the analysis and derivation of the distribution of anisotropy ratio in the SZ near the C-wells complex is presented in the *Saturated Zone In Situ Testing* report (BSC 2004 [DIRS 170010], Section 6.2.6), some background information and a short summary are presented here. Interpretation of well test data with analytical solutions consists of inferring the hydraulic properties of the system from its measured responses, based on an assumed flow geometry (i.e., radial). The problem becomes more complicated, however, when the system geometry cannot be specified with reasonable certainty. In a layered sedimentary system lacking extreme heterogeneity, flow might reasonably be expected to be radial during a hydraulic test. When hydraulic tests are conducted at some arbitrary point within a 3-D fractured rock mass, however, the flow geometry is complex. Radial flow would occur only if the test were performed in a single uniform fracture of effectively infinite extent, or within a network of fractures confined to a planar body in which the fractures were so densely interconnected that the network behaves like an equivalent porous medium. More likely, flow in fractured tuff is nonradial and variable, as fracture terminations and additional fracture intersections were reached. Therefore, it must be emphasized that assumptions required in the analytical treatment of anisotropy may not be strictly consistent with site geology.

Through the fractured tuff and alluvium near Yucca Mountain, there is significant heterogeneity in hydraulic properties, which not only vary spatially, but also differ depending upon the direction in which they are measured (both horizontally and vertically). In the fractured volcanic units near Yucca Mountain, preferential orientation of open fractures and/or faults can possibly impart significant anisotropy in horizontal permeability to the groundwater flow system. The uncertainty in horizontal anisotropy in permeability implicitly accounts for potential undetected features, such as fault and fracture zones, that impart preferential directional flow to groundwater. In this analysis, transmissivity and storativity are the hydrologic parameters required to calculate and define large-scale anisotropy, and their measured values reflect the heterogeneity of the media. The concept of anisotropy is typically associated with a homogeneous medium—a criterion not met here. Nevertheless, there are clearly spatial and directional variations in transmissivity, and the notion remains that, over a large enough representative elementary volume, there exists a preferential flow direction that can be termed anisotropy.

Data from the long-term pumping test conducted from May 8, 1996, to November 12, 1997, were used to evaluate the anisotropy in the vicinity of the C-wells complex in *Saturated Zone In-Situ Testing* (BSC 2004 [DIRS 170010], Section 6.2.6). After filtering the drawdown data in response to pumping at UE-25 c#3, transmissivity and storativity were calculated at four distant wells (USW H-4, UE-25 ONC1, UE-25 wt#3, and UE-25 wt#14).

A distribution of anisotropies must be specified so that an anisotropy ratio can be selected for each of the 200 stochastic model realizations used as input to the SZ flow and transport abstraction model. Because the current version of the FEHM V2.20 software code [DIRS 161725] can only implement anisotropy oriented in alignment with the grid direction, principal directions discussed above are not directly applicable in the model. The net result of being unable to specify a principal direction is that uncertainty in the anisotropy ratio increases. For example, the analytical result for anisotropy using the Cooper-Jacob (1946 [DIRS 150245]) method is a ratio of 3.3 in a direction 15º east of north. A projection that orients the principal direction north-south (0º) results in a new anisotropy ratio of 2.5. In fact, this line of reasoning suggests that it is possible for the projected north-south anisotropy ratio to be significantly less than one.

Based on consultations with United States Geological Survey (USGS) staff and with the YMP Parameters Team, and on scientific judgment and results from the analytical anisotropy analyses, Figure 6-20a represents the best estimate of the PDF for the anisotropy ratio (north-south/east-west) in the SZ near the C-wells complex. Figure 6-20b is the corresponding CDF.

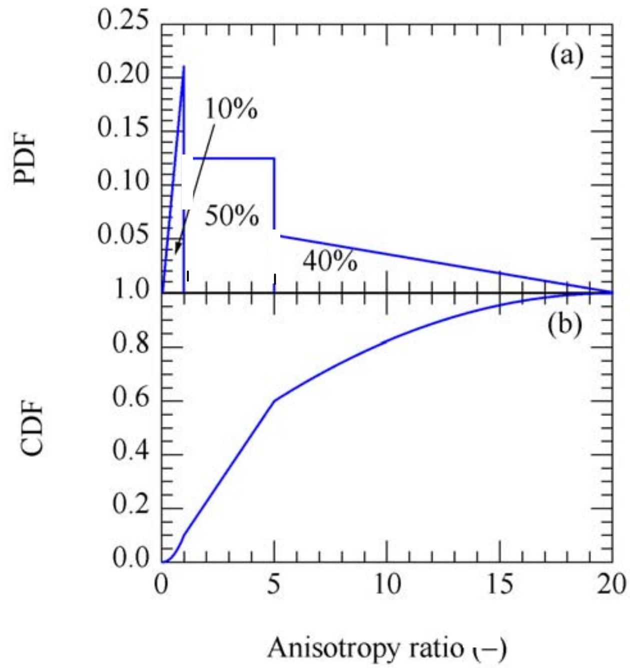

Source: DTN: SN0302T0502203.001 [DIRS 163563].

Figure 6-20. Probability Density Function (a) and Corresponding CDF (b) for the Uncertainty in North-South/East-West Anisotropy Ratio

There are several noteworthy points based on three distinct regions of the anisotropy ratio distribution (DTN: SN0302T0502203.001 [DIRS 163563]).

- *Anisotropy ratio between 5 and 20*. The maximum anisotropy ratio of 20:1 is based upon the highest calculated anisotropy ratio of 17:1 reported by Ferrill et al. (1999 [DIRS 118941], p. 7). The maximum reported value of 17:1 was rounded to 20:1 and set as the upper limit for horizontal anisotropy. Furthermore, although features such as high transmissivity zones and fractures can yield very large anisotropy ratios locally, globally, their effects are attenuated, and 20 is a reasonable maximum. The 5.5 anisotropy ratio calculated by the second approach of the modified Papadopulos-PEST method (see *Saturated Zone In-Situ Testing* (BSC 2004 [DIRS 170010], Section 6.2.6)) lies in this range, near its highest probability point. Therefore, between 5 and 20, a triangular distribution of anisotropy ratio is constructed that decreases to zero probability at 20. A 40-percent probability is assigned to this portion of the probability density function.

- *Anisotropy ratio between 0.05 and 1*. Discussions among Sandia National Laboratories (SNL) and USGS staff established that, although it is likely the SZ is anisotropic with a principal direction approximately northeast, it is possible the media could be isotropic, as well as a small probability that the principal direction could be significantly different from north-northeast. Correspondingly, an anisotropy ratio of less than one is possible, and the minimum anisotropy ratio is set equal to the inverse of the maximum, 1:20, with a triangular distribution of 10 percent probability decreasing to zero at a ratio of 0.05.

An additional Papadopulos solution yielding an anisotropy ratio of 3.5 at 79 west of north (BSC 2004 [DIRS 170010], Section 6.2.6) falls in this range.

- *Anisotropy ratio between 1 and 5.* A uniformly distributed 50 percent probability is assigned to the range of anisotropy ratio between 1 and 5. This interval comprises the more likely values of anisotropy ratios, with no specific value more likely than any other. It should be noted that in a previous model of the SZ near Yucca Mountain (CRWMS M&O 2000 [DIRS 153246], Section 3.8.1.3), anisotropy was binomially distributed with a 50 percent probability of isotropy (1:1) and a 50 percent probability of a 5:1 ratio.

It is assumed that the potential anisotropy of permeability in the horizontal direction is adequately represented by a permeability tensor that is oriented in the north-south and east-west directions. This approach is carried forward from the *Saturated Zone In-Situ Testing* scientific analysis report (BSC 2004 [DIRS 170010], Section 6.2.6). The numerical grid in the SZ site-scale flow and transport model is aligned in the north-south and east-west directions, and values of permeability may only be specified in directions parallel to the grid. Analysis of the probable direction of horizontal anisotropy shows that the direction of maximum transmissivity may be about N 15° E, indicating that the anisotropy applied on the SZ flow and transport abstraction model grid is within approximately 15° of the inferred anisotropy.

Figure 6-20(a) and Figure 6-20(b) are the best estimates for the PDF and the CDF, respectively, of north-south anisotropy ratios in the SZ to be modeled with the FEHM V2.20 software code [DIRS 161725] in the SZ flow and transport abstraction model. Horizontal anisotropy in permeability is determined for a particular realization by the parameter HAVO.

6.5.2.11 Retardation of Colloids with Irreversibly Sorbed Radionuclides

For TSPA-LA, colloid-facilitated transport of radionuclides in the SZ is simulated to occur by two basic modes. In the first mode, radionuclides that are irreversibly attached to colloids are transported at the same rate as the colloids, which are themselves retarded by interaction with the aquifer material. In the second mode, radionuclides that are reversibly attached to colloids are in equilibrium with the aqueous phase and the aquifer material. In this mode of transport, the effective retardation of these radionuclides during transport in the SZ is dependent on the sorption coefficient of the radionuclide onto colloids, the concentration of colloids, and the sorption coefficient of the radionuclide onto the aquifer material. This section deals with the first mode of colloid-facilitated transport; Section 6.5.2.12 addresses the second mode.

The SZ flow and transport simulations of radionuclides that are irreversibly attached to colloids are conducted for radioisotopes of plutonium and americium. The retardation of colloids with irreversibly attached radionuclides is a kinetically controlled process, which approaches equilibrium behavior for long transport times. For transport of colloids through the SZ, equilibrium behavior is nearly achieved. However, nonequilibrium behavior results in unimpeded migration of some of the colloids. Consequently, a small fraction of these colloids is transported through the SZ with no retardation, whereas the larger fraction is delayed by a retardation factor. For the SZ flow and transport simulations, a small fraction of the radionuclide mass irreversibly attached to colloids is transported without retardation, and the remaining fraction of the radionuclide mass is retarded. A discussion of the fraction of colloids transported with no retardation is in *Saturated Zone Colloid Transport* (BSC 2004 [DIRS 170006], Section 6.6). The fraction of irreversibly sorbed to reversibly sorbed radionuclides is determined in the waste-form component of TSPA-LA, and is used as input to the SZ flow and transport abstraction model and the SZ 1-D transport model.

The processes important to the transport of irreversible colloids in the volcanic units of the SZ are as follows: advection and dispersion of colloids in the fracture water, exclusion of the colloids from the matrix waters, and chemical filtration or adsorption of the colloids onto the fracture surfaces.

Modeling of the advective/dispersive processes is handled as if the colloids were solute in the SZ flow and transport abstraction model and the SZ 1-D transport model. Matrix exclusion (i.e., colloid transport only in the fractures) in the volcanic units is considered to be appropriate because of the large size and small diffusivities of the colloids compared to the solute, plus the possibility of similar electrostatic charge of the colloids and the tuff matrix. Matrix exclusion is implemented by reducing the values of the effective diffusion coefficients for radionuclides (see Section 6.5.2.6 for a discussion of the solute diffusion coefficient) by 10 orders of magnitude, thus preventing essentially all matrix diffusion. Chemical (i.e., reversible) filtration of irreversible colloids is modeled by applying a retardation factor to the transport in the fractures. The implementation of the retardation factor in the SZ flow and transport abstraction model is described in Section 6.5.1.

Saturated Zone Colloid Transport (BSC 2004 [DIRS 170006], Section 6.4) describes the development of colloid retardation factors for fractured tuff from field and experimental data. Figure 6-21 shows the CDF used for retardation factors in the volcanic units for the SZ flow and transport abstraction model and Table 6-8 provides the associated probabilities. This CDF is based on the uncertainty distribution developed in *Saturated Zone Colloid Transport* (BSC 2004 [DIRS 170006], Table 6-2). A log cumulative probability distribution is used because the retardation factors span slightly more than two orders of magnitude. Retardation of colloids with irreversibly sorbed radionuclides in the volcanic units is specified for a particular realization by the parameter CORVO.

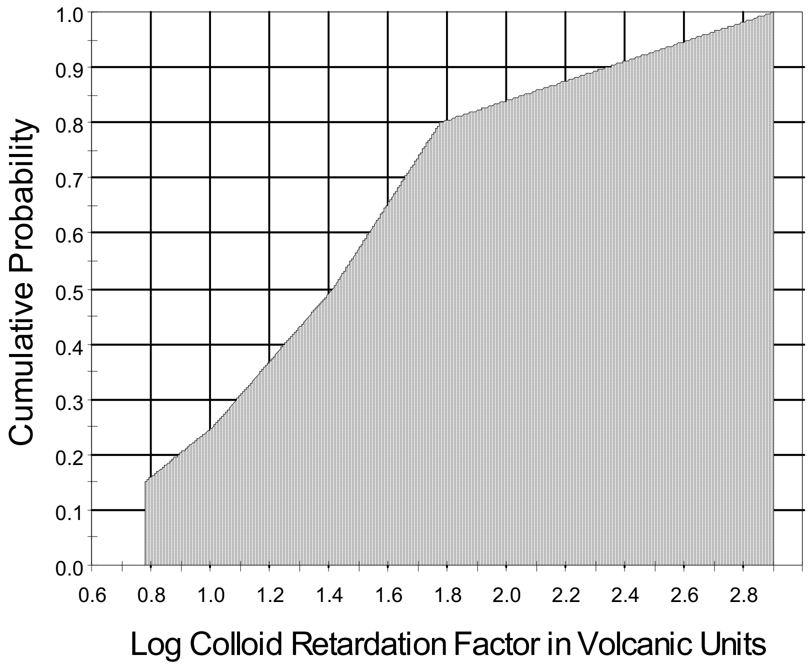

Source: DTN: LA0303HV831352.002 [DIRS 163558].

Figure 6-21. CDF of Uncertainty in Colloid Retardation Factor in Volcanic Units

The processes modeled for irreversible colloids in the alluvium are the same as those modeled for irreversible colloids in the volcanic units, with the exception of matrix exclusion, because the alluvium is modeled as a single porous medium. *Saturated Zone Colloid Transport* (BSC 2004 [DIRS 170006], Section 6.5) describes the development of colloid retardation parameters for the alluvium using experimental data specific to colloid transport in alluvial material from Yucca Mountain, as well as bacteriophage field studies in alluvial material, which are thought to be good analogues for colloid transport because of their colloidal size and passive transport characteristics. As with irreversible colloids in the volcanic units, filtration in the alluvium is modeled by applying a retardation factor to transport in the porous medium. Figure 6-22 shows the CDF used for retardation factors in the alluvium for the SZ flow and transport abstraction model, and Table 6-8 provides the associated probabilities. This CDF is based on the uncertainty distribution developed in *Saturated Zone Colloid Transport* (BSC 2004 [DIRS 170006], Table 6-3). A log cumulative probability distribution is used because the retardation factors span slightly more than three orders of magnitude. The implementation of the retardation factor in the SZ flow and transport abstraction model is described in Section 6.5.1. Retardation of colloids with irreversibly sorbed radionuclides in the alluvium is specified for a particular realization by the parameter CORAL.

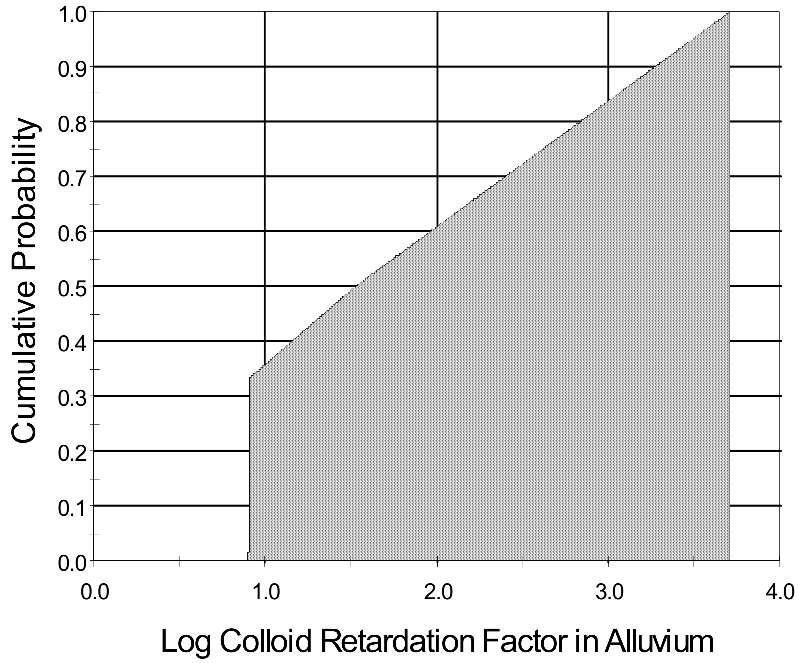

Source: DTN: LA0303HV831352.004 [DIRS 163559].

Figure 6-22. CDF of Uncertainty in Colloid Retardation Factor in Alluvium

6.5.2.12 Transport of Radionuclides Reversibly Sorbed on Colloids

Radionuclides that are reversibly sorbed onto colloids are modeled to be temporarily attached to the surface of colloids. Thus, these radionuclides are available for dissolution in the aqueous phase, and their transport characteristics are a combination of the transport characteristics of solute and colloids. The SZ flow and transport simulations of radionuclides that are reversibly attached to colloids are conducted for radioisotopes of plutonium, americium, thorium, protactinium, and cesium, which is consistent with the radionuclides selected for reversible sorption (BSC 2005 [DIRS 174290], Section 6.3.3.1). For these transport simulations, radioisotopes of plutonium are transported as one group, radioisotopes of americium, thorium, and protactinium are transported as a second group, and cesium is transported as a third species. Americium and plutonium can also be transported as irreversibly sorbed onto colloids; see Section 6.5.2.11.

The K_c parameter is a distribution coefficient that represents the equilibrium partitioning of radionuclides between the aqueous phase and the colloidal phase, as given in Equation 6-4. The K_c is a function of only radionuclide sorption properties, colloid substrate properties, and colloid mass concentration, and not any properties of the immobile media through which transport occurs; thus, the same K_c applies to transport of a radionuclide in both the volcanic units and the alluvium.

For TSPA-LA, the K_d^{coll} uncertainty distributions for plutonium, americium, thorium, protactinium, and cesium were developed in *Waste Form and In-Drift Colloids-Associated Radionuclide Concentrations: Abstraction and Summary* (BSC 2005 [DIRS 174290],

Table 6-6). Figures 6-23 to 6-25 show the uncertainty distributions input to the SZ transport abstraction model for sorption coefficients onto colloids.

The C_{col} uncertainty distribution was also developed in *Waste Form and In-Drift Colloids-Associated Radionuclide Concentrations: Abstraction and Summary* (BSC 2005 [DIRS 174290], Table 6-4) (see Figure 6-26). This distribution implements the uncertainty in the sampling probabilities for ionic strength less than 0.05 M, which corresponds to chemical conditions in the SZ. For ionic strengths greater than or equal to 0.05 M colloids are stipulated to be unstable (BSC 2005 [DIRS 174290], Section 6.3.2].

Retardation of colloids with reversibly sorbed radionuclides is determined for a particular realization by the following uncertain parameters:

- Conc_Col for groundwater colloid concentrations
- Kd_Cs_Col for cesium sorption coefficient onto colloids;
- Kd_Am_Col for americium, thorium, and protactinium sorption coefficients onto colloids
- Kd_Pu_Col for plutonium sorption coefficient onto colloids.

Implementation of the K_c model in the SZ flow and transport abstraction model is discussed in Section 6.5.1. Note that the values given for the parameter vectors of Kd_Pu_Col, Kd_Am_Col, and Kd_Cs_Col in Appendix A are the $\log_{10}$-transformed values.

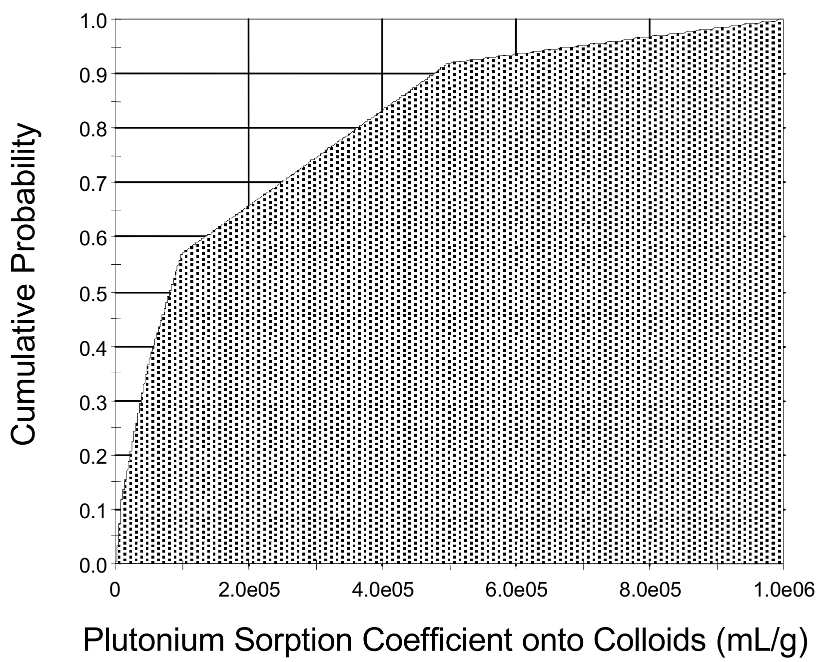

Source: DTN: SN0306T0504103.006 [DIRS 164131], Table 1.

Figure 6-23. CDF of Uncertainty in Plutonium Sorption Coefficient onto Colloids

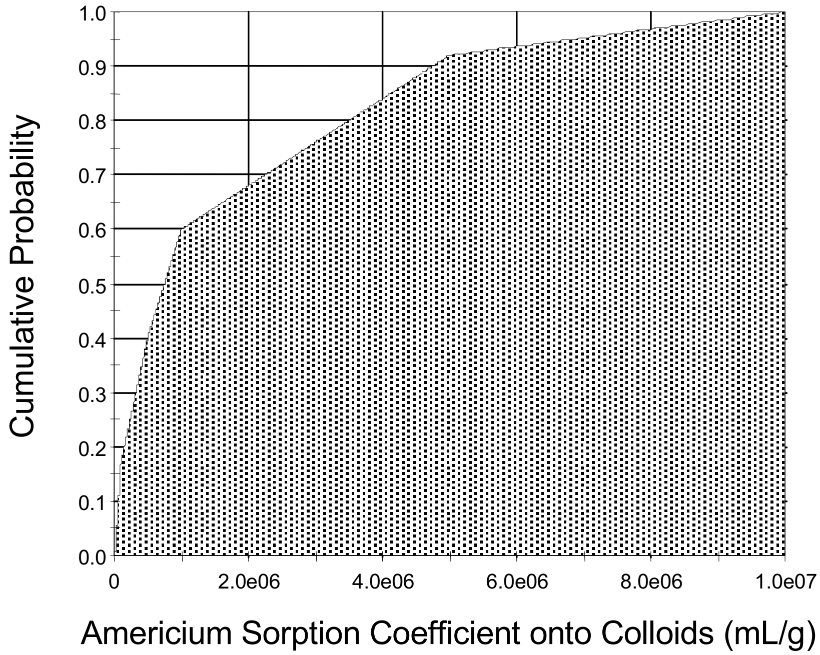

Source: DTN: SN0306T0504103.006 [DIRS 164131], Table 1.

Figure 6-24. CDF of Uncertainty in Americium Sorption Coefficient onto Colloids

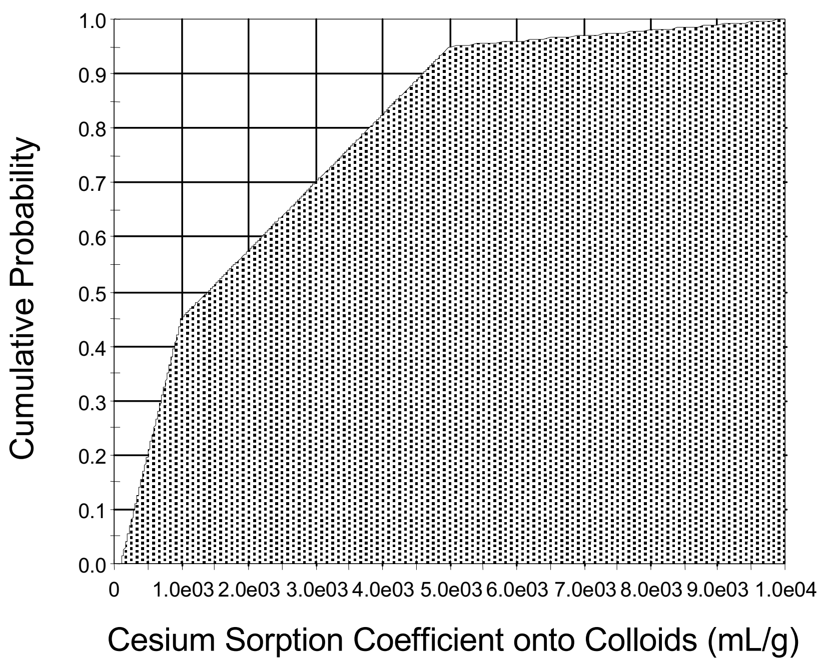

Source: DTN: SN0306T0504103.006 [DIRS 164131], Table 1.

Figure 6-25. CDF of Uncertainty in Cesium Sorption Coefficient onto Colloids

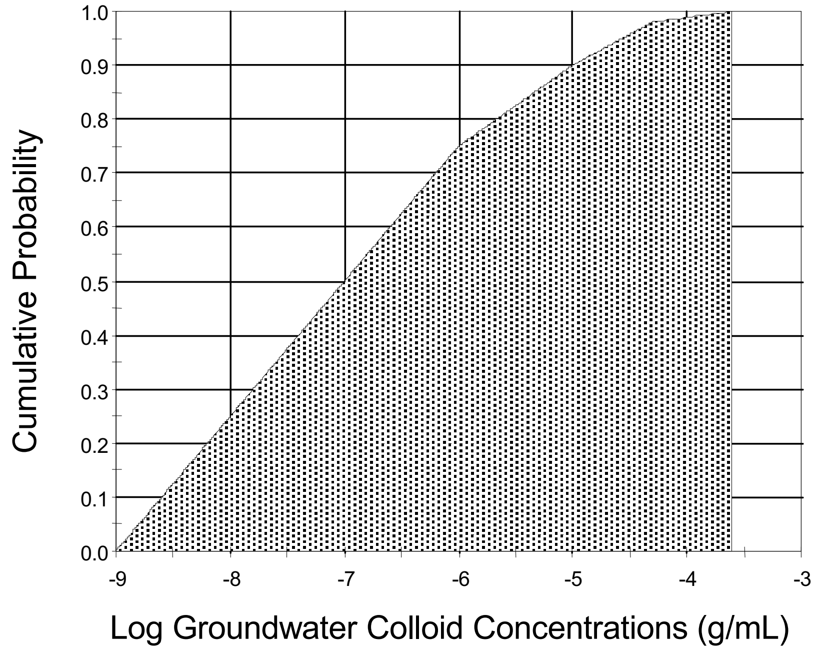

Source: DTN: SN0306T0504103.005 [DIRS 164132], Table 3.

NOTE: In constructing CDF of uncertainty in groundwater colloid concentrations it was assumed that the groundwater concentration of 200 mg/L=0.0002 g/mL (with log-transformed value of -3.7 g/mL) has probability of 0% (0.0) and the groundwater concentration of 50 mg/L=0.00005 g/mL (with log-transformed value of -4.3 g/mL) has probability of 2% (0.02).

Figure 6-26. CDF of Uncertainty in Groundwater Colloid Concentrations

Accompanying the K_c model is the partitioning of radionuclides between the aqueous phase and the sorbed phase onto the tuff matrix and the alluvium, as described by K_d for the radionuclide onto the aquifer material. The K_d uncertainty distributions for americium, plutonium, and cesium are described in Table 6-8 (DTN: LA0310AM831341.002, [DIRS 165891]).

6.5.2.13 Source Regions

Variations in radionuclide transport pathways and travel times in the SZ from various locations beneath the repository are considered by defining four radionuclide source regions at the water table. For any particular TSPA-LA realization, a point source of radionuclides is defined within each of the four regions for simulation of radionuclide transport in the SZ flow and transport abstraction model. A point source of radionuclides in the SZ is appropriate for a single leaking waste package or for highly focused groundwater flow along a fault or single fracture in the UZ. Whereas a more diffuse source of radionuclides at the water table may be more physically realistic for later times when numerous leaking waste packages occur, use of a point source in the SZ is an approach that overestimates the concentration of radionuclides near the source.

The SZ source region locations are based on the extent of the repository design and on the general pattern of groundwater flow in the UZ as simulated by the site-scale UZ flow and transport model. Variations in the pattern of groundwater flow from the repository to the water table exist among infiltration models, ACMs, and climate states for the site-scale UZ model

(BSC 2004 [DIRS 169861], Section 6.6). The UZ flow and transport simulations indicate varying degrees of lateral diversion of groundwater to the east of the repository, and downward redirection by interception of flow at major faults. The SZ source region locations are defined to accommodate the general range in UZ transport pathways simulated by the suite of site-scale UZ flow model simulations.

The four SZ radionuclide source regions are shown in Figure 6-27. Note that the CORPSCON software code (CORPSCON V5.11.08, STN: 10547-5.11.08-00 [DIRS 155082]) was used to convert the coordinates of the repository design (given in state plane coordinates, in meters) to Universal Transverse Mercator (UTM) coordinates. The coordinates of the corners of the source regions are given in Table 6-8. Source regions 1, 3, and part of 2 are located directly below the repository to capture radionuclide transport that occurs vertically downward in the site-scale UZ flow and transport model. In addition, regions 1, 2, and 3 are appropriate source locations for radionuclides arriving at the water table in the human intrusion scenario (see *Total System Performance Assessment for the Site Recommendation* (CRWMS M&O 2000 [DIRS 153246], Section 4.4)), in which a hypothetical borehole penetrates the repository and extends to the SZ. Source regions 2 and 4 are located to the east of the repository to capture radionuclide transport that is subject to lateral diversion of groundwater to the east along dipping volcanic strata in the UZ. Also note, that the northern part of source region 2 underlies a northeasterly extension of the repository.

The random locations of the radionuclide source term for each realization are defined by eight stochastic parameters. The parameters SRC1X, SRC1Y, SRC2X, SRC2Y, SRC3X, SRC3Y, SRC4X, and SRC4Y determine the x coordinate and y coordinate for the source location within regions 1 to 4, respectively. These parameter values are drawn from independent, uniform distributions from 0.0 to 1.0. The result is a randomly located point source within each of the four source regions for each realization of the SZ flow and transport abstraction model.

6.5.2.14 Maximum Alluvial Porosity

The value of maximum or total alluvial porosity is used to calculate the adjusted (or new) K_d value in the effective porosity conceptualization of transport in the alluvium (see Equation 6-3). The average total porosity of alluvium from corroborative data given in Table 6-10 is 0.35. The calculated value of average total porosity in alluvium from the borehole gravimeter data from well EWDP-19D1 is significantly lower, as shown in Table 6-11. The approximate average value of maximum alluvial porosity from these two sources is 0.30. The uncertainty distribution in effective porosity of alluvium is truncated at a maximum value of 0.30 (Figure 6-10).

6.5.2.15 Average Fracture Porosity

The value of average fracture porosity of volcanic rocks is used to calculate the retardation factor of sorbing radionuclides in the rubblized material of fracture zones. This retardation factor in the fracture zones only applies when the flowing interval porosity exceeds the average fracture porosity. The average fracture porosity is conceptualized to be the total fracture porosity of the volcanic units, not including any matrix porosity in the rubblized material of fracture zones. The average fracture porosity is taken as the median of the uncertainty distribution assigned to the flowing interval porosity (FPVO) (see Table 6-8), which is equal to 0.001.

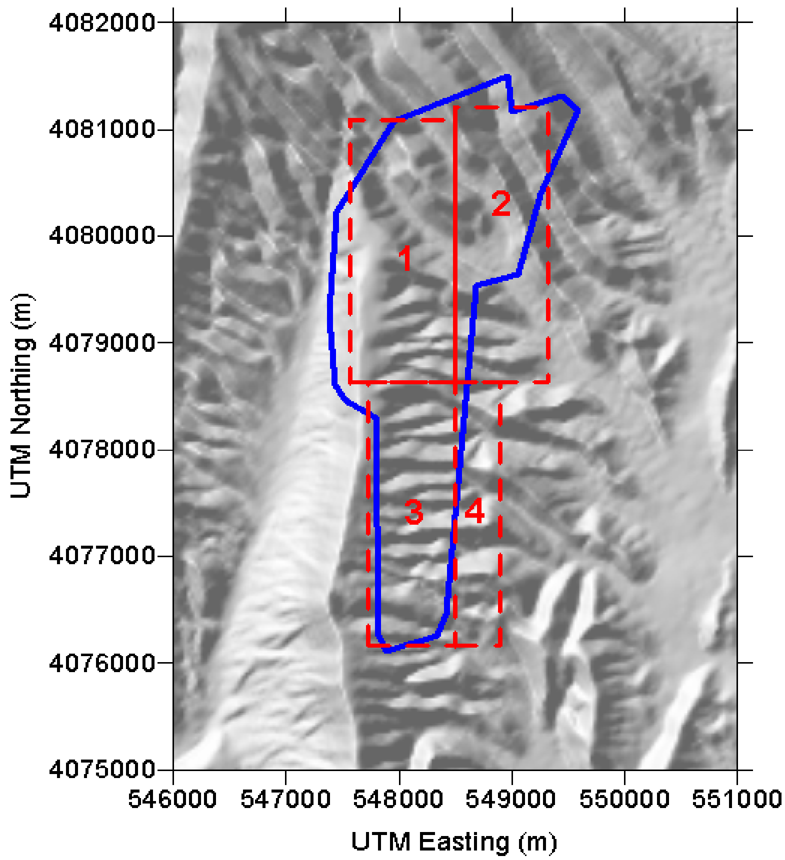

Sources: Repository outline from 800-IED-WIS0-00101-000-00B (BSC 2004 [DIRS 172801]).

NOTE: Repository outline is shown by the solid blue line and the four source regions are shown by the dashed red lines.

Figure 6-27. Source Regions for Radionuclide Release in the SZ Flow and Transport Abstraction Model

6.5.2.16 Average Matrix Porosity

The value of average matrix porosity of volcanic rocks is used to calculate the retardation factor of sorbing radionuclides in the SZ 1-D transport model and in the rubblized material of fracture zones. This retardation factor in the fracture zones only applies when the flowing interval porosity exceeds the average fracture porosity. The average matrix porosity of volcanic rocks is calculated as the average of matrix porosity in hydrogeologic Units 11 through 14, as given in Table 6-12. The calculated average matrix porosity is 0.22.

6.5.2.17 Average Bulk Density of the Volcanic Matrix

The value of average bulk density of the matrix in volcanic rocks is used to calculate the retardation factor of sorbing radionuclides in the SZ 1-D transport model and in the rubblized material of fracture zones. This retardation factor in the fracture zones only applies when the flowing interval porosity exceeds the average fracture porosity. The average bulk density of the volcanic matrix is calculated as the weighted average of bulk density in hydrogeologic Units 13 through 15, as given in Table 6-13, with double weighting given to Unit 13 because of its prominence in the flow path beneath the repository. The calculated average bulk density is 1.88 g/cm^3.

6.5.2.18 Matrix Porosity of Volcanic Units (Constant)

Matrix porosity (ϕ_m) is treated as a constant parameter for eight units of the nineteen SZ model hydrogeologic units. Constant, in this sense, means that ϕ_m will vary from one unit to another but, given a particular unit, the porosity is constant for all realizations. The porosity also remains spatially constant for each unit. The parameter values and input source(s) are shown in Section 4, Table 4-1, and discussed below.

The following discussion covers data sources used in constant porosity inputs for the affected hydrogeologic units. The volcanic Units 11 through 15 do lie in the expected flow paths (BSC 2004 [DIRS 170037], Figure 6-43) per the SZ site-scale flow model. All of the remaining units lie outside of any expected SZ model transport paths because they do not exist in this area of the model or they occur deeper than the expected flow paths. Thus, the values of matrix porosity assigned to the remaining units have no impact on the transport simulations. However, the model requires values for ϕ_m for all units, regardless of whether they play a role in transport simulations; therefore, values as representative as possible were used.

For the case of Units 15-13, the matrix porosity is based on the values from DTN: SN0004T0501399.003 [DIRS 155045]. The matrix porosity value for Units 12 and 11 were derived from matrix porosity data from the boreholes: UE-25P#1, USW H-3, SD7, USW G-3, USW H-1, USW G-4, USW H-5, and USW H-6 (DTNs: SN0004T0501399.003 [DIRS 155045], MO0109HYMXPROP.001 [DIRS 155989], MO0010CPORGLOG.002 [DIRS 155229]). Simple averages of the wells described above were calculated from the data for Units 12 and 11, as shown in spreadsheet *bulkd_matr_eff_La.xls* (DTN: SN0306T0502103.006).

Units 10 and 8 are both volcanic confining units. The value of ϕ_m for these units was obtained from the value for Unit 14, which is a volcanic confining unit for which there are site-specific data. The ϕ_m value for Unit 9 (volcanic unit) was obtained by averaging the values for the three overlying Crater Flat group units (Units 11 - 13). These averages were used as the matrix porosity inputs to the SZ site-scale model for their respective units, as shown in Table 6-12.

6.5.2.19 Bulk Density of the Volcanic Matrix

Bulk density (ρ_b) is defined by Freeze and Cherry (1979 [DIRS 101173], p. 337) as the "oven-dried mass of the sample divided by its field volume." It is a factor in Equation 6-2, used to determine retardation of a solute due to chemical adsorption in groundwater. That equation is employed in the SZ site-scale flow and transport model as part of the FEHM code (Zyvoloski et al. 1997 [DIRS 110491], p. 42).

Table 6-12. Values of Matrix Porosity (ϕ_m) for Several Units of the SZ Model

SZ Unit Name	SZ Unit Number	Matrix Porosity (ϕ_m)
Upper Volcanic Aquifer (Topopah)	15	0.15
Upper Volcanic Confining Unit (Calico Hills)	14	0.25
Lower Volcanic Aquifer, Prow Pass	13	0.23
Lower Volcanic Aquifer, Bullfrog	12	0.18
Lower Volcanic Aquifer, Tram	11	0.21
Lower Volcanic Confining Unit	10	0.25
Older Volcanic Aquifer	9	0.21
Older Volcanic Confining Unit	8	0.25

Output DTN: SN0310T0502103.010.

Bulk density is treated as a constant parameter for seventeen of the nineteen units of the SZ model hydrogeologic units. Constant, in this sense, means that ρ_b varies from one unit to another but, given a particular unit, the bulk density stays the same for all realizations. The bulk density also remains spatially constant for each unit. Bulk density in hydrogeologic Units 19 and 7 is treated as an uncertain parameter, and is discussed in Section 6.5.2.7. The parameter values and input source(s) are described in Section 4. This section contains a discussion of the analyses used to develop the values. The volcanic Units 11 through 15 do lie in the expected flow paths (BSC 2004 [DIRS 170037], Figure 6-43) per the SZ site-scale flow model. All of the remaining units lie outside of any expected SZ model transport paths, because they do not exist in this area of the model or they occur deeper than the expected flow paths. Thus, the values of bulk density assigned to the remaining units have no impact on the transport simulations.

Estimates for bulk density were either based on the use of an analogous unit, or a calculation was required, as discussed below. For some units, including part of the volcanic units and the carbonate units, the calculation involved averaging a group of referenced bulk density values. Some of the volcanic units required the use of a referenced graph to calculate bulk density as a certain function of matrix porosity (for which values had already been determined). Finally, two units (granite and lava flows) required the use of a general equation that relates bulk density to porosity. Many of the calculations required referencing either the matrix porosities or the effective porosities that were tabulated in Table 6-12 and Table 6-14, respectively.

The estimated bulk densities are summarized in Table 6-13, and the methods used to obtain these values are summarized in the discussion below.

Table 6-13. Values of Bulk Density (ρ_b) for All Units of the SZ Site-Scale Model

SZ Unit Name	SZ Unit Number	Bulk Density (ρ_b) (g/cm^3)
Valley Fill Confining Unit	18	2.50
Cenozoic Limestone	17	2.77
Lava Flows	16	2.44
Upper Volcanic Aquifer (Topopah)	15	2.08
Upper Volcanic Confining Unit (Calico Hills)	14	1.77
Lower Volcanic Aquifer, Prow Pass	13	1.84
Lower Volcanic Aquifer, Bullfrog	12	2.19
Lower Volcanic Aquifer, Tram	11	2.11
Lower Volcanic Confining Unit	10	1.77
Older Volcanic Aquifer	9	2.05
Older Volcanic Confining Unit	8	1.77
Upper Carbonate Aquifer	6	2.77
Lower Carbonate Aquifer Thrust	5	2.77
Upper Clastic Confining Unit	4	2.55
Lower Carbonate Aquifer	3	2.77
Lower Clastic Confining Unit	2	2.55
Granites	1	2.65

NOTE: Units 19 and 7 are treated as uncert ain parameters, and are discussed in Section 6.5.2.7.

Carbonates Units 3, 5, 6, and 17–Bulk density for Units 3, 5, 6, and 17 is determined from an average of a series of bulk density values from the Roberts Mountain Formation and the Lone Mountain Formation of Borehole UE-25p#1 (DTN: MO0010CPORGLOG.002 [DIRS 155229]). A simple average was calculated using these values (see spreadsheet *bulkd_matr_eff_La.xls* [DTN: SN0306T0502103.006]).

Clastic Units 2, 4, and 18–Bulk density values for Unit 4 are determined from an average of a series of sedimentary deposit formation bulk densities from Borehole UE-25P#1 (DTN: MO0010CPORGLOG.002 [DIRS 155229]). There are no bulk density data available for the Clastics hydrogeologic units. A simple average was calculated using these values (see spreadsheet *bulkd_matr_eff_La.xls* (DTN: SN0306T0502103.006)). The bulk density assigned to Unit 4 was used as an analogous value for Unit 2, because Unit 2 is also a clastic confining unit. Unit 4 is also used as an analogous unit for Unit 18 because data do not exist for this unit, and the value was rounded to 2.5.

Volcanic Units 8, 10, 13, 14, and 15-The rock properties model (BSC 2004 [DIRS 170032]) contains a graph (Figure 6.4-21) that relates point values of ρ_b to ϕ_m in volcanic tuff. The graph demonstrates a strong linear correlation between the two parameters. The equation for the straight-line fit to the scatterplot is shown below (DTN: SN0004T0501399.002 [DIRS 155046])

$$\rho_b = 2.5019 - 2.8924 \cdot \phi_m \qquad \text{(Eq. 6-30)}$$

Table 6-8 lists the values of ϕ_m for the units (Units 13 - 15) that were used to calculate ρ_b. Hydrogeologic Units 8 and 10 are volcanic confining units. The value of ρ_b for these units was obtained from the value for Unit 14, which is a volcanic confining unit for which we have site-specific data.

Volcanic Units 11 and 12–Bulk density for Units 11 and 12 is determined from values of the so-called "middle volcanic aquifer," which is equivalent to SZ Units 11 and 12 (DTNs: MO0109HYMXPROP.001 [DIRS 155989] and MO0010CPORGLOG.002 [DIRS 155229]). The bulk density values come from Boreholes SD7, USW H-1, UE-25b#1, J-13, UE-25a#1, USW GU-3, USW G-3, USW G-4, UE-25p#1, and USW G-1. A simple average was calculated from those values (see spreadsheet *bulkd_matr_eff_La.xls* [DTN: SN0306T0502103.006]).

Volcanic Unit 9–Unit 9 is a "volcanic aquifer." Its value was obtained by averaging the values for the three overlying volcanic Crater Flat group units (Units 11 - 13) and Unit 15.

Lava Flows (Unit 16) and Granites (Unit 1)–The values of bulk density for these units are calculated from Equation 6-25. A representative value that is appropriate for ρ_{grain} is 2.65g/cm^3 (Hillel 1980 [DIRS 101134], p. 9). As both of these units are not in the transport model path, it is suitable to use the particle density value and effective porosity to calculate bulk density (Equation 6-31) (see spreadsheet *bulkd_matr_eff_La.xls* (DTN: SN0306T0502103.006)). The effective porosity values were used for Equation 6-31 because the effective porosity is very similar to the total porosity for the lava flow and granite units. The porosity values were taken from Table 6-12. The lava flow unit has an effective porosity of 0.08, and the granite unit has a porosity of 0.0001. Therefore, the bulk densities assigned for those units are 2.44 and 2.65 g/cm^3, respectively.

6.5.2.20 Effective Porosity

Effective porosity (ϕ_e) is treated as a constant parameter for nine of the nineteen SZ model hydrogeologic units. Constant, in this sense, means that ϕ_e varies from one unit to another but, given a particular unit, the porosity is the same for all realizations. The effective porosity is also homogeneous within each unit. The input source(s) are described in Section 4, Table 4-1.

The nine hydrogeologic units discussed in this section do not occur within the flow path from beneath the repository; therefore, these values do not impact the simulated transport of radionuclides. However, representative values are used. The Bedinger et al. report (1989 [DIRS 129676], Table 1, p. A18) includes hydrogeologic data for the Basin and Range Province of the Southwestern U.S. The Bedinger et al. report covers a region that extends into eight states and includes the Yucca Mountain site. The Bedinger et al. report was used as the source for data on the Valley Fill Confining Unit (18), the Cenozoic Limestone Unit (17), Lava Flow Unit (16), Upper Carbonate Aquifer Unit (6), Lower Carbonate Aquifer Thrust Unit (5), Upper Clastic Confining Unit (4), Lower Carbonate Aquifer Unit (3), Lower Clastic Confining Unit (2) and the Granites Unit (1). All of the carbonate units were assigned the same value.

The effective porosity values (Bedinger et al. 1989 [DIRS 129676], Table 1, page A18; DTN: MO0105HCONEPOR.000 [DIRS 155044]) are used for all of the hydrogeologic units described in this paragraph. The upper carbonate aquifer, the lower carbonate aquifer, the lower carbonate thrust aquifer, and the Cenozoic limestone units (designated as Units 6, 3, 5, and 17 respectively) use the mean value of Carbonate Rocks. The Cenozoic Limestone Unit is assigned the same value as the carbonate units because it is a similar rock type to the carbonate rocks. The value for granites (Unit 1) is set equal to the estimate for metamorphic rock with a depth more than 300 m. Unit 16 is assigned the average of the Lava Flows, fractured and moderately dense, from the DTN: MO0105HCONEPOR.000 [DIRS 155044] source. Units 4 and 2 utilize the mean value from the Clastic Sedimentary Units. Unit 18 utilizes the Basin fill mean value for fine-grained clay and silt cited by Bedinger et al. (1989 [DIRS 129676], Table 1). This information is summarized in the spreadsheet *geonames.xls* (DTN: SN0306T0502103.006). Table 6-14 lists the constant values used for each unit, for the SZ flow and transport abstraction model for TSPA-LA.

Table 6-14. Values of Effective Porosity (ϕ_e) for Several Units of the SZ Flow and Transport Abstraction Model

SZ Unit Name	SZ Unit Number	Effective Porosity (ϕ_e)
Valley Fill Confining Unit	18	0.32
Cenozoic Limestone	17	0.01
Lava Flows	16	0.08
Upper Carbonate Aquifer	6	0.01
Lower Carbonate Aquifer Thrust	5	0.01
Upper Clastic Confining Unit	4	0.18
Lower Carbonate Aquifer	3	0.01
Lower Clastic Confining Unit	2	0.18
Granites	1	0.0001

Output DTN: SN0310T0502103.009.

6.5.3 Summary of Computational Models

Both the SZ flow and transport abstraction model and the SZ 1-D transport model are intended for use in the analyses for TSPA-LA. The results of the multiple realizations of SZ flow and transport with the SZ flow and transport abstraction model, in the form of multiple breakthrough curves, are coupled with the TSPA-LA simulations using the convolution integral method. The SZ 1-D transport model is intended for direct incorporation into the TSPA-LA model. The SZ 1-D transport model is developed independently of the TSPA-LA model, but contains the elements necessary for implementation within the TSPA-LA model.

The results of the SZ flow and transport abstraction model and the SZ 1-D transport model are combined for calculating dose for comparison to the individual protection standard in the following way: the mass arriving at the accessible environment of the following radionuclides is simulated, using the SZ flow and transport abstraction model: ^{14}C, ^{90}Sr, ^{99}Tc, ^{129}I, ^{135}Cs, ^{137}Cs, ^{232}U, ^{243}Am, ^{241}Am, ^{240}Pu, ^{242}Pu, ^{239}Pu, ^{237}Np, ^{236}U, ^{238}U, ^{238}Pu, and ^{234}U. Note, transport of the actinides listed above (with the exception of ^{232}U) is also simulated with the SZ 1-D transport model, but only the subsequent daughter products in the four decay chains are taken as output from the SZ 1-D transport model. The mass arriving at the accessible environment of the following radionuclides is simulated with the SZ 1-D transport model (or assumed to be in secular equilibrium with their respective parents): ^{235}U, ^{233}U, ^{232}Th, ^{231}Pa, ^{229}Th, ^{229}Ra, ^{230}Th, and ^{226}Ra.

6.5.3.1 SZ Flow and Transport Abstraction Model

The groups of radioelements for simulated transport in the SZ flow and transport abstraction model are summarized in Table 6-15. There are 10 groupings of radionuclides noted in the first column of Table 6-15. The modes of radionuclide transport are:

1. As solute,
2. As colloid-facilitated transport of radionuclides reversibly attached to colloids, and
3. As colloid-facilitated transport of radionuclides irreversibly attached to colloids.

As indicated in Table 6-15, the nonsorbing radionuclides of carbon, technetium, and iodine are grouped together because their migration is identical. Americium, thorium, and protactinium reversibly attached to colloids are grouped together because of their similar sorption characteristics. Note that plutonium and americium may be transported both reversibly and irreversibly attached to colloids.

Table 6-15. Radioelements Transported in the SZ Flow and Transport Abstraction Model

Radionuclide Number	Transport Mode	Radioelements
1	Solute	Carbon, Technetium, Iodine
2	Colloid-Facilitated (Reversible)	Americium, Thorium, Protactinium
3	Colloid-Facilitated (Reversible)	Cesium
4	Colloid-Facilitated (Reversible)	Plutonium
5	Solute	Neptunium
6	Colloid-Facilitated (Irreversible)	Plutonium, Americium
7	Solute	Radium
8	Solute	Strontium
9	Solute	Uranium
10	Colloid-Facilitated (Fast Fraction of Irreversible)	Plutonium, Americium

Output DTNs: SN0310T0502103.010, SN0310T0502103.012, and MO0506SPAINPUT.001.

The radionuclide breakthrough curves from the SZ flow and transport abstraction model for the 200 Monte Carlo realizations of SZ flow and transport are generated as follows: a steady-state groundwater flow field is produced for each of the 200 realizations prior to transport simulations. Variations in the groundwater specific discharge are included by scaling all values of permeability in the base-case SZ site-scale flow model (BSC 2004 [DIRS 170037]) and the values of specified recharge, using the value of the GWSPD parameter. Variations in horizontal anisotropy in permeability are included by scaling the values of north-south and east-west permeability within the zone of volcanic rocks influenced by anisotropy, using the value of the

HAVO parameter. Each steady-state groundwater flow solution is stored to be used as the initial conditions in the radionuclide transport simulations. The SZ_Pre V2.0 software code (STN: 10914-2.0-00, SNL 2003 [DIRS 163281]) is a preprocessor that is used to prepare the FEHM V2.20 software code [DIRS 161725] input files for each of the 200 realizations. The preprocessor reads the values of the parameters from an input file containing a table of values for all 200 realizations, performs relevant parameter transformations, and writes the appropriate values to the various FEHM V2.20 software code [DIRS 161725] input files. A total of 8,000 individual simulations (200 realizations × 10 radioelement groups × 4 source regions) of SZ flow and transport are conducted, and the particle tracking output files are saved. The particle tracking simulations of matrix diffusion use the type curves of the analytical solution for matrix diffusion in DTN: LA0302RP831228.001 [DIRS 163557]. The SZ_Post V3.0 software code (STN: 10915-3.0-00, SNL 2003 [DIRS 163571]) is a post-processor that is used to extract the breakthrough curves from the FEHM V2.20 software code [DIRS 161725] output files, and concatenate all 200 realizations into a single file for input to the SZ_Convolute V3.0 software code (STN: 10207-3.0-00, SNL 2003 [DIRS 164180]), for use in the TSPA-LA.

For implementation of the 3-D SZ flow and transport abstraction model in the TSPA-LA model, a control file must be provided that specifies solute and time control information for the SZ_Convolute V3.0 software code (STN: 10207-3.0-00, SNL 2003 [DIRS 164180]). The control file includes information on the maximum number of time steps and time step lengths. The number of species analyzed is provided along with a flag value for each species that determines the generic breakthrough curve to be used for that species. Information is also provided to specify which columns will be read from the breakthrough curve files (first column for time, third column for relative mass). The number of climate states (three) and the multiplier of groundwater flow rate in the SZ (relative to present conditions) for each climate state are also specified in the control file. The values for this factor are given in Table 6-5.

6.5.3.2 SZ 1-D Transport Model

Implementation of the SZ 1-D transport model in the TSPA-LA model requires that the "stand-alone" version of the model developed in this report be correctly integrated into the TSPA-LA model. The SZ 1-D transport model was developed in anticipation of integration into the TSPA-LA model, but the following aspects of the integration are required for implementation in the TSPA-LA model:

> The radionuclide flux into and out of the SZ 1-D transport model must be properly linked to the other components of the TSPA-LA model. The radionuclide decay and ingrowth chains and the corresponding half-life values of radionuclides must be consistent with the other components of the TSPA-LA model. The parameter values for the 200 realizations of the SZ flow and transport abstraction model are stored as a table in the TSPA-LA model, and the SZ 1-D transport model must be correctly linked with this table of values to ensure consistency with the SZ flow and transport abstraction model on a realization-by-realization basis. The parameter vectors used in the SZ flow and transport abstraction model that need to be incorporated into the table values used by the SZ 1-D transport model are contained in Appendix A of this report and in

DTN: SN0310T0502103.009. The variable controlling changes in climate state in the TSPA-LA model must be correctly linked with the SZ 1-D transport model.

6.6 BASE-CASE MODEL RESULTS

Base-case model results from the SZ flow and transport abstraction model consist of radionuclide mass breakthrough curves at the accessible environment of the biosphere, approximately 18 km downgradient from the repository. A suite of breakthrough curves is generated for each species or class of radionuclides based on multiple realizations of the model. Variability in the results among these multiple realizations reflects uncertainty in groundwater flow and radionuclide transport behavior in the SZ. Variations in transport behavior among the species are also represented in these results.

6.6.1 Overview

The results of the 200 SZ flow and transport abstraction model realizations are shown in Figures 6-28 to 6-36. Each figure shows the relative mass arriving at the accessible environment as a function of time and a histogram of median transport times, for a given category of radionuclides from Table 6-15. Note that the breakthrough curves and transport times shown in these figures are for a continuous, steady source at the water table below the repository (source region 1), initiated at time equal to zero. Transport simulation results for source region 1 are representative of results for all of the source regions; there are no dramatic variations among the source regions in simulated radionuclide transport times for any given realization. Note that the breakthrough curves shown in these figures are for present climatic conditions, and do not include the effects of radioactive decay. Recall that the process of radioactive decay is implemented in the SZ_Convolute V3.0 software code (STN: 10207-3.0-00, SNL 2003 [DIRS 164180]).

Although individual breakthrough curves can be difficult to discern in some of the figures, both the timing and the shapes of the breakthrough curves vary among the realizations. Variability in the timing of the breakthrough is reflected in the histograms of median transport time, for the bulk of the radionuclide mass arrival at the accessible environment. Variability in the shapes of the breakthrough curves is a function of differences in matrix diffusion and dispersivity among the realizations.

The results differ from the results presented in *SZ Flow and Transport Model Abstraction* (BSC 2003 [DIRS 164870], Section 6.6) for neptunium, plutonium reversibly attached to colloid, cesium reversibly attached to colloids, and uranium. However, the results presented here for the breakthrough curves do not differ significantly from the results in *SZ Flow and Transport Model Abstraction* (BSC 2003 [DIRS 164870]) for transport times of less than 100,000 years, given the overall uncertainty among the 200 realizations.

In addition, simulated breakthrough curves for the fast fraction of plutonium and americium irreversibly attached to colloids are developed for this report, as shown in Figure 6-37. Transport of these radionuclides in the SZ is simulated to occur with no retardation of colloids in the volcanic units or alluvium, and with no matrix diffusion in the volcanic units.

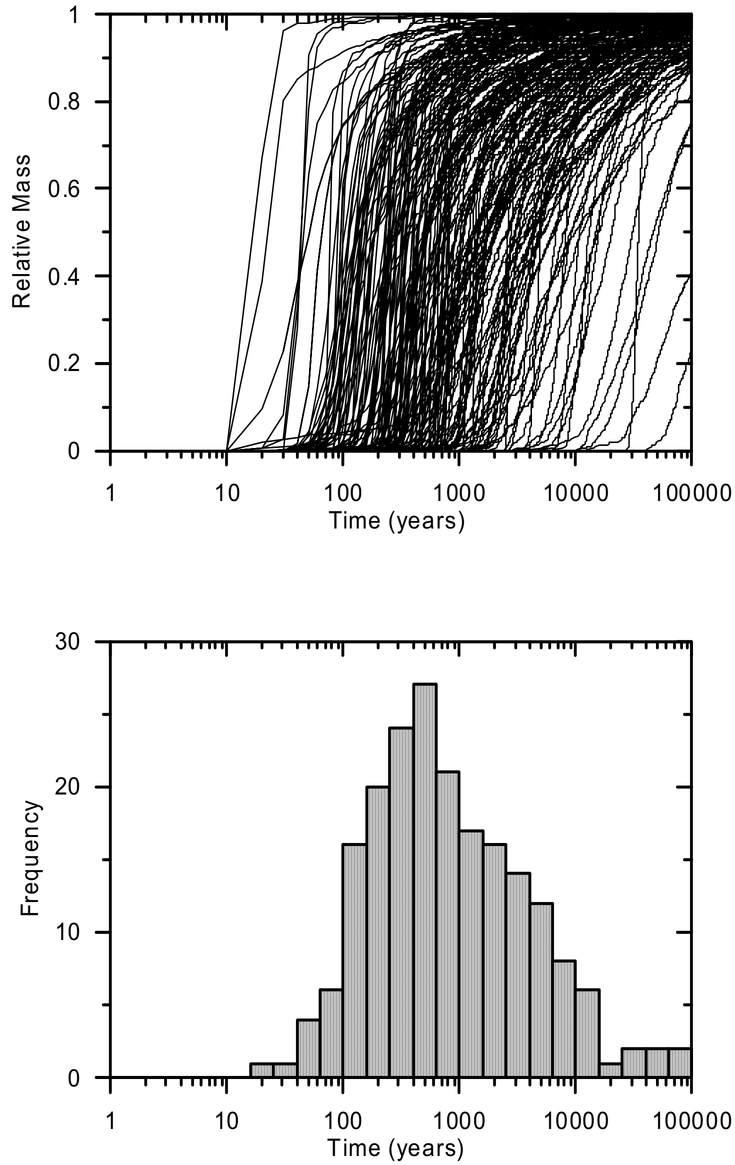

Output DTN: SN0310T0502103.010.

NOTE: Mass breakthrough curves and median transport times are for present-day climate, and do not include radionuclide decay. Results shown for 200 realizations from source region 1.

Figure 6-28. Mass Breakthrough Curves (upper) and Median Transport Times (lower) for Carbon, Technetium, and Iodine at 18-km Distance

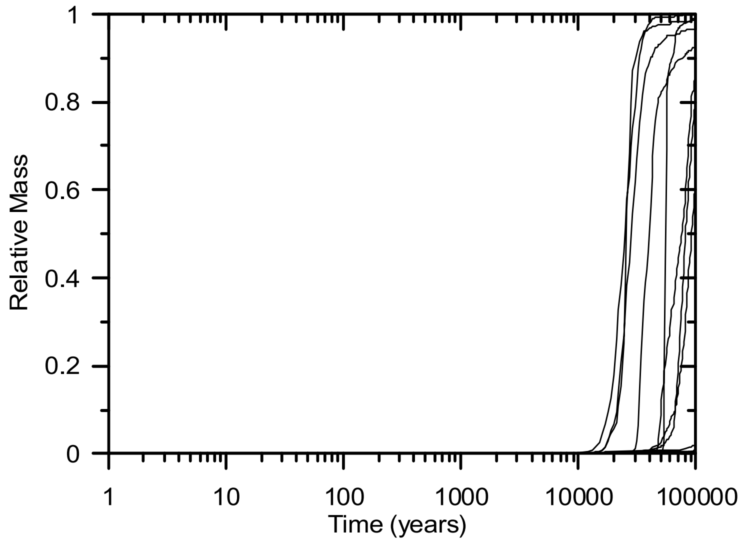

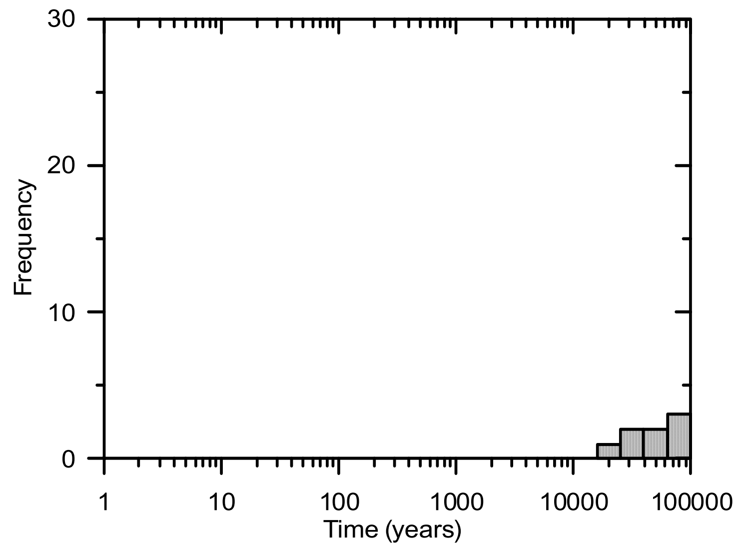

Output DTN: SN0310T0502103.010.

NOTE: Mass breakthrough curves and median transport times are for present-day climate, and do not include radionuclide decay. Results shown for 200 realizations from source region 1.

Figure 6-29. Mass Breakthrough Curves (upper) and Median Transport Times (lower) for Americium, Thorium, and Protactinium on Reversible Colloids at 18-km Distance

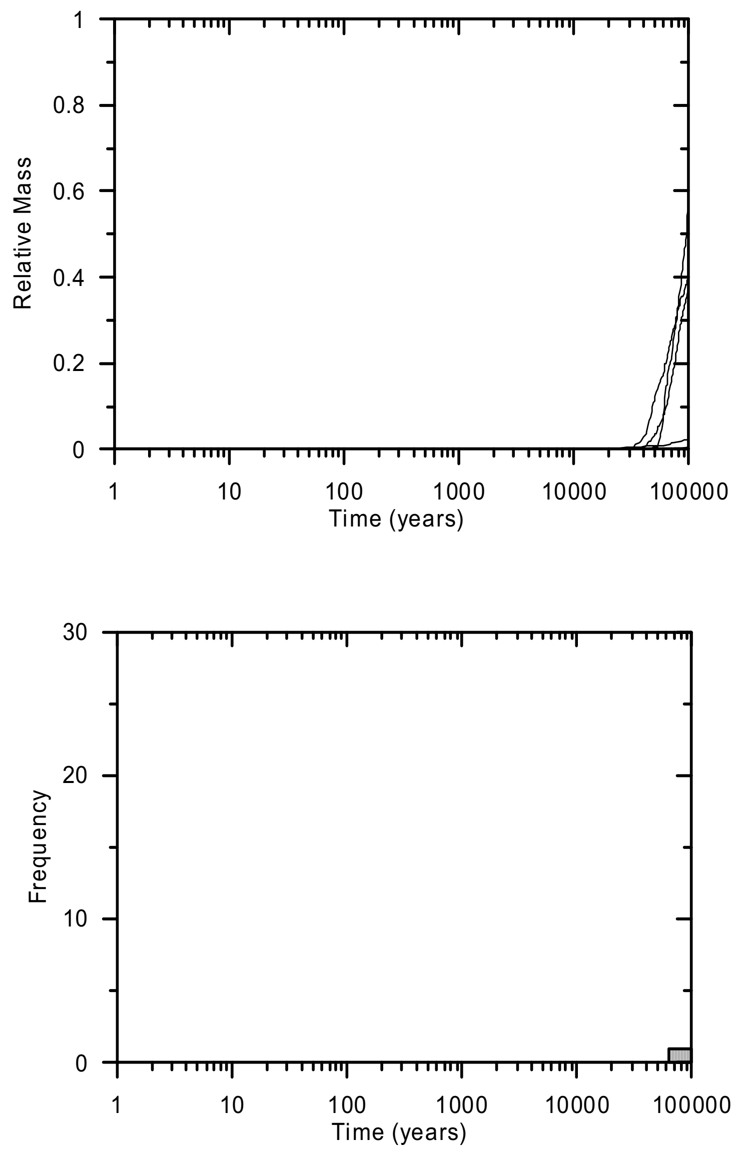

Output DTN: SN0310T0502103.010.

NOTE: Mass breakthrough curves and median transport times are for present-day climate, and do not include radionuclide decay. Results shown for 200 realizations from source region 1.

Figure 6-30. Mass Breakthrough Curves (upper) and Median Transport Times (lower) for Cesium on Reversible Colloids at 18-km Distance

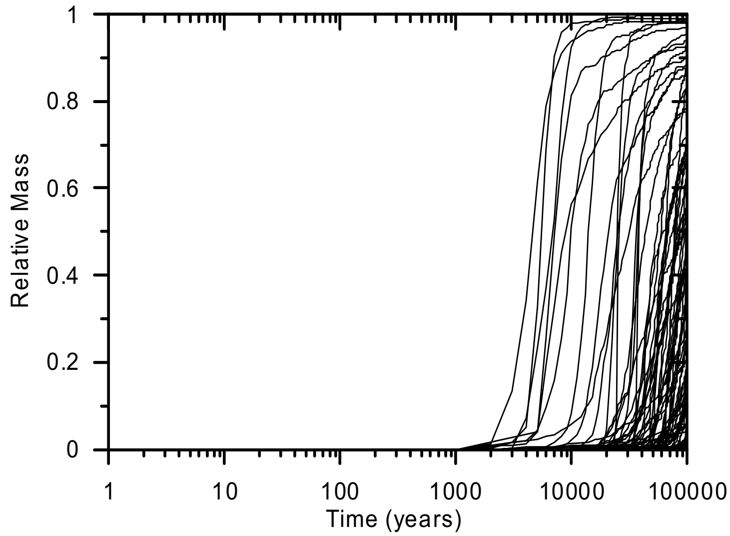

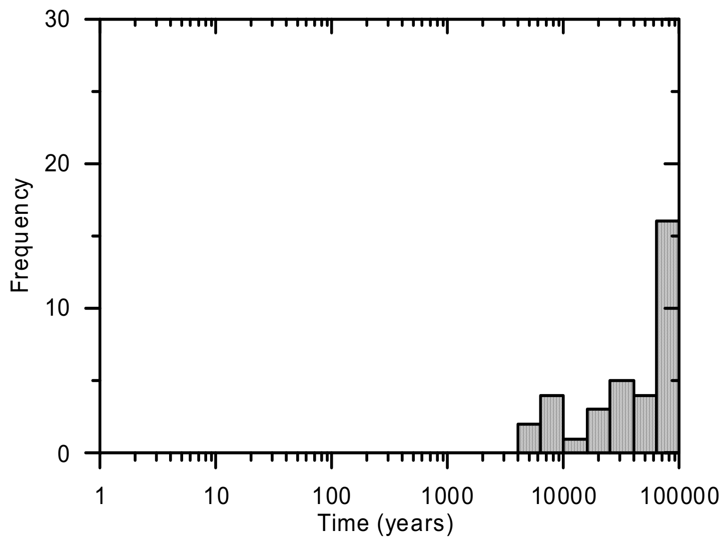

Output DTN: SN0310T0502103.010.

NOTE: Mass breakthrough curves and median transport times are for present-day climate, and do not include radionuclide decay. Results shown for 200 realizations from source region 1.

Figure 6-31. Mass Breakthrough Curves (upper) and Median Transport Times (lower) for Plutonium on Reversible Colloids at 18-km Distance

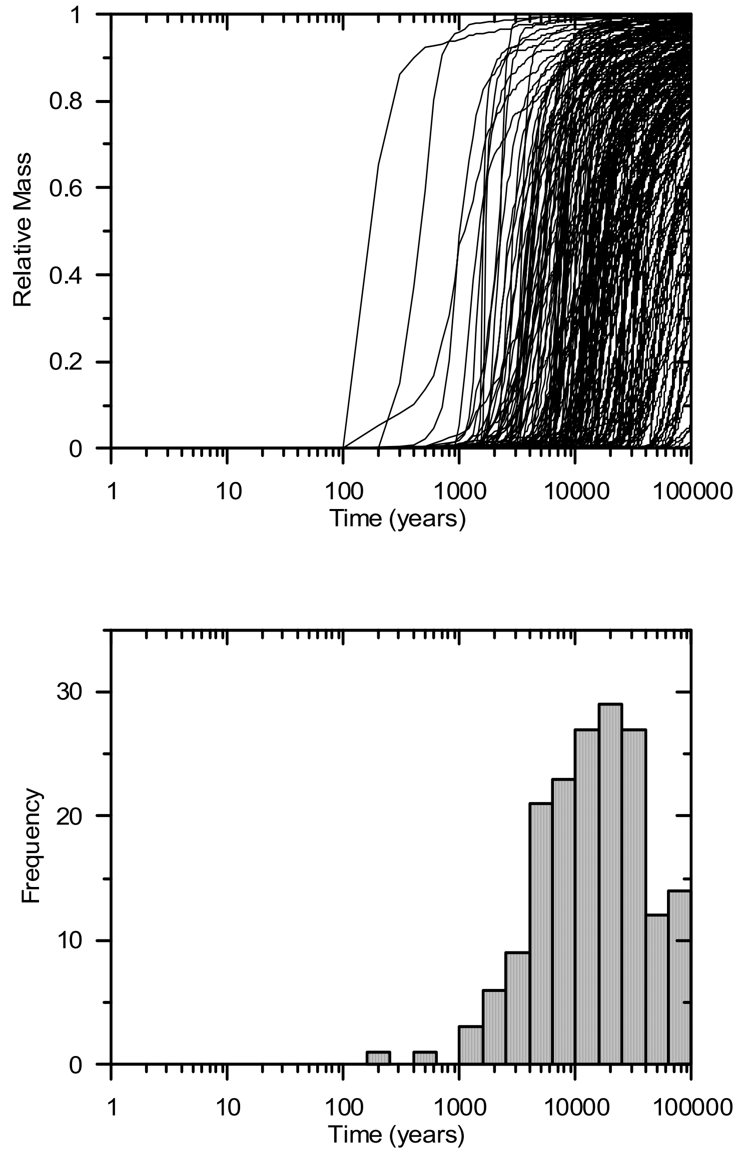

Output DTN: SN0310T0502103.010.

NOTE: Mass breakthrough curves and median transport times are for present-day climate, and do not include radionuclide decay. Results shown for 200 realizations from source region 1.

Figure 6-32. Mass Breakthrough Curves (upper) and Median Transport Times (lower) for Neptunium at 18-km Distance

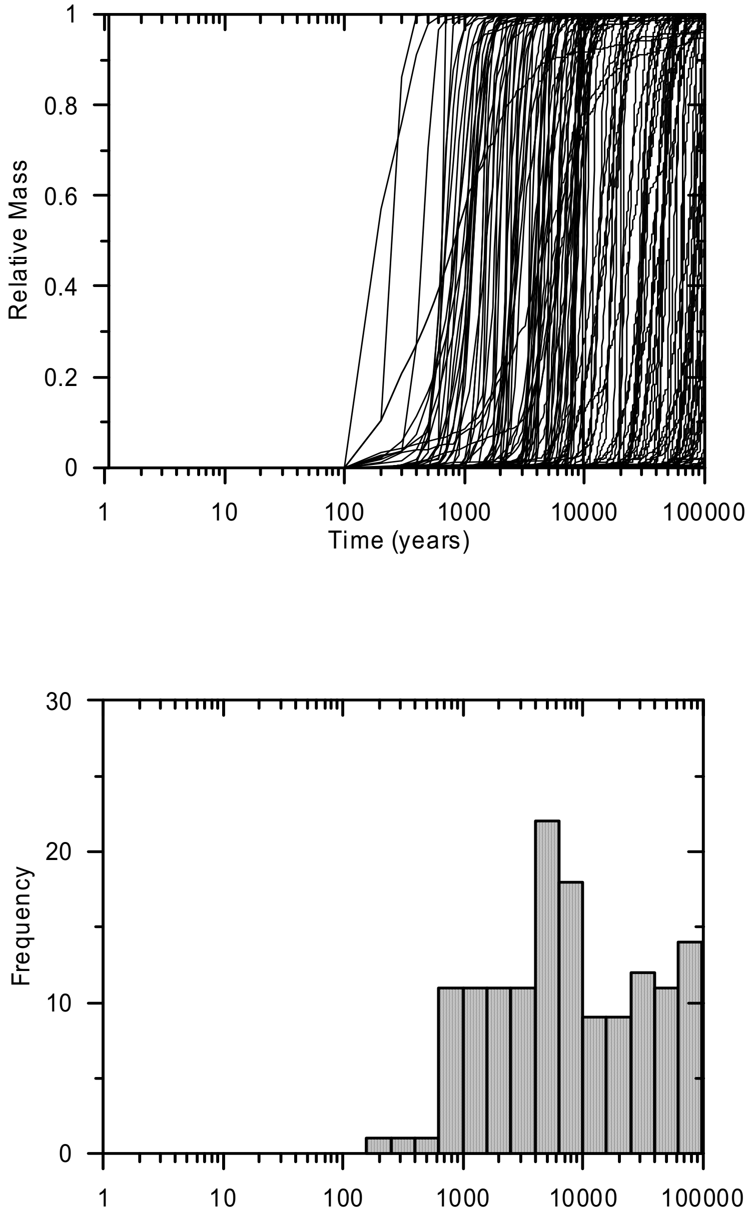

Output DTN: SN0310T0502103.010.

NOTE: Mass breakthrough curves and median transport times are for present-day climate, and do not include radionuclide decay. Results shown for 200 realizations from source region 1.

Figure 6-33. Mass Breakthrough Curves (upper) and Median Transport Times (lower) for Plutonium and Americium on Irreversible Colloids at 18-km Distance

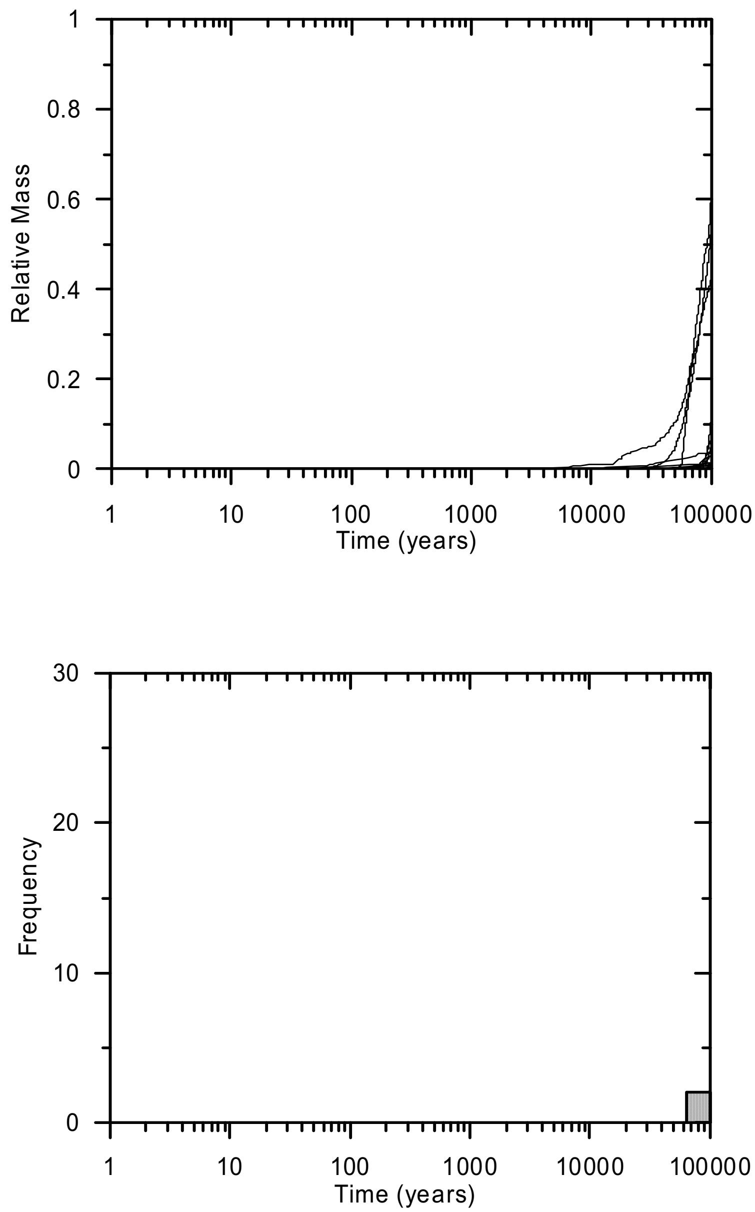

Output DTN: SN0310T0502103.010.

NOTE: Mass breakthrough curves and median transport times are for present-day climate, and do not include radionuclide decay. Results shown for 200 realizations from source region 1.

Figure 6-34. Mass Breakthrough Curves (upper) and Median Transport Times (lower) for Radium at 18-km Distance

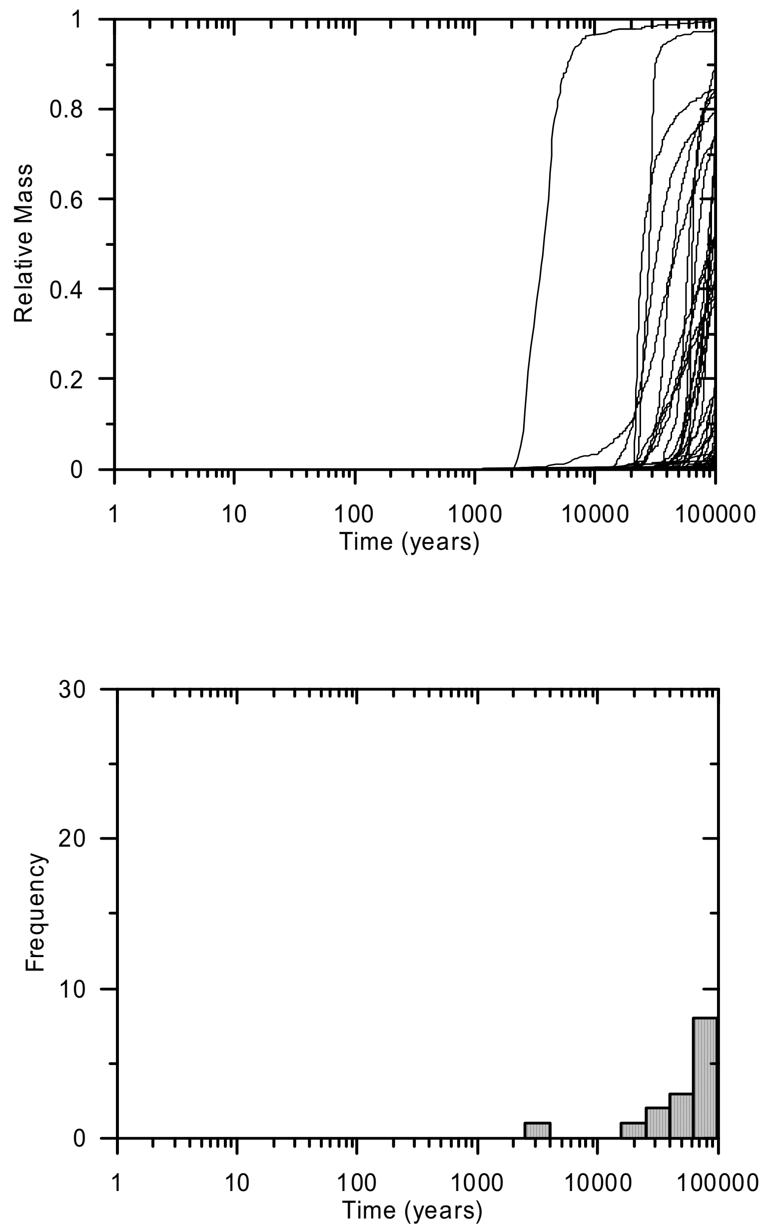

Output DTN: SN0310T0502103.010.

NOTE: Mass breakthrough curves and median transport times are for present-day climate, and do not include radionuclide decay. Results shown for 200 realizations from source region 1.

Figure 6-35. Mass Breakthrough Curves (upper) and Median Transport Times (lower) for Strontium at 18-km Distance

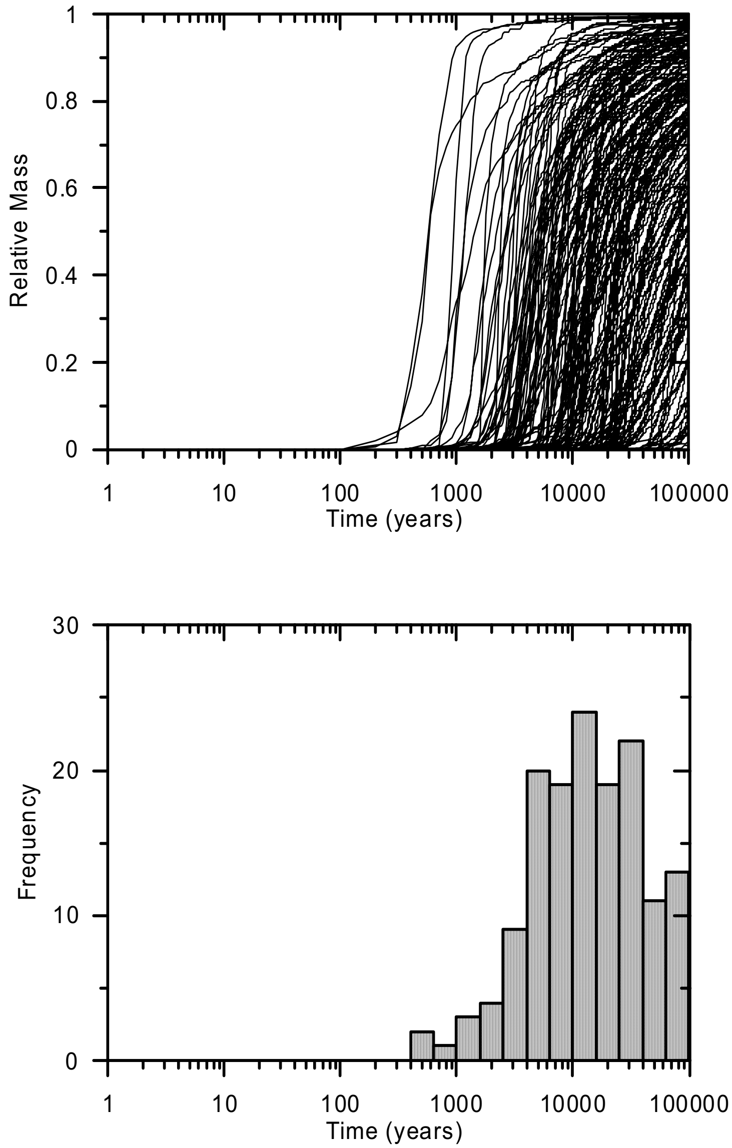

Output DTN: SN0310T0502103.010.

NOTE: Mass breakthrough curves and median transport times are for present-day climate, and do not include radionuclide decay. Results shown for 200 realizations from source region 1.

Figure 6-36. Mass Breakthrough Curves (upper) and Median Transport Times (lower) for Uranium at 18-km Distance

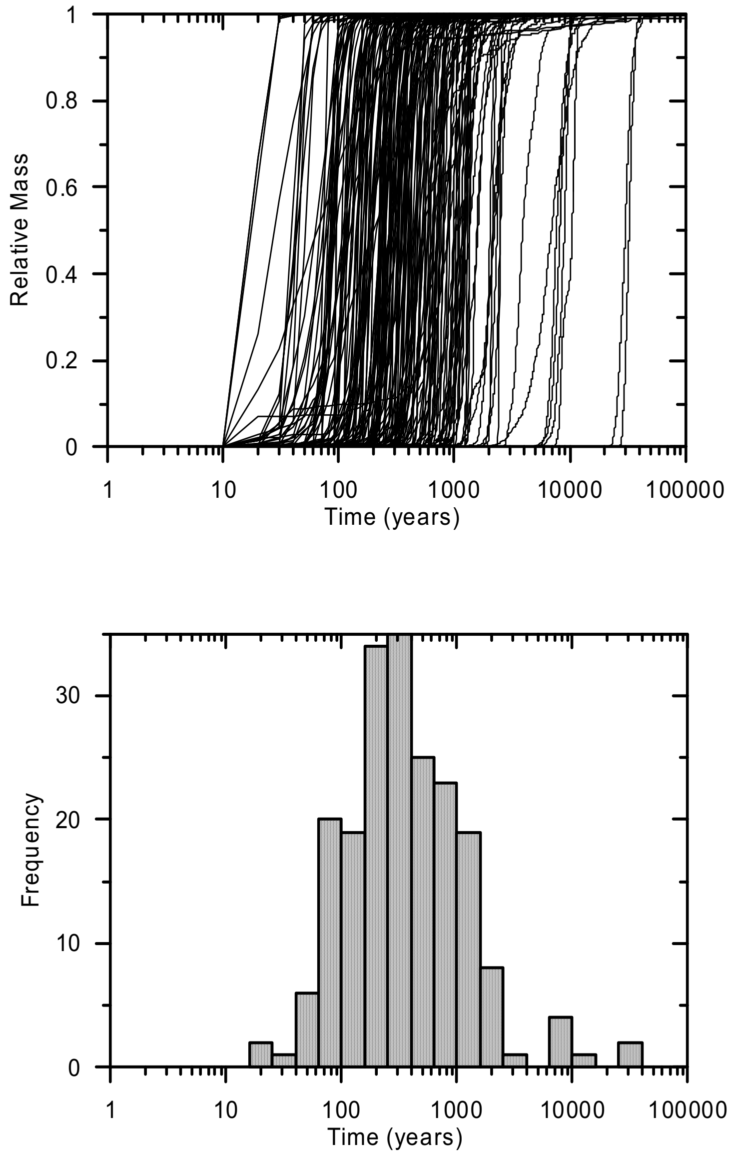

Output DTN: SN0310T0502103.012.

NOTE: Mass breakthrough curves and median transport times are for present-day climate, and do not include radionuclide decay. Results shown for 200 realizations from source region 1.

Figure 6-37. Mass Breakthrough Curves (upper) and Median Transport Times (lower) for the Fast Fraction of Plutonium and Americium on Irreversible Colloids at 18-km Distance

The simulated breakthrough curves from the SZ flow and transport abstraction model, as scaled for the glacial-transition climate state are shown in Figures 6-38 to 6-47. The results shown in these figures are for the same categories of radionuclides shown in Figures 6-28 to 6-37 and are derived from the breakthrough curves for present-day conditions, as implemented by the convolution method and the groundwater flow scaling factors for climate change, described in Section 6.5. The scaling factor is 3.9 (Table 6-5) and the maximum time is scaled from 100,000 years to approximately 26,000 years. The breakthrough curves and radionuclide transport times shown in Figures 6-38 to 6-47 are more representative of the long-term behavior of transport in the SZ because expected glacial-transition climatic conditions are applied in the TSPA-LA modeling from 2,000 years to 10,000 years following repository closure.

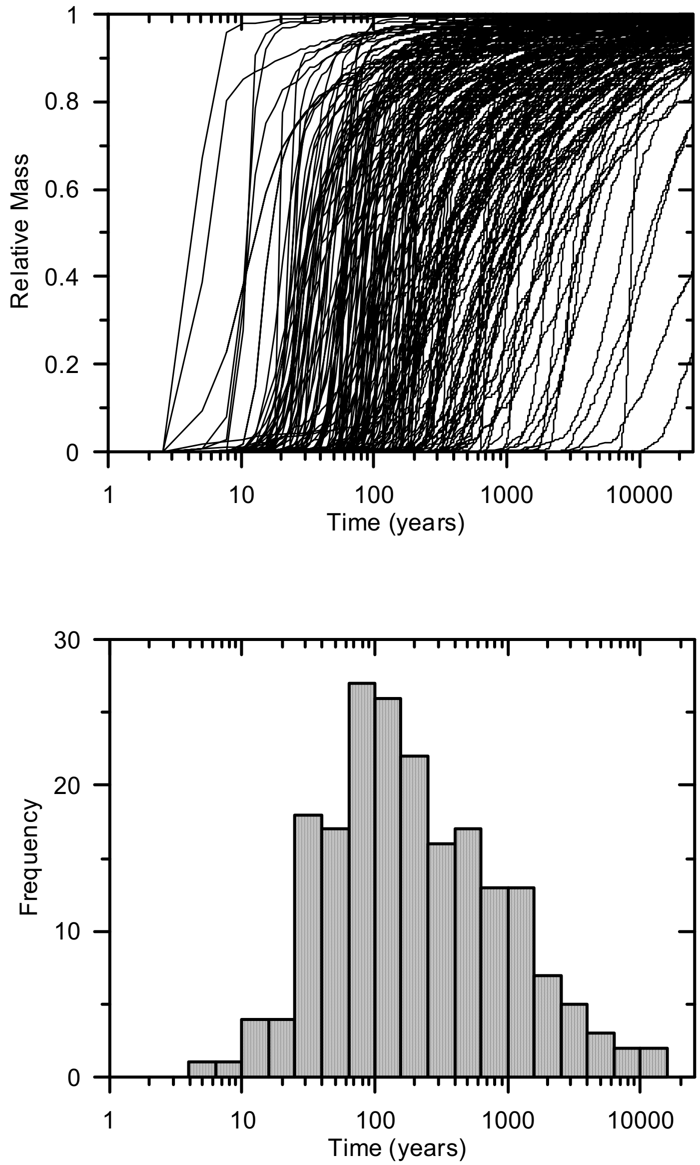

Output DTN: SN0310T0502103.010.

NOTE: Mass breakthrough curves and median transport times are derived from the breakthrough curves for present-day conditions and the groundwater flow scaling factors for climate change, described in Section 6.5. The scaling factor is 3.9 (Table 6-5) and the maximum time is scaled from 100,000 years to approximately 26,000 years for glacial-transition climate. Mass breakthrough curves do not include radionuclide decay. Results shown for 200 realizations from source region 1

Figure 6-38. Mass Breakthrough Curves (upper) and Median Transport Times (lower) for Carbon, Technetium, and Iodine at 18-km Distance

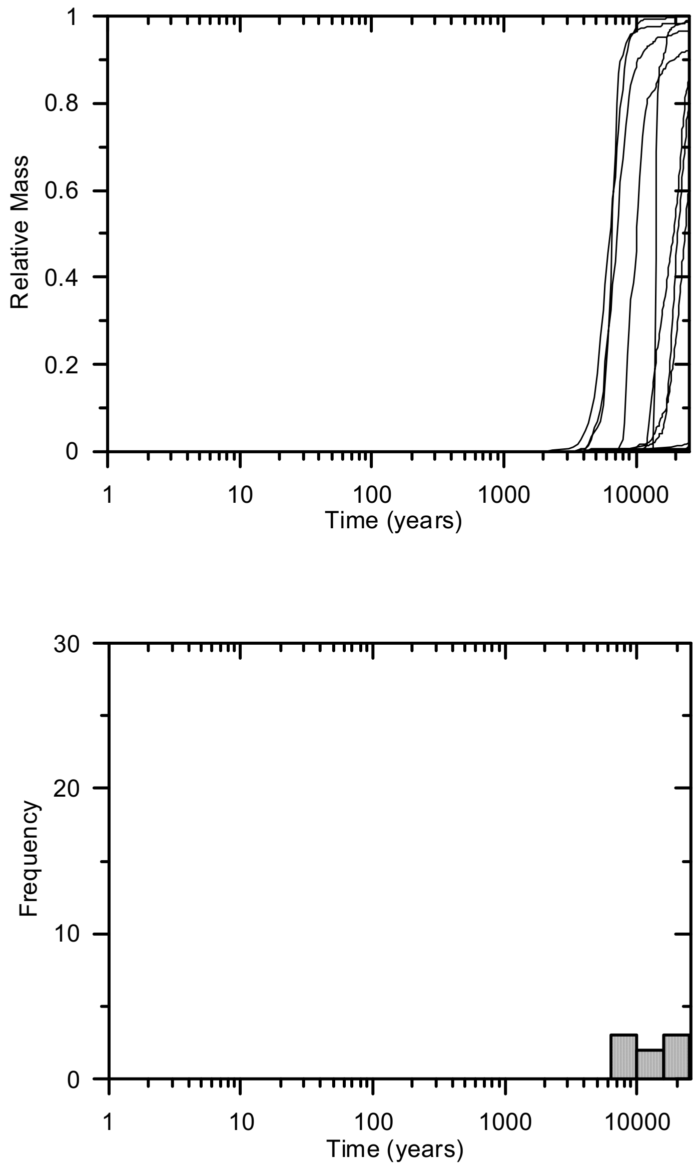

Output DTN: SN0310T0502103.010.

NOTE: Mass breakthrough curves and median transport times are derived from the breakthrough curves for present-day conditions and the groundwater flow scaling factors for climate change, described in Section 6.5. The scaling factor is 3.9 (Table 6-5) and the maximum time is scaled from 100,000 years to approximately 26,000 years for glacial-transition climate. Mass breakthrough curves do not include radionuclide decay. Results shown for 200 realizations from source region 1

Figure 6-39. Mass Breakthrough Curves (upper) and Median Transport Times (lower) for Americium, Thorium, and Protactinium on Reversible Colloids at 18-km Distance

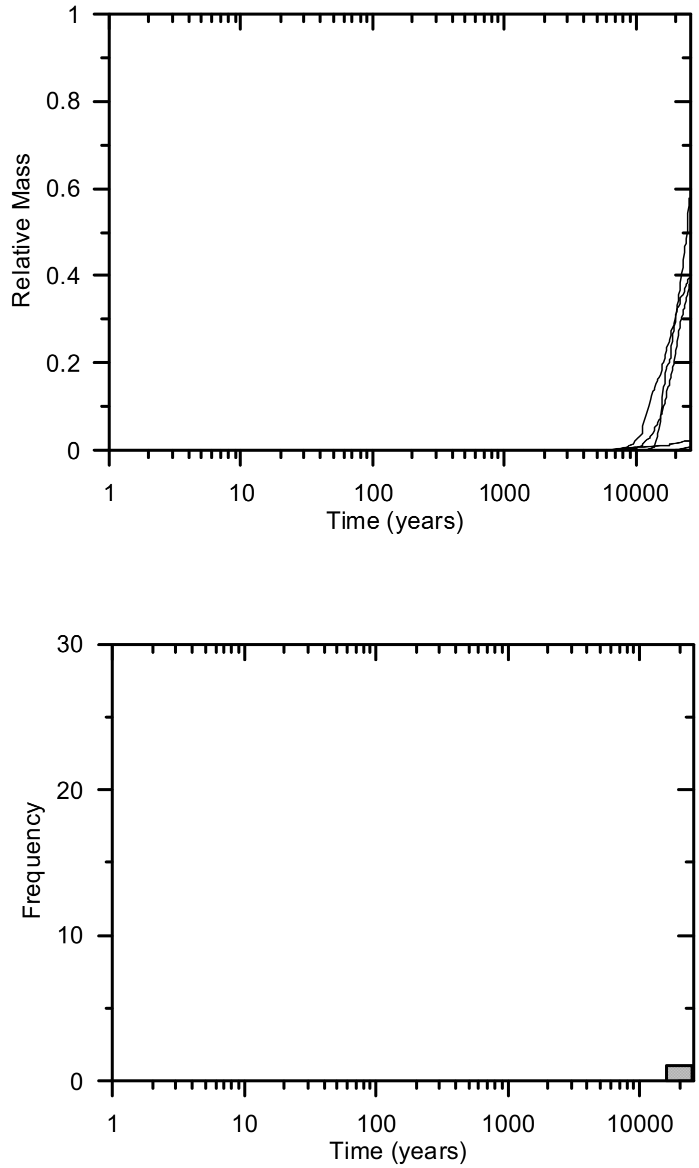

Output DTN: SN0310T0502103.010.

NOTE: Mass breakthrough curves and median transport times are derived from the breakthrough curves for present-day conditions and the groundwater flow scaling factors for climate change, described in Section 6.5. The scaling factor is 3.9 (Table 6-5) and the maximum time is scaled from 100,000 years to approximately 26,000 years for glacial-transition climate. Mass breakthrough curves do not include radionuclide decay. Results shown for 200 realizations from source region 1.

Figure 6-40. Mass Breakthrough Curves (upper) and Median Transport Times (lower) for Cesium on Reversible Colloids at 18-km Distance

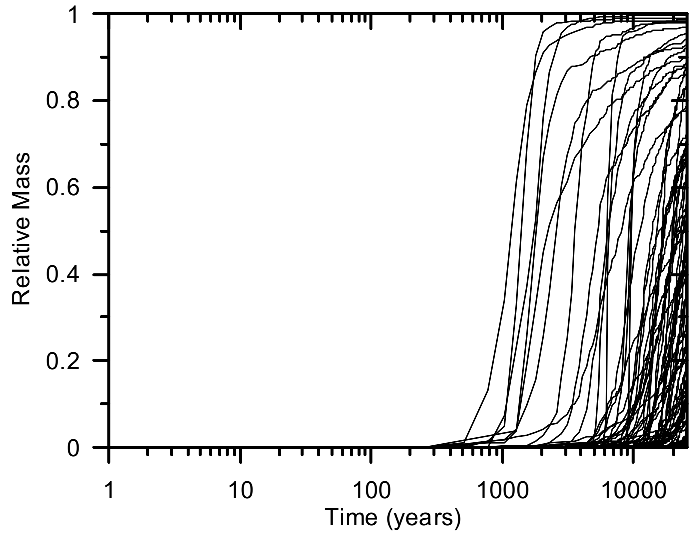

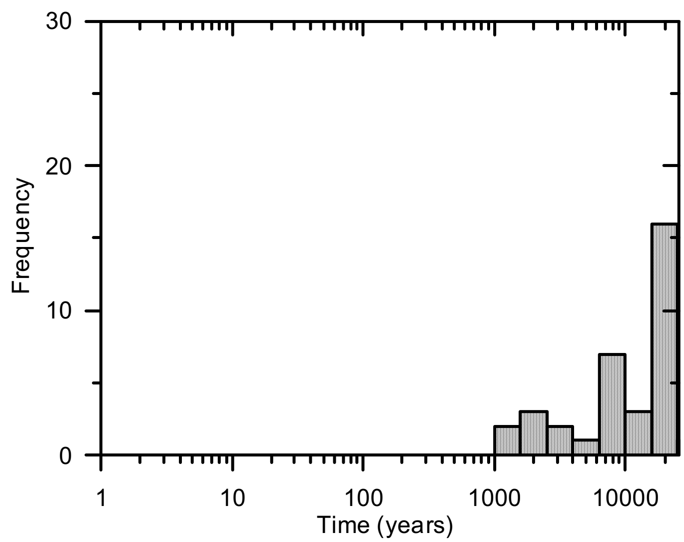

Output DTN: SN0310T0502103.010.

NOTE: Mass breakthrough curves and median transport times are derived from the breakthrough curves for present-day conditions and the groundwater flow scaling factors for climate change, described in Section 6.5. The scaling factor is 3.9 (Table 6-5) and the maximum time is scaled from 100,000 years to approximately 26,000 years for glacial-transition climate. Mass breakthrough curves do not include radionuclide decay. Results shown for 200 realizations from source region 1.

Figure 6-41. Mass Breakthrough Curves (upper) and Median Transport Times (lower) for Plutonium on Reversible Colloids at 18-km Distance

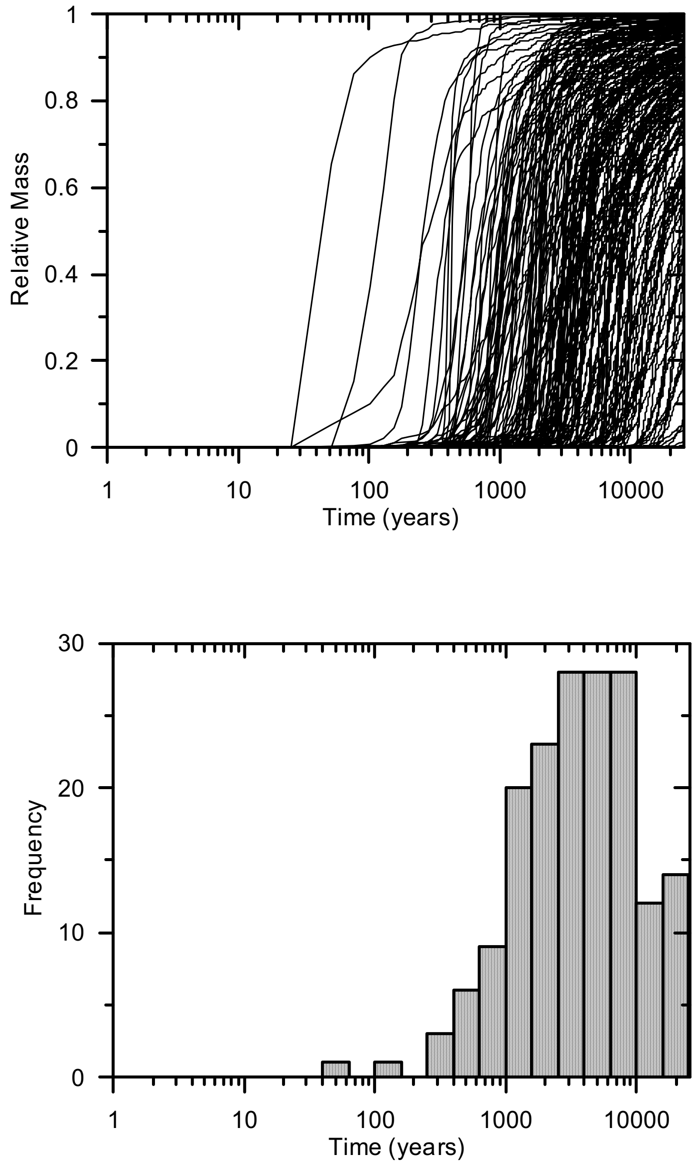

Output DTN: SN0310T0502103.010.

NOTE: Mass breakthrough curves and median transport times are derived from the breakthrough curves for present-day conditions and the groundwater flow scaling factors for climate change, described in Section 6.5. The scaling factor is 3.9 (Table 6-5) and the maximum time is scaled from 100,000 years to approximately 26,000 years for glacial-transition climate. Mass breakthrough curves do not include radionuclide decay. Results shown for 200 realizations from source region 1.

Figure 6-42. Mass Breakthrough Curves (upper) and Median Transport Times (lower) for Neptunium at 18-km Distance

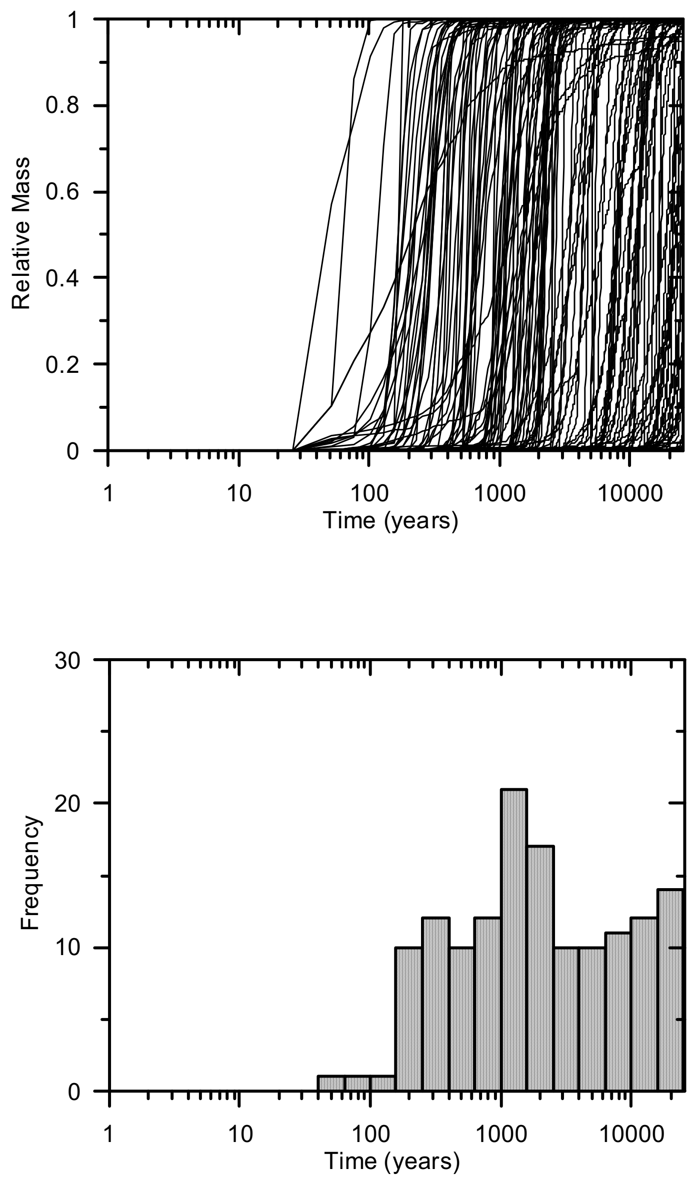

Output DTN: SN0310T0502103.010.

NOTE: Mass breakthrough curves and median transport times are derived from the breakthrough curves for present-day conditions and the groundwater flow scaling factors for climate change, described in Section 6.5. The scaling factor is 3.9 (Table 6-5) and the maximum time is scaled from 100,000 years to approximately 26,000 years for glacial-transition climate. Mass breakthrough curves do not include radionuclide decay. Results shown for 200 realizations from source region 1.

Figure 6-43. Mass Breakthrough Curves (upper) and Median Transport Times (lower) for Plutonium and Americium on Irreversible Colloids at 18-km Distance

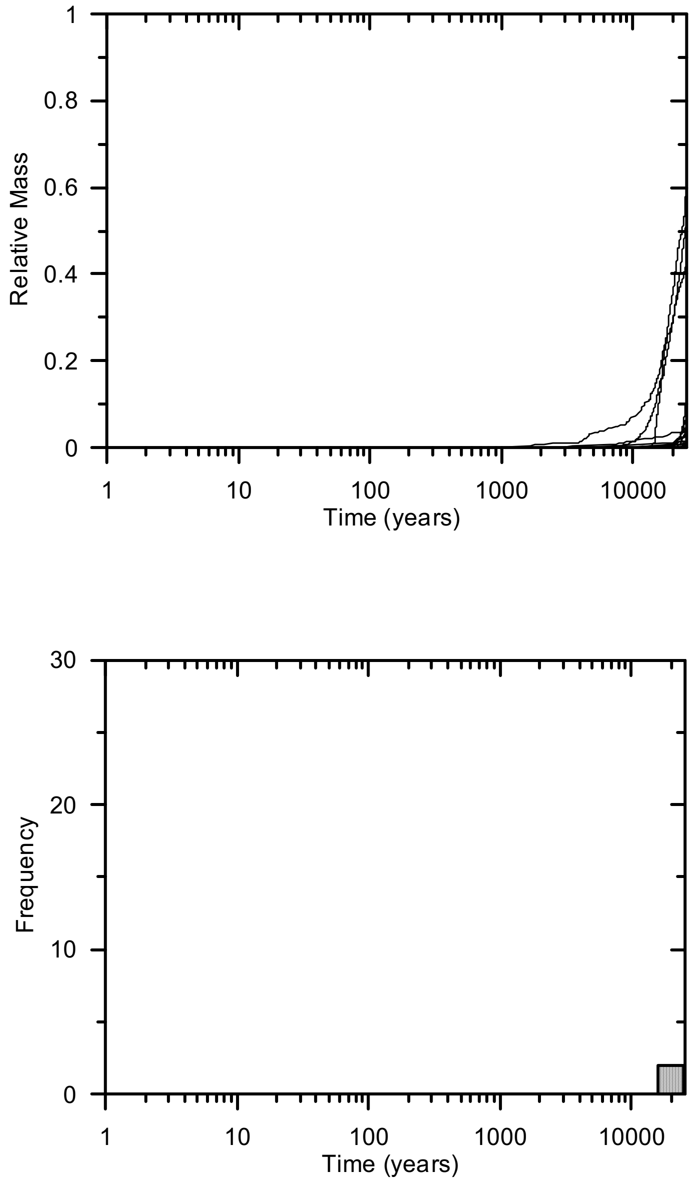

Output DTN: SN0310T0502103.010.

NOTE: Mass breakthrough curves and median transport times are derived from the breakthrough curves for present-day conditions and the groundwater flow scaling factors for climate change, described in Section 6.5. The scaling factor is 3.9 (Table 6-5) and the maximum time is scaled from 100,000 years to approximately 26,000 years for glacial-transition climate. Mass breakthrough curves do not include radionuclide decay. Results shown for 200 realizations from source region 1.

Figure 6-44. Mass Breakthrough Curves (upper) and Median Transport Times (lower) for Radium at 18-km Distance

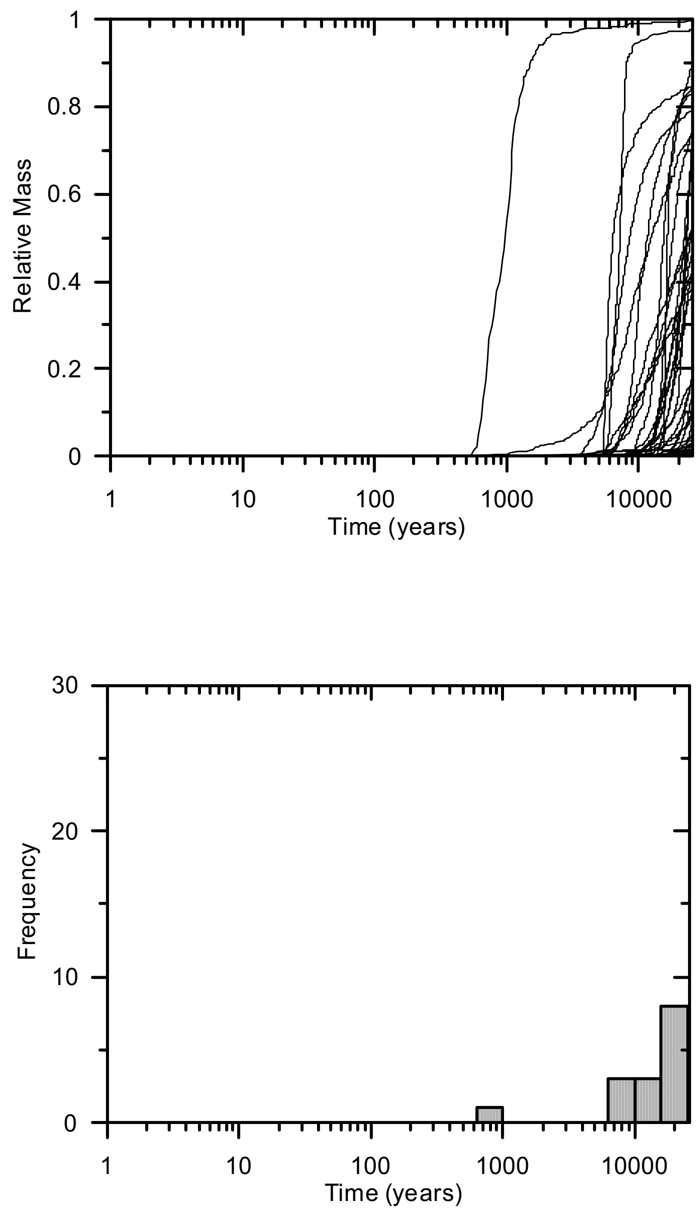

Output DTN: SN0310T0502103.010.

NOTE: Mass breakthrough curves and median transport times are derived from the breakthrough curves for present-day conditions and the groundwater flow scaling factors for climate change, described in Section 6.5. The scaling factor is 3.9 (Table 6-5) and the maximum time is scaled from 100,000 years to approximately 26,000 years for glacial-transition climate. Mass breakthrough curves do not include radionuclide decay. Results shown for 200 realizations from source region 1.

Figure 6-45. Mass Breakthrough Curves (upper) and Median Transport Times (lower) for Strontium at 18-km Distance

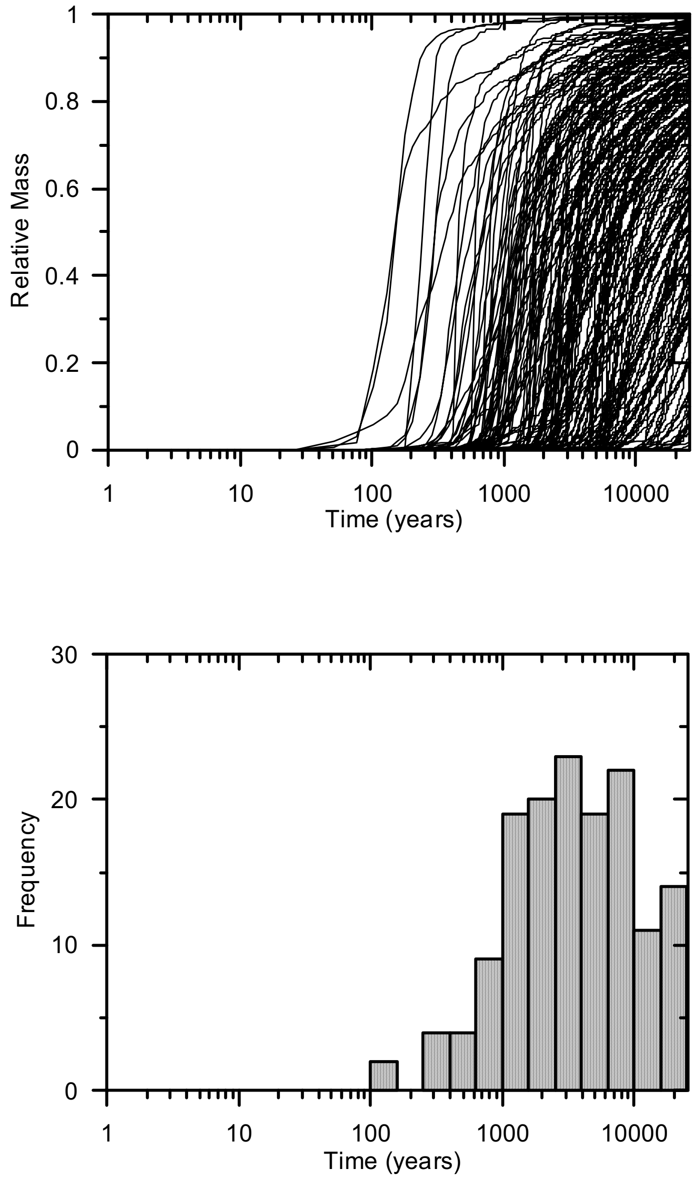

Output DTN: SN0310T0502103.010.

NOTE: Mass breakthrough curves and median transport times are derived from the breakthrough curves for present-day conditions and the groundwater flow scaling factors for climate change, described in Section 6.5. The scaling factor is 3.9 (Table 6-5) and the maximum time is scaled from 100,000 years to approximately 26,000 years for glacial-transition climate. Mass breakthrough curves do not include radionuclide decay. Results shown for 200 realizations from source region 1.

Figure 6-46. Mass Breakthrough Curves (upper) and Median Transport Times (lower) for Uranium at 18-km Distance

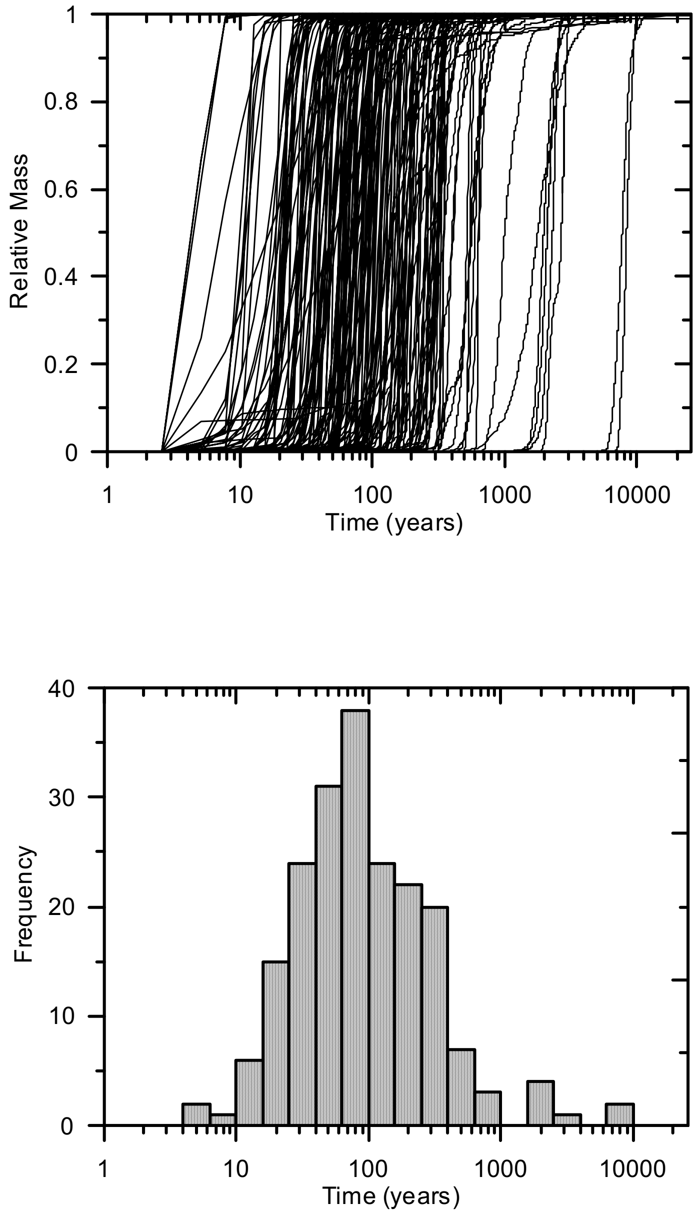

Output DTN: SN0310T0502103.012.

NOTE: Mass breakthrough curves and median transport times are derived from the breakthrough curves for present-day conditions and the groundwater flow scaling factors for climate change, described in Section 6.5. The scaling factor is 3.9 (Table 6-5) and the maximum time is scaled from 100,000 years to approximately 26,000 years for glacial-transition climate. Mass breakthrough curves do not include radionuclide decay. Results shown for 200 realizations from source region 1.

Figure 6-47. Mass Breakthrough Curves (upper) and Median Transport Times (lower) for the Fast Fraction of Plutonium and Americium on Irreversible Colloids at 18-km Distance

6.6.2 Summary of Results

SZ flow and transport simulation results with the SZ flow and transport abstraction model for the nonsorbing radionuclides of carbon, technetium, and iodine indicate that variability in simulated median transport times to the boundary of the accessible environment ranges from a few tens of years to 100,000 years. The bulk of the realizations show transport times ranging from a few hundred years to a few thousand years for nonsorbing species, and a median transport time among all of the realizations of about 640 years.

Approximately 97 percent of the realizations of americium, protactinium, and thorium transported as reversibly sorbed onto colloids have simulated transport times of greater than 100,000 years. Approximately 99 percent of the realizations of cesium transported as reversibly sorbed onto colloids have simulated transport times of greater than 100,000 years.

Simulated median transport times for plutonium reversibly sorbed on colloids range from a few thousand years to greater than 100,000 years, with a majority of the realizations indicating transport times of greater than 100,000 years. The simulated breakthrough curves for neptunium range from less than 100 years to greater than 100,000 years, with a median transport time among the realizations of about 18,000 years. Simulated median transport times for plutonium and americium irreversibly attached to colloids range from a few hundred years to greater than 100,000 years, with a median among the realizations of about 18,000 years.

About 99 percent of the realizations of radium transport have simulated transport times of greater than 100,000 years. Greater than 99 percent of the realizations of strontium transport have simulated transport times of greater than 10,000 years, with the majority of the realizations having median transport times of greater than 100,000 years. Simulated median transport times for uranium range from somewhat less than 1,000 years to greater than 100,000 years, with a median transport time among the realizations of about 24,000 years. Simulated median transport times for plutonium and americium irreversibly attached to the fast fraction of colloids (i.e., with no retardation) range from a few tens of years to greater than 10,000 years, with a median among the realizations of about 300 years.

6.7 DESCRIPTION OF BARRIER CAPABILITY

The SZ forms a barrier to the migration of radionuclides and to the exposure of the potential receptor population to these radionuclides in two ways. Delay in the release of radionuclides to the accessible environment during transport in the SZ allows radioactive decay to diminish the mass of radionuclides that are ultimately released. Dilution of radionuclide concentrations in groundwater used by the potential receptor population occurs during transport in the SZ and in the process of producing groundwater from wells. Further discussion of the SZ flow system as a barrier to radionuclide migration at Yucca Mountain is found in a report by Eddebbarh et al. (2003 [DIRS 163577]).

6.7.1 Analyses of Barrier Capability

The simulated transport times of radionuclides in the SZ give a direct indication of the barrier capability of the SZ with regard to the delay in the release of radionuclides to the accessible environment. Uncertainty in the radionuclide transport times in the SZ is represented in the multiple realizations of the SZ system with the SZ flow and transport abstraction model and shown in the breakthrough curves for various radionuclides in Figures 6-28 to 6-36. As shown by these figures, the effectiveness of the SZ as a barrier to transport varies significantly among the classes of radionuclides included in the analyses. The ranges of median transport times and the median transport times from all realizations for the various radionuclides are summarized in Table 6-16.

Variations in the radionuclide transport time among the realizations shown in Figures 6-28 to 6-36 reflect the aggregate uncertainty in the underlying input parameters to the SZ flow and transport abstraction model. Although formal sensitivity analyses have not been applied to these results, sensitivity analyses have been performed on similar previous SZ flow and transport modeling results (Arnold et al. 2003 [DIRS 163857]). The SZ flow and transport abstraction model has not been significantly changed and the parameter uncertainty distributions have not been dramatically changed in the present modeling, relative to the modeling analyzed in Arnold et al. (2003 [DIRS 163857]). Consequently, the general conclusions from the study are expected to apply to the current modeling. The analyses in Arnold et al. (2003 [DIRS 163857]) indicate that uncertainties in groundwater specific discharge, sorption coefficients, and retardation of colloids are major factors in the simulated uncertainty in radionuclide transport times. Parameters related to matrix diffusion and geologic uncertainty have significant, but secondary importance with regard to the uncertainty in radionuclide transport times.

For nonsorbing species, such as carbon, technetium, and iodine, the delay afforded by the SZ can be less than 100 years to as much as 100,000 years, within the range of uncertainty indicated by the simulation results shown in Figure 6-28. The median transport time for nonsorbing species among all realizations is about 620 years. For the moderately sorbing species of neptunium, simulated median transport times range from about 200 years to greater than 100,000 years, with a median transport time among all realizations of 17,100 years (see Table 6-16). For the strongly sorbing species of radium, simulated median transport times range from 80,200 to greater than 100,000 years, with a median transport time among all realizations of greater than 100,000 years (see Table 6-16).

Analyses with the SZ flow and transport abstraction model indicate that there is considerable uncertainty in the delay to release of radionuclides to the accessible environment for all radionuclides. The upper bounds of uncertainty in the transport times are greater than 100,000 years (the upper limit of time in the transport simulations) for all radionuclides, with the exception of the fast fraction of plutonium and americium irreversibly attached to colloids. The lower bounds of the uncertainty in transport times are indicated by the ranges given in Table 6-16.

It should be noted that the summary of simulated transport times presented in Table 6-16 is given for SZ groundwater flow under present climatic conditions. Under glacial-transition climatic conditions that are expected to occur within the next 10,000 years, the groundwater flow rate would be significantly higher. Groundwater flow rates in the SZ are estimated to be 3.9 times higher under glacial-transition climate conditions (see Section 6.5.1) corresponding to transport times shorter by approximately a factor of 3.9 (i.e., divided by a factor of 3.9) than those presented in Table 6-16.

Table 6-16. Summary of Simulated Transport Times in the SZ Under Present Climatic Conditions

Species	Range of Median Transport Time (years)	Median Transport Time Among All Realizations (years)
Carbon Technetium Iodine	20 - >100,000	620
Reversible Colloids: Americium Thorium Protactinium	25,000 - >100,000	>100,000
Reversible Colloids: Cesium	80,000 - >100,000	>100,000
Reversible Colloids: Plutonium	5,000 - >100,000	>100,000
Neptunium	200 - >100,000	17,100
Irreversible Colloids: Plutonium Americium	200 - >100,000	19,400
Radium	80,200 - >100,000	>100,000
Strontium	3,300 - >100,000	>100,000
Uranium	600 - >100,000	23,300
Fast Fraction of Irreversible Colloids: Plutonium Americium	20 – 32,620	310

Output DTNs: SN0310T0502103.010 and SN0310T0502103.012.

6.7.2 Summary of Barrier Capability

Taken as a whole, these analyses indicate that the SZ is expected to be a significant barrier to the transport of radionuclides to the accessible environment within the 10,000-year period of regulatory concern for the repository at Yucca Mountain. The expected behavior of the SZ system is to delay the transport of sorbing radionuclides and radionuclides associated with colloids for many thousands of years, even under future wetter climatic conditions. Nonsorbing radionuclides are expected to be delayed for hundreds of years during transport in the SZ.

However, analyses of uncertainty in radionuclide transport in the SZ indicate that delays in the release of nonsorbing radionuclides could be as small as tens of years. The transport times in the SZ of neptunium, uranium, and of plutonium and americium irreversibly attached to colloids could be as small as hundreds of years, based on the analyses of uncertainty conducted with the SZ flow and transport abstraction model. It is important to note that ranges of uncertainty based on analyses with 200 Monte Carlo realizations extend to relatively low probability (approximately 0.5 percent probability) and thus include relatively unlikely results. Nonetheless, lower values in the ranges of transport time are possible, given the degree of uncertainty included in the model.

The radioactive decay of radionuclides during transport in the SZ enhances the barrier capability of the SZ by reducing the mass of radionuclides ultimately released to the accessible environment. The effectiveness of the decay process in attenuating releases from the SZ is related to the delay in the SZ and the half-life of the radionuclide. For radionuclides with longer transport times in the SZ and relatively short half-lives, this process renders the SZ an extremely effective barrier. Strontium-90 and ^{137}Cs transport times would exceed several thousand half-lives, i.e., greater than 100,000 years, based on the median transport time among the realizations (Table 6-16). For comparison, the reduction in radioactivity after 20 half-lives is more than six orders of magnitude. For some radionuclides, a modest reduction in radionuclide mass would occur during transport in the SZ. Plutonium-239 that is irreversibly attached to colloids would be expected to experience about 0.8 half-lives, based on the median transport time among all realizations (Table 6-16). Several radionuclides would experience little attenuation due to radioactive decay during transport in the SZ. Technetium-99, ^{129}I, and ^{237}Np would have only very small reductions in mass during the delay in release afforded by the SZ, due to their long half-lives (2.13×10^5 years for ^{99}Tc to 1.59×10^7 years for ^{129}I).

The dilution of radionuclides in the SZ and during pumping from wells by the future hypothetical community in which the RMEI resides is not quantitatively assessed with the transport modeling approach used in the SZ flow and transport abstraction model. The relatively low values of transverse dispersivity in the uncertainty distribution for this parameter suggest that a large amount of dilution in radionuclide concentration during transport from beneath the repository to the accessible environment in the SZ is not expected.

6.8 GROSS ALPHA CONCENTRATION

Regulations in 10 CFR 63.331 (10 CFR 63 [DIRS 173273]) limit the gross alpha concentration and ^{226}Ra and ^{228}Ra concentration in groundwater. These groundwater protection standards apply to the accessible environment in the Yucca Mountain region and potential impacts of the repository must be compared to them. One aspect of the analysis is an assessment of the natural background concentrations in groundwater near the site because the standards for both gross alpha activity and combined ^{226}Ra and ^{228}Ra activity concentrations (15 picocuries per liter (pCi/L) and 5 pCi/L, respectively, 10 CFR 63 [DIRS 173273], Section 63.331, Table 1) are inclusive of natural background concentrations. Measurements of gross alpha concentrations and ^{226}Ra and ^{228}Ra activity concentrations are taken as representative of natural background concentrations in groundwater under future conditions. Although climatic conditions are expected to change in the future, present-day groundwater samples from multiple locations and of varying groundwater ages provide a reasonable average assessment of natural background concentrations for future climatic conditions because the older groundwater samples retain information from previous climate states.

6.8.1 Gross Alpha Activity Data

A testing program to measure ambient radiation levels in groundwater was conducted in FY 1998. This work was performed under the YMP QA program. Groundwater samples were collected in June, July, and September of 1998 from each of six wells and two springs. The details and findings of this evaluation were reported in *Radioactivity in FY 1998 Groundwater Samples from Wells and Springs Near Yucca Mountain* (CRWMS M&O 1999 [DIRS 150420]). The data of interest for this study are the reported gross alpha concentrations (pCi/L) (CRWMS M&O 1999 [DIRS 150420], Section 3.2.1, Table 3), which were submitted with gross beta measurements, to the Total Management Data System as DTN: MO9904RWSJJS98.000 [DIRS 165866].

In *Radioactivity in FY 1998 Groundwater Samples from Wells and Springs Near Yucca Mountain* (CRWMS M&O 1999 [DIRS 150420], p. 9) it was stated that, when gross alpha concentrations in groundwater exceed 5 pCi/L, calculation of average combined ^{226}Ra and ^{228}Ra concentration was required. However, *Radioactivity in FY 1998 Groundwater Samples from Wells and Springs Near Yucca Mountain* (CRWMS M&O 1999 [DIRS 150420], Section 3.2.1) demonstrates the mean gross alpha concentration at each sample location was below 5 pCi/L in FY 1998, and continues by stating that in such cases, it was not necessary to calculate combined ^{226}Ra and ^{228}Ra concentration. As a consequence, data concerning ^{226}Ra and ^{228}Ra concentrations were not presented.

6.8.2 Counting Statistics and Error Prediction

Because of the random nature of radioactive decay and the relatively low concentrations of alpha emitting radionuclides in natural groundwater, it is necessary to understand the statistical fluctuations of the analytical method in relation to uncertainty. This will explain why negative radiation concentrations may be reported.

6.8.2.1 Counting Statistics and Uncertainty for a Single Measurement

The following discussions on the statistics of radioactive decay measurements are taken from *Radiation Detection and Measurement* (Knoll 1989 [DIRS 161052], Chapter 3). A detector is used to count the number of radioactive decays in a given time period (a trial). The counts from multiple trials have a Poisson distribution. Clearly, if a trial comprises n counts, then the estimate of the actual (average) number of counts ($\overline{n}$) in that trial is n (Knoll 1989 [DIRS 161052], p.84). Furthermore, the sample variance (σ^2) is also n, implying that the standard deviation (σ) is $n^{0.5}$ (Knoll 1989 [DIRS 161052], p. 85). For large values of n, the Poisson distribution for multiple trials can be approximated by a normal (i.e., Gaussian) distribution, thereby allowing confidence limits for the true mean ($\overline{n}$) to be established. Measurements involving radioactive decay are generally conducted for sufficient time to establish conditions for this approximation to be valid. One example given by Knoll (1989 [DIRS 161052], Table 3-6), is for a measurement of n = 100 (σ in this example is equal to $100^{0.5} = 10$). There is a 90 percent probability that the true mean ($\overline{n}$) is in the interval $n \pm 1.64\sigma$, or 83.6 to 116.4. The symmetry of the normal distribution indicates that in this example, there is a 5 percent chance of the true mean being below 83.6 and a 5 percent chance of it being above 116.4.

6.8.2.2 Uncertainty Propagation

Measurements involving the counting of radioactive decay events are subject to spurious counts from natural background radiation. The effect of this natural background on the desired results can be negated to a certain extent by performing the measurement twice, once with the sample to be quantified and once without the sample. The former measurement gives a count of the desired signal plus unwanted background noise, while the latter provides an estimate of the background noise only. If the counting times for both trials are equal, then the net counts from the sample to be characterized is the difference between the two measured counts.

Following the approach presented by Knoll (1989 [DIRS 161052], p. 88), if there were two counts taken, the first series x being associated with the sample and background noise and the second y corresponding to the background noise, then the net counts attributable to the sample being assessed is the difference between x and y. The variance (σ^2) associated with the net value is the sum of the variances of the two measurements:

$$\sigma_{net}^2 = \sigma_x^2 + \sigma_y^2 \qquad \text{(Eq. 6-31)}$$

Because of the stochastic nature of both radioactive decay and background radiation, it is possible for a sample of low activity to give rise to a total count that is lower than the independently measured background count. These cases produce a negative estimate for the net sample activity. Although a negative value for gross alpha activity is physically unrealistic, such estimates are an expected outcome for some measurements of low-activity samples because of variations in the decay process. For statistical consistency it is necessary to retain these negative estimates of activity when calculating average values of activity. Inclusion of negative measurements in calculations of average values is in accordance with U.S. Environmental Protection Agency recommendations and statistical theory (Watson 1980 [DIRS 173955], p. 6-1 and Gilbert 1987 [DIRS 163705], Chapter 14).

6.8.2.3 Statistical Analysis of Multiple Measurements

If these measurements to quantify a small level of activity were to be repeated several times, then the stochastic nature of the processes will result in a range of net activity estimates. Some of these results would underestimate the true activity while others would overestimate the true value. Combining the data sets allows the random fluctuations observed in single measurements to be averaged over multiple measurements and thereby reduce statistical variations. This approach is adopted here.

If there are n measurements of a variable x, where measurement i is denoted by x_i having a variance of σ_i^2 (number of counts) then the average ($\bar{x}$) is given by:

$$\bar{x} = \frac{1}{n}\sum_{1}^{n} x_i \qquad \text{(Eq. 6-32)}$$

Knoll (1989 [DIRS 161052], Equations 3-38 and 3-40) provides an estimate of the standard deviation (σ_x) in $\bar{x}$ as:

$$\sigma_{\bar{x}} = \frac{1}{n}\sqrt{\sum_{1}^{n}\sigma_i^2} \qquad \text{(Eq. 6-33)}$$

6.8.3 Applicable Sample Locations

Gross alpha concentration data in groundwater from eight locations in the vicinity of a potential future receptor were collected in *Radioactivity in FY 1998 Groundwater Samples from Wells and Springs Near Yucca Mountain* (CRWMS M&O 1999 [DIRS 150420]). Six of these locations were identified as being in the subbasin (Alkali Flat-Furnace Creek Subbasin) that contains Yucca Mountain, as shown in the first column of Table 6-17 (DTN: MO9904RWSJJS98.000 [DIRS 165866]). The data from these six locations were selected to be the basis of estimating the groundwater gross alpha concentration at the receptor's location. The data from the Cherry Patch Well and Fairbanks Spring were not used, because these locations are not in the groundwater subbasin containing the repository.

It was recognized that other weighting schemes to obtain a mean activity level from these data were available. Weights could be based on some function of distance of the sampled wells from the receptor location or on the uncertainties of the individual measurements. In the interests of keeping the analysis simple without having to provide justification from any particular scheme, simple averaging was used.

6.8.4 Data Analysis

The calculation of the mean activity values and the estimated standard deviation, using data from DTN: MO9904RWSJJS98.000 [DIRS 165866] is shown in Table 6-17. It should be noted that the reported values of gross alpha concentration on these groundwater samples exclude the contributions of radon and uranium, consistent with the regulations in 10 CFR 63.331 (10 CFR 63 [DIRS 173273]) governing gross alpha activity in groundwater.

Table 6-17. Data Table Showing Calculation of Mean and Standard Deviation of Gross Alpha Concentration

Location	Date	Gross Alpha (x_i) (pCi/L)	Uncertainty[a] ($2\sigma_i$) (pCi/L)	Sigma (σ_i) (pCi/L)	σ_i^2 (pCi/L)^2
NDOT Well	24-Jun-98	-0.08	1.56	0.78	0.608
	29-Jul-98	0.32	1.1	0.55	0.303
	23-Sep-98	-1.40	0.79	0.40	0.156
Gilgan's South Well	24-Jun-98	-0.63	0.86	0.43	0.185
	29-Jul-98	0.64	0.86	0.43	0.185
	23-Sep-98	-0.74	0.69	0.35	0.119
UE-25 J-12	23-Jun-98	0.06	0.96	0.48	0.230
	28-Jul-98	0.27	0.72	0.36	0.130
	22-Sep-98	0.27	0.8	0.40	0.160
UE-25 J-13	23-Jun-98	0.05	0.94	0.47	0.221
	28-Jul-98	0.50	0.73	0.37	0.133
	22-Sep-98	-0.18	1.2	0.60	0.360

Table 6-17. Data Table Showing Calculation of Mean and Standard Deviation of Gross Alpha Concentration (Continued)

Location	Date	Gross Alpha (x_i) (pCi/L)	Uncertainty[a] ($2\sigma_i$) (pCi/L)	Sigma (σ_i) (pCi/L)	σ_i^2 $(pCi/L)^2$
UE-25 c#2	23-Jun-98	1.20	1.33	0.67	0.442
	28-Jul-98	1.49	0.94	0.47	0.221
	22-Sep-98	0.73	1.67	0.84	0.697
Crystal Pool	22-Jun-98	1.04	1.27	0.64	0.403
	27-Jul-98	1.75	1.64	0.82	0.672
	25-Sep-98	-0.85	1.21	0.61	0.366
	Σx_i =	4.44		$\Sigma \sigma_i^2$ =	5.59
	Mean Gross Alpha $\bar{x}$ =	0.25[b]		$\sigma_{\bar{x}}$ =	0.13[c]

Source: DTN: MO9904RWSJJS98.000 [DIRS 165866].

[a] Uncertainty is defined as being two standard deviations (sigma) (CRWMS M&O 1999 [DIRS 150420], Section 3.2.1, Note to Table 3 given on p. 9).
[b] Calculated using Equation 6-32.
[c] Calculated using Equation 6-33.

6.8.5 Results

From the discussion in Section 6.8.2 from Knoll (1989 [DIRS 161052], p. 86), there is a 90 percent chance that the true mean of a parameter (μ) will fall in the interval of $\bar{x} \pm 1.64\sigma_{\bar{x}}$ and that in only 5 percent of the cases will the true value exceed $\bar{x} + 1.64\sigma_{\bar{x}}$. As was discussed in Section 6.8.2 this estimate is valid for the large values of counts when the Poisson distribution can be approximated by a normal distribution and confidence limits for the true mean can be established. From the values presented in Table 6-17 to two decimal places, the best estimate for the mean gross alpha concentration in groundwater is 0.25 pCi/L with a 95 percent confidence that the concentration will not exceed 0.46 pCi/L. The overall uncertainty in the mean gross alpha concentration has a physically defined lower bound of 0.0 pCi/L. The upper bound of the uncertainty in the gross alpha concentration can be reasonably defined using a value that is 3 times the standard deviation above the expected value, which can be calculated as 0.64 pCi/L. A value that is 3 times the standard deviation above the expected value corresponds approximately to the 99.9th percentile in a normal distribution. The overall uncertainty distribution of the mean gross alpha concentration can thus be defined as a truncated normal distribution with a mean of 0.25 pCi/L, a standard deviation of 0.13 pCi/L, a lower bound of 0.0 pCi/L, and an upper bound of 0.64 pCi/L.

In the absence of data on the combined concentrations of ^{226}Ra and ^{228}Ra, it should be conservatively assumed for the standards involving these radionuclides that they are responsible for all gross alpha activity. For ^{226}Ra and ^{228}Ra, the mean concentration is 0.25 pCi/L with a 95 percent confidence that the concentration will not exceed 0.46 pCi/L. These results are summarized in Table 6-18.

Table 6-18. Summary of Alpha Concentration Results in Amargosa Valley Groundwater

Parameter	Expected Value pCi/L	Upper (95%) Limit pCi/L
Gross Alpha Concentration	0.25	0.46
Combined Concentration of ^{226}Ra and ^{228}Ra	0.25	0.46

Source: DTN: MO9904RWSJJS98.000 [DIRS 165866].

6.8.6 Additional Data

There are several sources of additional non-QA data on gross alpha and radium concentrations in groundwater in the vicinity of the receptor that can be used to augment the data on the concentrations derived to demonstrate compliance with the groundwater protection standards. These sources are discussed below and data from them were combined with the QA data used in the analysis in Section 6.8.4.

In *Yucca Mountain Site Characterization Project Radiological Programs, Radioactivity in FY 1997 Groundwater Samples from Wells and Springs Near Yucca Mountain* (CRWMS M&O 1998 [DIRS 104963]) data on gross alpha concentration and combined ^{226}Ra and ^{228}Ra concentration are reported for the same locations analyzed in Section 6.8.4. The gross alpha concentrations reported in CRWMS M&O (1998 [DIRS 104963], Table E-1) have been corrected to exclude the contributions of radon and uranium. The gross alpha concentration data from *Yucca Mountain Site Characterization Project Radiological Programs, Radioactivity in FY 1997 Groundwater Samples from Wells and Springs Near Yucca Mountain* (CRWMS M&O 1998 [DIRS 104963], Table E-1) are included in Table 6-19. Combined ^{226}Ra and ^{228}Ra concentrations for the same locations are also reported in *Yucca Mountain Site Characterization Project Radiological Programs, Radioactivity in FY 1997 Groundwater Samples from Wells and Springs Near Yucca Mountain* (CRWMS M&O 1998 [DIRS 104963], Table D-1). The average combined ^{226}Ra and ^{228}Ra concentration from 23 water samples is 0.42 pCi/L. This average value is above the expected value, but below the upper 95 percent confidence limit of combined ^{226}Ra and ^{228}Ra concentration estimated in Section 6.8.5.

In *Nevada Test Site Annual Site Environmental Report for Calendar Year 2000* (Townsend and Grossman 2001 [DIRS 156604], Table 8.3), data on gross alpha concentration for a total of 11 water samples are reported for wells UE-25 J-12, UE-25 J-13, Amargosa Valley RV Park, and Crystal Pool. The gross alpha concentrations reported are not corrected for the contributions of radon and uranium, so these values overestimate the gross alpha activity excluding radon and uranium. The approximately corrected values and uncertainty in gross alpha concentration from Townsend and Grossman (2001 [DIRS 156604], Table 8.3) are included in Table 6-19. Estimated concentrations of ^{226}Ra and ^{228}Ra for the same locations are reported by Townsend and Grossman (2001 [DIRS 156604], Table 8.6 and Table 8.7). The sum of the average concentration for ^{226}Ra and the average concentration for ^{228}Ra is 0.51 pCi/L. This average value is above the expected value and somewhat above the upper 95 percent confidence limit of combined ^{226}Ra and ^{228}Ra concentration estimated in Section 6.8.5.

The gross alpha concentrations reported in Townsend and Grossman 2001 [DIRS 156604], Table 8.3 are approximately corrected to exclude the contribution of uranium as follows.

Uranium concentrations in groundwater samples are not reported in Townsend and Grossman 2001 [DIRS 156604]. However, average uranium concentrations at these sampling locations are taken from DTN: MO9904RWSJJS98.000 [DIRS 165866] and used for the correction of gross alpha concentrations from Townsend and Grossman 2001 [DIRS 156604]. In the case of the Amargosa Valley RV Park well, no measurements of uranium concentration are available from DTN: MO9904RWSJJS98.000 [DIRS 165866], but average uranium concentration from the nearby NDOT well is used to make the correction. Average uranium concentration values from DTN: MO9904RWSJJS98.000 [DIRS 165866] used in the corrections are as follows: NDOT well – 2.60 μg/L, Crystal Pool - 2.82 μg/L, UE-25 J-12 – 0.64 μg/L, and UE-25 J-13 – 0.56 μg/L. The uranium concentration is converted from units of μg/L to units of pCi/L by multiplying by 0.68 (CRWMS M&O 1998 [DIRS 104963], Table 6 note). The same approximate correction method is used for gross alpha concentration data from Townsend and Grossman 2002 [DIRS 173960] (Table 8.3), Townsend and Grossman 2003 [DIRS 168841] (Table 8.3), and Wills 2004 [DIRS 173956] (Table 3-1, 3-2, and 3-3).

In *Nevada Test Site Annual Site Environmental Report for Calendar Year 2000* (Townsend and Grossman 2001 [DIRS 156604], p. 8-1), the preamble to Section 8: Groundwater Monitoring, identifies that for the calendar year covered by the report (CY 2000), some results for radioactivity analysis were higher than historical data. It was also mentioned that the (unidentified) organization providing oversight of groundwater monitoring activities had also experienced similar difficulty in obtaining accurate analytical data. Because, there was no indication as to whether this caveat applied to specific data sets or to all data, it must be assumed that all data based on radioactivity analysis were systematically biased to higher values.

In *Nevada Test Site Annual Site Environmental Report for Calendar Year 2001* (Townsend and Grossman 2002 [DIRS 173960], Table 8.3), data on gross alpha concentration for a total of nine water samples are reported for wells UE-25 J-12, UE-25 J-13, and Crystal Pool. There is no indication that the gross alpha concentrations reported are corrected for the contributions of radon and uranium, so these values overestimate the gross alpha activity excluding radon and uranium. The approximately corrected values and uncertainty in gross alpha concentration from Townsend and Grossman (2002 [DIRS 173960], Table 8.3) are included in Table 6-19. Estimated concentrations of ^{226}Ra and ^{228}Ra for wells UE-25 J-12 and UE-25 J-13 are reported by Townsend and Grossman (2002 [DIRS 173960], Table 8.6 and Table 8.7). The sum of the average concentration for ^{226}Ra and the average concentration for ^{228}Ra is 0.64 pCi/L. This average value is above the expected value and the upper 95 percent confidence limit of combined ^{226}Ra and ^{228}Ra concentration estimated in Section 6.8.5.

In *Nevada Test Site Annual Site Environmental Report for Calendar Year 2002* (Townsend and Grossman 2003 [DIRS 168841], Table 8.3), data on gross alpha concentration for a total of nine water samples are reported for wells UE-25 J-12, UE-25 J-13, and Crystal Pool. There is no indication that the gross alpha concentrations reported are corrected for the contributions of radon and uranium, so these values overestimate the gross alpha activity excluding radon and uranium. The approximately values and uncertainty in gross alpha concentration from Townsend and Grossman (2003 [DIRS 168841], Table 8.3) are included in Table 6-19. Estimated concentrations of ^{226}Ra and ^{228}Ra for wells UE-25 J-12 and UE-25 J-13 for a total of four samples are reported by Townsend and Grossman (2003 [DIRS 168841], Table 8.5 and Table 8.6). The sum of the average concentration for ^{226}Ra and the average concentration for

^{228}Ra is 0.63 pCi/L. This average value is above the expected value and the upper 95 percent confidence limit of combined ^{226}Ra and ^{228}Ra concentration estimated in Section 6.8.5.

In *Nevada Test Site Environmental Report 2003* (Wills 2004 [DIRS 173956], Table 3-3, Table 3-1, and Table 3-2), data on gross alpha concentration for a total of eight water samples are reported for wells UE-25 J-12, UE-25 J-13, Amargosa Valley RV Park, and Crystal Pool. There is no indication that the gross alpha concentrations reported are corrected for the contributions of radon and uranium, so these values overestimate the gross alpha activity excluding radon and uranium. The approximately corrected values and uncertainty in gross alpha concentration from Wills (2004 [DIRS 173956], Table 3-3, Table 3-1, and Table 3-2) are included in Table 6-19. Estimated concentrations of ^{226}Ra and ^{228}Ra for wells UE-25 J-12 and UE-25 J-13 for a total of six samples are reported by Wills (2004 [DIRS 173956], Table 3-3). The sum of the average concentration for ^{226}Ra and the average concentration for ^{228}Ra is 0.08 pCi/L. This average value is below the expected value and the upper 95 percent confidence limit of combined ^{226}Ra and ^{228}Ra concentration estimated in Section 6.8.5.

Combining data on the gross alpha concentration in groundwater near Yucca Mountain from a variety of sources has several advantages. Stochastic fluctuations in the radioactive decay process and measurement methods can be averaged over a larger number of measurements, leading to a more representative average value and greater precision. Potential variations in groundwater concentrations as a function of time would also be more effectively averaged over several data sets collected during different years. Most importantly, variations in sampling and analytical methods may be significant and using data on gross alpha concentration from several studies results in a more representative estimate of the average value.

Histograms of the 79 estimated values of gross alpha concentration in groundwater near Yucca Mountain are plotted in Figure 6-48. The upper plot in Figure 6-48 shows the values of gross alpha concentration that have been corrected for uranium concentration in red (from DTN: MO9904RWSJJS98.000 [DIRS 165866] and CRWMS M&O 1998 [DIRS 104963], Table E-1). The upper plot in Figure 6-48 also shows the values of gross alpha concentration that have not been corrected for uranium concentration in blue (from Townsend and Grossman 2001 [DIRS 156604], Table 8.3, Townsend and Grossman 2002 [DIRS 173960], Table 8.3, Townsend and Grossman 2003 [DIRS 168841], Table 8.3, and Wills 2004 [DIRS 173956], Tables 3-1 to 3-3). The upper plot in Figure 6-48 shows that the uncorrected values of gross alpha concentration are on the higher side of the distribution, as expected. The lower plot in Figure 6-48 shows the values of gross alpha concentration from all sources, corrected for uranium concentration. This histogram shows that the distribution of estimated gross alpha concentration is approximately normally distributed with a clear central tendency toward a value somewhat less than 1.0 pCi/L. A few of the highest and lowest values are potential outliers, but their impact on the overall distribution is minor.

The same analysis of the data applied in Section 6.8.4 to the 18 measurements from DTN: MO9904RWSJJS98.000 ([DIRS 165866]) can be used on the combined data set in Table 6-19. The results of this analysis, using 79 measurements, indicate that the estimate of the mean value of the gross alpha concentration is 0.50 pCi/L. Furthermore the standard deviation of the estimate of the mean value is 0.13 pCi/L.

Table 6-19. Data Table Showing Calculation of Mean and Standard Deviation of Gross Alpha Concentration Using Qualified and Corroborative Data

Location	Date	Gross Alpha[b] (x_i) (pCi/L)	Uncertainty[a] ($2\sigma_i$) (pCi/L)	Sigma (σ_i) (pCi/L)	σ_i^2 $(pCi/L)^2$	Source
NDOT Well	24-Jun-98	-0.08	1.56	0.780	0.608	DTN: MO9904RWSJJS98.000 [DIRS 165866]
NDOT Well	29-Jul-98	0.32	1.1	0.550	0.303	DTN: MO9904RWSJJS98.000 [DIRS 165866]
NDOT Well	23-Sep-98	-1.40	0.79	0.395	0.156	DTN: MO9904RWSJJS98.000 [DIRS 165866]
Gilgan's South Well	24-Jun-98	-0.63	0.86	0.430	0.185	DTN: MO9904RWSJJS98.000 [DIRS 165866]
Gilgan's South Well	29-Jul-98	0.64	0.86	0.430	0.185	DTN: MO9904RWSJJS98.000 [DIRS 165866]
Gilgan's South Well	23-Sep-98	-0.74	0.69	0.345	0.119	DTN: MO9904RWSJJS98.000 [DIRS 165866]
UE-25 J-12	23-Jun-98	0.06	0.96	0.480	0.230	DTN: MO9904RWSJJS98.000 [DIRS 165866]
UE-25 J-12	28-Jul-98	0.27	0.72	0.360	0.130	DTN: MO9904RWSJJS98.000 [DIRS 165866]
UE-25 J-12	22-Sep-98	0.27	0.8	0.400	0.160	DTN: MO9904RWSJJS98.000 [DIRS 165866]
UE-25 J-13	23-Jun-98	0.05	0.94	0.470	0.221	DTN: MO9904RWSJJS98.000 [DIRS 165866]
UE-25 J-13	28-Jul-98	0.50	0.73	0.365	0.133	DTN: MO9904RWSJJS98.000 [DIRS 165866]
UE-25 J-13	22-Sep-98	-0.18	1.2	0.600	0.360	DTN: MO9904RWSJJS98.000 [DIRS 165866]
UE-25 c#2	23-Jun-98	1.20	1.33	0.665	0.442	DTN: MO9904RWSJJS98.000 [DIRS 165866]
UE-25 c#2	28-Jul-98	1.49	0.94	0.470	0.221	DTN: MO9904RWSJJS98.000 [DIRS 165866]
UE-25 c#2	22-Sep-98	0.73	1.67	0.835	0.697	DTN: MO9904RWSJJS98.000 [DIRS 165866]
Crystal Pool	22-Jun-98	1.04	1.27	0.635	0.403	DTN: MO9904RWSJJS98.000 [DIRS 165866]
Crystal Pool	27-Jul-98	1.75	1.64	0.820	0.672	DTN: MO9904RWSJJS98.000 [DIRS 165866]
Crystal Pool	25-Sep-98	-0.85	1.21	0.605	0.366	DTN: MO9904RWSJJS98.000 [DIRS 165866]
NDOT Well	first quarter	-0.14	2.63	1.315	1.729	CRWMS M&O 1998 [DIRS 104963], Table E-1
NDOT Well	second quarter	-0.67	2.17	1.085	1.177	CRWMS M&O 1998 [DIRS 104963], Table E-1
NDOT Well	third quarter	-2.61	2.14	1.070	1.145	CRWMS M&O 1998 [DIRS 104963], Table E-1
NDOT Well	fourth quarter	1.26	2.57	1.285	1.651	CRWMS M&O 1998 [DIRS 104963], Table E-1
Gilgan's South Well	first quarter	-0.94	1.36	0.680	0.462	CRWMS M&O 1998 [DIRS 104963], Table E-1

Table 6-19. Data Table Showing Calculation of Mean and Standard Deviation of Gross Alpha Concentration Using Qualified and Corroborative Data (Continued)

Location	Date	Gross Alpha[b] (x_i) (pCi/L)	Uncertainty[a] ($2\sigma_i$) (pCi/L)	Sigma (σ_i) (pCi/L)	σ_i^2 $(pCi/L)^2$	Source
Gilgan's South Well	second quarter	-1.05	1.29	0.645	0.416	CRWMS M&O 1998 [DIRS 104963], Table E-1
Gilgan's South Well	third quarter	0.96	2.18	1.090	1.188	CRWMS M&O 1998 [DIRS 104963], Table E-1
Gilgan's South Well	fourth quarter	1.40	2.00	1.000	1.000	CRWMS M&O 1998 [DIRS 104963], Table E-1
Crystal Pool	first quarter	-1.56	2.91	1.455	2.117	CRWMS M&O 1998 [DIRS 104963], Table E-1
Crystal Pool	second quarter	-0.57	2.89	1.445	2.088	CRWMS M&O 1998 [DIRS 104963], Table E-1
Crystal Pool	third quarter	0.49	3.48	1.740	3.028	CRWMS M&O 1998 [DIRS 104963], Table E-1
Crystal Pool	fourth quarter	-1.01	2.70	1.350	1.823	CRWMS M&O 1998 [DIRS 104963], Table E-1
UE-25 c#3	first quarter	-2.67	1.67	0.835	0.697	CRWMS M&O 1998 [DIRS 104963], Table E-1
UE-25 c#3	second quarter	1.43	1.87	0.935	0.874	CRWMS M&O 1998 [DIRS 104963], Table E-1
UE-25 c#3	third quarter	4.57	2.71	1.355	1.836	CRWMS M&O 1998 [DIRS 104963], Table E-1
UE-25 c#3	fourth quarter	2.02	2.02	1.010	1.020	CRWMS M&O 1998 [DIRS 104963], Table E-1
UE-25 J-12	first quarter	-0.79	1.47	0.735	0.540	CRWMS M&O 1998 [DIRS 104963], Table E-1
UE-25 J-12	second quarter	0.13	1.49	0.745	0.555	CRWMS M&O 1998 [DIRS 104963], Table E-1
UE-25 J-12	third quarter	-4.52	15.6	7.800	60.840	CRWMS M&O 1998 [DIRS 104963], Table E-1
UE-25 J-12	fourth quarter	-0.51	1.39	0.695	0.483	CRWMS M&O 1998 [DIRS 104963], Table E-1
UE-25 J-13	first quarter	-1.06	1.55	0.775	0.601	CRWMS M&O 1998 [DIRS 104963], Table E-1
UE-25 J-13	second quarter	0.00	1.52	0.760	0.578	CRWMS M&O 1998 [DIRS 104963], Table E-1
UE-25 J-13	third quarter	-0.36	1.72	0.860	0.740	CRWMS M&O 1998 [DIRS 104963], Table E-1
UE-25 J-13	fourth quarter	0.98	1.80	0.900	0.810	CRWMS M&O 1998 [DIRS 104963], Table E-1
UE-25 J-12	26-Jan-00	3.02	1.11	0.555	0.308	Townsend and Grossman 2001 [DIRS 156604], Table 8.3
UE-25 J-12	19-Apr-00	1.64	1.00	0.500	0.250	Townsend and Grossman 2001 [DIRS 156604], Table 8.3
UE-25 J-12	19-Apr-00	2.13	0.98	0.490	0.240	Townsend and Grossman 2001 [DIRS 156604], Table 8.3
UE-25 J-12	25-Jul-00	1.12	0.96	0.480	0.230	Townsend and Grossman 2001 [DIRS 156604], Table 8.3
UE-25 J-12	24-Oct-00	0.57	0.38	0.190	0.036	Townsend and Grossman 2001 [DIRS 156604], Table 8.3
UE-25 J-13	26-Jan-00	3.34	1.13	0.565	0.319	Townsend and Grossman 2001 [DIRS 156604], Table 8.3
UE-25 J-13	25-Jul-00	1.94	1.04	0.520	0.270	Townsend and Grossman 2001 [DIRS 156604], Table 8.3

Table 6-19. Data Table Showing Calculation of Mean and Standard Deviation of Gross Alpha Concentration Using Qualified and Corroborative Data (Continued)

Location	Date	Gross Alpha[b] (x_i) (pCi/L)	Uncertainty[a] ($2\sigma_i$) (pCi/L)	Sigma (σ_i) (pCi/L)	σ_i^2 $(pCi/L)^2$	Source
UE-25 J-13	24-Oct-00	0.53	0.85	0.425	0.181	Townsend and Grossman 2001 [DIRS 156604], Table 8.3
Amargosa Valley RV Park	14-Nov-00	-0.99	0.50	0.250	0.063	Townsend and Grossman 2001 [DIRS 156604], Table 8.3
Crystal Pool	16-Jun-00	2.76	2.22	1.110	1.232	Townsend and Grossman 2001 [DIRS 156604], Table 8.3
Crystal Pool	16-Nov-00	3.03	0.90	0.450	0.203	Townsend and Grossman 2001 [DIRS 156604], Table 8.3
UE-25 J-12	7-Feb-01	0.81	1.01	0.505	0.255	Townsend and Grossman 2002 [DIRS 173960], Table 8.3
UE-25 J-12	4-Apr-01	0.55	0.946	0.473	0.224	Townsend and Grossman 2002 [DIRS 173960], Table 8.3
UE-25 J-12	1-Aug-01	-0.10	1.03	0.515	0.265	Townsend and Grossman 2002 [DIRS 173960], Table 8.3
UE-25 J-12	31-Oct-01	1.56	0.84	0.420	0.176	Townsend and Grossman 2002 [DIRS 173960], Table 8.3
UE-25 J-13	7-Feb-01	1.02	1.08	0.540	0.292	Townsend and Grossman 2002 [DIRS 173960], Table 8.3
UE-25 J-13	4-Apr-01	0.18	0.976	0.488	0.238	Townsend and Grossman 2002 [DIRS 173960}, Table 8.3
UE-25 J-13	1-Aug-01	0.92	0.936	0.468	0.219	Townsend and Grossman 2002 [DIRS 173960], Table 8.3
UE-25 J-13	31-Oct-01	0.60	0.9	0.450	0.203	Townsend and Grossman 2002 [DIRS 173960], Table 8.3
Crystal Pool	23-Jul-01	1.83	2.13	1.065	1.134	Townsend and Grossman 2002 [DIRS 173960], Table 8.3
UE-25 J-12	20-Feb-02	1.36	1.58	0.790	0.624	Townsend and Grossman 2003 [DIRS 168841], Table 8.3
UE-25 J-12	24-Apr-02	1.09	1.08	0.540	0.292	Townsend and Grossman 2003 [DIRS 168841], Table 8.3
UE-25 J-12	17-Jul-02	-0.33	1.12	0.560	0.314	Townsend and Grossman 2003 [DIRS 168841], Table 8.3
UE-25 J-12	16-Oct-02	0.41	1.56	0.780	0.608	Townsend and Grossman 2003 [DIRS 168841], Table 8.3
UE-25 J-13	20-Feb-02	1.62	1.82	0.910	0.828	Townsend and Grossman 2003 [DIRS 168841], Table 8.3
UE-25 J-13	24-Apr-02	2.20	1.45	0.725	0.526	Townsend and Grossman 2003 [DIRS 168841], Table 8.3
UE-25 J-13	17-Jul-02	0.64	1.80	0.900	0.810	Townsend and Grossman 2003 [DIRS 168841], Table 8.3
UE-25 J-13	16-Oct-02	1.63	1.73	0.865	0.748	Townsend and Grossman 2003 [DIRS 168841], Table 8.3
Crystal Pool	18-Apr-02	2.83	2.22	1.110	1.232	Townsend and Grossman 2003 [DIRS 168841], Table 8.3
Amargosa Valley RV Park	20-Aug-03	-1.15	0.873	0.437	0.191	Wills 2004 [DIRS 173956], Table 3-1
Crystal Pool	13-Aug-03	0.21	0.673	0.337	0.113	Wills 2004 [DIRS 173956], Table 3-2
UE-25 J-12	29-Jan-03	1.33	0.730	0.365	0.133	Wills 2004 [DIRS 173956], Table 3-3
UE-25 J-12	30-Apr-03	0.30	0.642	0.321	0.103	Wills 2004 [DIRS 173956], Table 3-3
UE-25 J-12	2-Jul-03	-0.33	0.424	0.212	0.045	Wills 2004 [DIRS 173956], Table 3-3

Table 6-19. Data Table Showing Calculation of Mean and Standard Deviation of Gross Alpha Concentration Using Qualified and Corroborative Data (Continued)

Location	Date	Gross Alpha[b] (x_i) (pCi/L)	Uncertainty[a] ($2\sigma_i$) (pCi/L)	Sigma (σ_i) (pCi/L)	σ_i^2 $(pCi/L)^2$	Source
UE-25 J-12	8-Oct-03	0.04	0.753	0.377	0.142	Wills 2004 [DIRS 173956], Table 3-3
UE-25 J-13	29-Jan-03	1.62	1.17	0.585	0.342	Wills 2004 [DIRS 173956], Table 3-3
UE-25 J-13	8-Oct-03	0.27	0.710	0.355	0.126	Wills 2004 [DIRS 173956], Table 3-3
	Σx_i =	39.42		$\Sigma\sigma_i^2$ =	106.504	
	Mean Gross Alpha $\bar{x}$ =	0.50		$\sigma_{\bar{x}}$ =	0.13	

[a]Uncertainty is defined as being two standard deviations (sigma).

[b]Estimated values of gross alpha concentration from Townsend and Grossman 2001 [DIRS 156604], Table 8.3, Townsend and Grossman 2002 [DIRS 173960], Table 8.3, Townsend and Grossman 2003 [DIRS 168841], Table 8.3, and Wills 2004 [DIRS 173956], Tables 3-1 to 3-3 have been approximately corrected for uranium concentration, as described in Section 6.8.6.

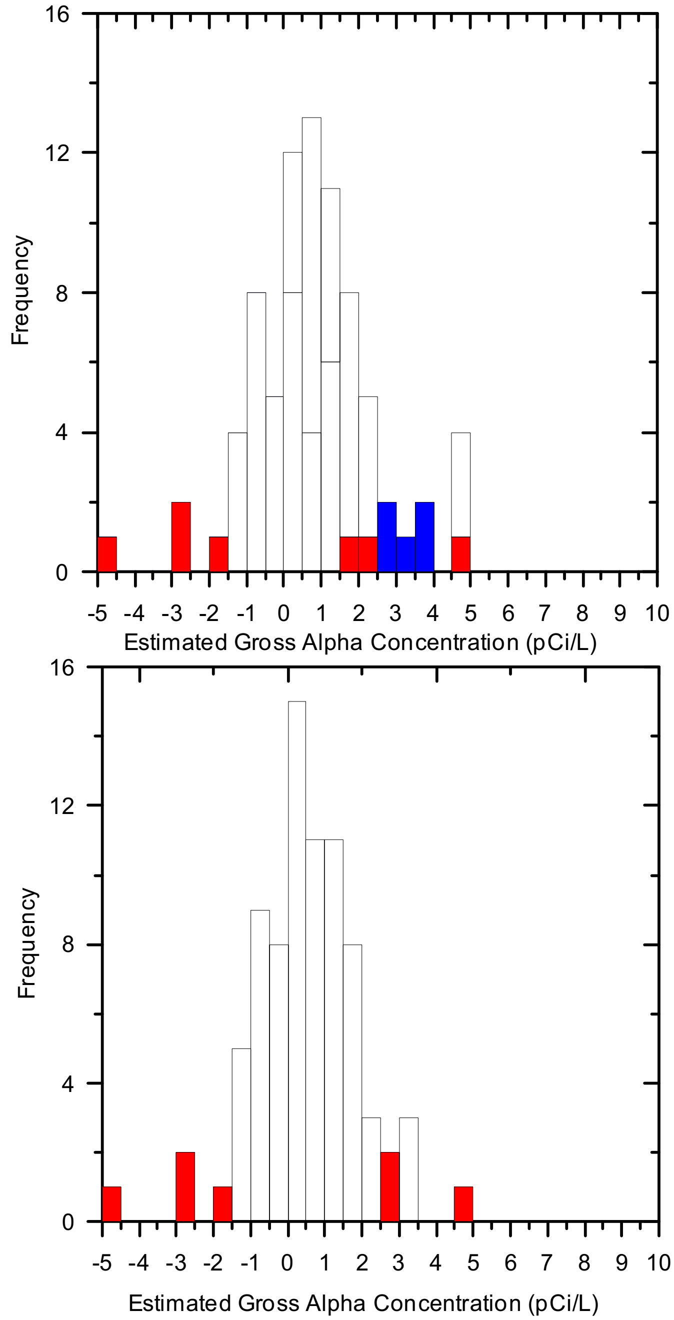

NOTE: Upper plot shows values of gross alpha concentration that have been corrected for uranium concentration in red and values that are uncorrected in blue. Lower plot shows all values corrected for uranium concentration

Source: The sources are listed in Table 6-19.

Figure 6-48. Histograms of Gross Alpha Concentration in Groundwater Near Yucca Mountain from Qualified and Additional Data

Applying the same logic presented in Section 6.8.5, the expected value and upper 95 percent limit of gross alpha concentration from the analysis using qualified and corroborative data are given in Table 6-20. The best estimate for the mean gross alpha concentration in groundwater from the combined data set is 0.50 pCi/L with a 95 percent confidence that the concentration will not exceed 0.71 pCi/L. These estimates of the expected value and the upper limit are higher than those derived from the smaller qualified data set and presented in Table 6-18.

The higher value of gross alpha concentration given in Table 6-20 is more conservative for the purpose of regulatory analyses than the value given in Table 6-18 and is more reliable, given the larger number of measurements used in the analysis. In addition, some of the estimated values of combined ^{226}Ra and ^{228}Ra concentrations are greater than the estimated upper limit given in Table 6-18, but they are all less than the upper limit given in Table 6-20.

Table 6-20. Summary of Alpha Concentration Results in Amargosa Valley Groundwater for Qualified and Corroborative Data

Parameter	Expected Value pCi/L	Upper (95%) Limit pCi/L
Gross Alpha Concentration	0.50	0.71
Combined Concentration of ^{226}Ra and ^{228}Ra	0.50	0.71

7. VALIDATION

This section of the report documents the validation of the SZ flow and transport abstraction model and the SZ 1-D transport model. For the SZ flow and transport abstraction model, a comparison is made between the abstraction model and the underlying process model, which is discussed in the report *Site-Scale Saturated Zone Transport* (BSC 2004 [DIRS 170036]). This comparison tests the appropriateness and accuracy of the convolution integral method used in the SZ flow and transport abstraction model. Similarly, the validation of the SZ 1-D transport model consists of a qualitative comparison between the abstraction model and the site-scale process model mentioned above (BSC 2004 [DIRS 170036]). In all cases, the validations of these models are performed for a range of behavior that is representative of the uncertainties being evaluated for the TSPA-LA analyses. In addition, this section documents corrections to the SZ 1-D transport model and evaluates the impacts of these corrections (see Section 7.5).

7.1 VALIDATION PROCEDURES

As discussed above, validation of the SZ flow and transport abstraction model and the SZ 1-D transport model involves comparison with the underlying process model (BSC 2004 [DIRS 170036]). In making these comparisons, three cases for radionuclide transport are defined for implementation: median case, fast case, and slow case. The median case uses median values from uncertainty distributions for the relevant flow and transport parameters. The fast case uses parameter values set at the 90th percentile or the 10th percentile, depending on the parameter, that result in more rapid transport of radionuclides through the SZ. For example, the flowing interval spacing is set to its 90th percentile value, and the sorption coefficient is set to its 10th percentile value for transport of neptunium in the fast case. The slow case uses parameter values set at the 90th percentile or 10th percentile that result in less rapid transport of radionuclides through the SZ. These three cases approximately span the range of uncertainty in results of the SZ flow and transport abstraction model with regard to radionuclide transport in the SZ, as shown in Figures 6-28 and 6-32. The parameter values used in the median, fast, and slow cases are summarized in Table 7-1.

The SZ site-scale transport model (BSC 2004 [DIRS 170036]) was run for each of the three model validation cases by varying the input parameters to conform to the values given in Table 7-1. The steady-state groundwater flow solution for each case was first established by running the flow model (BSC 2004 [DIRS 170037]) to equilibrium with the specified values of the parameters GWSPD and HAVO. The particle-tracking algorithm in the FEHM V2.20 software code [DIRS 161725] was then used to obtain the simulated mass breakthrough curves with the SZ site-scale transport model at the regulatory boundary of the accessible environment.

Table 7-1. Parameter Values in the Three Cases for SZ Flow and Transport Model Validation

Parameter Name	Parameter Description	Median Case	Fast Case	Slow Case
FISVO	Flowing interval spacing in volcanic units	1.29 (19.5 m)	1.82 (66.1 m)	0.67 (4.68 m)
HAVO	Ratio of horizontal anisotropy in permeability	4.2	16.25	1.0
LDISP	Longitudinal dispersivity	2.0 (100 m)	2.96 (920 m)	1.03 (10.9 m)
FPLAW	Western boundary of the alluvial uncertainty zone	0.5	0.1	0.9
FPLAN	Northern boundary of the alluvial uncertainty zone	0.5	0.1	0.9
NVF19	Effective porosity in shallow alluvium	0.18	0.114	0.245
NVF7	Effective porosity in undifferentiated valley fill	0.18	0.114	0.245
FPVO	Fracture porosity in volcanic units	-3.0 (10^{-3})	-3.89 (1.29×10^{-4})	-1.50 (0.0316)
DCVO	Effective diffusion coefficient in volcanic units	-10.3 (5.0×10^{-11} m^2/s)	-10.68 (2.08×10^{-11} m^2/s)	-9.65 (2.22×10^{-10} m^2/s)
GWSPD	Groundwater specific discharge multiplier	0.0 (1.0)	0.477 (3.0)	-0.477 (0.333)
bulkdensity	Bulk density of alluvium	1910 kg/m^3	1810 kg/m^3	2010 kg/m^3
KDNPVO	Neptunium sorption coefficient in volcanic units	1.3 mL/g	1.04 mL/g	1.6 mL/g
KDNPAL	Neptunium sorption coefficient in alluvium	6.35 mL/g	4.26 mL/g	8.44 mL/g

NOTE: Values in parentheses are the parameter values from log-transformed uncertainty distributions.

Source: Sources for the uncertainty distributions are provided in Table 6-8.

7.1.1 SZ Flow and Transport Abstraction Model

Validation of the SZ flow and transport abstraction model is accomplished by running this model using the breakthrough curves for the three validation cases from the SZ site-scale transport model (BSC 2004 [DIRS 170036]). The SZ flow and transport abstraction model uses the convolution integral method as implemented by the SZ_Convolute V3.0 software code (STN: 10207-3.0-00, SNL 2003 [DIRS 164180]) to produce the radionuclide mass breakthrough to the accessible environment, given the time-varying input of mass at the water table below the repository for the TSPA-LA. Note that model validation tests were performed with the SZ_Convolute V2.2 software code (STN: 10207-2.2-00, SNL 2003 [DIRS 163344]).

For the first validation test, a constant input of 1 g/year from the UZ is applied at the water table beneath the repository in the SZ flow and transport abstraction model. This is essentially the same transport boundary condition used in the SZ site-scale transport model (BSC 2004 [DIRS 170036]) to derive the SZ breakthrough curves for input to the abstraction model. Consequently, the output of the SZ flow and transport abstraction model should reproduce the breakthrough curve used as the input in the validation test. This validation test is conducted for both a nonsorbing species and for neptunium. The validation test is also run for the three validation cases described in the previous section. To facilitate comparison of the results, the transport simulations in both the SZ site-scale transport model and the SZ flow and transport abstraction model are performed without radioactive decay.

As a second validation test, the mass balance of radionuclides transported in the SZ flow and transport abstraction model is checked. This check is performed by setting the upstream boundary condition equal to 1 g/year for time up to 1,000 years and reducing this to 0 g/year for the remainder of the simulation. Thus, the total radionuclide mass input to the SZ flow and transport abstraction model is 1,000 grams. Since radioactive decay is not included in this validation test, the cumulative output of the model over a long simulation time should also be 1,000 grams. This second validation test is also run for the three validation cases described in the previous section (Table 7-1).

It should be noted that several additional test cases for the SZ_Convolute V2.2 software code (SZ_Convolute V2.2, STN: 10207-2.2-00, [DIRS 163344]) have been conducted for the purposes of software verification (BSC 2003, [DIRS 163587]). These tests verify the ability of the convolution integral method, as implemented by the SZ_Convolute V2.2 software code (STN: 10207-2.2-00, SNL 2003 [DIRS 163344]), to simulate accurately radionuclide transport with variable input boundary conditions, radioactive decay, and variations in groundwater flux with climate change. Although not directly applied to the radionuclide transport results of the SZ flow and transport abstraction model presented in this report, the numerical testing of the software code used in this model provides additional confidence in the validity of the model.

7.1.2 SZ 1-D Transport Model

Validation of the SZ 1-D transport model is conducted by running this model and comparing the results to the output of the SZ site-scale transport model (BSC 2004 [DIRS 170036] and DTN: LA0306SK831231.001 [DIRS 164362]). The SZ 1-D transport model is implemented using the GoldSim V7.50.100 software code. Ultimately, the SZ 1-D transport model is fully integrated into the TSPA-LA model; however, for the purposes of model development and validation, a stand-alone version of this model is used.

For the validation test, a constant input of 1 g/year from the UZ is applied at the upstream boundary of the SZ 1-D transport model. This is the same radionuclide mass boundary condition used in the SZ site-scale transport model (BSC 2004 [DIRS 170036]). The breakthrough curves from the SZ 1-D model should approximately match the output of the site-scale transport model. This validation test is conducted for both a nonsorbing species and for neptunium, and is run for the three validation cases described in the previous section. To facilitate comparison of the results, the transport simulations in both the SZ site-scale transport model and the SZ 1-D transport model are performed without radioactive decay.

It should be noted that several additional test cases for the GoldSim V7.50.100-00 software code have been conducted for the purposes of software verification (BSC 2002 [DIRS 163962]). These tests verify the ability of the GoldSim V7.50.100-00 software code to accurately simulate radioactive decay and ingrowth. Although not directly applied to the radionuclide transport results of the SZ 1-D transport model presented in this report, the numerical testing of the software code used in this model provides additional confidence in the validity of the model. It should also be noted that a problem in the GoldSim V7.50.100-00 software code with regard to parameter sampling was identified subsequent to the validation testing documented in this report and this problem is reported in CR 2222 (*Evaluate Revised LH Sampling Algorithm on the Results of ANL-EBS-PA-000009*). The parameter-sampling component of the GoldSim V7.50.100-00 software code was not used in the validation testing of the SZ 1-D transport model and the problem reported in CR 2222 is thus not relevant to the validation testing conducted for this report.

Groundwater flow rates and flow-path lengths derived from the SZ site-scale transport model (BSC 2004 [DIRS 170036]) were used in the development of the SZ 1-D transport model. However, both the approximate nature of the equivalency between the two models and the reduction in dimensionality in the 1-D transport model limit the ability of the 1-D model to match the results of the site-scale transport model. Among the realizations of SZ flow and transport in the TSPA-LA analyses, the source locations within each of the four source regions beneath the repository are varied in the SZ flow and transport abstraction model. However, the impact of this variability on flow paths and flow-path lengths is not captured in the SZ 1-D transport model. This limitation of the SZ 1-D transport model results in some differences in simulation results between the SZ flow and transport abstraction model and the SZ 1-D transport model for any given realization in the TSPA-LA analyses. These differences are evaluated for a sampling of realizations and the results are also documented in Section 7.3.2. The results of this evaluation indicate acceptable agreement between the SZ 1-D transport model and the SZ site-scale transport model, from which it was abstracted.

7.2 VALIDATION CRITERIA

The *Technical Work Plan For: Natural System – Saturated Zone Analysis and Model Report Integration* (BSC 2004 [DIRS 171421], Section 2.2.1.1) states that model validation was completed following criteria in the previous version of the technical work plan (TWP). Model validation presented in Section 7 of this report follows the *Technical Work Plan for: Saturated Zone Flow and Transport Modeling and Testing* (BSC 2003 [DIRS 166034], Section 2.5). The previous TWP (BSC 2003 [DIRS 166034], Section 2.5) states that Level-II validation will be achieved through confidence building activities during model development and by implementing one post-development validation method. In the cases of the SZ flow and transport abstraction model and the SZ 1-D transport model, the post-development method was chosen to be the corroboration of the abstraction model results to the results of the validated process model from which the abstraction was derived (BSC 2003 [DIRS 166034], Section 2.5). This is the most appropriate method of model validation because the underlying process model (the SZ site-scale transport model) has undergone validation independently, and the SZ flow and transport abstraction model and the SZ 1-D transport model are derived directly from this process model. In addition, the TWP validation plan for the SZ Flow and transport abstraction model includes a check of output for mass balance.

The acceptance criterion for validation of both the SZ flow and transport abstraction model and the SZ 1-D transport model is a favorable qualitative comparison between the simulated SZ breakthrough curves from these two models and the breakthrough curve from the SZ site-scale transport model conducted by visual examination of graphs made of the breakthrough curves (BSC 2004 [DIRS 170036] and DTN: LA0306SK831231.001 [DIRS 164362]). The breakthrough curves are compared at 10 percent, 50 percent, and 90 percent mass breakthrough in the evaluation of this criterion. Breakthrough curves are compared for a nonsorbing species and for neptunium. Breakthrough curves for the median, fast, and slow cases outlined above are compared.

An additional acceptance criterion for the validation of the SZ flow and transport abstraction model is a check of the radionuclide mass balance in the model. The mass input to the model should equal the mass output from the model over long time periods. Discrepancies of a few percent are acceptable due to both less-than-complete discharge of radionuclide mass from the model and numerical (truncation) errors in the computer software implementing the numerical integration used in the convolution integral method.

These acceptance criteria reflect the essential functions of the SZ system with regard to the transport time and radionuclide mass delivery to the accessible environment.

7.2.1 Confidence Building During Model Development to Establish Scientific Basis and Accuracy for Intended Use

For Level II validation, the development of the models should be documented in accordance with the requirements of Section 5.3.2(b) of *LP-SIII.10Q-BSC*. The development of the SZ flow and transport abstraction model and the SZ 1-D transport model has been conducted in accordance with these criteria, as follows:

1. *Selection of input parameters and/or input data, and a discussion of how the selection process builds confidence in the model. [LP-SIII.10Q-BSC 5.3.2(b) (1) and LP-2.29Q-BSC Attachment 3 Level I (a)]*

   The inputs to the SZ flow and transport abstraction model and the SZ 1-D transport model have all been obtained from controlled sources (see Tables 4-1, 4-2, and 4-3), including discussion about selection of input and design parameters (Section 4.1). The SZ flow and transport abstraction model takes the SZ site-scale transport model, which has been independently validated (BSC 2004 [DIRS 170036]), as a direct input. Model assumptions have been described in Section 5. Detailed discussion about model concepts can be found in Section 6.3. Section 6.5.2 contains detailed discussion and analyses of data sources and parameter uncertainty, leading to increased confidence in the parameters that are used in the models presented in this report. Thus, this requirement is considered satisfied.

2. *Description of calibration activities, and/or initial boundary condition runs, and/or run convergences, simulation conditions set up to span the range of intended use and avoid inconsistent outputs, and a discussion of how the activity or activities build confidence in the model. Inclusion of a discussion of impacts of any non-convergence runs [(LP-SIII.10Q-BSC 5.3.2(b)(2) and LP-2.27Q-BSC Attachment 3 Level I (e)].*

   The SZ flow and transport abstraction model and the SZ 1-D transport model use the SZ site-scale transport model (BSC 2004 [DIRS 170036]), which is itself based on the calibrated SZ site-scale flow model (BSC 2004 [DIRS 170037]), as a starting point.

The SZ flow and transport abstraction model generates breakthrough curves for a unit point source, hence initial and boundary conditions for radionuclide mass transport are established through linkage to the UZ transport model in TSPA-LA model simulations. The SZ 1-D transport model obtains boundary conditions for radionuclide mass from the UZ in the TSPA-LA model. Section 6.3.3 discusses the source term for the models. Section 6.6 provides detailed discussion of model results. Discussion about nonconvergence runs is not relevant for this model report. Thus, this requirement is considered satisfied.

3. *Discussion of the impacts of uncertainties to the model results including how the model results represent the range of possible outcomes consistent with important uncertainties. [(LP-SIII.10Q-BSC 5.3.2(b)(3) and LP-2.29Q-BSC Attachment 3 Level 1 (d) and (f)].*

   Results of 200 realizations of the SZ flow and transport abstraction model are presented in Section 6.6. These results constitute an assessment of the impacts of uncertainty in model parameters and provide this information as a direct feed to the probabilistic analyses of the TSPA-LA model.

4. *Formulation of defensible assumptions and simplifications. [LP-2.29Q-BSC Attachment 3 Level I (b)].*

   Discussion of assumptions and simplifications are provided in Section 5 and Section 6.3. The conceptual model of transport in the SZ and the components of the model are discussed in Section 6.3. Justification of assumptions and discussion of their implications for the models are also provided.

5. *Consistency with physical principles, such as conservation of mass, energy, and momentum. [LP-2.29Q-BSC Attachment 3 Level I (c)]*

   Consistency with physical principles is demonstrated by the conceptual and mathematical formulation of the SZ flow and transport abstraction model and the SZ 1-D transport model in Sections 6.3 and 6.5.1, and the selection and use of the FEHM and GoldSim V7.50.100 software codes in Section 3. Thus, this requirement is considered satisfied.

7.2.2 Confidence Building After Model Development to Support the Scientific Basis of the Model

Model validation requires mathematical models be validated by one or more of several methods given in Section 5.3.2(c and d) of LP-SIII.10Q-BSC. Validation of the SZ flow and transport abstraction model and the SZ 1-D transport model is documented in Section 7 of this report and is related to the procedural requirements as follows:

1. *LP-SIII.10Q-BSC 5.3.2(c), Method 6: Corroboration of abstraction model results to the results of the validated mathematical model from which the abstraction model is derived.*

The SZ flow and transport abstraction model and the SZ 1-D transport model are validated by comparing results from these models with the SZ site-scale transport model, which is the underlying validated mathematical (process) model from which they are derived. The validation criteria, testing, and results are described in detail in Section 7 of this report.

2. *LP-SIII.10Q-BSC 5.3.2(d): Technical review through publication in a refereed professional journal.*

   The SZ flow and transport abstraction model and its results are described in the refereed professional publication of Arnold et al. (2003 [DIRS 163857]). This publication demonstrates additional confidence in the model, when taken in conjunction with the model validation activity described in item 1 above.

7.3 RESULTS OF VALIDATION ACTIVITIES

The numerical results of the model validation activities described above are presented primarily as a series of plots of simulated breakthrough curves. A quantitative comparison of models with regard to radionuclide mass balance is also presented for the SZ flow and transport abstraction model.

7.3.1 SZ Flow and Transport Abstraction Model Validation Results

Results of the SZ flow and transport abstraction model and the SZ site-scale transport model (BSC 2004 [DIRS 170036]) for a nonsorbing species are shown as simulated breakthrough curves in Figure 7-1. This figure shows results for the median, fast and slow cases of SZ flow and transport. Note that all simulations were conducted without radioactive decay. The simulated breakthrough curves from the SZ site-scale transport model are shown with the solid and dashed lines for the three cases. The results from the SZ flow and transport abstraction model are shown as the open symbols that are superimposed on the breakthrough curves from the site-scale model.

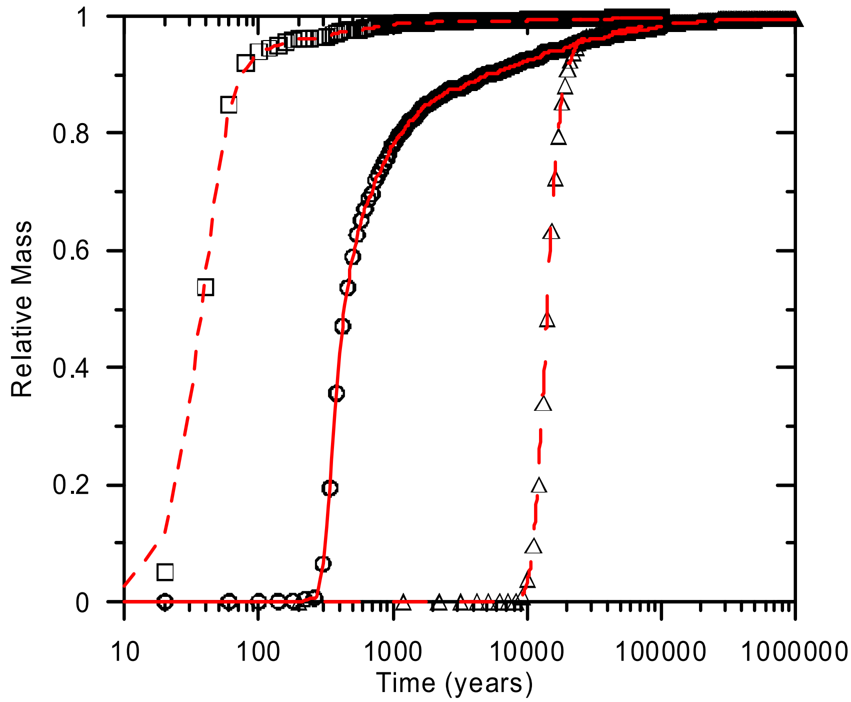

NOTE: Results from the SZ site-scale transport model (BSC 2004 [DIRS 170036]) are shown for the median case (solid line), fast case (short-dashed line), and slow case (long-dashed line). Results from the SZ flow and transport abstraction model are shown for the median case (open circle), fast case (open square), and slow case (open triangle). Breakthrough curves do not include radioactive decay.

Figure 7-1. Simulated Breakthrough Curves Comparing the Results of the SZ Flow and Transport Abstraction Model and the SZ Site-Scale Transport Model for a Nonsorbing Radionuclide

Visual comparison of the open symbols and the lines in Figure 7-1 indicates agreement within a few percent of relative mass in the results from the SZ flow and transport abstraction model and the SZ site-scale transport model for all three cases of SZ flow and transport. The one exception is the first point in the results of the SZ flow and transport abstraction model for the fast case, which is lower than the corresponding breakthrough curve from the SZ site-scale transport model. It should be noted that the time step used in the abstraction model is 20 years, which differs from the 10-year time step used in the site-scale model for the fast case. This difference in time-step size accounts for the small discrepancy between the models at the first time step.

Results of the SZ flow and transport abstraction model and the SZ site-scale transport model (BSC 2004 [DIRS 170036] and DTN: LA0306SK831231.001 [DIRS 164362]) for neptunium are shown as simulated breakthrough curves in Figure 7-2. This figure shows results for the median, fast, and slow cases of SZ flow and transport. Note that all simulations were conducted without radioactive decay. The simulated breakthrough curves from the SZ site-scale transport model are shown with the solid and dashed lines for the three cases. The results from the SZ flow and transport abstraction model are shown as the open symbols that are superimposed on the breakthrough curves from the site-scale model.

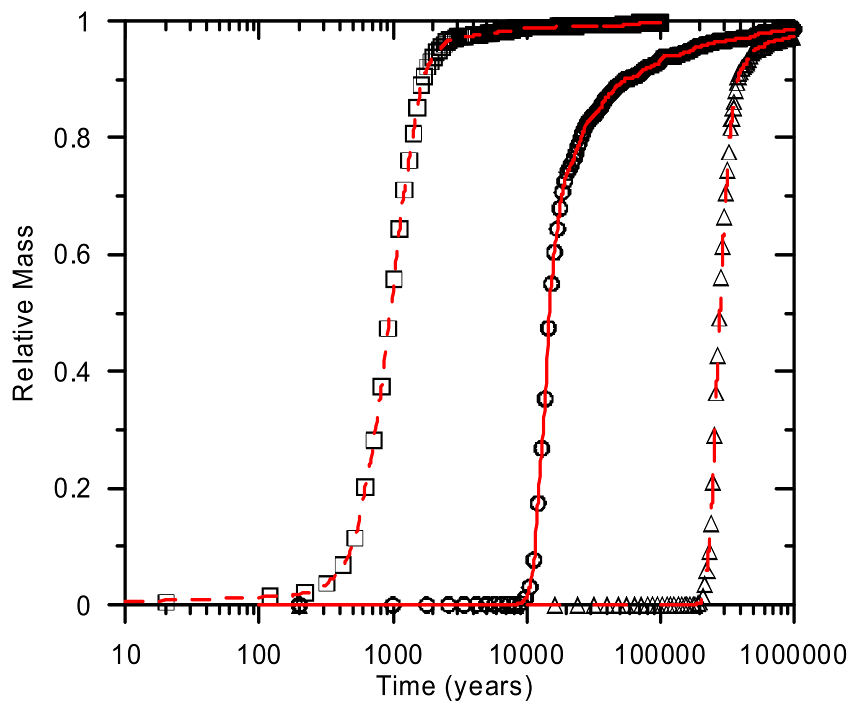

NOTE: Results from the SZ site-scale transport model (BSC 2004 [DIRS 170036]) are shown for the median case (solid line), fast case (short-dashed line), and slow case (long-dashed line). Results from the SZ flow and transport abstraction model are shown for the median case (open circle), fast case (open square), and slow case (open triangle). Breakthrough curves do not include radioactive decay.

Figure 7-2. Simulated Breakthrough Curves Comparing the Results of the SZ Flow and Transport Abstraction Model and the SZ Site-Scale Transport Model for Neptunium

Visual comparison of the open symbols and the lines in Figure 7-2 indicates agreement within a few percent of relative mass in the results from the SZ flow and transport abstraction model and the SZ site-scale transport model for all three cases of SZ flow and transport of neptunium.

Figure 7-3 shows the simulated breakthrough curve from the SZ flow and transport abstraction model of a nonsorbing species for the median case. This simulation applies a radionuclide mass influx boundary condition of 1 g/year for the first 1,000 years of the simulation, which results in a total mass input of 1,000 grams. The mass balance in the SZ flow and transport abstraction model is checked by summing the total mass output from the simulated breakthrough curve shown in Figure 7-3 over the 100,000 years of the simulation. The output sum is 981 grams, which is 98.1 percent of the input mass. Examination of the simulated breakthrough curve from the SZ site-scale transport model for the median case indicates that 98 percent of the mass has reached the accessible environment within 100,000 years. Consequently, the discrepancy between total input mass and total output mass can be explained as the radionuclide mass retained in the SZ system after 100,000 years. The total output mass from the SZ flow and transport abstraction model for the fast case and the slow case is 99.8 percent and 99.5 percent of the input mass, respectively. Mass breakthrough for the median case has a longer “tail” than the slow and fast cases due to matrix diffusion. Consequently, the total mass output is somewhat lower for the median case than the slow and fast cases in this validation test.

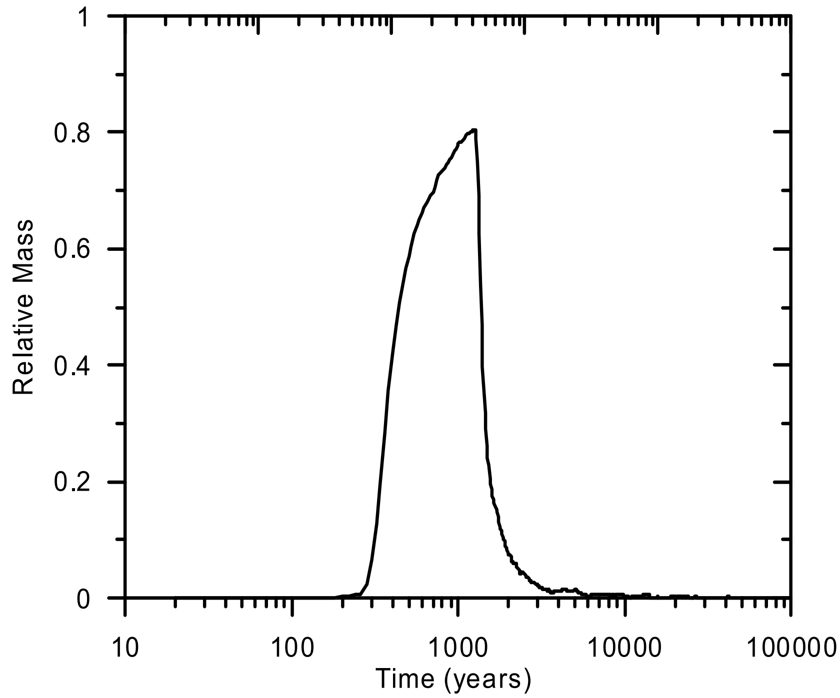

NOTE: Results from the SZ flow and transport abstraction model are shown for the median case. The breakthrough curve does not include radioactive decay.

Figure 7-3. Simulated Breakthrough Curve for a Nonsorbing Radionuclide from a 1000-Year-Duration Source

7.3.2 SZ 1-D Transport Model Validation Results

Results of the SZ 1-D transport model and the SZ site-scale transport model for a nonsorbing species are shown as simulated breakthrough curves in Figure 7-4. This figure shows results for the median, fast, and slow cases of SZ flow and transport. Note that all simulations were conducted without radioactive decay. The simulated breakthrough curves from the SZ site-scale transport model are shown with the solid and dashed lines for the three cases. The results from the SZ 1-D transport model are shown as the open symbols superimposed on the breakthrough curves from the SZ site-scale transport model.

Visual comparison of the open symbols and the lines in Figure 7-4 indicates close agreement in the results for a nonsorbing species from the SZ 1-D transport model and the SZ site-scale transport model for the median case of SZ flow and transport. There is generally close comparison in the overall shapes of the breakthrough curves from the SZ 1-D transport model and the SZ site-scale transport model, as indicated by the times of 10 percent, 50 percent, and 90 percent of mass breakthrough, with somewhat greater deviation for the upper tails of the breakthrough curves.

Results of the SZ 1-D transport model and the SZ site-scale transport model for neptunium are shown as simulated breakthrough curves in Figure 7-5. This figure shows results for the median, fast and slow cases of SZ flow and transport. Note that all simulations were conducted without radioactive decay. The simulated breakthrough curves from the SZ site-scale transport model are shown with the solid and dashed lines for the three cases. The results from the SZ 1-D transport model are shown as the open symbols superimposed on the breakthrough curves from the SZ site-scale transport model.

Visual comparison of the open symbols and the lines in Figure 7-5 indicates close agreement in the results for neptunium from the SZ 1-D transport model and the SZ site-scale transport model for the median case of SZ flow and transport. The comparison is slightly less close for the fast case and slow case. There is generally close comparison in the overall shapes of the breakthrough curves from the SZ 1-D transport model and the SZ site-scale transport model.

Results of the SZ 1-D transport model and the SZ flow and transport abstraction model for a nonsorbing species and neptunium are shown and compared in Figure 7-6. These results are for a single realization (above) and for the average of 15 realizations (below). Comparison between the simulated breakthrough curves for the SZ 1-D transport model and the SZ flow and transport abstraction model for a single realization shows differences between the simulated results, particularly for neptunium transport in this realization. However, there are small differences between the simulated breakthrough curves when the results are averaged over 15 realizations of the models, as shown in the lower plot in Figure 7-6. For the case of nonsorbing species, the average of the SZ 1-D transport model simulations shows somewhat earlier breakthrough for the tail of the breakthrough curve, relative to the SZ flow and transport abstraction model.

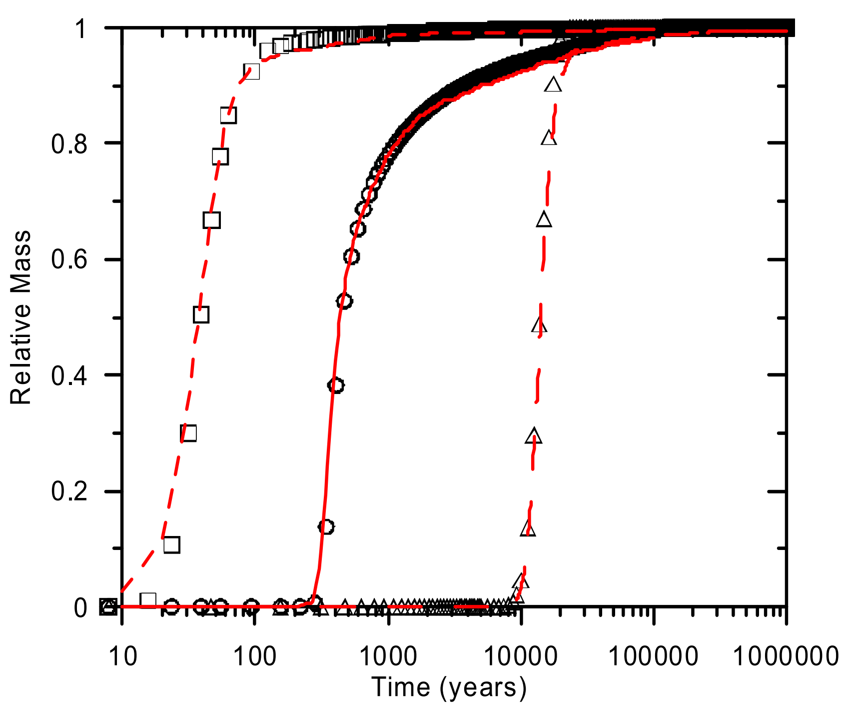

Output DTN: SN0306T0502103.005.

NOTE: Results from the SZ site-scale transport model (BSC 2004 [DIRS 170036]) are shown for the median case (solid line), fast case (short-dashed line), and slow case (long-dashed line). Results from the SZ 1-D transport model are shown for the median case (open circle), fast case (open square), and slow case (open triangle). Breakthrough curves do not include radioactive decay.

Figure 7-4. Simulated Breakthrough Curves Comparing the Results of the SZ 1-D Transport Model and the SZ Site-Scale Transport Model for a Nonsorbing Radionuclide

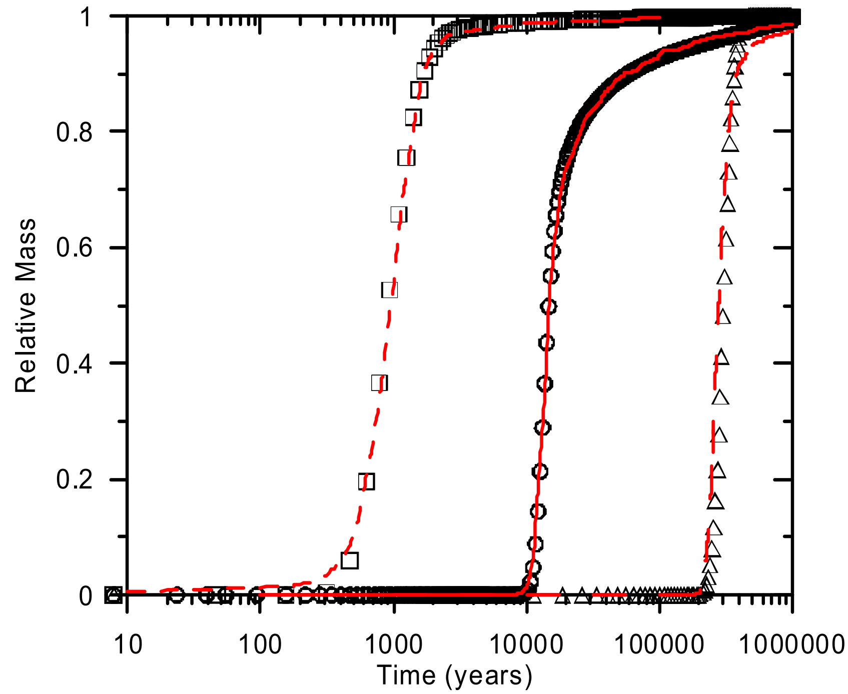

Output DTN: SN0306T0502103.005.

NOTE: Results from the SZ site-scale transport model (BSC 2004 [DIRS 170036]) are shown for the median case (solid line), fast case (short-dashed line), and slow case (long-dashed line). Results from the SZ 1-D transport model are shown for the median case (open circle), fast case (open square), and slow case (open triangle). Breakthrough curves do not include radioactive decay.

Figure 7-5 Simulated Breakthrough Curves Comparing the Results of the SZ 1-D Transport Model and the SZ Site-Scale Transport Model for Neptunium

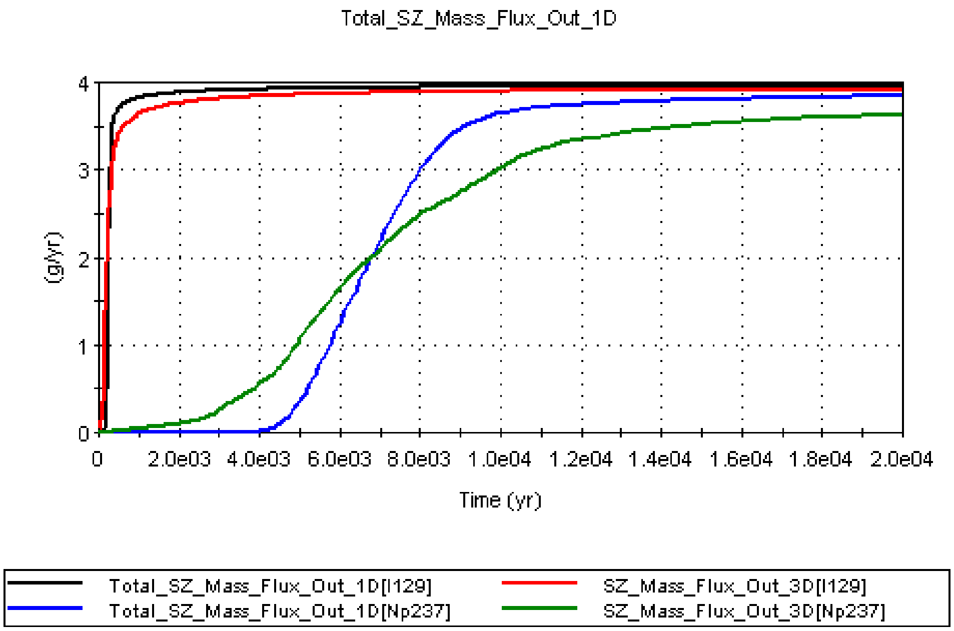

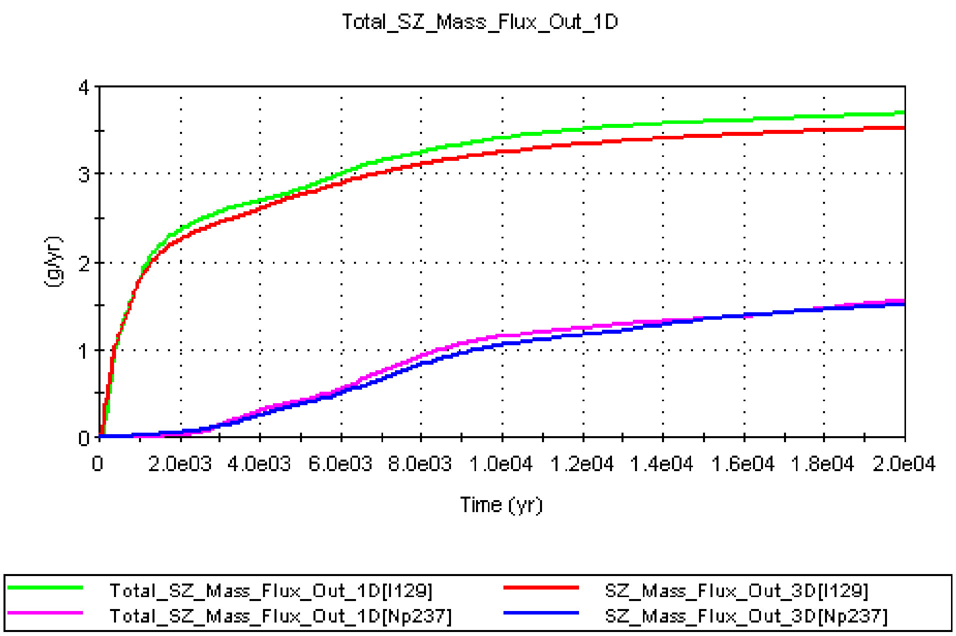

Output DTN: SN0306T0502103.005.

Figure 7-6. Simulated Breakthrough Curves Comparing the Results of the SZ 1-D Transport Model (1D) and the SZ Flow and Transport Abstraction Model (3D) for a Nonsorbing Radionuclide (I129) and Neptunium (^{237}Np) for a Single Realization (Above) and for the Average of 15 Realizations (Below)

7.4 CONCLUSIONS

7.4.1 SZ Flow and Transport Abstraction Model Validation

Validation testing of the SZ flow and transport abstraction model indicates good agreement with the SZ site-scale transport model (BSC 2004 [DIRS 170036]). Acceptance criteria established for the model validation regarding the qualitative comparison of simulated breakthrough curves and the quantitative evaluation of radionuclide mass balance are met. Results of the validation testing indicate that the SZ flow and transport abstraction model is valid for the approximate range of uncertainty incorporated into the model through parameter uncertainty distributions. Results also indicate that the SZ flow and transport abstraction model is valid for both nonsorbing and sorbing radionuclide species for its intended use.

It should be noted that the SZ is more effective as a barrier for highly sorbing, short-lived radionuclides such as ^{90}Sr and ^{137}Cs, relative to neptunium, as used in this validation testing. The validation testing does not demonstrate the delay afforded by the SZ in the migration of these radionuclides; nor does it demonstrate the impact of radionuclide decay. However, the importance of the SZ as a barrier to ^{90}Sr and ^{137}Cs transport, with regard to both delay and decay, is discussed in Section 6.7.

The small deviation from the SZ site-scale transport model results at early times for the fast case is a result of the time-step size used in the simulation. Such deviations in the abstraction model for realizations with very fast transport in the SZ would not be significant within the context of the TSPA-LA analyses using this model. The discrepancy in radionuclide mass balance identified in the validation testing is a small percentage and is readily understood with regard to long-term mass retention in the SZ due to the matrix diffusion process. No future activities are needed to complete this model validation for its intended use.

7.4.2 SZ 1-D Transport Model Validation

Validation testing of the SZ 1-D transport model indicates acceptable agreement with the SZ site-scale transport model (BSC 2004 [DIRS 170036]). Qualitative acceptance criteria regarding the comparison of the simulated breakthrough curves with the results of the SZ site-scale transport model are met. Results of the validation testing indicate that the SZ 1-D transport model is valid for the approximate range of uncertainty incorporated into the model through parameter uncertainty distributions. Results also indicate that the SZ 1-D transport model is valid for both nonsorbing and sorbing radionuclide species for its intended use.

It is relevant to consider the purpose and use of the SZ 1-D transport model in the evaluation of validation testing results. This model is used for the purpose of simulating radioactive decay and ingrowth for four decay chains. This simplified model is required because the SZ flow and transport abstraction model is not capable of simulating ingrowth by radioactive decay. It is not anticipated that the decay products in these decay chains would be significant contributors to total radiological dose; however, groundwater protection regulations require assessment of groundwater concentrations for some of these decay products. The results of the SZ 1-D transport model are used only for the decay products in these decay chains within the TSPA-LA analyses.

It must also be considered that there are fundamental differences between the SZ 1-D transport model and the SZ site-scale transport model that limit the degree of consistency that can be expected between these two models. Groundwater flow and radionuclide transport simulation in the SZ site-scale transport model occur in three dimensions with a relatively complex representation of geological heterogeneity from the hydrogeologic framework model. Radionuclide transport in the SZ 1-D transport model is simulated in a significantly simplified representation of the SZ system consisting of three pipe segments. Each pipe segment has properties that represent the average characteristics in that area of the SZ site-scale transport model. There are also variations in the source location within the four source regions beneath the repository simulated by the SZ flow and transport abstraction model that are not incorporated in the SZ 1-D transport model on a realization-by-realization basis, as discussed in Section 7.1.2.

Another difference between the SZ 1-D transport model and the SZ flow and transport abstraction model is the way in which changes in groundwater flux related to climate change are handled. A fundamental limitation to the Laplace transform solution used by the GoldSim V7.50.100 software code to simulate radionuclide transport in the “pipe” module is that radionuclide mass in transit through a particular pipe segment does not change in response to changes in specified groundwater flow rate. Consequently, radionuclide mass that has entered a pipe segment in the SZ 1-D transport model before increased flow rates are imposed at 600 and 2,000 years for the monsoonal and glacial-transition climate states in the TSPA-LA model, would not be instantaneously accelerated, as it is in the SZ flow and transport abstraction model. Because peak releases of radionuclides to the SZ are not expected to occur within the first 2,000 years of the TSPA-LA simulations, this limitation to the SZ 1-D transport model is unlikely to have a significant impact on the simulation results.

Comparison of simulation results from the SZ 1-D transport model and the SZ flow and transport abstraction model shows that there are differences for individual realizations, as used in the TSPA-LA analyses. However, when results are averaged over several realizations the ensemble behavior of the SZ 1-D transport model is very similar to the SZ flow and transport abstraction model. This indicates that there is no consistent bias in the simulation results from the SZ 1-D transport model relative to the SZ flow and transport abstraction model. Given this finding and the intended use of the SZ 1-D transport model for the simulation of decay chain products only, differences in the results with the SZ flow and transport abstraction model for individual realizations are acceptable.

Considering these factors, the SZ 1-D transport model provides a good approximation of simulated radionuclide transport in the 3-D system of the SZ. No future activities are needed to complete this model validation for its intended use.

7.4.3 Validation Summary

The SZ flow and transport abstraction model and the SZ 1-D transport model have been validated by applying acceptance criteria based on an evaluation of the models’ relative importance to the potential performance of the repository system. All relevant validation requirements have been fulfilled, including corroboration of model results with comparison to the model from which they were derived and publication in a refereed professional journal. Activities requirements for confidence building during model development have also been satisfied. The model development activities and post-development validation activities described establish the scientific bases for the SZ flow and transport abstraction model and the SZ 1-D transport model. Models used to simulate the transport of radionuclides in the SZ are sufficiently accurate and adequate for intended use if they model radionuclide mass output as a function of time, consistent with the underlying transport model (SZ site-scale transport model), given that uncertainty of input parameters may impact simulated transport times by several orders of magnitude. Other criteria for accuracy and adequacy are radionuclide mass balance and non-biased ensemble transport behavior among multiple realizations, which were addressed in model validation activities. Based on these criteria, the SZ flow and transport abstraction model and the SZ 1-D transport model used in this report are considered to be sufficiently accurate and adequate for the intended purpose and to the level of confidence required by the models' relative importance to the potential performance of the repository system.

7.5 CORRECTION TO THE SZ 1-D TRANSPORT MODEL

Reevaluation of the SZ 1-D transport model has indicated two corrections to the model relative to the model file contained in output DTN: SN0306T0502103.005. This section of the report describes those corrections and evaluates their impact with regard to radionuclide transport simulation results in the SZ 1-D transport model. The first correction is for the value of average matrix porosity of the volcanic units used to divide the free water diffusion coefficient. The value used in the original model file is 0.20, but it should be 0.21 to be consistent with the value used in the pipe segments to analyze matrix diffusion. The second correction is to the effective value of the flowing interval spacing used in the pipe segments to simulate matrix diffusion. In the original model file the value of flowing interval spacing (FISVO) was converted from the log-transformed value to the actual value and divided by 4. The corrected calculation is to divide the value by 2.

The impact of these corrections is evaluated by comparing the original results with the corrected results for the average breakthrough curves of a nonsorbing species and of neptunium with the SZ 1-D transport model. The model results for this comparison are shown in Figure 7-7. Examination of these results indicates that the agreement between the average breakthrough curves for the SZ 1-D transport model and the SZ flow and transport abstraction model is better for the corrected SZ 1-D transport model than for the original SZ 1-D transport model. This is particularly true for the transport of nonsorbing radionuclides; the differences between the original and corrected versions of the SZ 1-D transport model are minimal for the transport of neptunium.

Based on these results it is concluded that the impacts of the corrections to the SZ 1-D transport model are small with regard to validation of the SZ 1-D transport model. Further more, for the 15 realizations used in the impact analysis, the original SZ 1-D transport model overpredicts the rate of migration of nonsorbing species in the tail of the average breakthrough curve, relative to the SZ flow and transport abstraction model. Overprediction of the rate of migration of radionuclides results in higher simulated dose in the TSPA-LA model.

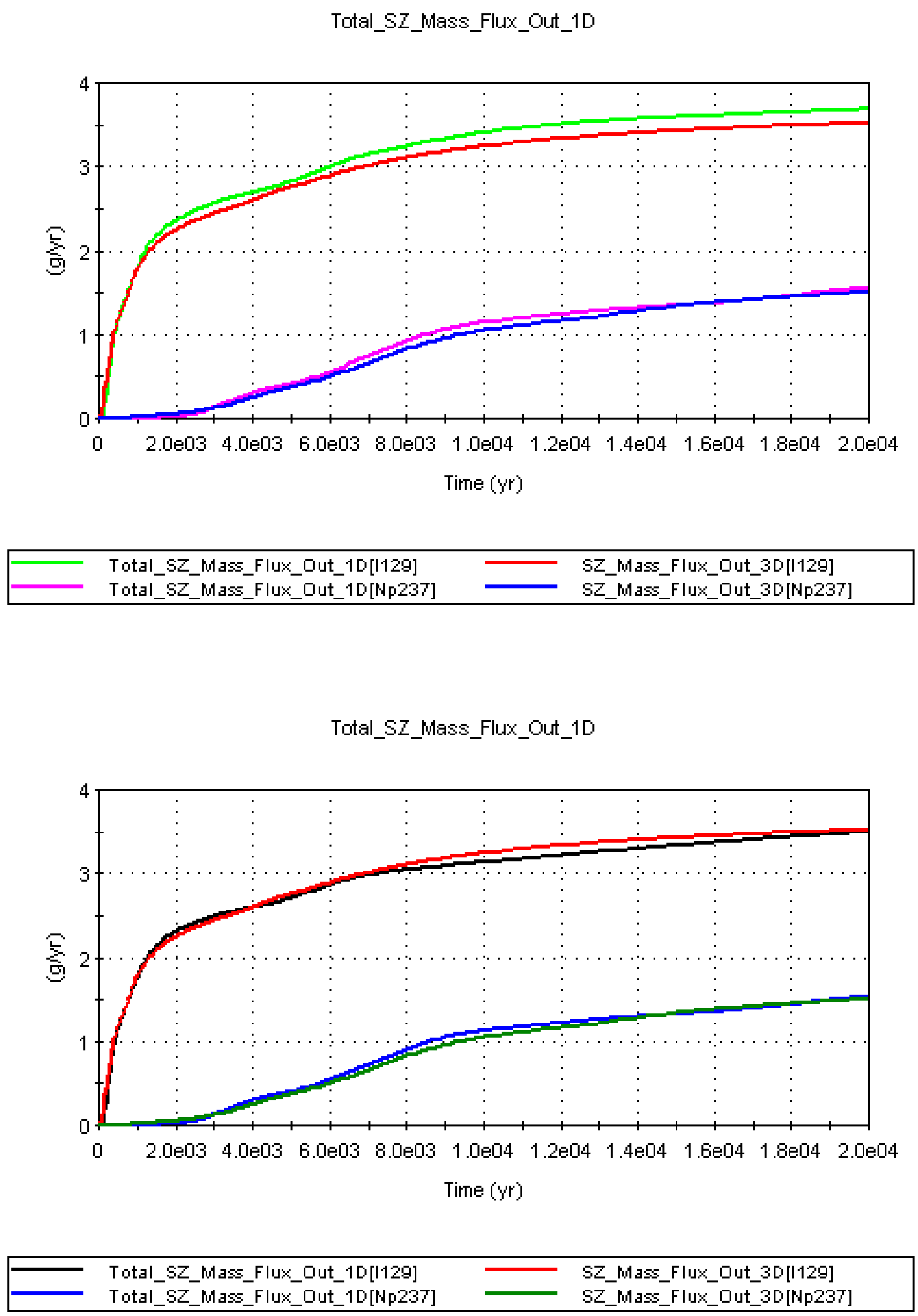

Output DTN: SN0306T0502103.005.

Figure 7-7. Simulated Breakthrough Curves Comparing the Results of the SZ 1-D transport model (1D) and the SZ Flow and Transport Abstraction Model (3D) for a Nonsorbing Radionuclide (I129) and Neptunium (^{237}Np) for the Average of 15 Realizations for the Original (Above) and Corrected SZ 1-D Transport Model (Below)

INTENTIONALLY LEFT BLANK

8. CONCLUSIONS

8.1 SUMMARY OF MODELING ACTIVITY

The SZ flow and transport abstraction model and the SZ 1-D transport model are developed for use in the TSPA-LA analyses. In addition, analyses of uncertainty in input parameters for these models are conducted, and the results are documented as uncertainty distributions. Values of uncertain parameters are sampled for 200 realizations of the SZ flow and transport system. Simulations using the SZ flow and transport abstraction model are conducted for these 200 realizations, and the results are documented in this report.

Analyses of parameter uncertainty and of multiple realizations of the SZ system, using the SZ flow and transport abstraction model, constitute an assessment of uncertainty in the SZ system that is useful for direct implementation in the TSPA-LA model. The simulated radionuclide mass breakthrough curves from the SZ flow and transport abstraction model are coupled to the TSPA-LA analyses using the convolution integral method (via the SZ_Convolute V3.0 software code (STN: 10207-3.0-00, SNL 2003 [DIRS 164180])).

In addition, the SZ 1-D transport model is developed for direct implementation, in conjunction with the GoldSim V7.50.100 software code, in the TSPA-LA. The uncertain input parameters defined for the SZ flow and transport abstraction model are used in the SZ 1-D transport model, to provide consistency between the two models when they are used in the probabilistic analyses of the TSPA-LA.

The SZ flow and transport abstraction model and the SZ 1-D transport model are validated, and the results of these validation activities are documented in this report. Validation of the SZ flow and transport abstraction model indicates very close agreement with the underlying SZ site-scale transport model when the convolution integral method is used. Although the SZ 1-D transport model is much simpler than the 3-D SZ flow and transport abstraction model, validation of the SZ 1-D transport model indicates there is close agreement, over a broad range of uncertainty, between the 1-D and 3-D models with respect to each model's assessment of transport behavior of representative radionuclides.

The technical bases of FEPs included in the models are presented in this report, and are provided to clarify the parameters and components of the SZ flow and transport abstraction model and the SZ 1-D transport model. The role of the SZ as a natural barrier to the transport of radionuclides is assessed in relation to the results of the SZ flow and transport abstraction model. In addition, the model development and analyses presented in this report address those YMRP acceptance criteria (NRC 2003 [DIRS 163274]) that are listed in Section 4.2 of this report.

Information on the correlation between distribution coefficients (K_ds) used in the sampling of uncertain parameters for the SZ flow and transport abstraction model and for the SZ 1-D transport model is provided in Table 4-3 and Table 6-8. Positive correlation between the distribution coefficient for uranium in volcanic units and alluvium is specified, based on potentially similar hydrochemical conditions in the two aquifers. Positive correlation between the distribution coefficient for neptunium in volcanic units and alluvium is specified, based on potentially similar hydrochemical conditions in the two aquifers. Positive correlation between the distribution coefficient for plutonium in volcanic units and alluvium is specified, based on potentially similar hydrochemical conditions in the two aquifers. Positive correlation between the distribution coefficients for uranium and neptunium is specified, based on similarities in the chemical behavior of these radioelements. The technical bases for correlations between distribution coefficients (or the lack thereof) are documented in *Site-Scale Saturated Zone Transport* (BSC 2004 [DIRS 170036], Section C1.2.1).

Evaluation of uncertainty in horizontal anisotropy in permeability is summarized in Section 6.5.2.10. Complete documentation of the technical basis for this evaluation of uncertainty is given in *Saturated Zone In-Situ Testing* (BSC 2004 [DIRS 170010]), Section 6.2.6. Results of this evaluation indicate that there is a greater probability of enhanced permeability in the north-south direction, but a small probability of greater permeability in the east-west direction. Implementation of uncertainty in horizontal anisotropy in the SZ flow and transport abstraction model and in the SZ 1-D transport model is discussed in Section 6.5.3.1 and Section 6.5.1.2, respectively.

The impacts of spatial variability of parameters affecting radionuclide transport in the alluvium are incorporated in the evaluation of uncertainties in model parameters in Section 6.5.2.3, Section 6.5.2.7, Section 6.5.2.8, Section 6.5.2.9, and Section 6.5.2.11. Uncertainties in individual parameters affecting radionuclide transport, as influenced by spatial variability, are combined in the probabilistic analyses with the SZ transport abstraction model. The technical bases for uncertainty in distribution coefficients are documented in *Site-Scale Saturated Zone Transport* (BSC 2004 [DIRS 170036], Appendix A).

Information on geological uncertainty in the location of the contact between tuff and alluvium, and the consequent uncertainty in flow-path lengths in the alluvium, is presented in Section 6.5.2.2. This evaluation of uncertainty includes information from the Nye County drilling program. Reevaluation of the uncertainty in the northern and western extent of the alluvium resulted in significant reduction in this uncertainty, in comparison to the previous evaluation (CRWMS M&O 2000 [DIRS 147972], Section 6.2).

The sensitivity analysis of matrix diffusion in the SZ transport abstraction model is presented in the assessment of ACMs in Section 6.4. The results of this sensitivity analysis indicate that a minimal matrix diffusion ACM is captured within the range of uncertainty used in the SZ transport abstraction model.

8.2 MODEL OUTPUTS

8.2.1 Developed Output

The technical output from this report is given in seven DTNs; these DTNs are summarized in Table 8-1.

Table 8-1. Summary of Developed Output

Output DTN	Description
SN0310T0502103.009	Uncertainty distributions for parameters used in the SZ transport abstraction model. Sampling output of uncertain parameters for 200 realizations is also included (see Appendix I). This DTN also includes a description of each uncertain parameter.
SN0310T0502103.010	Input and output files for the SZ transport abstraction model. This DTN also contains the output breakthrough curves for use in the TSPA-LA analyses.
SN0306T0502103.005	Input and output files for the SZ 1-D transport model.
SN0306T0502103.006	Data spreadsheets to support data uncertainty development.
SN0310T0502103.012	Input and output files for the SZ transport abstraction model for the fast fraction of radionuclides irreversibly attached to colloids. This DTN also contains the output breakthrough curves for use in the TSPA-LA analyses.
SN0407T0502103.013	Input and output files for the SZ transport abstraction model with re-sampling of input parameters to address CR 2222 (*Evaluate Revised LH Sampling Algorithm on the Results of ANL-EBS-PA-000009*). This DTN also contains the output breakthrough curves for use in the TSPA-LA analyses.
MO0310SPANGRAC.000	Results of the background gross alpha concentration analysis.
SN0507T0502103.014	Revised results of the background gross alpha concentration analysis.
MO0506SPAINPUT.001	Parameter definitions and values for the SZ 1-D transport model for use in the TSPA-LA model.

Results of the parameter uncertainty analyses from this report are given in DTN: SN0310T0502103.009. These results include the uncertainty distributions for parameters that were developed in this analysis or incorporated from other analyses and the input file for the GoldSim V7.50.100 software code for sampling 200 realizations from these uncertainty distributions. DTN: SN0310T0502103.009 also contains the output file from the GoldSim V7.50.100 software code, which includes the parameter vectors to be used in the SZ transport abstraction model.

Results of the SZ transport abstraction model from this report are given in DTN: SN0310T0502103.010. These results consist of the input and output files from the FEHM V2.20 software code (STN: 10086-2.20-00), the SZ_Pre V2.0 software code (STN: 10914-2.0-00), and the SZ_Post V3.0 software code (STN: 10915-3.0-00) used in the analyses. The results that form a direct input to the TSPA-LA model are the files that contain the breakthrough curves (from the SZ transport abstraction model) from the 200 realizations of radionuclide transport. The breakthrough curves used in the TSPA-LA model (i.e., the breakthrough curves at the regulatory boundary of the accessible environment) are defined in the output files in the first column (“time”) and the third column (“relative mass”).

The input and output files for the SZ 1-D transport model are given in DTN: SN0306T0502103.005. The input file of the SZ 1-D transport model for the GoldSim V7.50.100 software code is intended for incorporation into the TSPA-LA model. Output pertaining to parameter values for use in the SZ 1-D transport model is also found in Section 6.5.1.2 of this report. Estimates of groundwater specific discharge for the three pipe segments (in the SZ 1-D transport model) taken from the SZ transport abstraction model are given in Table 6-6, as a function of horizontal anisotropy in permeability. Estimates of the minimum and maximum pipe lengths for the second and third pipe segments in the SZ 1-D transport model are given in Table 6-7 as a function of source region and horizontal anisotropy in permeability.

The data spreadsheets in DTN: SN0306T0502103.006 have the data used in the analyses of parameter uncertainty summarized in this report and in DTN: SN0310T0502103.009. The spreadsheets mentioned by filename in this report are included in DTN: SN0306T0502103.006.

Results of the SZ transport abstraction model that used re-sampling of the input parameters from Appendix B of this report are given in DTN: SN0407T0502103.013. These results were generated primarily to address CR 2222 (*Evaluate Revised LH Sampling Algorithm on the Results of ANL-EBS-PA-000009*) with respect to evaluation of the impact of the sampling difference in the GoldSim V7.50.100 software code. These radionuclide transport simulation results are also appropriate for use as input to the TSPA-LA for purposes of evaluating the impacts of the problem identified in CR 2222 at the total-system level, if necessary. These results consist of the input and output files from the following codes used in the analyses: the FEHM V2.20 software code (STN: 10086-2.20-00), the SZ_Pre V2.0 software code (STN: 10914-2.0-00), and the SZ_Post V3.0 software code (STN: 10915-3.0-00). The breakthrough curves accepted for use in the TSPA-LA model (i.e., the breakthrough curves at the regulatory boundary of the accessible environment) are defined in the output files, in the first column ("time") and the third column ("relative mass").

This report's results of the SZ transport abstraction model for the fast fraction of radionuclides irreversibly attached to colloids are given in DTN: SN0310T0502103.012. These results consist of the input and output files from the following codes used in the analyses: the FEHM V2.20 software code (STN: 10086-2.20-00), the SZ_Pre V2.0 software code (STN: 10914-2.0-00), and the SZ_Post V3.0 software code (STN: 10915-3.0-00). The results that form a direct input to the TSPA-LA model are the files that contain the breakthrough curves (from the SZ transport abstraction model) used for the 200 realizations of radionuclide transport. The breakthrough curves accepted for use in the TSPA-LA model (i.e., the breakthrough curves at the regulatory boundary of the accessible environment) are defined in the output files, in the first column ("time") and the third column ("relative mass").

The results of the background gross alpha concentration analysis (as documented in Section 6.8) are given in DTN: MO0310SPANGRAC.000. The results of the revised background gross alpha concentration analysis using additional data are given in DTN: SN0507T0502103.014. Parameter definitions and values for the SZ 1-D transport model for use in the TSPA-LA model are given in DTN: MO0506SPAINPUT.001.

8.2.2 Output Uncertainties and Limitations

The assessment of uncertainty in model parameters and model outputs is an integral part of the performed analyses in this report. Uncertainty in model parameters is quantitatively represented by the statistical distributions developed and given in DTN: SN0310T0502103.009. Uncertainty in radionuclide transport in the SZ transport abstraction model is embodied in the breakthrough curves for the 200 realizations given in DTN: SN0310T0502103.010. The SZ 1-D transport model is intended for direct incorporation into the TSPA-LA model, with which uncertainty will be assessed using Monte Carlo probabilistic analyses.

All relevant uncertainties in data and model parameters, with respect to their affect upon groundwater flow and radionuclide transport, have been included in both the SZ transport abstraction model and the SZ 1-D transport model. Uncertainties have been propagated through the results of the SZ transport abstraction model (i.e., the radionuclide breakthrough curves for multiple realizations) documented in this report. These output uncertainties address the requirements of acceptance criterion 3 of the YMRP (NRC 2003 [DIRS 163274]) for the propagation of data uncertainty through model abstraction for flow paths in the SZ and for radionuclide transport in the SZ.

Use of the SZ transport abstraction model and the SZ 1-D transport model is subject to the limitations and restrictions imposed by the assumptions listed in Sections 5, 6.3, and 6.5 of this report. Limitations in knowledge of specific parameter values are addressed in this report in the analysis of parameter uncertainties. The radionuclide breakthrough curves generated for the SZ Transport Abstraction model are limited to 100,000 years duration for present climatic conditions; this limits the time period that can be simulated with the TSPA-LA model when using these breakthrough curves for the SZ. Because the SZ breakthrough curves are scaled for higher groundwater flow rates under future climatic conditions, the time period that can be simulated with the TSPA-LA model would be less than 100,000 years. If the glacial-transition climate state is applied for most of the simulation period in the TSPA-LA model, the SZ breakthrough curves would be scaled by a factor of approximately 3.9, thereby limiting the TSPA-LA model simulation time to about 26,000 years.

8.3 YUCCA MOUNTAIN REVIEW PLAN ACCEPTANCE CRITERIA

The following information describes how this analysis addresses the acceptance criteria in the Yucca Mountain Review Plan (NRC 2003 [DIRS 163274], Sections 2.2.1.3.8.3 and 2.2.1.3.9.3). Only those acceptance criteria that are applicable to this report (see Section 4.2) are discussed. In most cases, the applicable acceptance criteria are not addressed solely by this report; rather, the acceptance criteria are fully addressed when this report is considered in conjunction with other analysis and model reports that describe flow and transport in the saturated zone. Where a subcriterion includes several components, only some of those components may be addressed. How these components are addressed is summarized below.

Acceptance Criteria from Section 2.2.1.3.8.3 Flow Paths in the Saturated Zone

Acceptance Criterion 1: System Description and Model Integration Are Adequate

> Subcriterion (1): Total system performance assessment adequately incorporates important design features, physical phenomena, and couplings, and uses consistent and appropriate assumptions, throughout the flow paths in the saturated zone abstraction process;

Important physical phenomena and couplings are incorporated into the SZ flow and transport model abstraction through application of the best relevant, qualified data from the Yucca Mountain site and region (Sections 4.1.1 and 4.1.2). Consistent and appropriate assumptions noted in Sections 5 and 6.3 are used throughout this abstraction report and other abstractions, model reports, and analysis reports related to flow paths in the SZ. Integration of the SZ abstraction models for the TSPA-LA is described in Sections 6.3.3 and 6.5.3.

> Subcriterion (2): The description of the aspects of hydrology, geology, geochemistry, design features, physical phenomena, and couplings that affect flow paths in the saturated zone, is adequate. Conditions and assumptions in the abstraction of flow paths in the saturated zone are readily identified, and consistent with the body of data presented in the description;

This abstraction provides fully adequate descriptions of the aspects of hydrology, geology, geochemistry, physical phenomena, and couplings that may affect flow paths in the saturated zone through reference to supporting analysis and model reports in Table 4-1, discussion of incorporated features, events, and processes in Table 6-1, and detailed discussions of base-case conceptual model and inputs in Sections 6.3 and 6.5.2. Additional and more detailed descriptions of these aspects of the system are provided in supporting documents, particularly *Site-Scale Saturated Zone Flow Model* (BSC 2004 [DIRS 170037]) and BSC 2004 [DIRS 170036]. Conditions and assumptions in the abstraction of flow paths in the saturated zone are readily identified in Sections 5 and 6.3, and they are consistent with the body of data presented in the descriptions (Sections 4.1, 6.2, 6.3, and 6.5).

> Subcriterion (3): The abstraction of flow paths in the saturated zone uses assumptions, technical bases, data, and models that are appropriate and consistent with other related U.S. Department of Energy abstractions. For example, the assumptions used for flow paths in the saturated zone are consistent with the total system performance assessment abstraction of representative volume (Section 2.2.1.3.12 of the Yucca Mountain Review Plan). The descriptions and technical bases provide transparent and traceable support for the abstraction of flow paths in the saturated zone;

Assumptions, described in Section 5, are consistent with those used in other model and analysis reports. For example, two of the six assumptions are carried forward directly from the *Saturated Zone Colloid Transport* scientific analysis report (BSC 2004 [DIRS 170006], Section 6.3). Technical bases, data, models, and local modeling assumptions are described in Section 6.3. Transparent and traceable support for the abstraction of flow paths in the SZ is provided for the SZ transport abstraction and the SZ 1-D transport model. For example, estimates of the variation in groundwater specific discharge and flow-path lengths in the SZ 1-D transport model are explained and illustrated in Section 6.5.1.2.

> Subcriterion (4): Boundary and initial conditions used in the total system performance assessment abstraction of flow paths in the saturated zone are propagated throughout its abstraction approaches. For example, abstractions are based on initial and boundary conditions consistent with site-scale modeling and regional models of the Death Valley ground water flow system;

Boundary conditions used in the TSPA-LA abstraction of flow paths in the SZ are taken from the SZ site-scale flow model, as described in Section 6.5. These boundary conditions are based on analyses that use the regional model of the Death Valley groundwater flow system, as described in *Site-Scale Saturated Zone Flow Model* (BSC 2004 [DIRS 170037]). The effects of these boundary conditions are implicitly propagated to the SZ 1-D transport model through estimates of flow rates and pipe-segment lengths, as described in Section 6.5.1.2. Initial conditions are not used in the abstraction of flow paths because steady-state conditions are assumed.

> Subcriterion (5): Sufficient data and technical bases to assess the degree to which features, events, and processes have been included in this abstraction are provided;

FEPs addressed in this model report are documented in Section 6.2. Table 6-1 summarizes those SZ FEPs for which the technical bases are provided in this report, and includes the location within this report of the information providing sufficient data and bases.

> Subcriterion (7): Long-term climate change, based on known patterns of climatic cycles during the Quaternary period, particularly the last 500,000 years, and other paleoclimate data, are adequately evaluated;

The patterns of climatic cycles used for modeling were provided in BSC 2004 [DIRS 170002], and were adequately evaluated for impacts on groundwater flow paths and flow rates in the SZ. The USGS analyzed known patterns of climatic cycles covering the last 500,000 years and correlated them with relevant paleoclimate data to produce the climate projections incorporated in this report. The application of climate information in modeling is described in Section 6.5.

> Subcriterion (9): The impact of the expected water table rise on potentiometric heads and flow directions, and consequently on repository performance, is adequately considered;

The impact of expected water table rise has been adequately considered in Section 5 of this report by conservatively scaling transport rates in the SZ. Water table rise directly beneath the repository would place flow in hydrogeologic units with lower values of permeability (Section 5, item 6). This approximation of climate change with unaltered SZ flow paths is shown to underestimate radionuclide transport times in sensitivity studies documented in *Site-Scale Saturated Zone Transport* (BSC 2004 [DIRS 170036], Attachment E).

> Subcriterion (10): Guidance in NUREG–1297 [DIRS 103597] and NUREG-1298 (Altman, et al., 1988) [DIRS 103750], or other acceptable approaches for peer review and data qualification is followed.

This report was developed in accordance with the *Quality Assurance Requirements and Description* (QARD) (DOE 2004 [DIRS 171539]), which commits to NUREGs 1297 [DIRS 103597] and 1298 [DIRS 103750]. Moreover, compliance with the DOE procedures, which are designed to ensure compliance with the QARD, is verified by audits by QA and other oversight activities. Accordingly, the guidance in NUREGs 1297 and 1298 has been followed as appropriate.

Acceptance Criterion 2: Data Are Sufficient for Model Justification

> Subcriterion (1): Geological, hydrological, and geochemical values used in the license application to evaluate flow paths in the saturated zone are adequately justified. Adequate descriptions of how the data were used, interpreted, and appropriately synthesized into the parameters are provided;

Section 6.5.2 of this report provides thorough explanations that adequately justify the use of geological, hydrological, and geochemical values in the evaluation of flow paths. Section 6.5.2 also adequately describes the interpretation of data and development of parameter values and distributions. Additional and more detailed descriptions of these aspects of the analysis are provided in supporting documents, particularly, *Site-Scale Saturated Zone Flow Model* (BSC 2004 [DIRS 170037]) and BSC 2004 [DIRS 170036].

> Subcriterion (3): Data on the geology, hydrology, and geochemistry of the saturated zone used in the total system performance assessment abstraction are based on appropriate techniques. These techniques may include laboratory experiments, site-specific field measurements, natural analog research, and process-level modeling studies. As appropriate, sensitivity or uncertainty analyses used to support the U.S. Department of Energy total system performance assessment abstraction are adequate to determine the possible need for additional data;

Section 6.5.2 of this report describes the sources of data that were used in the development of modeling parameters in the TSPA-LA abstraction, the techniques used to evaluate these data, and the sufficiency of the data; the section also shows these techniques were appropriate. Table 6-8 includes the sources of input data, and associated uncertainty types.

Acceptance Criterion 3: Data Uncertainty Is Characterized and Propagated Through the Model Abstraction

> Subcriterion (1): Models use parameter values, assumed ranges, probability distributions, and bounding assumptions that are technically defensible, reasonably account for uncertainties and variabilities, and do not result in an under-representation of the risk estimate;

The development of parameter values, bounding values, and probability distributions is described in Section 6.5.2. The development was conducted in a technically defensible manner that reasonably accounts for uncertainty and variability. Two bounding assumptions are also described in Section 5, and model-specific assumptions are discussed in Section 6.3. Table 6-8 shows probability distributions associated with the parameters, and Section 6.5.2 explains the sources of uncertainties in the parameters. The conservative simplifications and assumptions used for the abstraction models reasonably account for uncertainties and variabilities, and do not result in an under-representation of the risk estimate (Sections 5 and 6.3).

> Subcriterion (2): Uncertainty is appropriately incorporated in model abstractions of hydrologic effects of climate change, based on a reasonably complete search of paleoclimate data;

The treatment of climate change and associated changes in infiltration are explained in Section 6.5 and Table 6-5. Applicable paleoclimate data was incorporated in the development of the climate phases adopted through BSC 2004 [170002].

> Subcriterion (3): Uncertainty is adequately represented in parameter development for conceptual models, process-level models, and alternative conceptual models considered in developing the abstraction of flow paths in the saturated zone. This may be done either through sensitivity analyses or use of conservative limits. For example, sensitivity analyses and/or similar analyses are sufficient to identify saturated zone flow parameters that are expected to significantly affect the abstraction model outcome;

Section 6.5.2 includes detailed explanations of parameter representations and uncertainty sources of parameters that were used in the development of flow paths. Alternative conceptual models and associated sensitivity analyses used to address uncertainty are discussed in Section 6.4.

> Subcriterion (4): Where sufficient data do not exist, the definition of parameter values and conceptual models is based on appropriate use of expert elicitation, conducted in accordance with NUREG–1563 (Kotra et al. 1996) ([DIRS 100909]). If other approaches are used, the U.S. Department of Energy adequately justifies their uses.

Expert elicitation was used in the determination of groundwater specific discharge in the SZ. The expert elicitation process was conducted in accordance with DOE procedures that conform to NUREG-1563 (Kotra et al. 1996) ([DIRS 100909]) and use of these results in quantifying uncertainty in specific discharge is described, with references, in Section 6.5.2.1.

Acceptance Criterion 4: Model Uncertainty Is Characterized and Propagated Through the Model Abstraction

> Subcriterion (1): Alternative modeling approaches of features, events, and processes are considered and are consistent with available data and current scientific understanding, and the results and limitations are appropriately considered in the abstraction;

The process of minimal matrix diffusion and the feature of horizontal anisotropy in permeability are considered in alternative conceptual models, as described in Section 6.4 and Table 6-4. The models are shown to be consistent with available data and current scientific knowledge and are considered appropriately in the abstraction through the ranges of parameter uncertainties in the base-case model.

> Subcriterion (2): Conceptual model uncertainties are adequately defined and documented, and effects on conclusions regarding performance are properly assessed. For example, uncertainty in data interpretations is considered by analyzing reasonable conceptual flow models that are supported by site data, or by demonstrating through sensitivity studies that the uncertainties have little impact on repository performance;

Alternative conceptual models are discussed in Section 6.4. ACMs are also listed in Table 6-4, which includes key assumptions and bases for screening decisions. A sensitivity analysis was used to determine the impact of these alternatives on repository performance. Additional descriptions of ACMs of the SZ flow system are provided in the supporting document, *Site-Scale Saturated Zone Flow Model* (BSC 2004 [DIRS 170037]).

> Subcriterion (3): Consideration of conceptual model uncertainty is consistent with available site characterization data, laboratory experiments, field measurements, natural analog information and process-level modeling studies; and the treatment of conceptual model uncertainty does not result in an under-representation of the risk estimate.

The parameters and parameter uncertainty related to groundwater flow from external sources used directly in the modeling documented in this report are shown in Table 4-3. Spatial variability in rock properties is encompassed within uncertainty distributions for key parameters (Tables 6-1 and 6-8). The uncertainty distributions incorporate uncertainties associated with Yucca Mountain field or laboratory data, knowledge of how the parameter will be used in the model, and theoretical considerations (Section 6.5.2). The probabilistic analysis of uncertainty in groundwater flow is implemented through Monte Carlo realizations of the SZ flow and transport system, in a manner consistent with the TSPA-LA simulations (Section 6.3). Variability in the results of multiple radionuclide breakthrough curves reflects the uncertainty in groundwater flow and radionuclide transport behavior in the SZ (Section 6.6). These results are intended for direct incorporation into the TSPA-LA model (Section 8.2.2), and as such, do not contribute to an under-representation of the risk estimate as determined in the TSPA-LA.

> Subcriterion (4): Appropriate alternative modeling approaches are consistent with available data and current scientific knowledge, and appropriately consider their results and limitations, using tests and analyses that are sensitive to the processes modeled.

The process, bases, and results for alternative modeling approaches are discussed in Section 6.4. Results obtained by use of an ACM are also shown in Figure 6-3. Additional descriptions of ACMs of the SZ flow system are provided in the supporting document, *Site-Scale Saturated Zone Flow Model* (BSC 2004 [DIRS 170037]). An example is an alternative model based on different interpretations of pump test results in the fractured volcanic units.

Acceptance Criterion 5: Model Abstraction Output Is Supported by Objective Comparisons

> Subcriterion (1): The models implemented in this total system performance assessment abstraction provide results consistent with output from detailed process-level models and/or empirical observations (laboratory and field testings and/or natural analogs);

Results of TSPA-LA abstraction modeling are compared with results of detailed process-level models in Section 7. Graphical representations of these comparisons between the results of the SZ transport abstraction model and the SZ site-scale transport model, and between the results of the SZ 1-D transport model and the SZ site-scale transport model, are shown in Figures 7-1, 7-2, 7-4, and 7-5. These figures show consistent results between the abstraction models and detailed process-level models.

> Subcriterion (2): Outputs of flow paths in the saturated zone abstractions reasonably produce or bound the results of corresponding process-level models, empirical observations, or both;

Model outputs, in the form of breakthrough curves, are presented in Section 6.6. In Section 7, results are compared with those of process models. The analysis abstracting the flow-path lengths from the SZ site-scale transport model, for use in the SZ 1-D transport model, is described in Section 6.5.1.2.

> Subcriterion (3): Well-documented procedures that have been accepted by the scientific community to construct and test the mathematical and numerical models are used to simulate flow paths in the saturated zone; and

Section 7.2 documents the procedures that were followed in the testing and validation of the abstraction models developed in this model report. Approved QA procedures identified in the TWP (BSC 2005 [DIRS 173859], Section 4) have been used to conduct and document the activities described in this model report. Section 7.2 documents the procedures accepted by the scientific community that were followed in the testing and validation of the abstraction models developed in this model report.

> Subcriterion (4): Sensitivity analyses or bounding analyses are provided to support the abstraction of flow paths in the saturated zone, that cover ranges consistent with site data, field or laboratory experiments and tests, and natural analog research.

Bounding analyses consistent with Yucca Mountain field and laboratory data were conducted to support the TSPA abstraction of flow paths in the saturated zone. These analyses considered uncertainties in the parameter that characterizes horizontal anisotropy. In addition, analyses were completed to bound the effects of uncertainty in the geometry of the alluvial uncertainty zone (Section 6.5.1.2) and the flow paths represented therein.

Acceptance Criteria from Section 2.2.1.3.9, Radionuclide Transport in the Saturated Zone

Acceptance Criterion 1: System Description and Model Integration Are Adequate

> Subcriterion (1): Total system performance assessment adequately incorporates important design features, physical phenomena, and couplings, and uses consistent and appropriate assumptions, throughout the radionuclide transport in the saturated zone abstraction process;

Important physical phenomena and couplings are incorporated into the SZ flow and transport model abstraction through application of the best relevant, qualified data from the Yucca Mountain site and region (Sections 4.1.1 and 4.1.2). Consistent and appropriate assumptions noted in Sections 5 and 6.3 are used throughout this abstraction report and other abstractions, model reports, and analysis reports related to radionuclide transport in the SZ.

> Subcriterion (2): The description of the aspects of hydrology, geology, geochemistry, design features, physical phenomena, and couplings that may affect radionuclide transport in the saturated zone, is adequate. For example, the description includes changes into transport properties in the saturated zone, from water-rock interaction. Conditions and assumptions in the abstraction of radionuclide transport in the saturated zone are readily identified, and consistent with the body of data presented in the description;

The abstraction in Section 6.3 of this report adequately describes the physical phenomena for the base-case conceptual model because it includes the aspects of hydrology, geology, geochemistry, physical phenomena, and couplings that may affect radionuclide transport in the saturated zone through reference to supporting analysis and model reports in Table 4-1, discussion of incorporated features, events, and processes in Table 6-1, and detailed discussions of important model considerations and inputs in Sections 6.3 and 6.5.2. Additional and more detailed descriptions of these aspects of the system are provided in supporting documents, particularly, *Site-Scale Saturated Zone Flow Model* (BSC 2004 [DIRS 170037]) and BSC 2004 [DIRS 170036]. Conditions and assumptions in the abstraction of radionuclide transport in the saturated zone are readily identified in Sections 5, 6.3, and 6.5, and they are consistent with the body of data presented in the descriptions (Sections 4.1, 6.2, 6.3, and 6.5).

> Subcriterion (3): The abstraction of radionuclide transport in the saturated zone uses assumptions, technical bases, data, and models that are appropriate and consistent with other, related U.S. Department of Energy abstractions. For example, assumptions used for radionuclide transport in the saturated zone are consistent with the total system performance assessment abstractions of radionuclide release rates and solubility limits, and flow paths in the saturated zone (Sections 2.2.1.3.4 and 2.2.1.3.8 of the Yucca Mountain Review Plan, respectively). The descriptions and technical bases provide transparent and traceable support for the abstraction of radionuclide transport in the saturated zone;

Assumptions, described in Section 5, are consistent with those used in other model and analysis reports. For example, two of the six assumptions are carried forward directly from the *Saturated Zone Colloid Transport* scientific analysis report (BSC 2003 [DIRS 170006], Section 6.3). Section 6.3.3 addresses the issue of consistency with interfacing UZ and biosphere models. Technical bases, data, models, and local modeling assumptions are described in Section 6.3. Transparent and traceable support for the abstraction of radionuclide transport in the SZ is provided for the SZ transport abstraction and the SZ 1-D transport model. For example, estimates of the variation in groundwater-specific discharge and flow-path lengths in the SZ 1-D transport model are explained and illustrated in Section 6.5.1.2.

> Subcriterion (4): Boundary and initial conditions used in the abstraction of radionuclide transport in the saturated zone are propagated throughout its abstraction approaches. For example, the conditions and assumptions used to

> generate transport parameter values are consistent with other geological, hydrological, and geochemical conditions in the total system performance assessment abstraction of the saturated zone;

Section 6.5 discusses boundary and initial conditions used in transport modeling. The groundwater flow boundary conditions for the SZ site-scale flow model, the SZ site-scale transport model, and the SZ transport abstraction model are specified head at the lateral boundaries and specified groundwater flux for recharge at the upper boundary. These boundary conditions are described in detail in *Site-Scale Saturated Zone Flow Model* (BSC 2004 [DIRS 170037], Section 6.3.2).

> Subcriterion (5): Sufficient data and technical bases for the inclusion of features, events, and processes related to radionuclide transport in the saturated zone in the total system performance assessment abstraction are provided; and

FEPs addressed in this model report are documented in Section 6.2. Table 6-1 summarizes those SZ FEPs for which the technical bases are provided in this report, and includes the location within this report of the technical information.

> Subcriterion (6): Guidance in NUREG–1297 [DIRS 103597] and NUREG–1298 (Altman et al. 1988 [DIRS 103750]), or other acceptable approaches for peer review and data qualification is followed.

This report was developed in accordance with the QARD (DOE 2004 [DIRS 171539]), which commits to NUREGs 1297 [DIRS 103597] and 1298 [DIRS 103750]. Moreover, compliance with the DOE procedures, which are designed to ensure compliance with the QARD, is verified by audits by QA and other oversight activities. Accordingly, the guidance in NUREGs 1297 [DIRS 103597] and 1298 [DIRS 103750] has been followed as appropriate.

Acceptance Criterion 2: Data Are Sufficient for Model Justification

> Subcriterion (1): Geological, hydrological, and geochemical values used in the license application are adequately justified (e.g., flow path lengths, sorption coefficients, retardation factors, colloid concentrations, etc.). Adequate descriptions of how the data were used, interpreted, and appropriately synthesized into the parameters are provided;

Section 6.5.2 of this report provides adequate and thorough explanations of the use of geological, hydrological, and geochemical values in evaluating flow, sorption, and colloid retardation. Section 6.5.2 also documents the interpretation of data, and the development of parameter values and uncertainty distributions.

> Subcriterion (2): Sufficient data have been collected on the characteristics of the natural system to establish initial and boundary conditions for the total system performance assessment abstraction of radionuclide transport in the saturated zone;

The boundary conditions and interfaces between radionuclide transport in the SZ and the UZ and the biosphere are described in Section 6.3.3. An analysis of background gross alpha concentrations in groundwater, which represent the initial conditions of the system with regard to groundwater protection standards, is presented in Section 6.8.

Acceptance Criterion 3: Data Uncertainty Is Characterized and Propagated Through the Model Abstraction

> Subcriterion (1): Models use parameter values, assumed ranges, probability distributions, and bounding assumptions that are technically defensible, reasonably account for uncertainties and variabilities, and do not result in an under-representation of the risk estimate;

The development of parameter values, bounding values, and probability distributions is described in Section 6.5.2. The development was conducted in a technically defensible manner that reasonably accounts for uncertainty and variability. Two bounding assumptions are also described in Section 5. Table 6-8 shows probability distributions associated with the parameters, and Section 6.5.2 explains the sources of uncertainties in the parameters. The probabilistic analysis of uncertainty is implemented through Monte Carlo realizations of the SZ flow and transport system, in a manner consistent with the TSPA-LA simulations (Section 6.3).

> Subcriterion (4): Parameter values for processes, such as matrix diffusion, dispersion, and ground water mixing, are based on reasonable assumptions about climate, aquifer properties, and ground water volumetric fluxes (Section 2.2.1.3.8 of the Yucca Mountain Review Plan);

The conceptual model descriptions of processes such as advection, dispersion, and matrix diffusion are found in Section 6.3. Section 6.5.2 includes detailed explanations of the development of parameters used in these SZ flow processes, including discussions on the assumptions (e.g., climate changes, aquifer properties, and colloid transport properties) and bases upon which the parameter values are developed.

> Subcriterion (5): Uncertainty is adequately represented in parameter development for conceptual models, process-level models, and alternative conceptual models considered in developing the abstraction of radionuclide transport in the saturated zone. This may be done either through sensitivity analyses or use of conservative limits;

Uncertainty in parameter values is adequately represented in Sections 6.3 and 6.4 of this report, in the context of conceptual models and alternative conceptual models. Parameter uncertainty at the process and abstraction level is discussed in detail in Sections 6.5.1 and 6.5.2. A probabilistic analysis of uncertainty in key model parameters is implemented through Monte Carlo realizations of the SZ flow and transport system, in a manner consistent with the TSPA-LA simulations.

> Subcriterion (6): Where sufficient data do not exist, the definition of parameter values and conceptual models is based on appropriate use of other sources, such as expert elicitation conducted in accordance with NUREG–1563 (Kotra, et al., 1996). If other approaches are used, the U.S. Department of Energy adequately justifies their use.

Expert elicitation was used in the determination of dispersivity in the SZ. The expert elicitation process was conducted in accordance with DOE procedures that conform to NUREG-1563 (Kotra, et al., 1996) [DIRS 100909], and use of these results in quantifying uncertainty in dispersivity is described, with references, in Section 6.5.2.9.

Acceptance Criterion 4: Model Uncertainty Is Characterized and Propagated Through the Model Abstraction

> Subcriterion (1): Alternative modeling approaches of features, events, and processes are considered, and are consistent with available data and current scientific understanding, and the results and limitations are appropriately considered in the abstraction;

The process of minimal matrix diffusion and the feature of horizontal anisotropy in permeability are considered in alternative conceptual models, as described in Section 6.4 and Table 6-4. The models are shown to be consistent with available Data and current scientific knowledge and are considered appropriately in the abstraction through the ranges of parameter uncertainties in the base-case model.

> Subcriterion (2): Conceptual model uncertainties are adequately defined and documented, and effects on conclusions regarding performance are properly assessed;

Conceptual model uncertainties are adequately defined and documented in Sections 6.3 and 6.5 of this report. The effects of the uncertainties on conclusions regarding performance of the conceptual model are discussed and shown in curves presented in Section 6.6 figures.

> Subcriterion (3): Consideration of conceptual model uncertainty is consistent with available site characterization data, laboratory experiments, field measurements, natural analog information and process-level modeling studies; and the treatment of conceptual model uncertainty does not result in an under-representation of the risk estimate; and

The parameters and parameter uncertainty from external sources used directly in the modeling documented in this report are shown in Table 4-3. Spatial variability in rock properties is encompassed within uncertainty distributions for key parameters (Tables 6-1 and 6-8). The uncertainty distributions incorporate uncertainties associated with Yucca Mountain field or laboratory data, knowledge of how the parameter will be used in the model, and theoretical considerations (Section 6.5.2). The probabilistic analysis of uncertainty is implemented through Monte Carlo realizations of the SZ flow and transport system, in a manner consistent with the TSPA-LA simulations (Section 6.3). Variability in the results of multiple radionuclide breakthrough curves reflects the uncertainty in groundwater flow and radionuclide transport behavior in the SZ (Section 6.6). These results are intended for direct incorporation into the TSPA-LA model (Section 8.2.2), and as such, do not contribute to an under-representation of the risk estimate as determined in the TSPA-LA.

> Subcriterion (4): Appropriate alternative modeling approaches are consistent with available data and current scientific knowledge, and appropriately consider their

> results and limitations, using tests and analyses that are sensitive to the processes modeled. For example, for radionuclide transport through fractures, the U.S. Department of Energy adequately considers alternative modeling approaches to develop its understanding of fracture distributions and ranges of fracture flow and transport properties in the saturated zone.

Alternative model approaches discussed in Section 6.4 are consistent with alternative interpretations of available data. Alternative conceptual models are also listed in Table 6-4, which includes key assumptions and bases for screening decisions. Alternative modeling approaches of fracture distributions and ranges of fracture flow and transport properties in the SZ are incorporated in upstream model reports. The conclusion of sensitivity analyses with regard to matrix diffusion in fractured media is that the alternative model of essentially no matrix diffusion is incorporated in the range of parameter uncertainties in the SZ transport abstraction model, as described in Section 6.4.

Acceptance Criterion 5: Model Abstraction Output Is Supported by Objective Comparisons

> Subcriterion (1): The models implemented in this total system performance assessment abstraction provide results consistent with output from detailed process-level models and/or empirical observations (laboratory and field testings and/or natural analogs);

Results of TSPA-LA abstraction modeling are compared with results of detailed process-level models in Section 7. Graphical representations of these comparisons between the results of the SZ transport abstraction model and the SZ site-scale transport model, and between the results of the SZ 1-D transport model and the SZ site-scale transport model, are shown in Figures 7-1, 7-2, 7-4, and 7-5. These figures show consistent results between the abstraction models and detailed process-level models.

> Subcriterion (2): Outputs of radionuclide transport in the saturated zone abstractions reasonably produce or bound the results of corresponding process-level models, empirical observations, or both. The U.S. Department of Energy-abstracted models for radionuclide transport in the saturated zone are based on the same hydrological, geological, and geochemical assumptions and approximations shown to be appropriate for closely analogous natural systems or laboratory experimental systems;

Results of TSPA abstraction modeling are compared with results of detailed process-level models in Section 7. Graphical representations of these comparisons between the results of the SZ transport abstraction model and the SZ site-scale transport model, and between the results of the SZ 1-D transport model and the SZ site-scale transport model, are shown in Figures 7-1, 7-2, 7-4, and 7-5. These figures show consistent results between the abstraction models and detailed process-level models.

> Subcriterion (3): Well-documented procedures that have been accepted by the scientific community to construct and test the mathematical and numerical models are used to simulate radionuclide transport through the saturated zone; and

Section 7.2 documents the procedures accepted by the scientific community that were followed in the testing and validation of the abstraction models developed in this model report. Approved QA procedures identified in the TWP (BSC 2005 [DIRS 173859], Section 4) have been used to conduct and document the activities described in this model report. Section 7.2 documents the procedures that were followed in the testing and validation of the abstraction models developed in this report.

> Subcriterion (4): Sensitivity analyses or bounding analyses are provided to support the total system performance assessment abstraction of radionuclide transport in the saturated zone, that cover ranges consistent with site data, field or laboratory experiments and tests, and natural analog research).

Sensitivity analyses consistent with Yucca Mountain field and laboratory data were conducted to support the TSPA abstraction of radionuclide transport in the saturated zone. In particular, a sensitivity analysis of matrix diffusion in the SZ transport abstraction model is presented in the assessment of alternative conceptual models in Section 6.4. This analysis used the SZ transport abstraction model to show that the minimal matrix diffusion alternate model is included within the range of parameter uncertainties considered. Sensitivity analyses have also been performed on previous SZ transport modeling results (Arnold et al. 2003 [DIRS 163857]) (Section 6.7).

INTENTIONALLY LEFT BLANK

9. INPUTS AND REFERENCES

The following is a list of the references cited in this document. Column 2 represents the unique six digit numerical identifier (the Document Input Reference System number), which is placed in the text following the reference callout (e.g., BSC 2004 [DIRS 170014]). The purpose of these numbers is to assist in locating a specific reference. Within the reference list, multiple sources by the same author (e.g., BSC 2004) are sorted alphabetically by title.

9.1 DOCUMENTS CITED

Altman, W.D.; Donnelly, J.P.; and Kennedy, J.E. 1988. *Qualification of Existing Data for High-Level Nuclear Waste Repositories: Generic Technical Position.* NUREG-1298. Washington, D.C.: U.S. Nuclear Regulatory Commission. TIC: 200652. 103750

Altman, W.D.; Donnelly, J.P.; and Kennedy, J.E. 1988. *Peer Review for High-Level Nuclear Waste Repositories: Generic Technical Position.* NUREG-1297. Washington, D.C.: U.S. Nuclear Regulatory Commission. TIC: 200651. 103597

Arnold, B.W.; Kuzio, S.P.; and Robinson, B.A. 2003. "Radionuclide Transport Simulation and Uncertainty Analyses with the Saturated-Zone Site-Scale Model at Yucca Mountain, Nevada." *Journal of Contaminant Hydrology, 62-63,* 401-419. New York, New York: Elsevier. TIC: 254205. 163857

Bear, J. 1972. *Dynamics of Fluids in Porous Media.* Environmental Science Series. Biswas, A.K., ed. New York, New York: Elsevier. TIC: 217356. 156269

Bedinger, M.S.; Sargent, K.A.; Langer, W.H.; Sherman, F.B.; Reed, J.E.; and Brady, B.T. 1989. *Studies of Geology and Hydrology in the Basin and Range Province, Southwestern United States, for Isolation of High-Level Radioactive Waste—Basis of Characterization and Evalu*ation. U.S. Geological Survey Professional Paper 1370-A. Washington, D.C.: U.S. Government Printing Office. ACC: NNA.19910524.0125. 129676

Bower, K.M.; Gable, C.W.; and Zyvoloski, G.A. 2000. *Effect of Grid Resolution on Control Volume Finite Element Groundwater Modeling of Realistic Geology.* LA-UR-001870. Los Alamos, New Mexico: Los Alamos National Laboratory. TIC: 248256. 149161

BSC (Bechtel SAIC Company) 2001. *Data Qualification Report: Calculated Porosity and Porosity-Derived Values for Lithostratigraphic Units for Use on the Yucca Mountain Project*. TDR-NBS-GS-000020 REV 00. Las Vegas, Nevada: Bechtel SAIC Company. ACC: MOL.20010531.0193. 163479

BSC 2001. *Data Qualification Report: Matrix Hydrologic Properties and Alcove 1 Infiltration Rate Data for Use on the Yucca Mountain Project*. TDR-NBS-HS-000014 REV 00. Las Vegas, Nevada: Bechtel SAIC Company. ACC: MOL.20010924.0268. 163566

BSC 2002. *Guidelines for Developing and Documenting Alternative Conceptual Models, Model Abstractions, and Parameter Uncertainty in the Total System Performance Assessment for the License Application*. TDR-WIS-PA-000008 REV 00, ICN 01. Las Vegas, Nevada: Bechtel SAIC Company. ACC: MOL.20020904.0002. 158794

BSC 2002. *Validation Test Report, GoldSim Version 7.50.100.* SDN: 10344-VTR-7.50.100-00. Las Vegas, Nevada: BSC (Bechtel SAIC Company). ACC: MOL.20030312.0227. 163962

BSC 2003. *SZ Flow and Transport Model Abstraction.* MDL-NBS-HS-000021 REV 00. Las Vegas, Nevada: Bechtel SAIC Company. ACC: DOC.20030818.0007. 164870

BSC 2003. *Technical Work Plan for: Saturated Zone Flow and Transport Modeling and Testing.* TWP-NBS-MD-000002 REV 01 ICN 01. Las Vegas, Nevada: Bechtel SAIC Company. ACC: DOC.20031203.0002. 166034

BSC 2003. *Validation Test Report, SZ_Convolute Version 2.2.* SDN: 10207-VTR-2.2-00. Las Vegas, Nevada: Bechtel SAIC Company. ACC: MOL.20021202.0341. 163587

BSC 2004. *Analysis of Hydrologic Properties Data.* ANL-NBS-HS-000042, Rev. 00. Las Vegas, Nevada: Bechtel SAIC Company. 170038

BSC (Bechtel SAIC Company) 2004. *D&E/RIT IED Subsurface Facilities [Sheet 1 of 4]. 800-IED-WIS0-00101-000-00B*. Las Vegas, Nevada: Bechtel SAIC Company. ACC: ENG.20041130.0002. 172801

BSC (Bechtel SAIC Company) 2004. *Future Climate Analysis*. ANL-NBS-GS-000008 REV 01. Las Vegas, Nevada: Bechtel SAIC Company. ACC: DOC.20040908.0005. 170002

BSC 2004. *Hydrogeologic Framework Model for the Saturated Zone Site Scale Flow and Transport Model*. MDL-NBS-HS-000024, Rev. 00. Las Vegas, Nevada: Bechtel SAIC Company. 170008

BSC 2004. *Probability Distribution for Flowing Interval Spacing.* ANL-NBS-MD-000003, Rev. 01. Las Vegas, Nevada: Bechtel SAIC Company. 170014

BSC 2004. *Recharge and Lateral Groundwater Flow Boundary Conditions for the Saturated Zone Site-Scale Flow and Transport Model*. ANL-NBS-MD-000010 REV 01. Las Vegas, Nevada: Bechtel SAIC Company. ACC: DOC.20041008.0004. 170015

BSC 2004. *Rock Properties Model.* MDL-NBS-GS-000004, Rev. 01. Las Vegas, Nevada: Bechtel SAIC Company. ACC: DOC.20040915.0011; DOC.20050214.0003. 170032

BSC 2004. *Saturated Zone Colloid Transport.* ANL-NBS-HS-000031, Rev. 02. Las Vegas, Nevada: Bechtel SAIC Company. ACC: DOC.20041008.0007. 170006

BSC 2004. *Saturated Zone Flow and Transport Model Abstraction*. MDL-NBS-HS-000021 REV 02. Las Vegas, Nevada: Bechtel SAIC Company. ACC: DOC.20041028.0003.

BSC 2004. *Saturated Zone In-Situ Testing.* ANL-NBS-HS-000039, Rev. 01. Las Vegas, Nevada: Bechtel SAIC Company. ACC: DOC.20041115.0008. 170010

BSC 2004. *Saturated Zone Site-Scale Flow Model.* MDL-NBS-HS-000011, Rev. 02. Las Vegas, Nevada: Bechtel SAIC Company. ACC: DOC.20041122.0001. 170037

BSC 2004. *Site-Scale Saturated Zone Transport.* MDL-NBS-HS-000010, Rev. 02. Las Vegas, Nevada: Bechtel SAIC Company. ACC: DOC.20041103.0004; DOC.20050405.0008. 170036

BSC 2004. *Technical Work Plan for: Natural System - Saturated Zone Analysis and Model Report Integration.* TWP-NBS-MD-000002 REV 02 ICN 01. Las Vegas, Nevada: Bechtel SAIC Company. ACC: DOC.20040818.0004. 171421

BSC 2004. *UZ Flow Models and Submodels.* MDL-NBS-HS-000006, Rev. 02. Las Vegas, Nevada: Bechtel SAIC Company. ACC: DOC.20041101.0004; DOC.20050629.0003. 169861

BSC 2005. *Waste Form and In-Drift Colloids-Associated Radionuclide Concentrations: Abstraction and Summary*. MDL-EBS-PA-000004 REV 02. Las Vegas, Nevada: Bechtel SAIC Company. 174290

BSC 2004. *Water-Level Data Analysis for the Saturated Zone Site-Scale Flow and Transport Model.* ANL-NBS-HS-000034, Rev. 02. Las Vegas, Nevada: Bechtel SAIC Company. ACC: DOC.20041012.0002. 170009

BSC 2005. *Features, Events, and Processes in SZ Flow and Transport.* ANL-NBS-MD-000002 REV 04. Las Vegas, Nevada: Bechtel SAIC Company. TBV#7421 174190

BSC 2005. *Q-List*. 000-30R-MGR0-00500-000-001. Las Vegas, Nevada: Bechtel SAIC Company. ACC: ENG.20050217.0010. 171190

BSC 2005. *Technical Work Plan for Saturated Zone Flow and Transport Modeling.* TWP-NBS-MD-000006 REV 01. Las Vegas, Nevada: Bechtel SAIC Company. ACC: DOC.20050525.0002. 173859

BSC 2005. *Total System Performance Assessment Model/Analysis for the License Application.* MDL-WIS-PA-000004 REV 01. Las Vegas, Nevada: Bechtel SAIC Company. 174227

Buchholtz ten Brink, M.; Phinney, D.L.; and Smith, D.K. 1991. "Actinide Transport in Topopah Spring Tuff: Pore Size, Particle Size and Diffusion." *Scientific Basis for Nuclear Waste Management XIV, Symposium held November 26-29, 1990, Boston, Massachusetts*. Abrajano, T.A., Jr. and Johnson, L.H., eds. *212*, 641-648. Pittsburgh, Pennsylvania: Materials Research Society. TIC: 203656. 162954

Buesch, D.C.; Spengler, R.W.; Moyer, T.C.; and Geslin, J.K. 1996. *Proposed Stratigraphic Nomenclature and Macroscopic Identification of Lithostratigraphic Units of the Paintbrush Group Exposed at Yucca Mountain, Nevada.* Open-File Report 94-469. Denver, Colorado: U.S. Geological Survey. ACC: MOL.19970205.0061. 100106

Burbey, T.J. and Wheatcraft, S.W. 1986. *Tritium and Chlorine-36 Migration from a Nuclear Explosion Cavity.* DOE/NV/10384-09. Reno, Nevada: University of Nevada, Desert Research Institute, Water Resources Center. TIC: 201927. 129679

Callahan, T.J.; Reimus, P.W.; Bowman, R.S.; and Haga, M.J. 2000. "Using Multiple Experimental Methods to Determine Fracture/Matrix Interactions and Dispersion of Nonreactive Solutes in Saturated Volcanic Tuff. "*Water Resources Research, 36,* (12), 3547-3558. Washington, D.C.: American Geophysical Union. TIC: 250760. 156648

Canori, G.F. and Leitner, M.M. 2003. *Project Requirements Document.* TER-MGR-MD-000001 REV 02. Las Vegas, Nevada: Bechtel SAIC Company. ACC: DOC.20031222.0006. 166275

Cooper, H.H., Jr. and Jacob, C.E. 1946. "A Generalized Graphical Method for Evaluating Formation Constants and Summarizing Well-Field History." *Transactions, American Geophysical Union, 27,* (IV), 526-534. Washington, D.C.: American Geophysical Union. TIC: 225279. 150245

CRWMS (Civilian Radioactive Waste Management System) M&O (Management & Operating Contractor) 1997. *Report of Results of Hydraulic and Tracer Tests at the C-Holes Complex.* Deliverable SP23APM3. Las Vegas, Nevada: CRWMS M&O. ACC: MOL.19971024.0074. 100328

CRWMS M&O 1997. *The Site-Scale Unsaturated Zone Transport Model of Yucca Mountain.* Milestone SP25BM3, Rev. 1. Las Vegas, Nevada: CRWMS M&O. ACC: MOL.19980224.0314. 124052

CRWMS M&O 1998. "Saturated Zone Flow and Transport." Chapter 8 of *Total System Performance Assessment-Viability Assessment (TSPA-VA) Analyses Technical Basis Document.* B00000000-01717-4301-00008 REV 01. Las Vegas, Nevada: CRWMS M&O. ACC: MOL.19981008.0008. 100365

CRWMS M&O 1998. *Saturated Zone Flow and Transport Expert Elicitation Project.* Deliverable SL5X4AM3. Las Vegas, Nevada: CRWMS M&O. ACC: MOL.19980825.0008. 100353

CRWMS M&O 1998. *Supplier Evaluation Report for Teledyne Environmental, Inc., June 19, 1998, Radiological Analysis of Air, Filter, Soil, Vegetation, Andimal, and Water Samples*. Las Vegas, Nevada: CRWMS M&O. ACC: MOL.19980807.0251. 174521

CRWMS M&O 1998. *Yucca Mountain Site Characterization Project Radiological Programs, Radioactivity in FY 1997 Groundwater Samples from Wells and Springs Near Yucca Mountain.* Rev. 00. Las Vegas, Nevada: CRWMS M&O. ACC: MOL.19990218.0213. 104963

CRWMS M&O 1999. *Radioactivity in FY 1998 Groundwater Samples from Wells and Springs Near Yucca Mountain.* BA0000000-01717-5705-00029 REV 00. Las Vegas, Nevada: CRWMS M&O. ACC: MOL.19990622.0219. 150420

CRWMS M&O 2000. *Modeling Sub Gridblock Scale Dispersion in Three-Dimensional Heterogeneous Fractured Media (S0015).* ANL-NBS-HS-000022 REV 00 ICN 01. Las Vegas, Nevada: CRWMS M&O. ACC: MOL.20001107.0376. 152259

CRWMS M&O 2000. *Total System Performance Assessment for the Site Recommendation.* TDR-WIS-PA-000001 REV 00 ICN 01. Las Vegas, Nevada: CRWMS M&O. ACC: MOL.20001220.0045. 153246

CRWMS M&O 2000. *Uncertainty Distribution for Stochastic Parameters.* ANL-NBS-MD-000011 REV 00. Las Vegas, Nevada: CRWMS M&O. ACC: MOL.20000526.0328. 147972

CRWMS M&O 2000. *Unsaturated Zone and Saturated Zone Transport Properties (U0100).* ANL-NBS-HS-000019 REV 00. Las Vegas, Nevada: CRWMS M&O. ACC: MOL.20000829.0006. 152773

D'Agnese, F.A.; O'Brien, G.M.; Faunt, C.C.; and San Juan, C.A. 1999. *Simulated Effects of Climate Change on the Death Valley Regional Ground-Water Flow System, Nevada and California.* Water-Resources Investigations Report 98-4041. Denver, Colorado: U.S. Geological Survey. TIC: 243555. 120425

DOE (U.S. Department of Energy) 1997. *Regional Groundwater Flow and Tritium Transport Modeling and Risk Assessment of the Underground Test Area, Nevada Test Site, Nevada.* DOE/NV-477. Las Vegas, Nevada: U.S. Department of Energy. ACC: MOL.20010731.0303. 103021

DOE 2003. *Design Document for: SZ_CONVOLUTE Version 3.0.* 10207-DD-3.0-00. Las Vegas, Nevada: U.S. Department of Energy, Office of Repository Development. ACC: MOL.20030717.0479. 167588

DOE 2004. *Quality Assurance Requirements and Description.* DOE/RW-0333P, Rev. 16. Washington, D.C.: U.S. Department of Energy, Office of Civilian Radioactive Waste Management. ACC: DOC.20040907.0002. Replacement for 171386. 171539

Domenico, P.A. and Schwartz, F.W. 1990. *Physical and Chemical Hydrogeology.* New York, New York: John Wiley & Sons. TIC: 234782. 100569

EDCON. 2000. *Report for the Borehole Gravity Survey in the NC-EWDP-19D Well in Nye County, Nevada on Behalf of TRW Corp.* EDCON Job# 00011. Denver, Colorado: EDCON. TIC: 249823. 154704

Eddebbarh, A.A.; Zyvoloski, G.A.; Robinson, B.A.; Kwicklis, E.M.; Reimus, P.W.; Arnold, B.W.; Corbet, T.; Kuzio, S.P.; and Faunt, C. 2003. "The Saturated Zone at Yucca Mountain: An Overview of the Characterization and Assessment of the Saturated Zone as a Barrier to Potential Radionuclide Migration." *Journal of Contaminant Hydrology, 62-63,* 477-493. New York, New York: Elsevier. TIC: 254205. 163577

Ferrill, D.A.; Winterle, J.; Wittmeyer, G.; Sims, D.; Colton, S.; Armstrong, A.; and Morris, A.P. 1999. "Stressed Rock Strains Groundwater at Yucca Mountain, Nevada." *GSA Today, 9,* (5), 1-8. Boulder, Colorado: Geological Society of America. TIC: 246229. 118941

Flint, L.E. 1998. *Characterization of Hydrogeologic Units Using Matrix Properties, Yucca Mountain, Nevada.* Water-Resources Investigations Report 97-4243. Denver, Colorado: U.S. Geological Survey. ACC: MOL.19980429.0512. 100033

Freeze, R.A. and Cherry, J.A. 1979. *Groundwater.* Englewood Cliffs, New Jersey: Prentice-Hall. TIC: 217571. 101173

Gelhar, L.W. 1986. "Stochastic Subsurface Hydrology from Theory to Applications." *Water Resources Research, 22,* (9), 135S-145S. Washington, D.C.: American Geophysical Union. TIC: 240749. 101131

Gilbert, R.O. 1987. *Statistical Methods for Environmental Pollution Monitoring*. Van Nostrand Reinhold, New York. TIC: 252619. 163705

Hillel, D. 1980. *Fundamentals of Soil Physics.* New York, New York: Academic Press. TIC: 215655. 101134

Howard, N.W. 1985. *Variation in Properties of Nuclear Test Areas and Media at the Nevada Test Site.* UCRL-53721. Livermore, California: Lawrence Livermore National Laboratory. TIC: 229690. 153266

Jury, W.A.; Sposito, G.; and White, R.E. 1986. "A Transfer Function Model of Solute Transport Through Soil. 1. Fundamental Concepts." *Water Resources Research, 22,* (2), 243-247. Washington, D.C.: American Geophysical Union. TIC: 254552. 164314

Knoll, G.F. 1989. *Radiation Detection and Measurement.* 2nd Edition. New York, New York: John Wiley & Sons. TIC: 233703. 161052

Kotra, J.P.; Lee, M.P.; Eisenberg, N.A.; and DeWispelare, A.R. 1996. *Branch Technical Position on the Use of Expert Elicitation in the High-Level Radioactive Waste Program.* NUREG-1563. Washington, D.C.: U.S. Nuclear Regulatory Commission. TIC: 226832. 100909

Kreft, A. and Zuber, A. 1978. "On the Physical Meaning of the Dispersion Equation and Its Solutions for Different Initial and Boundary Conditions." *Chemical Engineering Science, 33,* (11), 1471-1480. New York, New York: Pergamon Press. TIC: 245365. 107306

Li, Y-H. and Gregory, S. 1974. "Diffusion of Ions in Sea Water and Deep-Sea Sediments." *Geochimica et Cosmochimica Acta, 38,* (5), 703-714. New York, New York: Pergamon Press. TIC: 246823. 129827

Luckey, R.R.; Tucci, P.; Faunt, C.C.; Ervin, E.M.; Steinkampf, W.C.; D'Agnese, F.A.; and Patterson, G.L. 1996. *Status of Understanding of the Saturated-Zone Ground-Water Flow System at Yucca Mountain, Nevada, as of 1995.* Water-Resources Investigations Report 96-4077. Denver, Colorado: U.S. Geological Survey. ACC: MOL.19970513.0209. 100465

Manger, G.E. 1963. *Porosity and Bulk Density of Sedimentary Rocks.* Geological Survey Bulletin 1144-E. Washington, D.C.: U.S. Government Printing Office. TIC: 249699. 154474

McKenna, S.A.; Walker, D.D.; and Arnold, B. 2003. *"Modeling Dispersion in Three-Dimensional Heterogeneous Fractured Media at Yucca Mountain*." Journal of Contaminant Hydrology, 62-63, 577-594. New York, New York: Elsevier. TIC: 254205. 163578

Miller, I. and Kossik, R. 1998. *Repository Integration Program RIP Integrated Probabilistic Simulator for Environmental Systems Theory Manual and User's Guide.* Redmond, Washington: Golder Associates. ACC: MOL.19980526.0374. 100449

Moyer, T.C. and Geslin, J.K. 1995. *Lithostratigraphy of the Calico Hills Formation and Prow Pass Tuff (Crater Flat Group) at Yucca Mountain, Nevada.* Open-File Report 94-460. Denver, Colorado: U.S. Geological Survey. ACC: MOL.19941208.0003. 101269

Newman, J. 1973. *Electrochemical Systems.* Englewood Cliffs, New Jersey: Prentice-Hall. TIC: 210201. 148719

NRC (U.S. Nuclear Regulatory Commission) 2003. *Yucca Mountain Review Plan, Final Report.* NUREG-1804, Rev. 2. Washington, D.C.: U.S. Nuclear Regulatory Commission, Office of Nuclear Material Safety and Safeguards. TIC: 254568. 163274

Reimus, P.W.; Haga, M.J.; Adams, A.I.; Callahan, T.J.; Turin, H.J.; and Counce, D.A. 2003. "Testing and Parameterizing a Conceptual Solute Transport Model in Saturated Fractured Tuff Using Sorbing and Nonsorbing Tracers in Cross-Hole Tracer Tests." *Journal of Contaminant Hydrology, 62-63,* 613-636. New York, New York: Elsevier. TIC: 254205. 162950

Reimus, P.W.; Haga, M.J.; Humphrey, A.R.; Counce, D.A.; Callahan, T.J.; and Ware, S.D. 2002. *Diffusion Cell and Fracture Transport Experiments to Support Interpretations of the BULLION Forced-Gradient Experiment.* LA-UR-02-6884. Los Alamos, New Mexico: Los Alamos National Laboratory. TIC: 253859. 162956

Reimus, P.W.; Ware, S.D.; Benedict, F.C.; Warren, R.G.; Humphrey, A.; Adams, A.; Wilson, B.; and Gonzales, D. 2002. *Diffusive and Advective Transport of ^{3}H, ^{14}C, and ^{99}Tc in Saturated, Fractured Volcanic Rocks from Pahute Mesa, Nevada.* LA-13891-MS. Los Alamos, New Mexico: Los Alamos National Laboratory. TIC: 253905. 163008

Rundberg, R.S.; Partom, I.; Ott, M.A.; Mitchell, A.J.; and Birdsell, K. 1987. *Diffusion of Nonsorbing Tracers in Yucca Mountain Tuff.* Milestone R524. Los Alamos, New Mexico: Los Alamos National Laboratory. ACC: NNA.19930405.0074. 106481

Simpson, J.H and Carr, H.Y. 1958. "Diffusion and Nuclear Spin Relaxation in Water. "*The Physical Review, Second Series, 111,* (5), 1201-1202. New York, New York: American Physical Society. TIC: 246907. 139449

Skagius, K. and Neretnieks, I. 1986. "Porosities and Diffusivities of Some Nonsorbing Species in Crystalline Rocks. "*Water Resources Research, 22,* (3), 389-398. Washington, D.C.: American Geophysical Union. TIC: 225291. 156862

Sudicky, E.A. and Frind, E.O. 1982. "Contaminant Transport in Fractured Porous Media: Analytical Solutions for a System of Parallel Fractures. "*Water Resources Research, 18,* (6), 1634-1642. Washington, D.C.: American Geophysical Union. TIC: 217475. 105043

Townsend, Y.E. and Grossman, R.F., eds. 2001. *Nevada Test Site Annual Site Environmental Report for Calendar Year 2000.* DOE/NV/11718-605. Las Vegas, Nevada: U.S. Department of Energy, Nevada Operations Office. TIC: 251545. 156604

Townsend, Y.E. and Grossman, R.F., eds. 2002. *Nevada Test Site Annual Site Environmental Report for Calendar Year 2001.* DOE/NV/11718-747. Las Vegas, Nevada: U.S. Department of Energy, Nevada Operations Office. ACC: MOL.20050728.0313. 173960

Townsend, Y.E. and Grossman, R.F., eds. 2003. *Nevada Test Site Annual Site Environmental Report for Calendar Year 2002.* DOE/NV/11718-842. Las Vegas, Nevada: U.S. Department of Energy, Nevada Operations Office. ACC: MOL.20040413.0146. 168841

Triay, I.R.; Birdsell, K.H.; Mitchell, A.J.; and Ott, M.A. 1993. "Diffusion of Sorbing and Non-Sorbing Radionuclides. "*High Level Radioactive Waste Management, Proceedings of the Fourth Annual International Conference, Las Vegas, Nevada, April 26-30, 1993. 2,* 1527-1532. La Grange Park, Illinois: American Nuclear Society. TIC: 208542. 145123

USGS 2001. *Water-Level Data Analysis for the Saturated Zone Site-Scale Flow and Transport Model.* ANL-NBS-HS-000034 REV 01. Denver, Colorado: U.S. Geological Survey. ACC: MOL.20020209.0058. 157611

USGS n.d. Bulk Density. Denver, Colorado: U.S. Geological Survey. ACC: NNA.19940406.0076. 154495

Watson, J.E.1980. *Upgrading Environmental Radiation Data*. Health Physics Society Committee Report HPSR-1, EPA 520/1-80-012. Washington, D.C.: U.S. Environmental Protection Agency. TIC: 228385 173955

Wills, C.A., senior author. 2004. *Nevada Test Site Environmental Report 2003*. DOE/NV/11718-971. Las Vegas, Nevada: U.S. Department of Energy, Nevada Operations Office. ACC: MOL.20050728.0314. 173956

Wilson, M.L.; Gauthier, J.H.; Barnard, R.W.; Barr, G.E.; Dockery, H.A.; Dunn, E.; Eaton, R.R.; Guerin, D.C.; Lu, N.; Martinez, M.J.; Nilson, R.; Rautman, C.A.; Robey, T.H.; Ross, B.; Ryder, E.E.; Schenker, A.R.; Shannon, S.A.; Skinner, L.H.; Halsey, W.G.; Gansemer, J.D.; Lewis, L.C.; Lamont, A.D.; Triay, I.R.; Meijer, A.; and Morris, D.E. 1994. *Total-System Performance Assessment for Yucca Mountain – SNL Second Iteration (TSPA-1993).* SAND93-2675. Executive Summary and two volumes. Albuquerque, New Mexico: Sandia National Laboratories. ACC: NNA.19940112.0123. 100191

Viswanath, D.S. and Natarajan, G. 1989. *Data Book on the Viscosity of Liquids.* 714-715. New York, New York: Hemisphere Publishing Corporation. TIC: 247513. 129867

Zyvoloski, G.; Kwicklis, E.; Eddebbarh, A.A.; Arnold, B.; Faunt, C.; and Robinson, B.A. 2003. "The Site-Scale Saturated Zone Flow Model for Yucca Mountain: Calibration of Different Conceptual Models and their Impact on Flow Paths." *Journal of Contaminant Hydrology, 62-63,* 731-750. New York, New York: Elsevier. TIC: 254340. 163341

Zyvoloski, G.A.; Robinson, B.A.; Dash, Z.V.; and Trease, L.L. 1997. *Summary of the Models and Methods for the FEHM Application—A Finite-Element Heat-and Mass-Transfer Code.* LA-13307-MS. Los Alamos, New Mexico: Los Alamos National Laboratory. TIC: 235587. 110491

9.2 CODES, STANDARDS, REGULATIONS, AND PROCEDURES

10 CFR 63. 2005 Energy: *Disposal of High-Level Radioactive Wastes in a Geologic Repository at Yucca Mountain, Nevada.* ACC: MOL.20050405.0118. 173273

AP-2.22Q, Rev. 1, ICN 1. *Classification Analyses and Maintenance of the Q-List*. Washington, D.C.: U.S. Department of Energy, Office of Civilian Radioactive Waste Management. ACC: DOC.20040714.0002.

LP-AC.1Q-BSC, Rev. 0, ICN 1. *Expert Elicitation*. Washington, D.C.: U.S. Department of Energy, Office of Civilian Radioactive Waste Management. ACC: DOC.20050418.0004.

LP-2.27Q-BSC, Rev.0, ICN 0. Q*uality Assurance Surveillance.* Department of Energy, Office of Civilian Radioactive Waste Management. ACC: DOC.20040927.0040.

LP-SIII.10Q-BSC, Rev. 0, ICN 1. *Models*. Washington, D.C.: U.S. Department of Energy, Office of Civilian Radioactive Waste Management. ACC: DOC.20050623.0001.

LP-SI.11Q-BSC, Rev. 0, ICN 1. *Software Management.* Washington, D.C.: U.S. Department of Energy, Office of Civilian Radioactive Waste Management. ACC: DOC.20041005.0008.

9.3 SOURCE DATA, LISTED BY DATA TRACKING NUMBER

GS010908312332.002. Borehole Data from Water-Level Data Analysis for the Saturated Zone Site-Scale Flow and Transport Model. Submittal date: 10/02/2001. 163555

GS030108314211.001. Interpretation of the Lithostratigraphy in Deep Boreholes NC-EWDP-18P, NC-EWDP-22SA, NC-EWDP-10SA, NC-EWDP-23P, NC-EWDP-19IM1A, and NC-EWDP-19IM2A, Nye County Early Warning Drilling Program, Phase III. Submittal date: 02/11/2003. 163483

GS031008312315.002. Transport Parameters from Analysis of Conservative (Non-Sorbing) Tracer Tests Conducted in the Fractured Tuff at the C-Hole Complex from 1996 to 1999. Submittal date: 10/09/2003. 166261

LA0002JC831341.001. Depth Intervals and Bulk Densities of Alluviums. Submittal date: 03/08/2000. 147081

LA0302RP831228.001. Type Curve Data for FEHM Macro "SPTR" Based on Sudicky and Frind Solution. Submittal date: 02/11/2003. 163557

LA0303HV831352.002. Colloid Retardation Factors for the Saturated Zone Fractured Volcanics. Submittal date: 03/31/2003. 163558

LA0303HV831352.004. Colloid Retardation Factors for the Saturated Zone Alluvium. Submittal date: 03/31/2003. 163559

LA0303PR831231.002. Estimation of Groundwater Drift Velocity from Tracer Responses in Single-Well Tracer Tests at Alluvium Testing Complex. Submittal date: 03/18/2003. 163561

LA0303PR831231.005. Simple Calculations for SZ In-Situ Testing AMR. Submittal date: 03/19/2003. 166259

LA0306SK831231.001. SZ Site-Scale Transport Model, FEHM Files for Base Case. Submittal date: 06/25/2003. 164362

LA0310AM831341.002. Saturated Zone Distribution Coefficients (Kds) for U, Np, Pu, Cs, Am, Pa, SR, Th, Ra, C, Tc, and I. Submittal date: 10/21/2003. 165891

LB0205REVUZPRP.001. Fracture Properties for UZ Model Layers Developed from Field Data. Submittal date: 05/14/2002. 159525

LB03023DSSCP9I.001. 3-D Site Scale UZ Flow Field Simulations for 9 Infiltration Scenarios. Submittal date: 02/28/2003. 163044

MO0003SZFWTEEP.000. Data Resulting from the Saturated Zone Flow and Transport Expert Elicitation Project. Submittal date: 03/06/2000. 148744

MO0010CPORGLOG.002. Calculated Porosity from Geophysical Logs Data from "Old 40" Boreholes. Submittal date: 10/16/2000. 155229

MO0105GPLOG19D.000. Geophysical Log Data from Borehole NC EWDP 19D. Submittal date: 05/31/2001. 163480

MO0105HCONEPOR.000. Hydraulic Conductivity and Effective Porosity for the Basin and Range Province, Southwestern United States. Submittal date: 05/02/2001. 155044

MO0109HYMXPROP.001. Matrix Hydrologic Properties Data. Submittal date: 09/17/2001. 155989

MO0501SEPFEPLA.001. LA FEP List. Submittal date: 07/20/2004. 172601

MO9904RWSJJS98.000. Radioanalytical Water Data for Samples Collected in June, July, and September 1998. Submittal date: 04/08/1999. 165866

SN0004T0501399.002. Correlation of RH (Relative Humidity) Porosity and Bulk Density. Submittal date: 04/13/2000. 155046

SN0004T0501399.003. Statistical Summary of Porosity Data. Submittal date: 04/13/2000. 155045

SN0302T0502203.001. Saturated Zone Anisotropy Distribution Near the C-Wells. Submittal date: 02/26/2003. 163563

SN0306T0504103.005. Revised Groundwater Colloid Mass Concentration Parameters for TSPA (Total System Performance Assessment). Submittal date: 06/30/2003. 164132

SN0306T0504103.006. Revised Sorption Partition Coefficients (Kd Values) for Selected Radionuclides Modeled in the TSPA (Total System Performance Assessment). Submittal date: 06/30/2003. 164131

SN9907T0571599.001. Probability Distribution of Flowing Interval Spacing. Submittal date: 07/15/1999. 122261

9.4 OUTPUT DATA, LISTED BY DATA TRACKING NUMBER

MO0310SPANGRAC.000. Natural Gross Alpha Concentration In Amargosa Valley Groundwater. Submittal date: 10/23/2003.

MO0506SPAINPUT.001. Input Data for the SZ 1-D Transport Model. Submittal date: 06/07/2005.

SN0306T0502103.005. SZ (SZ) 1-D Transport Model. Submittal date: 06/05/2003.

SN0306T0502103.006. Data Spreadsheets To Support Parameter Uncertainty Development. Submittal date: 06/05/2003.

SN0310T0502103.009. Revised Sz Transport Abstraction Model Uncertain Inputs. Submittal date: 10/09/2003.

SN0310T0502103.010. Revised Sz Flow And Transport Model Abstraction Inputs And Results. Submittal date: 10/09/2003.

SN0310T0502103.012. SZ Flow And Transport Model Abstraction Inputs And Results For Fast Fraction Of Irreversible Colloids. Submittal date: 10/24/2003.

SN0407T0502103.013. Re-Sampled Sz Flow And Transport Model Abstraction Inputs And Results. Submittal date: 7/13/2004.

SN0507T0502103.014. Natural Gross Alpha Concentration In Amargosa Valley Groundwater. Submittal date: 07/12/05.

9.5 SOFTWARE CODES

BSC (Bechtel SAIC Company) 2003. *Software Code: GoldSim.* V7.50.100. PC. 10344-7.50.100-00. 161572

BSC 2004. *Software Code: GoldSim.* V8.01 Service Pack 4. PC, Windows 2000. 10344-8.01SP4-00. 169695

LANL (Los Alamos National Laboratory) 2001. *Software Code: CORPSCON.* V5.11.08. 10547-5.11.08-00. 155082

LANL 2003. *Software Code: FEHM.* V2.20. SUN, PC. 10086-2.20-00. 161725

SNL (Sandia National Laboratories) 2003. *Software Code: SZ_Convolute.* V2.2. PC, Windows 2000. 10207-2.2-00. 163344

SNL 2003. *Software Code: SZ_Convolute.* V3.0. PC, Windows 2000. 10207-3.0-00. 164180

SNL 2003. *Software Code: SZ_Post.* V3.0. Sun, SunO.S. 5.7. 10915-3.0-00. 163571

SNL 2003. *Software Code: SZ_Pre.* V2.0. Sun, Solaris 7. 10914-2.0-00. 163281

INTENTIONALLY LEFT BLANK

APPENDIX A

STOCHASTIC PARAMETER VALUES

This appendix contains a table listing the stochastic parameter values sampled for the SZ transport abstraction model and the SZ 1-D transport model. These parameter vectors for 200 realizations were sampled using the uncertainty distributions described in Section 6.5.2. The base-case model results described in Section 6.6 correspond to the input parameter values tabulated in Table A-1.

Table A-1. Stochastic Parameter Values

real. #	FPLAW	FPLAN	NVF19	NVF7	FISVO	FPVO	DCVO	KDNPVO	KDNPAL	KDSRVO	KDSRAL
1	0.70451	0.028309	0.15851	0.11373	1.3862	-3.7026	-10.092	1.7762	6.3364	268.07	259.27
2	0.61702	0.70184	0.11408	0.081329	0.84234	-3.0161	-10.116	1.2311	4.8505	258.99	113.51
3	0.35217	0.61633	0.083152	0.20585	1.0234	-3.3666	-10.146	1.09	4.2112	113.11	290.67
4	0.43734	0.35304	0.20587	0.19441	0.83422	-3.8921	-10.539	1.3057	7.6552	290.9	159.82
5	0.3726	0.4368	0.19441	0.16058	0.92304	-4.461	-10.042	1.5285	6.1118	160.14	199.68
6	0.38137	0.37493	0.16033	0.17169	1.4084	-2.3306	-10.426	1.1931	6.4302	200.28	240.98
7	0.96095	0.38323	0.17133	0.16309	0.81193	-2.6095	-10.325	1.556	5.7365	240.86	85.61
8	0.96721	0.96199	0.1631	0.16459	1.1285	-3.3333	-10.197	1.2925	7.73	86.233	122.88
9	0.063508	0.96547	0.16442	0.26596	1.3996	-3.1397	-10.612	1.1273	4.6382	122.69	82.931
10	0.39763	0.063782	0.26525	0.26907	1.2126	-3.2812	-10.518	1.2363	7.7179	83.165	99.983
11	0.12641	0.39708	0.26845	0.1011	0.63908	-3.2658	-10.619	1.2345	6.2902	100.11	249.1
12	0.83363	0.12855	0.10207	0.16643	1.5206	-1.199	-10.572	1.8288	7.5701	248.31	79.438
13	0.82638	0.83084	0.16658	0.12153	1.3272	-1.15	-10.174	1.2777	6.451	79.842	156.96
14	0.46725	0.82571	0.12117	0.22766	0.62506	-3.976	-10.626	1.22	4.9316	156.83	245.64
15	0.11482	0.46679	0.2272	0.22709	1.6764	-3.2319	-10.431	1.4189	6.8839	244.94	185.29
16	0.24233	0.11166	0.22688	0.17505	1.0682	-3.8285	-10.185	1.5742	7.3231	183.88	46.974
17	0.8055	0.24472	0.17513	0.11746	1.2021	-1.8383	-10.366	1.6247	7.8869	47.598	285.48
18	0.1329	0.80984	0.11813	0.14376	1.0712	-1.8602	-10.758	1.2913	5.1106	284.54	222.27
19	0.73058	0.13299	0.14387	0.22266	1.4018	-3.0689	-10.059	1.7072	5.8951	223.16	46.513
20	0.34072	0.73141	0.22261	0.12312	1.3451	-3.856	-10.26	1.7658	8.6697	45.328	329.38
21	0.048591	0.34315	0.12247	0.21023	1.0043	-3.5674	-10.801	1.5571	7.4175	327.85	136.96
22	0.74837	0.048613	0.21035	0.15875	1.4574	-1.9719	-9.921	1.6685	7.7301	137.24	181.17
23	0.93881	0.74785	0.15923	0.093691	1.2402	-3.8166	-10.485	1.5587	6.4626	180.92	138.35
24	0.55458	0.93563	0.09379	0.21283	1.1247	-2.2296	-10.372	1.0925	1.9633	139.62	247.14
25	0.79283	0.55378	0.21273	0.25453	1.668	-3.3458	-10.476	1.7332	6.3834	246.15	228.25
26	0.37734	0.79098	0.25543	0.18598	1.816	-4.0395	-10.185	5.906	7.6101	227.35	115.13

Table A-1. Stochastic Parameter Values (Continued)

real. #	FPLAW	FPLAN	NVF19	NVF7	FISVO	FPVO	DCVO	KDNPVO	KDNPAL	KDSRVO	KDSRAL
27	0.67108	0.37594	0.18625	0.2203	0.94555	-2.1743	-10.24	1.5551	7.8466	116.36	264.39
28	0.65266	0.67222	0.22046	0.16351	1.6175	-1.3137	-10.538	0.83687	6.7485	264.74	194.12
29	0.62918	0.65188	0.1638	0.20193	1.5918	-2.8203	-10.13	1.6876	10.779	194.18	155.64
30	0.24883	0.62618	0.20225	0.199	1.3545	-2.032	-10.341	1.135	2.4415	156.36	325.19
31	0.71164	0.2459	0.19922	0.19577	0.76344	-3.2677	-10.437	1.3511	6.4552	325.42	362
32	0.36584	0.7122	0.1961	0.14524	2.4058	-2.4327	-9.9314	1.5141	6.5489	361.97	105.28
33	0.47113	0.36787	0.14464	0.20748	1.2638	-2.4921	-9.6565	1.5069	6.2446	103.82	313.97
34	0.58157	0.47388	0.20749	0.16199	1.8275	-2.5698	-10.565	1.0319	5.3839	313.5	308.63
35	0.17154	0.58391	0.16242	0.17587	1.381	-3.5586	-9.9702	1.1229	4.5499	307.59	232.62
36	0.27276	0.17077	0.17593	0.19016	1.7866	-2.2884	-9.9878	1.2241	6.5466	230.98	72.64
37	0.16841	0.2727	0.18985	0.13151	1.3153	-3.2946	-10.231	1.4754	5.7734	71.65	395.34
38	0.21269	0.16757	0.13141	0.14914	1.5424	-3.0598	-10.645	1.0729	4.3751	395.81	200.88
39	0.60151	0.21358	0.14881	0.13017	1.6877	-2.7243	-9.3455	1.1663	4.6523	201.21	362.94
40	0.15729	0.60256	0.13036	0.13857	1.4451	-3.7297	-10.322	1.2935	5.863	363.36	239.29
41	0.3647	0.15605	0.13923	0.19281	1.2456	-3.5069	-9.6366	1.402	7.3494	238.67	353.32
42	0.59284	0.36398	0.19225	0.12862	1.5022	-3.7412	-10.208	1.1224	6.6715	353.63	219.29
43	0.43429	0.59413	0.1289	0.16172	1.0933	-3.6399	-9.7391	1.7931	4.4304	218.86	293.52
44	0.074964	0.43453	0.1616	0.1909	1.3933	-2.6663	-10.274	1.2546	6.7603	293.54	329.87
45	0.69768	0.072714	0.19154	0.17113	1.7338	-3.7591	-10.037	1.0482	4.24	329.95	260.63
46	0.53002	0.69555	0.17083	0.10469	0.60159	-3.3102	-9.9122	5.9484	12.998	260.58	195.92
47	0.066897	0.53497	0.10634	0.20539	1.5563	-2.6836	-10.14	1.3471	6.3144	195.81	278.81
48	0.81253	0.067039	0.20548	0.18333	1.629	-3.1487	-10.338	1.7807	8.2368	279.26	147.09
49	0.307	0.81175	0.18364	0.10332	1.1917	-3.954	-10.079	1.1421	5.1387	146.39	242.3
50	0.42421	0.30885	0.10441	0.2239	1.6554	-2.3446	-10.461	5.8964	12.116	242.61	342.55
51	0.31471	0.42162	0.22428	0.15377	1.015	-2.8939	-10.193	1.7596	7.6537	342.37	42.645
52	0.59783	0.31468	0.15362	0.16942	1.0887	-3.9623	-9.8347	1.3367	6.3723	41.049	296.42
53	0.54881	0.59673	0.16958	0.15458	0.92816	-1.937	-10.881	1.826	5.3289	296.98	317.67
54	0.25186	0.54916	0.15499	0.19171	1.3722	-3.4313	-10.022	2.9922	10.605	316.68	177.7
55	0.64107	0.25325	0.19159	0.18521	0.58809	-3.1758	-9.9578	1.4494	6.9642	177.84	322.55
56	0.45988	0.64197	0.18541	0.14594	0.70644	-3.4213	-10.38	1.3908	5.5995	322.77	120.09
57	0.35868	0.45653	0.14567	0.19779	1.1816	-2.6824	-9.9416	1.8202	8.3781	119.49	144.75

Table A-1. Stochastic Parameter Values (Continued)

real. #	FPLAW	FPLAN	NVF19	NVF7	FISVO	FPVO	DCVO	KDNPVO	KDNPAL	KDSRVO	KDSRAL
58	0.80213	0.35725	0.19771	0.17377	1.8448	-2.8405	-10.526	1.4432	8.2585	144.07	102.59
59	0.89925	0.80492	0.17397	0.16094	1.8056	-3.5446	-10.465	1.7504	8.3775	102.46	238.09
60	0.22248	0.89986	0.16077	0.22181	0.8828	-2.5185	-10.569	2.0366	7.6319	238.24	40.481
61	0.77121	0.22433	0.22181	0.24279	1.776	-3.0919	-10.209	4.6391	8.5555	39.125	60.504
62	0.75746	0.77304	0.24181	0.14055	1.4833	-3.3141	-10.914	1.3779	5.6484	61.745	174.98
63	0.55579	0.75953	0.14106	0.21688	0.29449	-1.9893	-10.676	1.5845	6.0788	175.27	368.07
64	0.13508	0.5581	0.2173	0.2146	0.97023	-1.5186	-10.388	1.6112	7.9421	368.85	358.4
65	0.9875	0.13511	0.21415	0.18662	0.67711	-3.6141	-9.5831	1.4423	7.3588	358.6	93.383
66	0.47965	0.98618	0.18644	0.12437	1.0221	-2.0912	-9.6872	1.6498	6.3947	93.089	351.55
67	0.90123	0.47822	0.12407	0.28381	1.3397	-2.146	-10.594	1.4092	4.8544	350.82	273.61
68	0.57866	0.90303	0.28224	0.17637	1.1865	-2.81	-9.7422	1.5295	7.097	272.91	29.222
69	0.87669	0.57844	0.17686	0.24362	1.3222	-3.8028	-10.099	1.7656	8.2015	29.194	109.73
70	0.52246	0.87687	0.24338	0.18948	1.4151	-1.0566	-11.127	1.689	7.9085	110.4	55.672
71	0.71788	0.52221	0.18946	0.23674	1.8942	-3.0485	-10.55	1.5342	7.2882	54.464	122.53
72	0.81847	0.71882	0.23781	0.182	1.7624	-1.4862	-10.686	1.0478	4.0931	122.07	225.24
73	0.63474	0.81922	0.18229	0.20867	0.738	-2.7404	-10.522	1.3844	5.8392	225.84	177.4
74	0.46117	0.63266	0.20818	0.22519	1.7318	-1.6079	-10.25	1.1146	5.563	177.5	220.21
75	0.68208	0.46283	0.22459	0.19667	1.533	-2.9264	-10.382	1.4729	4.6409	220.36	251.38
76	0.33346	0.68422	0.19617	0.1746	1.7237	-2.2736	-10.267	3.8397	5.4484	250.42	379.89
77	0.58661	0.33143	0.17454	0.2033	2.5288	-1.9123	-10.169	1.108	5.8758	379.91	348.05
78	0.84781	0.58957	0.20353	0.15752	0.18779	-2.5558	-9.4799	3.6575	8.1698	347.72	65.785
79	0.055061	0.84838	0.15727	0.1908	1.4319	-3.0857	-9.7859	1.7059	8.3184	65.77	340.28
80	0.72545	0.059548	0.19074	0.23065	0.65772	-2.3987	-10.66	1.0474	6.9709	340.32	288.61
81	0.78233	0.72652	0.23023	0.09896	1.0081	-3.3729	-9.8592	4.7524	7.3093	288.29	337.65
82	0.41537	0.78383	0.10033	0.21009	1.5687	-2.7055	-10.051	1.3448	4.2383	338.42	396.46
83	0.79615	0.4153	0.21009	0.21848	0.1867	-1.7701	-9.868	1.116	4.5096	396.97	24.361
84	0.26279	0.79769	0.21877	0.169	1.8692	-3.9839	-9.3285	1.3663	6.2532	24.087	256.82
85	0.32585	0.26149	0.16913	0.22126	1.0848	-2.2475	-11.197	3.2666	8.0548	257.05	51.292
86	0.21935	0.32771	0.22133	0.14731	0.43697	-2.0638	-10.149	1.2834	6.8038	50.403	118.69
87	0.57287	0.21868	0.14692	0.15714	1.0417	-3.1822	-10.698	1.1281	5.642	117.57	303.07
88	0.05408	0.5743	0.15668	0.14015	0.69929	-2.0111	-10.532	1.5478	6.9799	302.88	23.539

Table A-1. Stochastic Parameter Values (Continued)

real. #	FPLAW	FPLAN	NVF19	NVF7	FISVO	FPVO	DCVO	KDNPVO	KDNPAL	KDSRVO	KDSRAL
89	0.10576	0.054487	0.13962	0.18832	1.2717	-3.5333	-10.005	1.6866	5.067	22.372	375.01
90	0.40754	0.10529	0.18845	0.096424	1.6977	-3.3872	-11.258	2.6858	8.1054	374.3	142.05
91	0.91603	0.40782	0.098203	0.11647	0.90599	-3.6232	-9.5364	1.2958	7.3349	143.11	32.802
92	0.89135	0.91567	0.11686	0.16758	1.7454	-2.7577	-10.47	1.7117	6.3243	33.088	128.36
93	0.19019	0.89023	0.16751	0.24842	0.46766	-3.9928	-11.072	1.5973	5.532	129.99	59.201
94	0.87315	0.19372	0.24868	0.24104	1.2729	-3.8725	-10.503	1.4454	8.2211	58.595	204.12
95	0.66517	0.87134	0.24128	0.13522	1.7668	-3.2063	-10.678	1.3136	6.3196	203.25	333.28
96	0.024123	0.66764	0.13509	0.2357	0.79926	-1.415	-10.318	1.3962	5.1403	333.2	96.423
97	0.23899	0.022985	0.23591	0.20122	0.78641	-1.5294	-9.9071	1.6784	10.47	96.617	343.73
98	0.093079	0.23563	0.20126	0.079449	0.50753	-3.6823	-10.585	1.5156	6.2799	344.24	33.838
99	0.26953	0.090888	0.078007	0.14284	1.6105	-1.6374	-9.8223	2.0086	12.343	33.832	205.03
100	0.54079	0.26698	0.14297	0.1121	0.7266	-2.4384	-11.023	1.3193	4.8847	205.87	348.78
101	0.41165	0.54048	0.11173	0.14771	1.2905	-4.5523	-10.31	1.114	5.4429	349.62	77.497
102	0.52854	0.41152	0.14803	0.18493	1.053	-3.5782	-9.7593	5.3252	7.4087	77.534	76.842
103	0.60808	0.52661	0.18474	0.16809	1.8672	-3.9083	-10.633	1.6194	5.0404	76.359	36.081
104	0.94548	0.60856	0.1683	0.18302	1.8887	-3.5167	-10.633	1.0013	4.9632	36.121	311.98
105	0.86326	0.94988	0.18294	0.19313	1.9802	-2.8632	-10.973	1.2785	5.8423	312.49	63.968
106	0.12173	0.86184	0.19307	0.25889	2.2252	-3.196	-9.9776	1.5042	8.3694	64.993	210.78
107	0.84161	0.12403	0.259	0.23369	0.81543	-2.9144	-10.666	1.0022	4.0211	210.19	132.5
108	0.70681	0.84374	0.23391	0.12085	1.0518	-2.6365	-10.296	1.6652	8.0432	133.56	371.99
109	0.83677	0.70737	0.12071	0.22943	1.0756	-1.2562	-10.492	1.404	7.1784	372.31	378.64
110	0.99128	0.83905	0.22953	0.20708	1.0619	-1.6871	-9.5526	1.8088	6.2277	377.8	384.4
111	0.010519	0.99171	0.20724	0.2288	1.1152	-3.8399	-9.5112	1.5117	8.0958	383.78	389.32
112	0.62269	0.011542	0.22836	0.28924	1.5627	-1.7758	-9.4549	0.46893	2.0554	388.62	81.669
113	0.084204	0.62223	0.29036	0.067107	1.1593	-2.3046	-9.3949	1.3874	5.0674	81.049	131.2
114	0.25597	0.083179	0.063538	0.19537	1.7925	-1.8199	-10.623	1.0262	4.8538	131.47	141.54
115	0.74132	0.25944	0.19539	0.10837	1.8399	-1.0372	-10.499	1.4555	4.3711	140.73	134.5
116	0.007434	0.74115	0.10822	0.14618	1.3104	-4.793	-10.473	1.4463	4.6318	135.74	152.57
117	0.93236	0.008269	0.14655	0.21192	1.0318	-2.5914	-10.486	1.2589	4.8102	151.56	300.09
118	0.32035	0.93043	0.21235	0.049913	0.25923	-3.925	-10.447	1.6972	8.4928	299.64	166.3
119	0.030233	0.32271	0.054478	0.25292	1.8314	-3.5417	-10.015	1.3911	6.5942	167.99	355.78

Table A-1. Stochastic Parameter Values (Continued)

real. #	FPLAW	FPLAN	NVF19	NVF7	FISVO	FPVO	DCVO	KDNPVO	KDNPAL	KDSRVO	KDSRAL
120	0.28508	0.034057	0.25215	0.15635	1.6384	-2.197	-10.408	1.0517	4.3142	355.96	366.8
121	0.10144	0.28681	0.15579	0.084439	1.4232	-4.8885	-9.7061	4.1216	8.6042	365.99	216.81
122	0.48434	0.10353	0.087276	0.15092	1.2272	-1.3375	-9.6162	1.7822	10.632	216.07	125.11
123	0.82334	0.4826	0.15078	0.11532	1.2217	-3.394	-10.28	1.1916	6.8495	126.33	25.85
124	0.20394	0.82124	0.1155	0.17726	1.8577	-4.3628	-10.513	0.55633	5.2954	25.77	364.38
125	0.8532	0.20325	0.1773	0.2256	0.64581	-3.4685	-11.163	0.60824	5.5611	364.43	319.08
126	0.037624	0.85435	0.22552	0.13752	2.2805	-3.8812	-9.6208	1.6654	8.6597	318.59	252.72
127	0.48593	0.038573	0.1374	0.23209	1.8027	-3.0395	-9.9522	1.1375	4.852	253.06	189.7
128	0.86876	0.48711	0.2322	0.090398	1.4724	-1.8783	-10.167	1.5864	7.4125	189.11	188.25
129	0.1544	0.86639	0.087853	0.17752	0.8727	-3.6625	-10.349	1.2554	6.6315	189	371.09
130	0.14816	0.15141	0.17766	0.23528	1.4626	-1.7361	-10.354	1.7691	6.1952	371.34	48.507
131	0.043598	0.14898	0.2347	0.12704	0.8525	-4.2851	-9.5649	0.57225	6.1647	49.552	391
132	0.76846	0.043645	0.12788	0.12639	1.9175	-3.0322	-10.707	1.5393	8.5753	392.36	358.05
133	0.11602	0.76916	0.12658	0.091042	0.77682	-1.663	-9.3758	1.5539	6.1291	357.09	270.33
134	0.50019	0.11576	0.091188	0.21608	1.5858	-3.7717	-9.697	1.4248	5.1128	268.94	91.21
135	0.29848	0.50385	0.21619	0.11938	0.66707	-3.782	-10.108	1.7533	7.8604	91.012	266.13
136	0.92706	0.29908	0.11876	0.1795	0.9665	-4.1659	-10.598	1.3229	6.3067	266.24	87.774
137	0.94102	0.92914	0.17972	0.15236	1.6015	-2.1023	-10.123	1.4054	4.568	87.49	381.85
138	0.95563	0.94338	0.1525	0.25203	1.0371	-3.8468	-10.607	1.3532	6.9416	382.11	73.304
139	0.97152	0.95988	0.25117	0.25751	1.4984	-2.9884	-9.4764	1.4846	7.5599	75.05	305.76
140	0.16243	0.97467	0.25758	0.26263	1.3352	-3.4489	-10.64	1.4352	6.1782	306.58	52.742
141	0.29141	0.16433	0.26227	0.27269	1.3693	-1.3574	-9.9925	1.0025	4.2885	52.555	108.71
142	0.31613	0.29468	0.27054	0.12983	0.90791	-1.2856	-10.691	1.304	5.0186	107.51	310.21
143	0.30444	0.31977	0.12929	0.1517	1.1741	-1.2235	-10.553	1.2773	6.5328	309.31	127.74
144	0.34719	0.30198	0.15141	0.15513	2.5485	-1.1431	-9.9839	1.6238	4.665	126.78	278.2
145	0.73918	0.34993	0.15548	0.15306	1.2035	-3.7544	-10.508	1.5304	6.9865	278.09	224.01
146	0.38633	0.73982	0.15327	0.15945	0.94859	-3.4626	-10.086	1.7279	6.2592	223.97	234.71
147	0.88281	0.38841	0.15936	0.21123	1.7483	-3.4067	-10.258	1.4001	7.0045	235.6	98.655
148	0.91034	0.88286	0.21103	0.16498	1.5123	-3.4429	-10.217	0.9905	2.7287	98.884	173.85
149	0.51841	0.91188	0.16505	0.2382	0.12866	-3.3353	-10.578	0.96945	3.0842	172.58	398.45
150	0.27749	0.51972	0.23803	0.24697	1.4763	-2.2129	-10.391	1.8137	7.36	399.04	182.7

Table A-1. Stochastic Parameter Values (Continued)

real. #	FPLAW	FPLAN	NVF19	NVF7	FISVO	FPVO	DCVO	KDNPVO	KDNPAL	KDSRVO	KDSRAL
151	0.018691	0.27629	0.2464	0.18134	1.6242	-3.245	-9.3007	1.6874	6.8565	182.75	106.24
152	0.90977	0.017058	0.18162	0.14925	0.88989	-1.5786	-10.367	1.6278	7.3442	106.39	346.76
153	0.78691	0.90918	0.14972	0.071036	1.1644	-1.444	-10.56	1.7089	8.5463	345.34	282.36
154	0.61273	0.78833	0.073847	0.24478	1.5462	-2.9437	-9.806	1.532	4.5883	283.74	20.174
155	0.44835	0.61154	0.24491	0.21959	1.509	-3.4983	-10.066	1.644	6.1311	20.054	272.36
156	0.44417	0.44562	0.21926	0.19385	2.3672	-4.6266	-11.292	1.578	7.6511	270.96	316.33
157	0.92465	0.44049	0.19402	0.17247	1.2376	-1.4517	-10.102	1.5821	7.0916	315.47	94.793
158	0.076609	0.92395	0.17275	0.17226	1.297	-2.0342	-9.9661	1.036	4.1036	95.841	169.24
159	0.97647	0.077995	0.17184	0.25011	1.2888	-2.622	-10.589	1.8158	6.7876	169.73	294.38
160	0.88672	0.97946	0.24939	0.10731	1.3071	-3.1179	-10.4	1.4875	6.203	294.14	280.49
161	0.65647	0.88508	0.10708	0.27559	1.3647	-3.1224	-10.027	1.4853	7.3059	281.47	392.49
162	0.18665	0.65755	0.2747	0.2403	1.4503	-1.3913	-10.072	1.3696	4.7212	392.92	192.19
163	0.64606	0.18543	0.23956	0.19953	0.86176	-3.9385	-9.369	5.6796	11.544	192.4	212.7
164	0.17568	0.6463	0.19972	0.13401	1.2833	-1.1169	-10.347	1.0218	5.7699	212.65	209.44
165	0.95061	0.17555	0.13472	0.19829	1.1026	-1.5522	-10.29	3.2702	12.928	209.18	215.42
166	0.14335	0.95267	0.19855	0.13239	0.68419	-2.4821	-10.302	1.1476	4.9715	215.41	233.45
167	0.75389	0.14211	0.13248	0.26065	0.35455	-3.6937	-10.285	1.4987	6.0234	233.3	262.83
168	0.088815	0.75375	0.26063	0.12567	1.5235	-2.5044	-10.222	1.7817	7.7213	262.21	88.429
169	0.23232	0.08869	0.12491	0.21379	1.4276	-3.7156	-10.133	1.1922	5.8916	89.341	207.49
170	0.76434	0.23274	0.21353	0.11061	1.1196	-1.2367	-10.602	1.0342	6.3693	207.28	148.16
171	0.28202	0.7616	0.11071	0.14232	1.2168	-3.7935	-10.308	1.3828	7.5455	147.76	56.742
172	0.67838	0.28377	0.1421	0.21493	1.1411	-2.1576	-10.453	1.0248	4.8431	56.111	30.192
173	0.53511	0.67815	0.2155	0.15048	1.1566	-3.9196	-10.686	1.3506	7.8087	30.992	286.7
174	0.56885	0.53997	0.15046	0.20288	2.0937	-3.5938	-11.111	5.5651	10.593	286.98	254.82
175	0.20533	0.5681	0.20264	0.18426	2.1634	-2.1331	-10.054	5.0921	12.993	254.19	153.59
176	0.40471	0.20916	0.18434	0.18769	0.61684	-3.4847	-10.156	1.0081	2.0458	153.92	185.52
177	0.9995	0.40055	0.18774	0.13838	1.1696	-2.4075	-10.442	1.5078	6.559	186.74	162.09
178	0.42544	0.99674	0.13813	0.1669	0.74682	-2.8729	-10.359	1.76	6.093	160.92	166.26
179	0.22637	0.42607	0.16701	0.29202	1.7114	-2.7766	-10.421	1.8183	8.4675	165.99	386.06
180	0.85993	0.22959	0.29861	0.17001	1.7077	-3.649	-10.414	0.37838	4.25	385.73	387.44
181	0.69081	0.85616	0.17039	0.14118	1.2552	-3.218	-9.4402	1.5396	6.3219	388.13	42.922

Table A-1. Stochastic Parameter Values (Continued)

real. #	FPLAW	FPLAN	NVF19	NVF7	FISVO	FPVO	DCVO	KDNPVO	KDNPAL	KDSRVO	KDSRAL
182	0.000316	0.69391	0.14143	0.23223	0.71843	-1.0082	-9.4219	1.6811	7.6176	44.051	170.83
183	0.66425	0.000898	0.23224	0.20456	0.98249	-3.165	-10.84	0.82101	1.8184	170.21	68.282
184	0.77963	0.6644	0.20481	0.02251	1.6687	-3.6051	-10.4	1.2373	4.7156	67.757	336.51
185	0.19856	0.77701	0.026558	0.20066	0.75819	-1.714	-10.656	1.4965	5.9137	336.43	333.76
186	0.39325	0.19937	0.2007	0.21764	1.5619	-2.3599	-9.8929	1.3319	6.6568	334.86	197.72
187	0.72376	0.39066	0.21781	0.13599	1.1067	-4.9164	-9.9021	4.4429	10.666	197.9	62.435
188	0.68892	0.7222	0.13594	0.16567	0.55484	-2.4516	-10.331	1.063	4.4061	61.878	112.56
189	0.98274	0.6877	0.1656	0.2091	1.5759	-2.0718	-10.67	4.0276	8.2587	112.62	326.39
190	0.45275	0.98273	0.20896	0.20396	1.8807	-3.6752	-10.546	1.699	8.1244	326.54	71.187
191	0.50526	0.45272	0.20412	0.28052	1.3502	-3.2414	-9.9247	1.3218	7.4539	70.071	298.21
192	0.49598	0.50781	0.27675	0.17357	1.6501	-2.2593	-10.652	1.4167	6.163	298.79	151.05
193	0.51183	0.49782	0.17314	0.18015	1.1476	-2.3726	-10.017	1.5236	4.1231	150.2	38.786
194	0.56134	0.51179	0.18047	0.17902	1.4929	-1.0761	-10.45	0.036671	6.0078	38.545	304.18
195	0.63937	0.56322	0.17911	0.18073	1.469	-3.1087	-10.948	1.5217	5.8151	303.54	376.34
196	0.18288	0.63794	0.18074	0.18708	1.4386	-2.9756	-9.9997	1.0782	4.5618	376.21	230.27
197	0.49279	0.18439	0.18748	0.19706	0.99788	-3.0038	-9.5125	1.2419	5.6844	229.91	321.71
198	0.33957	0.49261	0.19742	0.13392	1.5377	-2.9649	-10.239	1.2661	7.7128	321.32	162.65
199	0.097933	0.33587	0.13394	0.17855	1.1373	-2.7936	-9.9428	1.1672	5.5324	163.61	275.46
200	0.02951	0.098121	0.17837	0.15841	1.2559	-2.5445	-10.415	0.37655	1.9883	274.65	268.56

Table A-1. Stochastic Parameter Values (Continued)

real. #	KDUVO	KDUAL	GWSPD	BULKDE NSITY	CORAL	CORVO	SRC4Y	SRC4X	SRC3X	SRC2Y	SRC2X
1	6.3929	4.0476	0.8181	1791.7	1.0875	1.0042	0.39801	0.12912	0.82832	0.11435	0.46636
2	5.4235	4.3547	-0.85495	1889.7	3.5582	1.6714	0.12714	0.83286	0.46792	0.2438	0.11184
3	6.091	4.121	-0.1215	1820.9	3.5695	1.1986	0.83439	0.82826	0.11009	0.80568	0.24456
4	6.0964	4.1487	-0.44224	1984.5	0.90319	1.3675	0.82819	0.4672	0.24114	0.13093	0.80542
5	7.4704	6.9729	0.39432	1983.7	1.1434	1.5138	0.46584	0.11053	0.80879	0.73468	0.13052
6	7.5767	7.1394	0.3885	1904.1	0.90338	0.83369	0.11165	0.24447	0.13119	0.34017	0.73259
7	6.7357	2.9464	-0.03684	1815.2	2.9725	1.0459	0.24061	0.80742	0.73112	0.046301	0.34463
8	6.9733	4.2057	-0.46085	1855.7	2.9604	0.81838	0.80897	0.13118	0.34463	0.7483	0.04631
9	5.4813	3.1882	-0.30786	1978.3	1.4071	0.91882	0.13468	0.73388	0.04603	0.93663	0.74671
10	6.1144	5.8512	0.36448	1823.5	0.90334	1.5367	0.73421	0.34146	0.74618	0.55383	0.93928
11	8.0149	5.8404	-0.43612	1957.8	0.90373	0.79926	0.34235	0.045831	0.93877	0.79495	0.55274
12	7.3052	4.4718	0.27522	1878.4	2.8768	1.1894	0.049235	0.74967	0.55011	0.37712	0.79438
13	5.7365	3.13	-0.19072	1777.8	0.9034	1.5267	0.74852	0.93563	0.79164	0.67425	0.37882
14	6.3898	3.6295	-0.97733	1961.7	2.5538	1.3075	0.93625	0.55419	0.37553	0.65406	0.67351
15	8.0955	5.7631	0.29233	2028.3	0.94105	0.77849	0.55335	0.79368	0.67241	0.62614	0.65251
16	5.418	3.2064	0.66404	1920	0.90314	1.6522	0.79004	0.37616	0.65068	0.24578	0.62768
17	7.2363	5.4719	0.059967	1973.9	2.6065	1.4544	0.37912	0.67379	0.62866	0.7112	0.24627
18	6.297	3.9963	0.3514	1885.7	3.4344	0.77844	0.67485	0.65038	0.24892	0.3687	0.71087
19	6.1532	2.8633	-0.14488	1944.9	1.7505	1.8446	0.65415	0.62701	0.711	0.47078	0.36665
20	6.3443	5.5418	0.20717	1940.3	2.8112	1.0993	0.62895	0.24539	0.36569	0.58084	0.47477
21	7.247	6.249	0.18479	1935.4	1.0695	1.288	0.24752	0.71071	0.47397	0.17007	0.5826
22	6.6527	4.799	0.15118	1856.8	2.2828	1.1135	0.71398	0.36774	0.58472	0.27474	0.1718
23	7.1839	5.711	-0.30353	1953.7	2.2025	1.5333	0.36813	0.47456	0.17021	0.1663	0.27316
24	6.3895	4.1293	0.25181	1883.7	2.0793	1.4721	0.47446	0.58489	0.27248	0.21154	0.16614
25	6.9776	5.251	-0.15875	1904.5	0.90375	1.0179	0.58135	0.17051	0.16512	0.60233	0.21337
26	14.466	5.1801	-0.03341	1925.9	2.4697	1.5852	0.17104	0.27259	0.21288	0.15556	0.60328
27	5.7245	5.0737	0.099475	1836.3	1.04	1.3493	0.27161	0.1696	0.60274	0.36263	0.15521
28	5.4412	3.6421	-0.38882	1862.7	1.4328	1.1809	0.16813	0.2111	0.15655	0.59017	0.36338

Table A-1. Stochastic Parameter Values (Continued)

real. #	KDUVO	KDUAL	GWSPD	BULKDE NSITY	CORAL	CORVO	SRC4Y	SRC4X	SRC3X	SRC2Y	SRC2X
29	7.345	5.3989	-0.27169	1834.9	1.8884	1.7837	0.21312	0.60029	0.36028	0.43416	0.59491
30	6.6146	4.1024	-0.39819	1847.3	0.90353	2.3132	0.60039	0.15621	0.59053	0.070562	0.43237
31	6.4572	4.4969	-0.34483	1930.7	0.90382	0.94597	0.15578	0.36256	0.43289	0.69568	0.072704
32	6.7446	4.9141	0.11944	1831.2	0.90351	1.7452	0.36078	0.59297	0.074871	0.53396	0.69861
33	6.5102	3.3664	-0.41112	1882.9	0.90364	1.7258	0.59401	0.43237	0.69566	0.066305	0.53255
34	6.3393	3.7497	-0.16609	1928.7	1.9686	1.4833	0.43426	0.073074	0.53246	0.81035	0.069985
35	5.9997	3.344	0.10967	1896.5	0.90348	0.77891	0.073323	0.6975	0.067696	0.30531	0.81321
36	5.9559	3.508	-0.07847	1796.8	1.0186	2.8271	0.6963	0.53488	0.81113	0.42313	0.30702
37	7.7597	4.9963	-0.76296	1950.8	1.9415	1.3809	0.53406	0.06581	0.30994	0.3125	0.42397
38	5.4215	3.3073	0.23755	1916.7	1.2853	2.3632	0.065321	0.81078	0.4221	0.59713	0.31337
39	7.5782	4.0865	0.037959	1792.3	0.90322	1.5062	0.81429	0.30812	0.31475	0.54755	0.59695
40	6.8481	4.9427	-0.81314	1978.7	2.3987	2.2149	0.30883	0.42455	0.59518	0.25434	0.54791
41	6.4336	4.348	0.37313	1870.6	1.6641	1.4434	0.42078	0.31241	0.54998	0.64335	0.25415
42	5.9679	2.9858	-0.23107	1894.9	0.9032	1.6805	0.31042	0.59809	0.25497	0.45955	0.64074
43	7.6914	5.3518	-0.08994	1872.4	2.8904	1.8892	0.59966	0.549	0.64079	0.35531	0.45927
44	6.5365	4.7282	-0.2259	1929.2	0.90393	1.5782	0.54701	0.25493	0.45549	0.80303	0.35881
45	3.8988	2.9717	0.11488	1919	1.2471	1.3553	0.25287	0.64012	0.35869	0.89767	0.8011
46	7.76	5.7864	0.054703	1857.7	0.90394	1.634	0.64341	0.45504	0.80265	0.22022	0.89575
47	6.9593	3.8645	-0.29576	1938.4	1.9461	1.1435	0.45681	0.35554	0.89736	0.77279	0.22201
48	6.3023	4.2993	0.16765	1902	1.729	1.5204	0.35767	0.8033	0.22106	0.75653	0.7745
49	7.1005	3.8948	-0.05232	1881.8	0.90376	2.0395	0.80219	0.8976	0.77391	0.55844	0.75595
50	7.2944	4.9688	-0.17085	1976.9	2.1536	0.77839	0.89527	0.22021	0.75624	0.13669	0.55693
51	6.9967	4.7739	0.35802	2009.1	1.3766	1.6906	0.22262	0.77394	0.55501	0.98761	0.13778
52	6.1107	3.6678	0.4722	1850.2	1.0029	1.7566	0.77311	0.75559	0.136	0.47673	0.98982
53	5.5058	5.1336	-0.32842	1968.2	2.8598	1.2814	0.75897	0.55733	0.98911	0.90165	0.47795
54	8.0283	4.4488	0.3249	1965	3.2589	1.7758	0.55928	0.13643	0.47798	0.57992	0.9017
55	7.1634	4.0579	0.30516	1921.4	0.90367	1.0305	0.13924	0.9852	0.90361	0.87597	0.57623
56	7.7182	5.7363	0.069194	1824.4	2.7248	1.1388	0.98859	0.47716	0.57516	0.52119	0.8799
57	16.934	6.1005	-0.43183	2082	2.6468	0.93337	0.47781	0.9021	0.87838	0.71927	0.52202
58	6.3677	3.5446	0.92526	1905.5	1.7898	1.5033	0.90019	0.57664	0.52429	0.81645	0.71732

Table A-1. Stochastic Parameter Values (Continued)

real. #	KDUVO	KDUAL	GWSPD	BULKDENSITY	CORAL	CORVO	SRC4Y	SRC4X	SRC3X	SRC2Y	SRC2X
59	8.0137	5.6306	-0.02427	2011	0.90342	0.77833	0.57734	0.87993	0.7155	0.63189	0.8157
60	7.5803	5.5676	0.47755	1925.5	3.6555	0.77871	0.87726	0.52225	0.81696	0.46085	0.63455
61	7.8045	4.8121	0.093825	2000.3	1.4533	1.2651	0.52405	0.71818	0.63403	0.6836	0.4645
62	6.8065	3.2399	0.44786	1914.8	3.2957	2.4448	0.71743	0.81913	0.46208	0.33488	0.68352
63	7.8024	8.2148	0.027231	1955.4	1.8794	2.2914	0.81684	0.63478	0.68113	0.58819	0.33071
64	6.3658	4.5135	0.26113	1979.9	3.1858	0.87284	0.63336	0.46033	0.33102	0.84547	0.58869
65	6.6401	6.1286	0.38063	1936	1.6237	2.1973	0.46483	0.68187	0.58955	0.056247	0.84656
66	8.0802	4.8948	0.15618	1902.7	2.4911	1.6189	0.68036	0.33279	0.84721	0.72827	0.058062
67	7.5176	6.0288	-0.04535	1947.4	2.9073	0.77816	0.33359	0.58683	0.055556	0.78499	0.72763
68	6.292	4.6899	0.21756	1876.5	2.1063	0.98331	0.5888	0.84941	0.72882	0.41564	0.78044
69	7.9056	5.4261	-0.19898	1927.3	1.3901	0.77861	0.84696	0.057968	0.78458	0.79874	0.41834
70	7.6321	5.7935	0.10325	1990.4	2.3218	1.0352	0.059202	0.72741	0.41612	0.26343	0.79713
71	7.3797	5.1016	0.41512	1786.2	0.91759	1.4684	0.72908	0.783	0.79694	0.32595	0.26112
72	6.5261	4.4622	-0.90291	1957.5	1.9062	1.2751	0.78309	0.41711	0.26183	0.21814	0.32885
73	7.6682	5.2846	0.2696	1971.2	3.0586	1.4506	0.41849	0.79753	0.3285	0.57109	0.21954
74	5.9958	3.9643	0.33449	1893.6	0.90317	1.5424	0.79539	0.26215	0.21556	0.051789	0.57407
75	6.3393	4.9391	-0.0988	1974.5	2.5336	2.6217	0.26288	0.32672	0.57298	0.10611	0.052027
76	7.6319	5.9195	0.3558	1860.1	2.769	2.1371	0.32568	0.21746	0.053163	0.40591	0.10719
77	5.7279	2.9262	-0.2854	1874.8	1.2181	0.7788	0.21624	0.57483	0.10741	0.91972	0.40777
78	7.3452	5.4588	-0.20391	1849.7	2.8383	2.0286	0.57311	0.052277	0.40829	0.8908	0.91655
79	7.8172	5.6723	-0.33597	1924.3	0.90379	1.6683	0.05449	0.10898	0.91926	0.19459	0.89262
80	7.2748	4.293	0.088795	1785.3	0.90398	1.9847	0.10825	0.4085	0.89123	0.87371	0.19373
81	13.835	5.7162	-0.95629	1813.8	0.90365	2.8559	0.40932	0.91507	0.19271	0.66865	0.87036
82	6.9084	3.6944	-0.46886	1891.7	1.847	0.77807	0.91592	0.89045	0.87402	0.022481	0.66851
83	6.2653	3.9482	-0.11054	2018.2	0.90316	1.5616	0.89293	0.19045	0.66901	0.23693	0.024774
84	5.4962	3.5414	0.57263	2006.8	0.90333	0.77854	0.19004	0.87062	0.023309	0.091047	0.2352
85	7.7176	4.87	0.47059	1842.7	1.1819	1.0206	0.87302	0.66938	0.2368	0.26906	0.091802
86	5.916	2.9113	-0.3659	1998.4	3.3469	1.7082	0.6656	0.024152	0.090667	0.54398	0.26823
87	5.885	3.1148	0.44164	1944.2	3.2399	0.77803	0.023333	0.23528	0.26661	0.41455	0.54303
88	6.5153	4.2502	0.19729	1751.8	0.90358	2.5253	0.23803	0.090919	0.54429	0.52672	0.41381

Table A-1. Stochastic Parameter Values (Continued)

real. #	KDUVO	KDUAL	GWSPD	BULKDE NSITY	CORAL	CORVO	SRC4Y	SRC4X	SRC3X	SRC2Y	SRC2X
89	18.883	6.1699	-1.2709	1853.8	3.1498	1.1287	0.093541	0.26709	0.4112	0.6066	0.52874
90	7.4636	6.0913	-0.31499	1806.3	2.2535	0.77822	0.26696	0.54419	0.52817	0.94606	0.60614
91	5.5562	3.4321	-0.57236	1861.2	0.90307	1.0671	0.54172	0.41108	0.60997	0.86265	0.94816
92	15.126	6.0081	-0.27432	1917.9	0.90372	0.77868	0.41491	0.52686	0.94891	0.12263	0.86301
93	7.5253	5.2247	0.050354	1892.7	0.90328	1.3907	0.52942	0.60533	0.86005	0.84008	0.12295
94	6.0635	2.2972	-0.10337	1915.2	0.9038	1.9143	0.60947	0.9471	0.12418	0.70779	0.84136
95	6.1259	3.6118	0.032758	1931.1	1.7069	0.90439	0.94625	0.86346	0.84482	0.83642	0.70974
96	6.019	3.0688	0.13087	2035.9	1.2067	2.0823	0.86403	0.12324	0.70673	0.9929	0.83838
97	6.7596	3.7298	0.73013	1995.7	1.6498	0.77824	0.12021	0.84037	0.83719	0.014448	0.9937
98	6.65	4.7642	0.43066	1819	1.9956	1.3968	0.84499	0.70858	0.99258	0.62177	0.010011
99	7.1823	4.2707	-0.45167	1988.1	3.4882	2.1656	0.70993	0.83907	0.011816	0.080484	0.62177
100	6.451	4.6949	0.40649	1952.6	3.1045	0.7812	0.83656	0.99291	0.62029	0.25668	0.084052
101	7.4039	4.9982	0.24501	1986.7	0.90337	0.77897	0.99369	0.011109	0.084139	0.74363	0.25783
102	7.4767	6.296	0.40263	2096.8	3.03	0.77829	0.012139	0.6206	0.25558	0.008536	0.74421
103	7.0457	5.9683	0.9646	1736.1	2.4303	1.7389	0.62312	0.083331	0.74082	0.93232	0.008844
104	5.7161	3.1765	-1.3741	1934.3	2.9977	0.77877	0.082851	0.25726	0.005755	0.32377	0.93333
105	5.9557	5.8845	0.14663	1800.5	3.6849	1.4182	0.25651	0.74433	0.93264	0.031595	0.32274
106	6.9747	5.3933	-0.65556	1859.7	0.90304	1.0833	0.74383	0.008921	0.32254	0.28928	0.032629
107	8.938	5.8838	-0.29014	1960.3	2.0719	2.503	0.007082	0.93162	0.032139	0.10235	0.28732
108	11.561	8.4623	0.28677	1711.5	0.90325	2.5914	0.9343	0.32226	0.28774	0.48315	0.10135
109	6.12	1.9755	-1.4049	2027.8	0.90377	2.6724	0.32398	0.033875	0.10227	0.82137	0.48128
110	6.9574	5.0698	0.65206	1874.1	2.5889	2.7358	0.034804	0.28617	0.48419	0.20142	0.82385
111	5.7228	3.0312	-0.2145	1765.8	0.90302	0.8074	0.28713	0.10452	0.82206	0.85408	0.20133
112	5.5625	3.6783	-1.1351	1866.8	3.4201	1.0809	0.10321	0.48255	0.20087	0.03713	0.85191
113	7.3147	5.5068	-0.25443	1811.7	0.90397	1.1169	0.48009	0.82013	0.85325	0.48798	0.038156
114	6.3164	1.9046	-0.47282	1906.2	0.9031	1.0955	0.82478	0.20143	0.036873	0.86745	0.48608
115	7.5921	6.2268	-0.02221	1981.5	0.90386	1.1662	0.20399	0.85208	0.48667	0.15011	0.86707
116	5.6012	3.9339	0.38733	1845.1	0.90331	1.7033	0.85464	0.036304	0.86896	0.14649	0.15383
117	1.2364	2.4753	-0.35313	1991.5	1.4715	1.2305	0.038431	0.48549	0.15269	0.041893	0.14705
118	6.6036	3.7894	0.42255	1773.4	2.934	2.2435	0.4888	0.86597	0.1496	0.76799	0.042585

Table A-1. Stochastic Parameter Values (Continued)

real. #	KDUVO	KDUAL	GWSPD	BULKDE NSITY	CORAL	CORVO	SRC4Y	SRC4X	SRC3X	SRC2Y	SRC2X
119	5.6675	3.1009	-1.0969	1907.4	0.90361	2.4104	0.86947	0.1505	0.041331	0.11687	0.76983
120	8.0168	4.5391	-0.01547	1997.7	3.0755	1.434	0.15471	0.14696	0.76917	0.50225	0.11804
121	7.805	5.8264	0.4368	1830.6	0.90311	1.0568	0.1482	0.041927	0.11919	0.29972	0.50172
122	7.3702	3.4667	-0.41438	1827.8	1.4778	0.77813	0.043749	0.76965	0.50249	0.92993	0.29938
123	6.7213	5.929	-0.41778	1776.7	3.1256	2.3797	0.76795	0.11768	0.29931	0.94398	0.92995
124	4.3306	2.6339	-1.0303	1966.5	0.90346	1.7621	0.11763	0.50186	0.92988	0.9591	0.94279
125	6.2064	4.5436	0.31744	1818.1	0.90345	1.5484	0.50125	0.29969	0.9417	0.9723	0.95904
126	7.6523	5.9877	-0.45746	1910.2	0.90312	1.3264	0.29829	0.92712	0.95959	0.16336	0.9735
127	5.563	3.2852	0.001514	1868.8	2.6949	1.3193	0.92626	0.94495	0.97011	0.29355	0.16075
128	6.1336	3.2702	-0.24028	2024.4	0.90336	2.4598	0.94317	0.95688	0.16089	0.31924	0.29198
129	6.3297	2.6876	0.63084	2032.1	1.5522	0.77853	0.95718	0.97024	0.29356	0.30068	0.31688
130	8.0247	5.6069	0.70954	2044.3	0.9039	2.7802	0.97338	0.16089	0.31924	0.34894	0.30226
131	5.8546	3.1558	0.77432	2060.7	3.4028	2.2586	0.16471	0.29112	0.30169	0.73742	0.34723
132	6.8369	4.6179	0.8669	1834	3.4585	1.6053	0.2919	0.31659	0.34685	0.38542	0.73879
133	7.0371	3.8323	-0.40523	1867.7	3.5324	0.86487	0.31639	0.30034	0.7382	0.8844	0.38707
134	8.0813	6.22	-0.24736	1873.1	3.5873	1.5948	0.30114	0.34737	0.38911	0.91417	0.88103
135	7.7775	6.2657	-0.21795	1869.7	0.9035	0.84208	0.34709	0.7389	0.8827	0.51527	0.91491
136	8.0432	6.5706	-0.23599	1879.7	0.90388	2.6439	0.73959	0.38723	0.91191	0.27739	0.51637
137	7.1933	7.4878	-0.18222	1959.9	0.90395	0.77896	0.3856	0.88123	0.51821	0.01555	0.27512
138	5.4294	3.3293	0.28472	1888.1	0.90392	1.721	0.8846	0.91276	0.27884	0.90859	0.015142
139	7.4959	3.8249	-0.13344	2003.3	0.96295	0.77857	0.91058	0.51807	0.019829	0.78559	0.9075
140	7.0592	3.9127	0.45875	2015.8	2.5618	0.96496	0.51863	0.27877	0.90669	0.61248	0.78753
141	5.8007	3.847	0.55231	1913.2	1.1215	1.7325	0.27928	0.018004	0.78506	0.44553	0.6123
142	6.8881	4.0184	0.022971	1864.3	3.212	1.0603	0.017035	0.90513	0.61484	0.44206	0.44827
143	7.4777	5.5041	-0.26788	1747.7	3.339	1.6273	0.90617	0.7874	0.44935	0.92037	0.44137
144	7.7513	4.1826	-1.319	2012.9	1.6067	1.4599	0.78778	0.61244	0.44289	0.077399	0.92211
145	7.312	6.0396	0.51974	1971.7	0.90383	1.4942	0.61002	0.44738	0.92177	0.9795	0.075209
146	14.261	6.1585	0.34072	1931.8	0.90305	0.9128	0.44868	0.44026	0.078919	0.88632	0.9771
147	6.8555	4.6736	0.13291	1900.1	3.3213	1.2546	0.44447	0.92422	0.97874	0.65608	0.88741
148	6.0243	3.7619	-0.06401	1898.7	2.7905	2.8905	0.92373	0.077673	0.88803	0.18793	0.65881

Table A-1. Stochastic Parameter Values (Continued)

real. #	KDUVO	KDUAL	GWSPD	BULKDENSITY	CORAL	CORVO	SRC4Y	SRC4X	SRC3X	SRC2Y	SRC2X
149	5.5135	2.0896	-0.07036	2019.6	2.0286	1.2974	0.076063	0.97623	0.65712	0.646	0.1872
150	10.004	6.1315	0.60144	1800.4	1.3319	0.95621	0.977	0.88897	0.18621	0.17963	0.6468
151	7.2786	5.6864	-0.70644	2065.3	1.3096	2.1114	0.88659	0.65894	0.64638	0.9533	0.17576
152	7.0625	5.0306	0.88838	2004.3	3.3771	1.6455	0.65842	0.18734	0.17977	0.14185	0.9527
153	7.3807	4.394	0.46244	1941.7	0.90323	0.77801	0.18664	0.64891	0.95287	0.75049	0.14379
154	5.5048	4.3793	0.1871	1840.8	3.6119	1.6096	0.64507	0.17691	0.14233	0.086316	0.75248
155	7.5409	6.1992	-0.37093	1939.2	3.2128	1.7536	0.17711	0.95118	0.75482	0.23203	0.087912
156	6.3404	2.9992	0.17419	1838.4	2.2216	0.88998	0.95059	0.14242	0.086579	0.7641	0.23087
157	6.1266	7.8565	-0.38192	2039.2	0.90356	1.2436	0.14252	0.75409	0.23232	0.28118	0.76162
158	6.9607	6.0621	0.75051	1826.1	2.1818	1.6866	0.75153	0.088803	0.76344	0.67984	0.28492
159	8.1312	5.1999	-0.42699	1963.6	0.90353	1.6433	0.08683	0.2337	0.28051	0.53945	0.67884
160	5.6327	3.4208	0.29815	1803.9	3.5015	2.797	0.23407	0.76141	0.67786	0.56739	0.53767
161	7.5186	5.1585	-0.61352	1852.5	0.90344	1.3361	0.76128	0.2824	0.53504	0.20679	0.5676
162	7.238	3.3742	-0.3168	1966.2	2.6324	1.4226	0.28348	0.67679	0.56754	0.4036	0.20555
163	8.0541	6.3283	0.31264	1864.5	0.90326	1.4115	0.6774	0.5359	0.20907	0.99995	0.40382
164	1.2445	3.2461	-0.26077	1945.8	0.9037	1.4326	0.53853	0.56976	0.40303	0.42927	0.99514
165	7.6782	5.5608	0.21202	1917.8	2.6793	1.4902	0.56716	0.20581	0.99747	0.22505	0.42972
166	4.29	3.0393	0.042953	1923.5	0.90386	1.5815	0.20914	0.40267	0.42578	0.85881	0.22675
167	7.0772	3.5934	0.082558	1846.9	2.304	0.85035	0.40148	0.99633	0.22882	0.69465	0.85692
168	8.1091	5.5989	-0.3463	1890.8	1.6854	1.4043	0.99946	0.429	0.85968	0.002816	0.69442
169	6.5584	3.7778	-0.11436	2150	1.8197	1.1554	0.42931	0.22809	0.69398	0.66467	0.004499
170	7.6312	5.2625	0.9848	1896.2	0.90363	0.77864	0.22617	0.85547	0.000323	0.77513	0.66304
171	6.7437	4.737	-0.08534	1851.6	1.1755	0.77818	0.85851	0.69354	0.66257	0.19757	0.77725
172	5.6544	4.8472	-0.32558	1992.9	3.6966	1.6616	0.69111	0.003257	0.77945	0.39292	0.19571
173	6.0848	3.487	0.42615	1949.6	1.2557	1.5596	0.003656	0.66345	0.19765	0.72304	0.3905
174	10.67	4.2364	0.23043	1675.6	0.90369	1.1742	0.66204	0.77506	0.39062	0.68608	0.72139
175	19.991	8.772	-1.4274	1942.6	3.1009	1.3104	0.77547	0.19838	0.72232	0.98368	0.68895
176	5.7069	4.3221	0.1918	1969.8	2.3748	1.2113	0.19977	0.39453	0.68752	0.45485	0.98231
177	5.8428	3.5686	0.32826	1844.1	0.903	1.2221	0.39164	0.72283	0.98031	0.50929	0.45473
178	14.033	5.9529	-0.36243	1888.8	2.2491	2.6986	0.72173	0.68745	0.45427	0.49792	0.50512

Table A-1. Stochastic Parameter Values (Continued)

real. #	KDUVO	KDUAL	GWSPD	BULKDENSITY	CORAL	CORVO	SRC4Y	SRC4X	SRC3X	SRC2Y	SRC2X
179	6.969	5.3194	-0.1308	1955.7	2.7377	2.7263	0.68811	0.98268	0.5089	0.51067	0.49559
180	4.8706	1.7248	0.26453	1948.5	0.90359	0.77843	0.98291	0.45113	0.49716	0.56127	0.51465
181	7.2743	5.2177	0.22384	2076	1.14	1.249	0.45143	0.50761	0.51411	0.63635	0.56495
182	14.003	5.6477	0.90461	1900.3	2.4991	0.77886	0.50641	0.4978	0.56414	0.18298	0.63987
183	5.5135	3.4549	-0.05683	1911.2	2.3608	1.9716	0.49998	0.51184	0.63908	0.49347	0.18035
184	7.4711	4.1951	0.010673	1909.7	3.6328	1.9303	0.51124	0.56314	0.18468	0.33757	0.49318
185	6.7534	5.4358	-0.00257	1912.2	1.3576	1.3653	0.56096	0.63868	0.49378	0.095147	0.339
186	7.6828	5.3098	0.015309	1922.2	1.5741	0.77876	0.63832	0.18425	0.33664	0.02893	0.098947
187	8.1434	7.9127	0.072474	1937	1.5171	0.98742	0.18035	0.4943	0.0968	0.70491	0.029299
188	6.7702	4.4289	0.16452	1839.5	1.5859	1.8086	0.49056	0.33741	0.026781	0.61604	0.70419
189	7.4674	4.637	-0.37947	1909	1.7945	0.77888	0.33874	0.096534	0.70431	0.35289	0.61966
190	6.9612	4.5943	-0.00717	1877.3	2.1272	1.6963	0.096831	0.029759	0.61591	0.43939	0.35146
191	6.5706	4.6492	-0.19088	1809	0.90355	1.1569	0.028917	0.70069	0.35311	0.37338	0.43794
192	6.4819	4.8274	-0.50508	1763.2	1.5065	0.77832	0.70456	0.6185	0.43943	0.38091	0.37255
193	6.2727	5.1259	-1.2166	1951.2	0.921	1.7169	0.61513	0.35035	0.37237	0.96251	0.38203
194	2.3318	3.4099	0.23869	1933.3	0.9033	2.5605	0.35362	0.43951	0.38267	0.96816	0.96337
195	6.6827	4.5729	0.13794	1880	0.90309	1.4774	0.43658	0.37213	0.96475	0.063027	0.96716
196	6.4829	3.9869	-0.176	1897.5	2.4068	1.766	0.37128	0.38098	0.96775	0.39953	0.061097
197	5.7686	3.0866	-0.07449	1884.9	2.0457	1.2188	0.38369	0.964	0.061914	0.1285	0.3971
198	6.1081	2.3548	-0.15273	1887.1	0.98501	1.6249	0.96476	0.96823	0.39947	0.83442	0.12711
199	6.5657	5.3679	-0.14182	2047.7	1.3082	1.601	0.96697	0.061409	0.12965	0.82773	0.83158
200	6.7453	5.0355	0.79534	2055	1.0649	1.5667	0.061482	0.39772	0.83314	0.46639	0.82855

Table A-1. Stochastic Parameter Values (Continued)

real. #	SRC3Y	SRC1Y	SRC1X	HAVO	LDISP	KDRAVO	KDRAAL	KD_PU_VO	KD_PU_AL	KD_PU_C0L
1	0.83233	0.24005	0.80624	14.221	1.9903	812.85	440.3	109.47	108.87	4.8775
2	0.82718	0.80526	0.13308	4.609	1.6863	438.05	704.33	129.6	92.939	5.0531
3	0.46566	0.13442	0.73247	9.336	1.0289	707.27	688.4	38.71	77.02	4.2620
4	0.11361	0.73275	0.34383	3.211	0.54985	688.19	663.39	79.503	109.71	4.5371
5	0.24003	0.34009	0.049709	6.490	2.4022	663.62	323.7	93.181	124.51	4.2375
6	0.80576	0.046205	0.7459	6.106	2.2194	321.01	742.97	102.03	100.9	4.3941
7	0.13452	0.74864	0.93901	5.590	1.7185	741.48	430.16	101.08	112.08	5.1399
8	0.73186	0.93694	0.55457	2.180	1.8825	429.34	525.79	96.651	94.367	4.2041
9	0.34145	0.55106	0.79371	7.319	1.7536	526.19	626.36	116.43	106.1	4.6918
10	0.047266	0.79274	0.37606	3.153	1.7716	626.1	256.08	94.687	105.03	5.1004
11	0.74875	0.37598	0.67186	3.965	3.3158	255.36	346.45	94.86	104.08	4.8134
12	0.9384	0.67431	0.65349	4.865	3.4105	344.48	252.75	107.78	89.193	3.8495
13	0.55426	0.65427	0.62915	1.599	0.85794	250.6	293.32	122.12	107.76	5.3892
14	0.79285	0.62833	0.24857	2.380	1.8079	289.57	644.32	104.11	93.974	4.9578
15	0.37977	0.24591	0.71151	1.533	1.1538	644.32	240.83	58.263	97.825	3.8205
16	0.67304	0.71226	0.36864	1.911	2.7247	241.27	425.57	112.1	102.21	5.5740
17	0.65016	0.36852	0.47149	5.094	2.7109	426.26	632.99	96.424	85.471	4.6028
18	0.62547	0.47303	0.58007	1.476	1.9399	631.8	489.65	114.56	90.109	4.8036
19	0.24894	0.58477	0.17326	3.117	1.099	489.47	166.43	98.307	85.408	4.6142
20	0.71268	0.17148	0.2719	4.941	1.4758	166.72	727.65	109.97	87.421	5.1106
21	0.36671	0.27358	0.16723	3.642	2.6485	726.02	580.16	67.302	102.9	4.9749
22	0.47389	0.16561	0.2131	0.834	1.1613	578.39	161.12	123.13	84.683	4.4990
23	0.58452	0.21367	0.60303	7.035	2.4699	159.62	829.77	91.467	93.664	5.2601
24	0.17185	0.60264	0.15762	4.458	1.6923	830.57	376.18	96.067	102.68	4.8586
25	0.27162	0.15986	0.36181	0.809	0.73272	375.4	481.98	91.381	96.375	4.6846
26	0.16981	0.36202	0.59096	9.867	2.4972	479.18	381.72	96.797	79.051	5.5658
27	0.21102	0.59494	0.43437	2.680	3.1595	381.7	638.55	129.53	107.22	5.6739
28	0.60015	0.43132	0.070798	3.579	2.1024	638.67	590.61	90.95	100.17	4.4166
29	0.15677	0.070876	0.69583	2.681	2.615	593.85	328.84	112.58	78.996	5.5237

Table A-1. Stochastic Parameter Values (Continued)

real. #	SRC3Y	SRC1Y	SRC1X	HAVO	LDISP	KDRAVO	KDRAAL	KD_PU_VO	KD_PU_AL	KD_PU_C0L
30	0.36158	0.69708	0.53266	5.000	1.7618	326.95	678.7	108.37	113.21	5.4983
31	0.59138	0.53117	0.065333	4.581	2.3314	677.42	509.58	94.841	91.582	4.9849
32	0.43049	0.068262	0.81193	2.210	2.2912	511.98	422.18	90.197	96.013	4.1083
33	0.074454	0.81122	0.30876	5.930	2.2459	422.1	820.66	58.974	91.679	5.9685
34	0.6978	0.3088	0.42281	3.841	1.4862	822.12	909.44	110.04	102.71	4.8878
35	0.53021	0.42103	0.3129	3.077	2.4162	909.46	300.12	126.65	100.7	5.6821
36	0.068291	0.31034	0.59624	9.575	1.7497	298.61	796.55	93.625	89.246	5.0253
37	0.81435	0.59788	0.5451	12.473	1.9504	794.22	779.79	103.89	104.64	5.6522
38	0.30796	0.54611	0.25403	1.983	2.1609	779.57	599.93	120.88	97.323	4.9442
39	0.42208	0.25262	0.64219	8.726	1.2938	599.68	224.14	73.613	93.554	5.4314
40	0.31087	0.64499	0.45689	8.364	1.5451	222.51	987.6	191.27	112.55	5.5843
41	0.59771	0.45948	0.35958	4.645	1.2728	987.07	529.6	124.49	119.63	5.2355
42	0.54692	0.35889	0.80226	1.284	1.4037	530.28	914.05	93.929	87.977	4.8650
43	0.2541	0.80481	0.89657	17.394	2.1923	910.33	620.16	179.01	110.89	5.3636
44	0.64387	0.89955	0.2211	4.001	1.2504	620.04	891.15	124.42	110	4.6416
45	0.45648	0.22056	0.77458	12.785	1.7351	891.41	571.89	54.883	101.28	5.0719
46	0.35594	0.77106	0.75751	4.813	2.1801	571.12	746.07	106.71	83.562	5.6180
47	0.8044	0.75705	0.55876	11.844	1.8744	747.9	837.75	111.76	135.96	3.7922
48	0.89716	0.55861	0.13615	4.372	0.91376	835.64	667.68	91.97	98.093	5.4487
49	0.22083	0.1361	0.98634	7.493	2.3907	670.09	514.51	98.776	120.19	5.5328
50	0.7728	0.98683	0.4783	9.902	2.0576	514.64	715.01	126.99	102.03	4.7887
51	0.75745	0.47635	0.90182	5.705	0.88603	712.87	399.44	83.962	118.01	5.5539
52	0.5575	0.90124	0.57823	3.901	2.6678	399.58	628.62	112.43	99.752	4.5138
53	0.13948	0.57826	0.87579	6.717	1.6269	627.55	864.64	126.74	107.99	4.6338
54	0.9886	0.87902	0.52465	2.859	1.849	864.15	150.75	258.23	113.65	4.4139
55	0.47636	0.52426	0.71777	4.903	1.6384	151.12	756.56	118.39	104.29	5.0128
56	0.90226	0.71853	0.81891	10.737	2.1894	754.26	803.41	127.89	97.509	3.7624
57	0.57565	0.81586	0.63343	0.739	2.0898	806.44	474.02	128.39	106.51	3.9613
58	0.87726	0.63481	0.46333	7.676	1.5057	476.79	818.8	83.831	92.659	4.7692
59	0.52271	0.46349	0.68074	9.049	2.2752	818.62	336.85	88.254	102.42	5.6955
60	0.71539	0.68244	0.33489	3.526	1.9216	336.49	394.56	122.77	115.57	5.6712

Table A-1. Stochastic Parameter Values (Continued)

real. #	SRC3Y	SRC1Y	SRC1X	HAVO	LDISP	KDRAVO	KDRAAL	KD_PU_VO	KD_PU_AL	KD_PU_C0L
61	0.81858	0.33278	0.58895	9.446	1.7264	394.68	294.57	81.37	78.053	4.3374
62	0.63424	0.58517	0.84543	2.290	2.6399	296.99	615.74	100.52	108.66	5.6464
63	0.46136	0.84982	0.056311	2.831	2.956	613.08	148.46	121.59	111.49	5.3243
64	0.68066	0.057841	0.72978	1.928	1.426	145.92	195.85	75.673	95.797	3.5267
65	0.33153	0.72969	0.78261	4.799	2.5599	198.3	467.99	108.21	112.44	4.4555
66	0.58726	0.78325	0.4167	0.690	2.5179	465.66	924.72	96.256	89.718	3.9177
67	0.84941	0.41653	0.79797	1.040	2.1075	926.22	903.86	105.75	92.376	4.5297
68	0.058578	0.79803	0.26066	3.457	1.1735	903.5	273.95	102.44	87.717	4.9694
69	0.728	0.26347	0.32972	13.311	3.6979	272.15	883.85	45.587	101.83	4.7835
70	0.78038	0.32548	0.21687	12.414	1.9618	885.32	702.03	43.519	77.264	4.9502
71	0.41596	0.21798	0.57346	1.751	2.9809	700.89	121.54	105.41	81.802	5.1614
72	0.79808	0.57228	0.054074	11.625	2.1481	119.34	314.87	94.86	95.495	5.8209
73	0.26002	0.052024	0.10657	6.408	2.8736	311.66	183.97	108.3	121.95	5.6385
74	0.32626	0.10795	0.40776	0.436	2.039	183.08	339.8	114.71	119.24	4.0269
75	0.21674	0.40841	0.91631	2.097	2.4268	339.18	589.62	63.997	86.459	5.6138
76	0.57425	0.91592	0.89188	0.955	2.6786	588.04	473.21	128.28	117.71	5.4099
77	0.053163	0.89356	0.19002	2.324	2.2583	471.84	575.22	84.112	105.81	5.6053
78	0.10825	0.19055	0.87486	4.521	1.933	572.68	648.88	112.64	73.738	5.9754
79	0.40749	0.87385	0.66564	3.502	2.361	646.51	950.64	76.018	88.667	3.3825
80	0.91533	0.66936	0.024592	4.407	1.6742	952.86	877.79	15.936	80.824	5.1987
81	0.89182	0.024802	0.238	5.160	2.1683	877.91	212.04	90.958	89.887	3.8823
82	0.19247	0.23768	0.092733	14.707	2.7659	208.9	860.23	125.16	100.63	4.5064
83	0.8716	0.093798	0.2697	11.234	0.82441	860.11	736.5	93.682	95.705	5.4698
84	0.66663	0.26782	0.54484	1.175	2.4578	738.68	855.93	123.3	100.03	3.2578
85	0.022039	0.54487	0.41286	10.610	2.5864	854.64	993.11	113.89	103.17	5.7672
86	0.23834	0.41297	0.5255	7.247	1.8464	994.47	110.54	118.18	126.14	4.6235
87	0.09303	0.52693	0.60617	10.538	2.6304	110.62	659.13	299.8	116.81	3.6374
88	0.26994	0.6098	0.94768	18.734	1.5209	658.39	174.16	120.3	82.794	4.5614
89	0.54397	0.94692	0.8623	0.348	1.6666	172.55	331.74	120.44	115.37	3.9564
90	0.41441	0.86116	0.12201	5.461	1.4188	329.82	767.45	106.38	107.69	4.8941
91	0.52656	0.12189	0.84487	0.899	2.1415	766.83	108.83	104.64	115.02	5.5922

Table A-1. Stochastic Parameter Values (Continued)

real. #	SRC3Y	SRC1Y	SRC1X	HAVO	LDISP	KDRAVO	KDRAAL	KD_PU_VO	KD_PU_AL	KD_PU_C0L
92	0.60929	0.84095	0.70556	2.267	0.76916	108.02	939.97	177.71	139.22	4.3696
93	0.94947	0.70568	0.83988	7.963	1.062	937.88	389.58	100.55	71.507	5.6284
94	0.8607	0.83864	0.99131	0.244	1.8277	388.79	129.98	92.897	103.93	3.6732
95	0.12496	0.99254	0.012151	13.874	3.0474	127.83	358.17	113.61	80.093	4.8986
96	0.84424	0.014322	0.6206	2.779	2.9291	359.12	191.36	125.2	89.546	5.6454
97	0.70863	0.62212	0.081579	0.537	1.3502	192.1	534.33	123.97	109.3	4.1823
98	0.83814	0.081611	0.25537	2.518	2.8488	534.89	840.2	69.572	68.715	4.1468
99	0.99153	0.25963	0.74219	1.040	2.3268	841.52	281.38	118.18	124.07	3.7073
100	0.01084	0.74266	0.00638	4.070	0.4986	282.1	868.25	94.204	92.211	5.5092
101	0.6226	0.008537	0.9333	10.121	1.4611	866.27	135.17	33.92	74.655	3.9941
102	0.082755	0.93024	0.32214	1.816	1.0042	131.91	540.77	81.289	90.751	4.9205
103	0.25772	0.32134	0.031583	10.910	1.5392	539	882.9	17.356	81.538	4.5873
104	0.74379	0.031874	0.28828	0.588	2.0766	880.48	236.85	95.217	98.315	5.7497
105	0.0066	0.28693	0.10244	4.092	1.833	238.35	232.4	121.57	113.88	5.8007
106	0.9304	0.10181	0.48385	11.375	2.0524	232.95	136.31	34.896	86.943	5.8716
107	0.32214	0.48365	0.82219	1.424	2.2089	139.73	790.5	109.12	116.02	5.9238
108	0.034931	0.82127	0.20133	1.361	3.2142	789.56	205.25	16.508	75.807	4.2303
109	0.28848	0.20343	0.85064	0.647	2.8115	204.97	554.05	83.719	98.454	4.5744
110	0.10153	0.85494	0.037852	8.580	1.131	552.51	367.97	106.86	117.35	4.6150
111	0.48488	0.039425	0.48927	1.134	2.7541	369.82	936.25	54.043	84.514	4.5945
112	0.82181	0.48703	0.86816	4.212	2.4064	935.32	947.4	101.16	84.306	4.6692
113	0.20309	0.86964	0.15423	2.581	2.735	949.48	963.04	98.817	76.071	5.4624
114	0.85318	0.15153	0.14775	13.639	3.9162	960.13	975.53	126.69	110.59	4.7348
115	0.037029	0.14723	0.043615	14.307	0.28545	973.13	244.95	80.878	82.558	5.6580
116	0.48919	0.044629	0.76977	15.467	2.2311	247.87	362.6	120.8	98.991	5.6920
117	0.86816	0.76877	0.11639	16.361	0.96482	361.16	385.18	93.073	91.229	4.9390
118	0.15324	0.11722	0.50208	1.506	1.5153	386.4	373.33	121.41	123.17	4.5446
119	0.14901	0.50107	0.29533	2.556	2.4838	370.58	412.47	115.09	124.87	3.4129
120	0.042737	0.29727	0.92996	2.757	0.24038	414.2	765.76	96.594	127.87	5.6875
121	0.76893	0.92623	0.94325	2.617	3.1079	763.07	449.47	204.67	130.96	5.5441
122	0.11682	0.94167	0.9558	2.972	1.6573	450.84	893.8	98.19	85.118	5.1761

Table A-1. Stochastic Parameter Values (Continued)

real. #	SRC3Y	SRC1Y	SRC1X	HAVO	LDISP	KDRAVO	KDRAAL	KD_PU_VO	KD_PU_AL	KD_PU_C0L
123	0.50185	0.95667	0.97337	7.856	0.63252	896.39	919.94	90.724	90.898	4.8374
124	0.29877	0.97469	0.16451	3.297	1.5766	920.24	564.89	81.361	92.057	4.8294
125	0.9262	0.16335	0.29046	12.053	1.0562	566.15	347.78	105.17	91.285	5.7118
126	0.94249	0.29347	0.31994	13.073	1.963	349.81	116.51	94.688	93.119	3.8728
127	0.95651	0.31629	0.30057	4.359	2.6953	115.03	915.08	98.763	109.14	5.9370
128	0.97227	0.30062	0.34665	2.407	1.3783	917.36	808.56	120.32	94.609	5.6665
129	0.16375	0.34816	0.73806	0.396	2.7931	807.17	653.26	56.345	118.5	5.3010
130	0.2908	0.73514	0.38982	12.887	0.64424	650.78	504.69	122.96	121.56	4.3202
131	0.31825	0.38902	0.88375	9.230	1.9739	502.29	497.53	96.43	99.609	5.2718
132	0.30346	0.8811	0.91445	5.287	2.8316	497.26	928.08	109.77	90.397	4.2901
133	0.34536	0.91351	0.51775	3.793	1.2279	932.09	167.74	96.177	71.682	5.8432
134	0.73979	0.51891	0.27618	3.753	1.2149	170.49	978.15	63.713	120.69	4.1248
135	0.38918	0.27944	0.017364	13.549	0.71527	981.81	900.52	33.543	111.8	5.4871
136	0.88142	0.018064	0.90692	0.871	2.5438	899.31	692.85	106.49	103.46	3.9044
137	0.91369	0.90812	0.78832	16.548	1.1016	691.49	268.16	89.996	96.932	4.4487
138	0.51854	0.78574	0.61055	12.129	2.0081	266.74	684.08	122.92	96.697	5.5024
139	0.27967	0.61066	0.44885	6.175	1.6021	682.82	261.21	108.67	122.43	4.5558
140	0.018437	0.44944	0.44473	1.681	3.1047	259.8	957.8	62.316	79.558	5.3464
141	0.90992	0.44492	0.92486	6.018	3.1925	959.02	228.62	117.29	132.79	4.9658
142	0.78977	0.92496	0.077725	1.626	3.2736	228.36	778.38	115.04	118.79	4.9995
143	0.61162	0.077621	0.97922	14.966	3.4137	776.75	180.78	105.11	105.23	4.3784
144	0.44672	0.97709	0.88689	1.355	1.2599	177.45	308.05	97.168	86.269	4.7661
145	0.44483	0.88694	0.65537	8.294	1.5851	307.83	787.18	29.899	104.91	5.9886
146	0.92381	0.65965	0.18644	0.932	1.6389	788.47	355.4	94.639	85.829	4.8111
147	0.077437	0.18566	0.64725	2.079	1.6102	354.67	709.36	126.18	127.33	4.4372
148	0.97688	0.64518	0.17796	8.446	1.7018	710.03	584.97	112.95	83.89	5.6345
149	0.88764	0.17513	0.95462	2.479	2.4779	585.05	611.31	110.25	109.74	5.3747
150	0.65902	0.95013	0.14251	6.661	1.7862	610.1	285.37	52.359	80.593	3.1110
151	0.18671	0.14065	0.75367	4.480	2.8909	285.78	461.67	21.46	88.309	5.3096
152	0.64903	0.75082	0.085452	4.723	3.0224	462.78	999.51	114.38	110.43	5.5276
153	0.17695	0.087076	0.23365	1.871	2.0351	999.67	483.77	93.823	90.563	4.3465

Table A-1. Stochastic Parameter Values (Continued)

real. #	SRC3Y	SRC1Y	SRC1X	HAVO	LDISP	KDRAVO	KDRAAL	KD_PU_VO	KD_PU_AL	KD_PU_C0L
154	0.9512	0.23467	0.76487	3.420	1.5586	484.97	306.89	113.63	106.18	4.7466
155	0.14091	0.76127	0.2801	19.238	0.38107	306.1	872.4	127.4	100.45	5.4393
156	0.75336	0.28179	0.67652	3.611	3.0035	871.12	725.39	116.87	101.58	5.3692
157	0.08953	0.67582	0.53817	2.021	2.5998	721.14	103.99	72.216	87.341	5.9484
158	0.23059	0.53548	0.56945	11.103	2.2116	101.08	695.4	40.23	95.224	4.8526
159	0.7646	0.56552	0.20822	6.888	1.8999	698.34	798.89	108.46	148.17	4.9279
160	0.28497	0.20529	0.40255	0.176	1.8931	798.55	277.25	197.34	96.195	4.9132
161	0.67504	0.40101	0.99992	6.311	3.0661	275.58	455.23	102.95	88.301	4.9346
162	0.53552	0.99938	0.42575	8.932	0.9365	455.05	748.2	111.1	116.45	4.9929
163	0.56653	0.42685	0.22858	1.774	3.5397	751.7	720.14	63.445	106.92	5.2455
164	0.20863	0.22935	0.85861	3.334	2.9012	718.67	983.76	123.47	63.959	4.3054
165	0.40195	0.85843	0.69288	7.557	2.3059	984.15	509.34	118.65	105.54	4.9098
166	0.99884	0.69375	0.001538	6.803	1.3307	505.59	556.96	116.61	111.26	4.6501
167	0.4295	0.00151	0.66146	16.959	2.2877	556.95	548.66	68.395	86.894	3.9386
168	0.22599	0.66498	0.77751	3.825	1.3026	547.43	562.63	110.89	94.915	3.5547
169	0.8586	0.77867	0.19755	4.276	3.2398	561.48	608.45	100.01	108.24	5.4048
170	0.69437	0.1954	0.39244	4.192	1.1982	608.46	671.99	99.386	106.64	5.1931
171	0.001231	0.39299	0.72459	4.305	2.514	671.82	265.99	231.89	134.49	4.6748
172	0.6606	0.72016	0.68846	4.690	0.97624	262.5	541.5	120.61	97.076	4.8286
173	0.77628	0.68789	0.98023	5.795	1.4467	545.05	402.29	113.14	99.164	4.7081
174	0.19637	0.98146	0.45478	1.678	2.5403	403.25	185.89	54.005	98.867	4.7295
175	0.39311	0.45483	0.50829	4.127	1.5639	189.74	125.45	122.69	99.409	5.8882
176	0.72453	0.50536	0.49776	2.894	2.3457	124.24	734.44	100.24	101.46	5.9004
177	0.68917	0.49845	0.51009	0.990	2.0682	731.22	654.92	95.999	104.55	3.8036
178	0.98396	0.51107	0.56335	0.488	2.1292	653.57	416.24	116.28	86.075	4.7517
179	0.45418	0.56394	0.63905	7.186	1.394	416.08	492.31	103.99	98.647	4.0583
180	0.50686	0.6384	0.18176	5.367	1.8196	493.18	435.53	118.77	92.833	5.6042
181	0.49959	0.18351	0.49236	3.002	4.0513	437.08	445.56	34.207	81.084	5.5955
182	0.51036	0.49117	0.33981	3.713	1.862	446.28	964.34	104.91	74.407	4.8724
183	0.56418	0.33823	0.098419	3.186	1.4389	965.64	970.23	124.85	107.46	3.9848
184	0.63522	0.098359	0.029148	3.280	2.8066	970.12	157.45	94.654	103.63	4.4748

Table A-1. Stochastic Parameter Values (Continued)

real. #	SRC3Y	SRC1Y	SRC1X	HAVO	LDISP	KDRAVO	KDRAAL	KD_PU_VO	KD_PU_AL	KD_PU_C0L
185	0.18001	0.028657	0.7049	15.790	2.3825	155.45	458.25	63.226	93.339	5.5682
186	0.49328	0.70242	0.61821	15.872	-0.00165	458.27	216.04	106.68	96.562	4.0889
187	0.33932	0.6174	0.35471	0.779	2.3105	213.33	848.03	116.92	94.132	5.4564
188	0.095855	0.35206	0.43994	3.371	2.5777	848.42	845.9	129.27	94.576	4.6564
189	0.025006	0.43563	0.37403	1.236	1.3627	843.72	521.17	120.76	129.18	3.7290
190	0.70291	0.37478	0.38384	10.428	1.7917	519.67	200.06	120.91	130.24	5.4786
191	0.61896	0.38398	0.96484	10.269	2.4475	199.43	316.94	103.58	78.41	5.7810
192	0.35329	0.96202	0.96738	3.958	2.3695	320.09	827.3	114.03	95.042	4.9796
193	0.43628	0.9654	0.062055	1.092	3.5458	826.09	219	85.037	83.247	5.5478
194	0.37169	0.061335	0.39868	2.121	1.9109	218.91	760.81	93.183	114.66	4.7098
195	0.38195	0.39667	0.12538	9.702	2.0123	761.17	408.2	93.174	114.11	5.3385
196	0.96264	0.12797	0.83326	1.247	1.9917	406.69	142.25	106.22	97.678	5.2878
197	0.96574	0.8321	0.82688	7.725	2.0208	144.67	773.83	28.908	82.048	5.2122
198	0.063634	0.82798	0.46962	2.930	2.1217	772.31	943.72	93.594	88.773	4.4856
199	0.39766	0.46669	0.11218	0.664	2.2674	943.38	595.47	114.98	113.09	5.4216
200	0.12612	0.1129	0.24114	8.080	1.3256	596.34	813.08	109.78	83.544	4.6979

Table A-1. Stochastic Parameter Values (Continued)

real. #	KD_AM_VO	KD_AM_AL	KD_AM_COL	KD_CS_VO	KD_CS_AL	KD_CS_COL	CONC_COL
1	6488.6	5700.9	5.6503	4168	178.08	3.4892	-4.4407
2	7769.2	6721	5.8331	2766.9	799.65	2.9211	-4.4107
3	5702.4	5037	5.9814	5772.4	945	3.0682	-8.7573
4	6712.4	6161.5	5.0086	6542.1	653.54	3.3114	-7.4077
5	5039.6	6078.9	5.4456	5006.4	833.8	2.6497	-8.4926
6	6166.2	5984.6	4.9920	5951.3	521.65	2.8072	-5.4465
7	6096	4478.6	5.2380	4312.3	744.24	2.6360	-5.476
8	5984.4	6343.7	6.0000	5475.1	729.51	2.7197	-7.1382
9	4483.4	4998.1	4.9762	5389.5	710.35	3.3486	-8.5426
10	6347.6	5398.5	5.6375	5296.6	405.6	2.6160	-8.0268
11	5003.5	5816.1	5.9903	3786	773.96	2.9143	-5.6308
12	5395.8	4080.1	5.7619	5640.9	512.41	3.3299	-8.4685
13	5804	4586.6	4.7149	4258.3	596.07	2.9856	-6.0663
14	4084.8	4056	6.3464	4687.9	676.07	2.3959	-7.6293
15	4591.2	4298.1	5.9175	5127.8	330.43	3.4717	-8.8063
16	4071.1	5882.9	4.6899	3493.9	431.82	3.2197	-6.018
17	4312.5	3986.6	6.5623	3882.3	328.73	2.3635	-4.6686
18	5887.7	4981.3	5.5315	3471	371.58	3.5901	-6.7922
19	3997.5	5842.8	5.7451	3656.9	692.74	2.8522	-5.715
20	4964.8	5254.5	5.5465	5206.8	318.51	2.9747	-7.4927
21	5841.3	3352.8	5.9978	3424.7	509.22	2.8589	-6.3092
22	5249.8	6267.7	5.9360	4246.1	684.76	3.3399	-6.3854
23	3350.7	5629.4	5.3838	5164.9	563.37	3.2550	-6.4937
24	6266.9	3265	6.1931	4532.5	211.99	2.7812	-8.015
25	5614	6838	5.8089	3093.9	761.1	3.4056	-6.1406
26	3268.8	4754.3	5.6274	5569	639.2	3.0266	-7.5392
27	6830	5203.4	6.5441	4917.6	203.9	2.9089	-7.1142
28	4752.1	4769.3	6.6739	3067.4	847.86	3.5824	-6.6703
29	5208.6	5863.3	5.2765	6042	461.44	3.6609	-8.3015
30	4760.6	5676.8	6.5011	4035.3	556.39	2.7344	-7.9093
31	5868	4504.5	6.4728	4490.8	466.35	3.5520	-8.3327

Table A-1. Stochastic Parameter Values (Continued)

real. #	KD_AM_VO	KD_AM_AL	KD_AM_COL	KD_CS_VO	KD_CS_AL	KD_CS_COL	CONC_COL
32	5686.4	6049.8	5.9494	4039.5	688.99	3.5412	-8.1408
33	4496.5	5340.1	4.9233	5173.5	651.93	3.2668	-6.5819
34	6054.1	4946	6.9605	4978.7	411.96	2.5760	-8.3777
35	5335.9	6784.5	5.8382	3800	720.52	3.9447	-7.556
36	4954.1	7395.9	6.6776	5350.2	582.95	3.0918	-6.6373
37	6768.2	4367.7	5.9759	4628	502.03	3.6629	-7.2777
38	7399.6	6606.1	6.6522	4233	839.43	3.3045	-8.7023
39	4349	6544.1	5.9085	5999.7	916.61	3.6457	-6.2199
40	6613.4	5717.4	6.3962	6377.4	383.48	3.2028	-6.8793
41	6556	3873.3	6.5717	3691.6	818.98	3.4953	-8.7381
42	5719.5	8732.1	6.1461	5871.8	808.27	3.5966	-5.5862
43	3858.1	5413.4	5.8195	5824.7	660.06	3.3930	-7.7721
44	8721.8	7419.7	6.3075	5026.1	294.01	3.0345	-7.3063
45	5413.9	5800.7	5.5809	3349.8	991.22	3.4557	-7.745
46	7437.8	7226.2	5.9859	6739.4	598.1	2.8849	-6.6174
47	5796.5	5589.3	6.6128	4704.9	919.06	3.3241	-6.8126
48	7243.6	6357.7	4.6388	6398.1	672.8	3.6195	-7.9985
49	5589.2	6861.8	6.4183	5104.8	899.64	2.3345	-6.4285
50	6364.8	6003.9	6.5159	6302.1	634.71	3.5066	-7.1708
51	6866	5353.2	5.7348	4883.7	777.9	3.5638	-7.5752
52	6008.3	6205.2	6.5366	5656.5	852.87	2.9709	-5.6643
53	5358	4858.7	5.4150	6057.5	712.71	3.5795	-5.0276
54	6218.9	5834.7	5.5775	5310.3	586.49	2.7970	-8.1064
55	4843	7046.9	5.2695	4642.6	750.31	2.8776	-5.8657
56	5831.9	3132.8	5.9717	5519.3	484.63	2.7310	-5.9515
57	7035.9	6410	4.6104	4131	681.99	3.2964	-6.7658
58	3173.9	6675	4.8343	5133.9	873.87	2.3122	-8.4411
59	6397.3	5193.9	5.7110	6175.2	194.82	2.4968	-4.1002
60	6670.5	6733.1	6.6972	3036.4	784.86	2.9609	-7.0941
61	5191.2	4558.9	6.6712	5688.1	825.8	3.6766	-4.9691
62	6755	4836.8	5.1367	5911.1	550.47	3.6582	-6.6998

Table A-1. Stochastic Parameter Values (Continued)

real. #	KD_AM_VO	KD_AM_AL	KD_AM_COL	KD_CS_VO	KD_CS_AL	KD_CS_COL	CONC_COL
63	4559.2	4322.6	6.6454	4468.5	836.11	2.6876	-5.161
64	4826	5767.5	6.2577	5976.8	421.28	3.6429	-6.9188
65	4342.6	3093.2	4.3501	3837.3	477.44	3.4355	-6.1259
66	5774	3650.4	5.3404	4101.5	378.03	2.1519	-5.5367
67	3112.8	5143.1	4.7901	3677.3	668.9	2.7602	-6.4733
68	3652.9	7554.3	5.4249	5088.1	186.91	2.4561	-7.1524
69	5141.2	7336	5.9355	3018.3	260.88	2.8035	-6.2729
70	7565.7	4199.1	5.7202	3230.6	545.33	3.2382	-7.6777
71	7361.4	7210.9	5.9101	4422.1	931.75	2.9685	-6.6509
72	4211.5	6137.8	6.0374	6460.7	911.36	3.2124	-5.3511
73	7212.3	2536.1	6.8306	6348.8	351.33	3.3517	-8.7724
74	6144.2	4428.3	6.6335	3560.8	896.71	3.6989	-6.0952
75	2583	3502.6	4.8833	6283.9	739.45	3.6343	-5.7992
76	4435.6	4576.3	6.6053	5466.5	142.3	2.5393	-7.3313
77	3519.2	5666.3	6.3674	1332.8	399.64	3.6162	-5.6828
78	4580.1	5162	6.5966	3743.7	241.47	3.4880	-7.9519
79	5656.1	5596.2	6.9741	3163.1	426.23	3.6116	-7.6875
80	5172.4	5914	4.2386	3858.5	647.46	3.9614	-8.1309
81	5609.8	7944.5	6.1038	4957.3	550.07	2.0951	-6.7135
82	5912.4	7132.6	4.7531	4448.8	634.96	3.3796	-8.7844
83	7914.7	3773.6	5.4065	4893.1	697.02	2.4256	-8.5657
84	7132.3	7012.5	6.4456	5219	955.7	2.7860	-7.3649
85	3753.5	6324.4	4.1847	6566.3	885.57	3.5229	-4.8334
86	6986.5	6980.9	6.7505	6234.4	276.95	2.0594	-5.0489
87	6306.8	8979.8	5.5658	3296	872.71	3.6879	-8.2303
88	6979.8	2198.1	4.4545	6153.4	769.22	2.8735	-5.1937
89	9020.7	5962.9	5.4814	5609.9	868.01	2.2234	-6.3262
90	2223.7	3419.5	4.8231	6129.4	995.38	2.8308	-8.9159
91	5959.5	4534.1	5.8457	6760.5	122.28	2.4814	-8.049
92	3435.1	6465.6	6.5752	698.84	707.86	3.1066	-8.6293
93	4518.4	1938.8	5.1959	5287.2	226.24	3.6012	-7.9308

Table A-1. Stochastic Parameter Values (Continued)

real. #	KD_AM_VO	KD_AM_AL	KD_AM_COL	KD_CS_VO	KD_CS_AL	KD_CS_COL	CONC_COL
94	6479.5	7749.4	6.6201	3126.2	418.09	2.7010	-6.8351
95	1944.9	4815.2	4.4834	3829.2	794.98	3.6242	-7.3558
96	7738.3	2757.9	5.8567	5762.7	116.33	2.2479	-6.8801
97	4813.7	4650.8	6.6405	669.12	943.93	3.1094	-6.5674
98	2752.3	3626	4.9596	6518.4	474.28	3.6371	-4.579
99	4668.5	5430.8	4.9532	4078.5	156.07	2.6025	-5.2514
100	3590.2	6886.2	4.5261	2047.5	445.26	2.5987	-8.5003
101	5437.2	4246.3	6.4871	3955.1	253.85	2.2623	-5.3798
102	6878.3	7050	4.8636	3207.5	602.23	3.5479	-6.1694
103	4242.2	2836.9	5.8808	4724.6	855.89	2.5293	-5.4229
104	7071.8	5458.1	5.5038	6071.5	365.43	3.1555	-3.9017
105	2849	7165.5	6.7372	3615.2	879.29	2.8449	-8.9485
106	5452	3968.1	6.8082	6203.8	161.11	3.6822	-6.5045
107	7180.6	3947.5	6.8733	2313.5	607.45	3.6947	-8.6754
108	3975.9	2963	6.9243	4750.4	889.84	3.7506	-7.9714
109	3949.9	6585	4.9802	6255.2	310.82	3.8465	-6.0296
110	2961.6	3722.4	5.4942	3405.5	306.56	2.6266	-8.9706
111	6583.9	5508.2	5.5563	3396.5	167.18	2.8365	-4.7113
112	3744.8	4713.2	5.5211	2566.2	815.33	2.8642	-7.7037
113	5502.7	7651.4	5.6117	5859.1	271.76	2.8499	-8.8791
114	4707.5	7827.8	6.4298	3276	619.25	2.9020	-7.8504
115	7668.2	8061.2	5.6812	4801.1	451.04	3.5209	-8.5921
116	7875.1	8371.1	6.6551	3985.2	937.03	2.9405	-7.0702
117	8054.6	4033.3	6.6920	6498.8	952.66	3.6481	-5.5235
118	8382.8	4674.7	5.9025	6550.2	965.4	3.6725	-8.1812
119	4032.2	4794.8	5.4548	6613.1	975.16	3.1876	-5.3301
120	4682.7	4727.1	4.3159	6665.6	320.43	2.8162	-8.8483
121	4789.7	4923.1	6.6857	3448.6	446.62	2.1361	-7.0482
122	4733.6	6446.1	6.5263	3960.9	470.86	3.6683	-5.226
123	4918.3	5066.3	6.0719	4064.5	456.71	3.5702	-8.3913
124	6457.4	7265.2	5.7917	4014.1	493.65	3.3600	-8.4006

Table A-1. Stochastic Parameter Values (Continued)

real. #	KD_AM_VO	KD_AM_AL	KD_AM_COL	KD_CS_VO	KD_CS_AL	KD_CS_COL	CONC_COL
125	5073.8	7501.7	5.7853	4190.3	792.72	2.9976	-8.8265
126	7269	5566.2	6.7024	5728.5	527.66	2.9937	-5.8902
127	7503.6	4620.7	4.7329	4350.1	902.78	3.6804	-8.5362
128	5573.1	2382.2	6.9325	6325	928.67	2.4095	-6.9813
129	4622.1	7497.1	6.6599	6426.1	629.98	3.8979	-7.8073
130	2420.4	6694.9	6.2405	4867.7	435.71	3.6530	-4.7451
131	7457.5	5934.5	5.1173	3908.3	127.29	3.4250	-4.6212
132	6679.9	5310	6.1987	995.09	924.13	2.6807	-4.4973
133	5936.4	5289	5.0374	6414.2	830.59	3.4087	-4.3664
134	5304.7	7600.3	6.8506	5940.5	698.01	2.6538	-8.3547
135	5285.5	3394.1	4.9341	5233.1	575.88	3.7269	-7.8364
136	7609.5	8528.2	6.4669	4588	572.62	2.5810	-7.7319
137	3398.2	7310.8	4.7676	4566.4	934.01	3.5342	-7.7884
138	8495.8	6104.3	5.3160	6480.9	220.56	2.4374	-7.6139
139	7329.9	4160.2	6.4786	3100.4	981.25	2.7538	-6.0479
140	6102.7	6062.9	5.4698	6693	907.73	3.5430	-7.4548
141	4166.5	4117.4	6.2900	6337.7	733.62	2.8222	-5.1313
142	6062	7991.4	5.9253	5422.8	349.23	3.4512	-4.9116
143	4131.1	3906.2	5.9633	3546.9	726.94	3.2263	-6.9204
144	8021.9	6524.3	5.2175	5384.1	336.27	3.2910	-7.891
145	3903.4	3468.8	5.7076	3509.5	960.78	2.7132	-8.9265
146	6511.8	4418.7	6.9969	6586.2	300.53	2.9582	-4.9539
147	3457.3	6579.8	5.7505	3359.8	803.03	3.9972	-5.7348
148	4404.6	4630.4	5.2945	5803.8	232.94	2.9797	-6.5489
149	6571.7	6183.3	6.6243	3147.6	394.75	2.7420	-7.2133
150	4650.1	5637.9	6.3304	3734.3	809.21	3.6309	-7.225
151	6185.5	5757.9	4.0403	5840.2	439.43	3.4709	-4.7824
152	5645.3	4276.8	6.2553	3929.5	747.16	2.0382	-8.6861
153	5748.4	5137.6	6.5065	5492.1	644.24	3.4298	-4.3303
154	4277.4	9300.6	5.1614	4944.8	668.14	3.5591	-5.0869
155	5131	5222.6	5.6857	5055.9	369.36	2.6922	-6.3617

Table A-1. Stochastic Parameter Values (Continued)

real. #	KD_AM_VO	KD_AM_AL	KD_AM_COL	KD_CS_VO	KD_CS_AL	KD_CS_COL	CONC_COL
156	9534.9	4376.2	6.3997	3628.1	540.59	2.9465	-8.2544
157	5223.8	7111.8	6.3160	4397.9	998.61	3.5045	-6.4036
158	4371.9	6245.4	6.9528	6778.5	559.62	3.4647	-8.2975
159	7107.4	1511.6	5.8035	4506.4	387.34	3.9291	-4.5372
160	6262.1	6123.3	5.8876	3710.1	884.11	3.0123	-8.4216
161	1345	6652.3	5.8745	6222	759.54	3.1609	-5.9679
162	6117.2	4216	5.8954	5553.8	106.16	3.1339	-8.6561
163	6648.8	5090.8	5.9552	133.63	737.64	3.1759	-8.0717
164	4235.5	6390.9	6.1584	5437.7	821.88	3.2811	-5.909
165	5089.3	6227.3	5.0969	5895.3	357.82	3.3966	-7.878
166	6385.7	8608	5.8603	3585.5	532.58	2.6703	-6.2949
167	6223.2	5321.4	5.5933	4356.9	781.14	3.1305	-6.8452
168	8546.8	5534.4	4.8125	5669.7	755.11	2.8881	-6.7339
169	5319.2	5483.1	4.4143	5538.5	983.03	2.4729	-8.1665
170	5521.6	5542.5	6.3617	6717.7	580.56	2.1921	-7.3829
171	5495.8	5731.1	6.0755	4608.6	622.03	3.4794	-3.6765
172	5549.6	6033.4	5.6232	4816.2	613.79	3.3727	-7.2856
173	5727.9	4140	5.7782	4782.9	623.75	2.9066	-8.0952
174	6023.7	5477.9	5.6590	4843.3	664.5	2.9908	-5.2724
175	4148.4	4872.6	5.6693	5042	719.54	2.9265	-6.2288
176	5479.6	3549.9	6.8814	5344	343.37	2.9380	-8.9859
177	4879.1	2624.6	6.9058	3534	608.71	3.8063	-6.3475
178	3562.2	6292.3	4.6491	4764.2	488.67	3.8289	-5.8284
179	2691.1	5944.7	5.6981	4144.2	248.32	2.3548	-8.2179
180	6293.7	4927.5	4.8968	3190.7	150.62	2.9539	-7.4396
181	5941.6	5265.2	6.5944	1697.7	766.1	2.5494	-6.1073
182	4940.1	5004.8	6.5843	5606.2	701.74	3.6094	-6.2584
183	5261.6	5043.6	5.8215	5251.5	497.44	3.6051	-4.1654
184	5020.3	8191.8	4.8495	4209.5	568.89	3.0603	-7.1812
185	5060.4	8242.6	5.3579	4551.7	517.51	2.5082	-6.9617
186	8136.4	3206.1	6.5563	4293.2	522.73	2.7668	-7.0139

Table A-1. Stochastic Parameter Values (Continued)

real. #	KD_AM_VO	KD_AM_AL	KD_AM_COL	KD_CS_VO	KD_CS_AL	KD_CS_COL	CONC_COL
187	8289.8	5112.5	4.9119	4326.7	967.88	3.5857	-6.9487
188	3212.5	3783.9	6.4232	6625	972.79	2.5597	-6.7548
189	5101.7	6943.9	5.6010	6654.5	199	3.5129	-6.4514
190	3797.2	6920.3	4.5707	3041.1	535.96	2.8922	-8.267
191	6929.3	5377.6	6.4533	4377.2	283.4	2.2913	-7.0285
192	6916.6	3672.1	6.7846	3319.1	863.42	3.5281	-7.651
193	5384	4451.3	5.9450	6111.5	861.69	3.6906	-8.615
194	3694.1	6790.8	6.5366	6096.6	590.15	3.2638	-8.8951
195	4459	3827.5	5.6646	4668.2	262.72	3.5723	-6.1974
196	6789.6	6419	6.2765	3248.5	403.04	2.9325	-6.5318
197	3839.3	4891.3	6.2175	3762.3	844.46	3.4436	-7.5985
198	6419.4	3017.7	6.1335	6014.8	285.99	3.4185	-7.2599
199	4889	6501.1	5.3766	3329.5	788.24	3.3858	-7.5095
200	3037	7780.9	6.3784	5721.1	489.71	2.7745	-7.4663

Output DTN: SN0310T0502103.009.

INTENTIONALLY LEFT BLANK

APPENDIX B

RE-SAMPLED STOCHASTIC PARAMETER VALUES

This appendix documents the results of the SZ transport abstraction model using a re-sampling of the uncertain input parameters. The re-sampling uses the same uncertainty distributions described in Section 6.5 of this model report, but utilizes a different sampling algorithm implemented in an updated version of the GoldSim software code.

The version of the GoldSim software code ([DIRS 161572]) used to sample the uncertain parameter vectors for the SZ transport abstraction model for the simulations presented in Section 6.6 contained a difference in the sampling routine relative to Latin Hypercube Sampling. This difference was reported in CR 2222 (*Evaluate Revised LH Sampling Algorithm on the Results of ANL-EBS-PA-000009*), and the problem was corrected in subsequent versions of the GoldSim software. Appendix B documents the impact analysis of this sampling difference on the SZ transport simulation results, as indicated by the plan in CR 2222. The inputs and outputs from the SZ transport abstraction model for the analysis documented in this appendix are contained in DTN: SN0407T0502103.013.

The impact analysis for SZ radionuclide transport results consists of the following steps. The uncertain parameter inputs to the SZ transport abstraction model are re-sampled using GoldSim V8.01 SP4 (STN: 10344-8.01SP4-00, BSC 2004 [DIRS 169695]), in which the sampling difference has been corrected. The re-sampled values of the stochastic parameters are given in Table B-1. The full suite of radionuclide transport simulations is conducted using the re-sampled parameter vectors. Among the 200 realizations for the 10 groups of radionuclides, the median transport times are extracted and ranked to determine the fifth percentile, median, and 95 percentile values out of the 200 realizations. The values of median transport time for these three levels of cumulative probability are then compared to the comparable values from the base-case results (as presented in Section 6.6). The comparison of median simulated transport times at these three levels of cumulative probability is presented in Table B-2.

The impact analysis plan in CR 2222 (*Evaluate Revised LH Sampling Algorithm on the Results of ANL-EBS-PA-000009*) gives a criterion of 10 percent difference between the base case SZ transport simulation results and the re-sampled parameter case for the impacts of the sampling difference in GoldSim to be considered significant. The results shown in Table B-2 indicate that this criterion for significant impact is exceeded for several of the radionuclide groups and for each of the levels of cumulative probability. In contrast, a graphical comparison of the CDFs for the median simulated transport times of nonsorbing species for the base case and the re-sampled parameters suggests little difference in the overall uncertainty distributions for the modeling results (see Figure B-1).

Table B-1. Resampled Stochastic Parameter Values

real. #	FPLAW	FPLAN	NVF19	NVF7	FISVO	FPVO	DCVO	KDNPVO	KDNPAL	KDSRVO	KDSRAL
1	0.15451	0.61331	0.17939	0.24512	0.82056	-3.8248	-11.253	1.7437	6.1641	102.77	160.47
2	0.47702	0.13684	0.11408	0.11487	1.2012	-2.1908	-10.542	1.1902	4.6904	127.89	398.51
3	0.56717	0.97133	0.18689	0.20301	1.1162	-1.0748	-10.369	1.2517	4.7706	230.91	100.67
4	0.10734	0.95304	0.15792	0.21281	2.1091	-4.0288	-10.449	1.4754	8.214	89.503	239.62
5	0.4026	0.3768	0.21127	0.083927	0.99514	-3.2734	-9.9334	1.1209	4.4149	329.24	382.08
6	0.84137	0.72993	0.14731	0.21163	1.1126	-3.0427	-10.626	0.75688	5.2304	261.08	41.482
7	0.31095	0.11323	0.10118	0.16575	1.1435	-3.1508	-9.5171	1.8229	7.0925	368.16	85.61
8	0.61721	0.30199	0.26624	0.10631	1.1633	-3.9555	-10.391	1.514	8.4012	86.233	246.38
9	0.64351	0.54047	0.22131	0.21951	1.33	-3.8841	-10.355	1.2195	5.0232	295.59	348.93
10	0.017634	0.69878	0.24485	0.09997	1.3982	-2.0052	-10.148	1.2513	7.772	366.26	232.98
11	0.36141	0.69208	0.16297	0.16612	1.7877	-3.4103	-9.8462	1.2362	6.2984	79.21	300.4
12	0.66863	0.51855	0.16177	0.17671	1.6181	-2.7493	-9.6179	1.8261	7.555	50.712	237.14
13	0.93638	0.86084	0.17432	0.18663	1.4548	-2.8833	-9.9251	1.7219	8.2876	39.942	221.56
14	0.54225	0.74071	0.12117	0.20404	1.0209	-2.114	-10.469	1.3192	5.3529	97.935	25.237
15	0.079818	0.14179	0.21335	0.19217	0.92842	-1.2718	-10.2	1.3252	6.4525	121.44	187.19
16	0.22733	0.53666	0.23757	0.22169	1.0914	-3.7174	-10.51	1.815	8.3339	153.48	35.574
17	0.9105	0.78472	0.1764	0.15444	1.4341	-2.8256	-10.457	1.7151	8.2226	87.498	154.38
18	0.7729	0.084835	0.14338	0.087999	1.1292	-3.9712	-10.267	1.5264	6.1475	339.64	53.169
19	0.22058	0.092993	0.16874	0.12009	1.8222	-1.1551	-9.3046	5.3108	7.0649	293.46	293.51
20	0.63572	0.22141	0.19893	0.18049	1.2755	-3.6338	-10.606	1.7728	8.6851	355.03	61.475
21	0.46859	0.15315	0.23131	0.07532	1.7139	-2.7178	-10.28	1.405	6.7432	248.05	306.06
22	0.55837	0.73861	0.14775	0.17517	1.8189	-2.5646	-10.364	1.6164	7.5053	188.54	285.67
23	0.93381	0.16285	0.20725	0.1593	1.4084	-1.4373	-11.221	1.1998	4.8646	393.72	71.854
24	0.27958	0.19563	0.18585	0.16883	1.5481	-2.2463	-10.472	1.0035	1.8242	71.215	171.14
25	0.67783	0.82878	0.19173	0.26284	1.2494	-4.7125	-10.179	1.8117	6.8152	213.85	129.45
26	0.14234	0.90098	0.15347	0.17201	2.1518	-3.2488	-10.428	5.9266	7.6134	331.85	113.23
27	0.63108	0.32094	0.11105	0.1861	1.8577	-4.1457	-10.082	1.5185	7.7077	370.96	182.69
28	0.97766	0.98722	0.23521	0.053929	1.2998	-3.9616	-10.998	1.0002	6.8603	133.64	281.52
29	0.094175	0.76688	0.12078	0.1676	1.6638	-1.4805	-9.8115	1.6107	9.075	66.879	77.741
30	0.57883	0.21118	0.17048	0.10311	1.5749	-1.3229	-10.564	1.0831	2.1409	135.46	95.29

Table B-1. Resampled Stochastic Parameter Values (Continued)

real. #	FPLAW	FPLAN	NVF19	NVF7	FISVO	FPVO	DCVO	KDNPVO	KDNPAL	KDSRVO	KDSRAL
31	0.94664	0.2609	0.10912	0.17843	2.4064	-3.3455	-10.769	1.653	7.7886	334.92	156.8
32	0.59584	0.3372	0.11284	0.19882	1.4641	-3.8551	-10.131	1.5419	6.679	132.07	207.88
33	0.32113	0.037874	0.2104	0.16284	0.91225	-1.2881	-10.259	1.7135	7.2404	286.22	108.77
34	0.29157	0.36888	0.18025	0.18707	1.0402	-4.319	-9.9468	0.99292	5.1509	110.2	394.13
35	0.74654	0.033906	0.15763	0.13045	1.8976	-2.3712	-10.312	1.1913	4.8234	163.19	90.119
36	0.27276	0.49577	0.13898	0.19081	1.1846	-3.1034	-10.459	1.4026	7.3466	386.78	224.64
37	0.37341	0.7327	0.064858	0.1695	1.2109	-1.7128	-10.317	1.4201	5.5295	301.55	313.64
38	0.81269	0.71257	0.17073	0.15785	2.2255	-3.9375	-10.273	1.3814	5.664	285.61	164.78
39	0.20651	0.81858	0.17469	0.1795	0.72671	-2.9076	-10.422	1.0858	4.3503	288.61	340.14
40	0.41729	0.39756	0.27779	0.11298	1.3697	-3.5408	-10.244	1.3096	5.9389	399.46	269.69
41	0.5347	0.10605	0.19533	0.17748	1.3558	-1.2155	-10.058	1.4409	7.5078	267.17	243.12
42	0.68784	0.35898	0.17567	0.15113	1.3862	-3.119	-10.399	1.5773	8.3875	61.025	304.79
43	0.20429	0.98413	0.18889	0.19525	1.0585	-3.9954	-9.6862	1.6986	4.2141	361.36	179.52
44	0.17996	0.079534	0.21288	0.19748	0.83332	-2.9663	-10.08	1.2322	6.6549	160.54	369.77
45	0.23268	0.70271	0.13104	0.095923	0.61091	-3.7591	-9.5589	1.2574	5.0532	111.45	135.23
46	0.94002	0.68555	0.17212	0.14843	2.499	-4.2914	-9.9183	5.4986	12.997	201.68	205.42
47	0.9219	0.62997	0.048637	0.21442	1.2257	-3.4446	-10.122	1.5445	7.2167	117.91	311.11
48	0.11753	0.38704	0.13991	0.20593	1.4879	-2.9231	-10.638	1.6764	7.8139	338.16	50.193
49	0.827	0.80175	0.25328	0.17901	1.4701	-3.0873	-9.9755	1.1679	5.2619	300.29	137.8
50	0.26421	0.52885	0.25032	0.19922	1.6234	-2.0279	-10.068	5.9955	12.169	311.01	319.75
51	0.064713	0.27162	0.15502	0.14136	1.1368	-1.8908	-10.284	1.726	7.4901	49.767	245.94
52	0.30783	0.76468	0.14528	0.22367	1.0829	-2.6102	-10.349	1.3565	6.4651	204.45	378.12
53	0.38381	0.55173	0.15182	0.14712	0.23855	-2.858	-10.671	1.7973	5.1993	36.678	97.266
54	0.72186	0.96916	0.18828	0.17131	1.6293	-1.9453	-9.8153	1.8224	9.4862	44.982	145.4
55	0.40607	0.83325	0.25785	0.096324	1.2842	-1.5205	-10.66	1.2942	6.2467	341.24	166.75
56	0.90988	0.84697	0.21523	0.2761	1.5133	-3.288	-10.051	1.1281	4.5134	90.968	395.59
57	0.19368	0.66653	0.28314	0.20833	1.025	-3.3438	-9.9961	1.6278	7.5936	320.89	283.45
58	0.75213	0.15725	0.20111	0.23127	1.4182	-4.4429	-10.254	1.3372	7.9413	202.97	321.09
59	0.51425	0.75492	0.1873	0.072509	1.8376	-3.1668	-10.11	1.5346	7.5754	379.86	105.09
60	0.33748	0.30986	0.1379	0.20891	2.3767	-2.6185	-10.321	3.5	7.8272	145.14	262.78
61	0.33121	0.47933	0.19631	0.18439	0.76825	-3.4808	-9.979	4.244	8.518	105.62	199.2

Table B-1. Resampled Stochastic Parameter Values (Continued)

real. #	FPLAW	FPLAN	NVF19	NVF7	FISVO	FPVO	DCVO	KDNPVO	KDNPAL	KDSRVO	KDSRAL
62	0.17246	0.77804	0.14847	0.19701	0.45371	-3.5141	-9.9163	1.6616	6.9774	23.745	273.78
63	0.11079	0.34953	0.17999	0.18161	1.459	-3.6508	-10.614	1.1611	4.379	194.27	37.474
64	0.77508	0.018099	0.22246	0.22977	1.1456	-3.6972	-9.5041	1.9761	8.666	298.55	126.6
65	0.9675	0.14511	0.15072	0.20751	1.2068	-2.2546	-9.9972	1.1835	6.1704	269.3	144.68
66	0.65465	0.78618	0.17502	0.18945	0.94653	-3.3942	-10.481	1.3794	5.1835	254.59	374.35
67	0.31623	0.058215	0.19715	0.19132	0.9235	-1.644	-10.129	1.1442	4.0732	174.12	362.92
68	0.053659	0.46803	0.2408	0.15517	0.73387	-2.0934	-10.4	1.7598	8.0943	377.41	397.82
69	0.49169	0.87844	0.22613	0.21365	1.5542	-3.0917	-10.733	1.4624	6.9132	31.094	257.93
70	0.48746	0.80687	0.18213	0.27987	0.68653	-2.2711	-10.492	1.689	7.9085	279.5	219.07
71	0.25288	0.062208	0.23415	0.26998	1.6942	-2.6728	-10.417	1.4776	7.0384	229.26	149.13
72	0.50847	0.60382	0.15427	0.17439	1.544	-2.3075	-10.155	0.68438	3.1663	72.667	141.64
73	0.29974	0.64922	0.24811	0.11975	0.41584	-2.4904	-10.536	1.3651	5.7509	108.04	369.3
74	0.001166	0.19266	0.21429	0.20577	1.8758	-3.0257	-10.341	1.2398	6.1983	377	279.11
75	0.042079	0.79283	0.21926	0.20281	1.4286	-1.3395	-10.616	1.3141	4.2133	64.565	29.08
76	0.45846	0.64422	0.18071	0.12158	1.4986	-3.6824	-10.693	1.7602	4.9213	43.315	271.59
77	0.95161	0.41143	0.20249	0.19316	1.5263	-3.8388	-11.053	1.5576	7.8909	186.11	348.05
78	0.26781	0.91957	0.19013	0.25676	1.6361	-1.5587	-10.004	2.3748	8.0176	262.22	335.59
79	0.41006	0.75838	0.11607	0.18122	0.90185	-2.9452	-10.574	1.4521	7.3697	345.07	47.677
80	0.51545	0.57455	0.22788	0.19986	1.0973	-2.6487	-9.7701	0.99093	6.6515	150.32	263.91
81	0.95733	0.066521	0.10282	0.22548	1.5359	-2.526	-10.375	1.7889	6.6458	81.188	250.25
82	0.88537	0.41883	0.22329	0.13661	0.77396	-2.1389	-11.108	1.3361	4.2183	290.92	231.16
83	0.36615	0.5453	0.13476	0.24087	1.1623	-3.7423	-10.506	1.301	5.2676	275.37	189.66
84	0.16779	0.45269	0.15697	0.11679	0.7852	-3.9283	-9.9037	1.6366	7.4887	227.39	112.42
85	0.16085	0.096493	0.17871	0.22874	1.777	-3.6095	-11.122	1.7966	7.708	323.55	64.592
86	0.72935	0.34271	0.12544	0.22486	1.2609	-3.7092	-9.4071	1.482	7.6459	211.9	342.89
87	0.83287	0.32868	0.13686	0.20156	0.80618	-2.5733	-10.297	1.4215	7.0502	168.87	303.07
88	0.76408	0.6793	0.17136	0.29058	1.0047	-3.0518	-9.4712	1.6056	7.2449	76.778	118.54
89	0.095763	0.40949	0.20964	0.16791	1.5617	-2.4667	-9.3754	1.6457	4.9158	41.372	196.41
90	0.48254	0.42029	0.24328	0.23031	1.6577	-3.8094	-10.49	3.1973	8.1647	250.8	105.95
91	0.19603	0.52282	0.17748	0.13717	1.2429	-1.5273	-10.554	1.2838	7.2846	21.507	287.4
92	0.18135	0.68067	0.21231	0.10727	1.1721	-1.0366	-10.499	1.7196	6.3647	384.59	265.16

Table B-1. Resampled Stochastic Parameter Values (Continued)

real. #	FPLAW	FPLAN	NVF19	NVF7	FISVO	FPVO	DCVO	KDNPVO	KDNPAL	KDSRVO	KDSRAL
93	0.24519	0.085228	0.22374	0.16178	1.2181	-2.7725	-10.142	1.2655	4.349	147.09	120
94	0.00815	0.88372	0.16053	0.21214	1.1511	-2.7587	-10.651	1.7821	11.569	157.39	295.32
95	0.88017	0.97634	0.13176	0.15667	0.75645	-4.8566	-10.544	1.4468	6.9344	58.853	346.58
96	0.65912	0.22764	0.070533	0.15584	1.7601	-1.59	-9.9109	1.4401	5.3184	314.2	43.223
97	0.61399	0.31798	0.23951	0.12847	0.85851	-3.1242	-10.582	1.5445	8.596	343.62	288.63
98	0.038079	0.28563	0.089285	0.21639	1.1241	-3.7934	-10.917	1.2656	5.1581	317.64	66.138
99	0.55453	0.63089	0.19061	0.22716	1.0105	-2.2082	-10.679	1.6838	9.6272	195.33	70.128
100	0.86079	0.48698	0.12253	0.20049	0.56076	-2.2218	-9.5403	1.4352	5.3442	190.67	259.48
101	0.78665	0.82048	0.052355	0.14924	0.19142	-2.4254	-10.035	1.1362	5.5581	207.12	372
102	0.01354	0.92652	0.20619	0.1519	1.2618	-2.7006	-10.672	2.7514	7.029	256.13	141.44
103	0.58308	0.70661	0.16817	0.1885	1.8112	-3.0639	-9.7574	1.4899	4.6051	220.76	75.981
104	0.13048	0.91356	0.1939	0.20205	1.7447	-1.7877	-9.4766	1.0647	5.3233	247.02	387.98
105	0.28326	0.59488	0.092197	0.16021	0.62008	-2.2965	-9.9623	1.1416	5.1875	211.79	240.67
106	0.74173	0.006837	0.18534	0.13162	1.438	-1.0161	-10.409	1.3379	7.8773	304.39	26.481
107	0.81661	0.94903	0.16504	0.15313	1.0701	-3.3763	-10.594	0.51139	3.3166	263.39	267.4
108	0.49681	0.84374	0.27156	0.23532	1.6115	-2.0365	-10.29	1.359	6.766	129.76	124.99
109	0.70677	0.50237	0.27545	0.23256	0.66038	-2.7875	-10.938	1.6052	7.9792	385.61	253.24
110	0.71628	0.20405	0.15244	0.2108	0.67724	-3.8943	-10.787	1.6233	5.338	140.3	323.6
111	0.020519	0.11671	0.13676	0.21789	1.8909	-1.3647	-10.447	1.466	7.9455	94.978	214.52
112	0.42269	0.86654	0.23582	0.18235	1.3075	-1.7508	-10.413	0.99845	2.3406	325.92	227.97
113	0.9942	0.25223	0.21716	0.17794	1.1071	-3.9809	-9.8537	1.4078	5.1478	96.249	366.8
114	0.89097	0.74818	0.25081	0.22697	0.69674	-2.0799	-10.604	1.3234	6.3414	104.87	59.842
115	0.62132	0.46444	0.18441	0.15	1.6799	-3.4277	-9.4566	1.1019	2.294	26.732	109.8
116	0.86743	0.63615	0.15577	0.12705	0.3135	-1.6733	-10.301	1.4408	4.6148	38.838	74.671
117	0.25736	0.88827	0.16637	0.15376	0.79901	-1.9871	-10.377	1.3022	4.9784	364.36	51.185
118	0.79535	0.53043	0.16581	0.28089	1.4781	-3.3028	-10.504	4.3222	11.776	356.64	210
119	0.82023	0.89271	0.17265	0.13346	1.7514	-2.6625	-10.885	1.7887	8.295	245.89	386.18
120	0.78008	0.029057	0.24583	0.22147	1.1758	-1.3955	-9.6455	1.0774	4.4117	63.359	34.305
121	0.99644	0.001809	0.25403	0.24598	1.7237	-3.2987	-10.619	1.7513	8.0951	348.89	254.81
122	0.43434	0.56853	0.21893	0.13887	0.70301	-1.8625	-10.015	3.8152	12.36	362.37	225.81
123	0.66334	0.9426	0.12918	0.15897	1.0999	-2.541	-10.646	1.0579	6.1532	284.03	20.15

Table B-1. Resampled Stochastic Parameter Values (Continued)

real. #	FPLAW	FPLAN	NVF19	NVF7	FISVO	FPVO	DCVO	KDNPVO	KDNPAL	KDSRVO	KDSRAL
124	0.34894	0.61624	0.1638	0.20696	1.4508	-1.6157	-9.7203	1.1641	6.4144	225.27	330.18
125	0.6482	0.55825	0.19996	0.14063	1.4038	-2.8694	-10.306	1.0934	6.2914	172.53	87.277
126	0.52262	0.47435	0.15944	0.15274	1.6703	-2.6884	-9.8678	1.3137	7.6635	52.594	353.42
127	0.12093	0.99857	0.14089	0.17042	1.521	-3.0728	-9.699	1.3607	5.8605	397.46	102.3
128	0.50376	0.40211	0.12462	0.24028	1.3506	-3.7681	-10.233	1.8162	8.3619	240.41	30.549
129	0.4494	0.58139	0.08441	0.15786	1.3227	-3.7514	-9.7281	1.4336	7.4172	219.4	277.99
130	0.87816	0.65641	0.20889	0.17611	1.834	-1.6861	-9.3586	1.7359	6.0229	48.342	160.61
131	0.8586	0.42898	0.11757	0.24908	1.2823	-3.265	-10.173	1.2161	7.4377	68.552	180.1
132	0.42846	0.043645	0.14276	0.19387	1.5002	-1.2474	-9.9678	1.6985	10.784	116.86	80.647
133	0.68102	0.87416	0.1497	0.14457	1.2919	-3.8169	-11.011	1.7445	7.0723	353.29	359.63
134	0.79019	0.44076	0.16073	0.16496	1.2304	-3.1606	-9.5735	1.0969	4.0565	270.84	248.91
135	0.24348	0.44885	0.11533	0.25325	0.37138	-1.7344	-10.023	1.5748	7.043	138.51	344.03
136	0.54706	0.014079	0.26015	0.17058	1.3755	-1.8165	-10.17	1.1307	5.3682	235.84	256.87
137	0.23602	0.39414	0.21771	0.26047	0.95554	-2.5023	-10.689	1.1687	3.9222	184.39	334.35
138	0.59063	0.43338	0.2567	0.19021	1.0313	-3.3801	-10.383	1.4407	7.3211	209.21	375.4
139	0.96152	0.33488	0.11912	0.23777	0.63887	-2.1551	-10.643	1.4238	7.3109	149.15	328.56
140	0.057431	0.90967	0.18381	0.14781	1.486	-2.39	-9.783	1.6775	7.3174	374.98	356.74
141	0.67141	0.24933	0.20516	0.24424	1.0503	-3.2255	-10.041	1.0837	4.6347	100.06	177.11
142	0.28613	0.99468	0.20035	0.12554	1.2671	-3.1936	-11.151	1.2299	4.7301	92.315	68.913
143	0.30444	0.35477	0.13232	0.25113	1.7961	-2.0657	-9.9496	1.0069	5.1081	265.61	310.14
144	0.18719	0.12198	0.075385	0.21826	1.6441	-1.4681	-9.9415	1.7274	5.0211	77.379	93.901
145	0.58918	0.45993	0.099761	0.2382	0.49254	-2.3316	-10.432	1.3627	6.2112	192.59	163.21
146	0.34133	0.04982	0.22967	0.10123	1.4409	-3.3182	-10.684	1.5502	5.4328	136.57	382.91
147	0.047805	0.29341	0.093901	0.1227	1.5628	-3.5622	-10.533	1.2252	6.1875	252.7	174.65
148	0.84534	0.58786	0.18263	0.14408	0.60164	-1.9215	-10.654	1.1387	4.179	155.88	132.05
149	0.87341	0.66188	0.12757	0.14625	1.7067	-4.6177	-10.15	1.0285	3.8389	125.08	314.85
150	0.73249	0.93472	0.16928	0.18818	1.597	-1.1944	-10.052	1.7162	6.8352	34.243	351.8
151	0.75869	0.56129	0.14396	0.26452	1.4149	-3.7228	-10.329	1.7684	7.2748	336.65	379.84
152	0.60477	0.10206	0.19316	0.13411	1.5702	-2.3524	-10.548	1.5811	7.1311	216.59	308.76
153	0.35691	0.37418	0.23304	0.20966	1.3384	-1.419	-11.288	1.9484	10.538	324.44	80.964
154	0.072725	0.27833	0.22884	0.14222	1.7334	-3.5069	-10.517	1.4743	4.4277	55.745	388.77

Table B-1. Resampled Stochastic Parameter Values (Continued)

real. #	FPLAW	FPLAN	NVF19	NVF7	FISVO	FPVO	DCVO	KDNPVO	KDNPAL	KDSRVO	KDSRAL
155	0.39335	0.71654	0.14475	0.16243	1.0566	-2.4475	-10.388	1.1995	4.3703	318.35	188.76
156	0.15917	0.96062	0.2046	0.19583	0.59304	-3.4141	-10.666	1.763	8.3527	170.26	173.83
157	0.39965	0.23549	0.17357	0.13773	1.7958	-3.9008	-10.217	1.3955	6.2267	114.07	115.69
158	0.56161	0.17895	0.22476	0.18496	1.529	-2.8009	-10.075	0.25242	2.953	234.54	290.84
159	0.47147	0.858	0.13501	0.13566	0.64763	-2.4053	-10.699	2.0714	6.9061	259.03	191.78
160	0.13672	0.85446	0.19772	0.22029	1.5876	-2.3436	-10.088	1.4322	5.9479	166.84	31.595
161	0.70147	0.62008	0.22654	0.14342	1.3647	-3.6558	-9.3177	1.5789	7.6938	239.67	324.09
162	0.066647	0.24255	0.19121	0.12682	0.85199	-3.4406	-10.359	1.3309	4.5934	280.82	213.09
163	0.89606	0.070428	0.096858	0.17308	1.0672	-2.1244	-10.328	2.7149	8.9685	152.5	229.8
164	0.02568	0.3813	0.10695	0.1826	1.3181	-3.4742	-10.485	1.0952	6.1953	182.25	298.74
165	0.35061	0.26555	0.21632	0.18526	1.1954	-3.3565	-10.435	1.6407	11.12	199.68	63.421
166	0.92835	0.49267	0.12642	0.21678	0.65329	-3.877	-10.588	1.4321	6.2817	143.21	39.647
167	0.71389	0.92211	0.24224	0.17395	1.9965	-3.5493	-10.097	1.4841	5.9563	176.3	194.43
168	0.62881	0.60875	0.19841	0.1838	1.878	-1.0817	-9.8839	1.4514	6.1409	307.81	97.929
169	0.69732	0.28369	0.18911	0.1926	1.2536	-3.0156	-10.187	1.1429	5.641	237.54	91.586
170	0.084344	0.89774	0.1668	0.16429	2.5922	-3.8607	-9.6075	1.1017	6.7401	123.68	216.56
171	0.85202	0.1316	0.19256	0.16686	1.1878	-3.0046	-10.56	1.3442	7.3912	389.06	22.542
172	0.38838	0.18377	0.15513	0.21493	1.3441	-3.1384	-10.015	1.0801	5.1351	118.81	184.09
173	0.085109	0.21815	0.13377	0.17292	1.868	-3.6307	-10.338	1.6482	8.6312	74.692	168.9
174	0.97385	0.16997	0.18179	0.16388	0.96591	-3.216	-10.581	5.5253	10.554	395.28	338.42
175	0.98033	0.5781	0.15892	0.12967	1.7293	-3.3332	-10.63	4.2776	12.983	31.891	316.99
176	0.69471	0.20916	0.12876	0.26707	1.3352	-3.6736	-10.162	1.1452	3.1774	180.52	219.72
177	0.2195	0.95555	0.20163	0.045592	0.74502	-3.4606	-10.226	1.6675	7.3099	348.24	152.59
178	0.44044	0.29674	0.14158	0.24225	1.507	-3.9153	-10.521	1.4003	4.6243	390.82	198.56
179	0.53637	0.18607	0.082572	0.10823	0.71592	-1.1148	-10.597	2.0903	8.5282	224.89	365.16
180	0.21493	0.024592	0.15055	0.091297	0.97907	-4.5409	-10.033	1.2357	5.5589	372.43	45.443
181	0.83581	0.12616	0.20355	0.19617	0.98965	-3.2402	-10.251	1.4982	6.1282	57.534	136.02
182	0.14532	0.81391	0.16419	0.13944	1.8493	-3.5703	-9.5983	1.3632	6.1587	25.051	326.63
183	0.73925	0.8359	0.20368	0.14546	1.0133	-1.8463	-10.84	0.80881	1.8179	305.11	123.38
184	0.91963	0.7744	0.23864	0.25804	2.2662	-3.5828	-9.3523	1.4038	5.3787	314.76	157.91
185	0.52856	0.59701	0.18463	0.086432	0.84059	-3.2062	-9.4032	1.6226	6.5072	330.73	54.46

Table B-1. Resampled Stochastic Parameter Values (Continued)

real. #	FPLAW	FPLAN	NVF19	NVF7	FISVO	FPVO	DCVO	KDNPVO	KDNPAL	KDSRVO	KDSRAL
186	0.32825	0.17437	0.23089	0.12394	1.691	-3.4955	-10.57	1.1034	5.5235	351.96	296.52
187	0.80375	0.67066	0.26343	0.1607	1.7672	-2.5861	-9.6591	3.1931	9.5432	161.8	360.73
188	0.76892	0.7972	0.20806	0.23394	0.86958	-3.6122	-10.103	1.145	4.7396	293.68	201.86
189	0.45274	0.052696	0.28832	0.22293	1.9214	-1.1328	-10.347	5.3608	8.4137	359.62	354.89
190	0.12775	0.25773	0.16217	0.11778	1.3804	-2.4795	-9.4334	1.7721	8.3851	28.238	150.99
191	0.030259	0.51272	0.19591	0.19479	0.15589	-3.5969	-10.21	1.2344	7.0844	381.67	275.41
192	0.43598	0.48281	0.14608	0.20493	1.2364	-3.5284	-10.442	1.3869	6.0249	222.79	392.35
193	0.80683	0.31282	0.29252	0.24753	0.8914	-3.7818	-10.525	1.4914	4.0691	197.7	122.39
194	0.98634	0.65179	0.10579	0.23597	1.0463	-4.9046	-10.115	0.029211	6.0052	274.14	209.18
195	0.37937	0.93822	0.19449	0.13212	1.0804	-2.1797	-10.465	1.2632	4.7519	242.74	235.74
196	0.46288	0.50794	0.16731	0.29215	1.593	-3.1837	-9.9573	1.2085	5.1291	178.61	203.67
197	0.57279	0.72439	0.26898	0.11042	0.1268	-2.9724	-10.203	1.4679	6.7437	309.71	84.214
198	0.60957	0.43761	0.17809	0.25562	1.3057	-2.9982	-10.196	1.4713	8.3448	83.824	132.25
199	0.90293	0.36087	0.20795	0.11238	1.3925	-1.9654	-10.234	1.1741	5.5667	277.61	332.46
200	0.10451	0.23312	0.22015	0.068105	0.87763	-2.8445	-9.9863	0.13075	1.9303	164.45	57.659

Table B-1. Resampled Stochastic Parameter Values (Continued)

real. #	KDUVO	KDUAL	GWSPD	BULKDEN SITY	CORAL	CORVO	SRC4Y	SRC4X	SRC3X	SRC2Y	SRC2X
1	6.1493	3.7076	-0.25613	1875.6	0.90315	1.249	0.14801	0.37912	0.95332	0.49935	0.55136
2	0.13979	2.9947	-0.90495	2066.2	1.1938	0.77885	0.092137	0.47786	0.91792	0.8188	0.97184
3	7.0802	5.5188	-0.04399	1936.2	0.90379	0.77851	0.60439	0.68826	0.66009	0.53068	0.82956
4	6.9144	5.3198	0.89094	1914	3.1598	1.4824	0.41319	0.8772	0.87114	0.76593	0.015416
5	5.4386	3.2889	-1.1703	1846.5	0.90303	1.5138	0.42084	0.42053	0.66879	0.14968	0.65052
6	5.707	3.7543	0.35869	1871.3	0.90329	1.1456	0.016647	0.81447	0.35119	0.19017	0.45259
7	15.582	5.9308	-0.22168	1957.1	3.4966	0.83018	0.54561	0.74242	0.22112	0.6963	0.84463
8	8.0173	5.9057	-1.3916	1895.9	0.90319	1.8458	0.48397	0.53618	0.81963	0.2233	0.06631
9	5.9674	4.076	0.12144	1972.7	0.90359	0.77867	0.20968	0.66388	0.56603	0.72163	0.16671
10	6.1912	5.9646	0.20946	1848.1	3.3813	0.77817	0.35921	0.91146	0.086184	0.26383	0.61428
11	8.0239	5.8593	0.57785	1955.5	3.0428	1.0566	0.25235	0.28583	0.14377	0.33995	0.37274
12	7.2804	4.434	0.978	1908.5	0.96748	2.6259	0.96923	0.38967	0.53011	0.37712	0.87938
13	7.9246	6.2089	-0.44711	1824	1.3524	1.436	0.91852	0.74563	0.60164	0.51425	0.28382
14	6.9083	4.3284	-0.01196	1860.2	0.90381	2.8391	0.061248	0.59919	0.035534	0.42406	0.12351
15	7.6659	4.8564	-0.46491	1901.3	1.0338	1.2741	0.18335	0.93868	0.44241	0.83114	0.66251
16	6.9608	5.7375	0.15593	1789.4	1.5556	2.8528	0.24504	0.23616	0.41568	0.56078	0.24768
17	7.723	6.1141	0.071892	1904.9	0.90311	2.1018	0.56412	0.71879	0.45866	0.6612	0.88127
18	7.4356	5.583	0.089054	1899.8	2.2769	1.4215	0.46985	0.17038	0.36892	0.4337	0.41587
19	15.261	6.4804	-0.2701	2008.9	3.3885	2.2946	0.15415	0.29201	0.926	0.13578	0.10665
20	6.398	5.6174	0.37412	1897.5	1.6537	0.90638	0.93395	0.38039	0.88069	0.83584	0.78477
21	6.5091	5.3612	0.14902	1967	2.8222	1.5622	0.70752	0.19571	0.96397	0.40507	0.072601
22	6.361	4.3835	0.26446	1941.6	2.4794	1.1297	0.89898	0.51774	0.51472	0.44474	0.076803
23	5.4631	3.0854	0.10788	1871.8	2.7048	0.77872	0.11813	0.97456	0.31021	0.6663	0.22816
24	5.6171	3.0148	-1.2654	1913.5	2.9966	0.8072	0.59446	0.50489	0.98748	0.23154	0.36614
25	7.5432	5.9876	-0.20048	1786.8	1.5056	1.554	0.95635	0.59051	0.050116	0.64233	0.45837
26	19.454	5.9545	0.27664	1876.9	0.90357	2.6816	0.74104	0.20259	0.33288	0.00056	0.94328
27	5.5521	4.6393	-0.30598	1905.6	3.2025	1.1549	0.48661	0.5346	0.40274	0.22763	0.38021
28	5.6577	4.1899	-0.34112	1986.6	1.743	2.5966	0.32813	0.3461	0.52155	0.30517	0.35838

Table B-1. Resampled Stochastic Parameter Values (Continued)

real. #	KDUVO	KDUAL	GWSPD	BULKDENSITY	CORAL	CORVO	SRC4Y	SRC4X	SRC3X	SRC2Y	SRC2X
29	6.9259	4.8134	-0.1107	1949.3	0.90353	1.2222	0.72812	0.35529	0.48028	0.18916	0.43491
30	6.2501	3.6112	0.61346	1917	0.90384	2.0319	0.57539	0.27621	0.90553	0.61556	0.49737
31	7.9127	8.0006	0.000996	1997.8	3.5195	2.0158	0.67078	0.43256	0.86789	0.37068	0.3227
32	6.8819	5.103	-0.13694	1826.2	2.9475	0.82037	0.63578	0.087969	0.059871	0.013958	0.61861
33	7.5956	4.9153	0.43555	1928.6	3.0686	1.0455	0.32401	0.28237	0.62066	0.27631	0.64255
34	5.8952	3.1641	-0.2913	1938	0.90391	2.405	0.57426	0.17807	0.63746	0.13035	0.049985
35	6.4071	3.8918	-0.05131	1857.7	0.90374	1.7737	0.38832	0.5125	0.7477	0.040306	0.80321
36	6.8402	4.7547	0.76045	1884.8	1.9106	0.77881	0.021301	0.00988	0.32113	0.24313	0.62202
37	7.5056	4.5429	-0.33819	1879.9	0.9031	1.6376	0.85906	0.67081	0.77494	0.5175	0.87397
38	7.0917	6.0084	-0.3587	1821.8	2.5739	1.3567	0.49032	0.78578	0.8421	0.92213	0.69837
39	7.0048	3.2365	-0.40327	1946.6	3.2872	1.7059	0.34929	0.10812	0.86475	0.26755	0.44695
40	6.9305	5.0561	-1.0631	1928.9	3.4907	0.77805	0.23383	0.96955	0.55518	0.21934	0.14791
41	6.6206	4.6125	-0.31852	1977.6	0.90347	0.78696	0.78578	0.67741	0.85998	0.44835	0.56415
42	14.413	8.5213	-0.81469	1867.6	0.90364	1.887	0.79542	0.48809	0.30997	0.68955	0.27574
43	7.0801	4.4074	0.23203	1829.1	2.3007	1.3741	0.054658	0.409	0.65079	0.16031	0.03927
44	6.4178	4.5582	0.42998	1896.6	2.8908	1.5358	0.44201	0.36493	0.58549	0.10303	0.34881
45	6.5805	5.1817	0.025447	1964	1.6772	2.5271	0.90287	0.84512	0.23369	0.88767	0.7561
46	6.7732	4.3508	0.17992	1906.4	0.9037	1.4949	0.76341	0.65504	0.38765	0.92522	0.81075
47	7.8863	5.3757	-0.6572	1839.2	2.7542	1.3217	0.55681	0.080545	0.68236	0.78279	0.68201
48	5.5915	3.1849	0.38826	1849.6	0.90382	1.4538	0.47267	0.5233	0.42106	0.49153	0.4295
49	7.2685	4.1403	0.33525	1887	1.5231	1.4289	0.30719	0.9826	0.97391	0.34844	0.30095
50	8.1591	7.477	0.46714	1907.9	1.9352	1.4188	0.75527	0.79521	0.79124	0.59169	0.94693
51	6.7672	4.4528	0.18511	1919.4	2.3538	1.6967	0.11262	0.78394	0.065009	0.96761	0.93778
52	6.2051	3.8	-0.0048	1843.4	0.90378	2.1284	0.21311	0.45059	0.101	0.87173	0.85482
53	0.001592	2.0902	-0.53103	2040	1.7023	1.7024	0.63397	0.75733	0.63411	0.59665	0.73295
54	7.7203	3.6933	0.48981	1940	2.5819	0.77875	0.74928	0.001434	0.017975	0.15992	0.5667
55	6.4049	3.0945	-0.12414	2075.6	0.90336	1.6481	0.59924	0.8652	0.39361	0.17097	0.78623
56	6.2952	3.7152	-0.19316	1881.2	2.2225	1.0983	0.46359	0.90716	0.64016	0.016186	0.5749
57	7.154	3.5316	-0.02042	1862.5	0.90385	2.182	0.98781	0.7921	0.91338	0.19927	0.20202
58	5.8708	2.9401	-0.26747	2097.2	0.90303	1.6425	0.10519	0.22164	0.62929	0.081447	0.65732

Table B-1. Resampled Stochastic Parameter Values (Continued)

real. #	KDUVO	KDUAL	GWSPD	BULKDENSITY	CORAL	CORVO	SRC4Y	SRC4X	SRC3X	SRC2Y	SRC2X
59	6.8836	3.7417	-0.13756	1890.7	3.4252	1.9758	0.16734	0.57493	0.6155	0.97189	0.060699
60	7.927	6.0964	-1.3759	1794.2	2.1267	1.3454	0.75226	0.55725	0.82696	0.85085	0.68955
61	7.6493	4.5099	-0.25796	1816.9	1.789	0.77828	0.20405	0.61318	0.76903	0.7736	0.5395
62	8.144	5.6387	-0.44055	1865.6	0.90313	1.6613	0.26243	0.87413	0.71708	0.71988	0.053525
63	5.7201	3.568	0.22399	1974.2	1.7265	0.86279	0.94684	0.43978	0.19613	0.63319	0.52571
64	7.8152	7.7093	-0.98719	2025.1	0.90356	2.794	0.088359	0.48033	0.84602	0.86047	0.96369
65	5.4064	3.8242	0.40448	1662.6	1.995	0.88188	0.19983	0.046866	0.94455	0.35625	0.19656
66	6.8026	1.7728	-0.45796	1930.3	1.967	0.77896	0.69036	0.15279	0.70221	0.95827	0.098062
67	6.1203	4.121	0.02024	1931.6	0.90386	0.77816	0.72359	0.12183	0.58056	0.039986	0.54263
68	7.5772	6.7573	-0.10442	1940.9	2.2592	2.2193	0.073801	0.96441	0.44882	0.88064	0.59544
69	6.2977	3.065	-0.23475	1963.3	2.7847	1.2303	0.97696	0.20797	0.084584	0.57374	0.70334
70	7.6321	5.7935	-0.03985	1780.6	3.5667	0.79181	0.7142	0.26741	0.78112	0.79843	0.88713
71	7.1083	4.7049	-0.35404	1952.3	0.91759	0.98496	0.99908	0.803	0.59694	0.31095	0.11612
72	5.6574	3.1777	0.04461	1852.1	0.90392	1.7219	0.45309	0.23211	0.34683	0.29814	0.033845
73	7.5767	5.1335	0.09073	1990.3	1.1033	1.4748	0.61349	0.70253	0.6485	0.95109	0.83954
74	6.7295	5.041	0.036364	1869.4	1.3657	1.2939	0.40039	0.22715	0.12556	0.84679	0.92907
75	5.6064	3.6735	0.32454	1947.8	2.1186	1.2692	0.13788	0.64172	0.39798	0.84111	0.76703
76	6.5068	4.3706	0.42735	1850.1	3.5552	1.1377	0.93568	0.052459	0.43316	0.27091	0.95719
77	8.0066	6.1562	0.39433	1883.3	2.1891	2.4279	0.036244	0.31983	0.85241	0.099715	0.98777
78	6.9771	4.9488	0.446	1977	0.90318	0.77863	0.52811	0.32228	0.69329	0.5458	0.17655
79	6.5367	3.7835	-0.84437	2036.5	3.0898	2.3931	0.23949	0.58398	0.51926	0.15459	0.62762
80	6.5752	3.3485	-0.29877	1968.9	2.9533	1.5442	0.79325	0.8985	0.93623	0.053707	0.48373
81	7.0924	3.2418	-0.70629	1962.3	0.9032	1.288	0.49932	0.12507	0.89771	0.82865	0.54536
82	6.8652	3.6377	-0.02764	1969.6	1.2058	1.7129	0.33092	0.65045	0.69902	0.23748	0.72851
83	7.3348	5.4404	-0.20594	1760	3.6174	1.5253	0.92293	0.72545	0.89401	0.91693	0.47477
84	6.8026	5.7136	-0.07956	2004.7	0.90395	1.1809	0.36004	0.035625	0.67331	0.77605	0.8152
85	7.085	3.85	-0.73072	1903	2.5396	2.4615	0.10302	0.13938	0.2868	0.79406	0.9918
86	6.8698	4.1013	-0.59536	1922.1	3.4561	1.4602	0.4156	0.099152	0.46067	0.50898	0.35323
87	7.4268	5.2303	0.4476	1909.9	2.9123	2.566	0.88833	0.71028	0.55161	0.029548	0.60303
88	6.8131	4.6657	0.92386	1840.5	1.3934	1.7451	0.33803	0.99092	0.099285	0.11672	0.40881

Table B-1. Resampled Stochastic Parameter Values (Continued)

real. #	KDUVO	KDUAL	GWSPD	BULKDEN SITY	CORAL	CORVO	SRC4Y	SRC4X	SRC3X	SRC2Y	SRC2X
89	8.1135	5.1499	-0.37491	1900.3	0.90326	1.2421	0.31854	0.46209	0.3012	0.5016	0.12874
90	7.596	6.2424	0.35281	1916.2	0.90397	0.77889	0.68696	0.76919	0.80317	0.94606	0.006143
91	5.503	3.3187	0.12577	1959.2	0.90339	1.0995	0.12672	0.92108	0.75997	0.99265	0.79816
92	18.034	6.2536	0.035734	1882.1	1.6093	0.77841	0.89491	0.92686	0.50891	0.30263	0.52301
93	5.9194	3.0336	0.062279	1942.7	0.90349	1.7296	0.029419	0.54533	0.97505	0.76008	0.082954
94	7.8762	5.3551	-0.08548	1993.1	0.90389	1.7347	0.004466	0.7771	0.81418	0.60279	0.77636
95	6.7676	4.4996	0.33088	1934.2	0.90367	0.779	0.27625	0.75346	0.94982	0.73642	0.92474
96	6.2249	3.3144	-0.46538	1815.1	3.5953	2.3636	0.50903	0.54324	0.52673	0.1679	0.64838
97	6.0388	2.7715	0.11734	1845.5	2.6544	1.0609	0.86021	0.61537	0.43719	0.29445	0.4137
98	5.4833	2.9698	0.84905	1994.9	1.2393	1.5103	0.53499	0.73858	0.54758	0.28177	0.71001
99	6.0469	2.608	-0.07007	1925.1	0.90337	1.4681	0.31493	0.44407	0.026816	0.41548	0.26677
100	7.0153	5.4693	0.7169	2131.4	1.3278	0.77801	0.37156	0.39791	0.34029	0.046676	0.71905
101	7.562	5.2438	0.53172	1863.9	1.8433	1.2537	0.52369	0.89111	0.72414	0.94363	0.97783
102	6.3275	4.8416	0.056803	1958.2	2.6805	1.3798	0.92714	0.1456	0.15558	0.32354	0.57921
103	6.3913	5.1183	0.9123	1809.1	3.6533	1.0224	0.61812	0.30333	0.26082	0.39232	0.38884
104	6.3176	4.0453	-0.16064	1765.8	0.9403	2.5396	0.66785	0.29726	0.31575	0.71377	0.40333
105	1.8792	3.8256	-0.43173	2012.3	2.3309	1.5695	0.88151	0.50933	0.15264	0.36659	0.76274
106	6.1733	4.26	-0.22998	2019.2	2.8064	1.0266	0.22383	0.85892	0.002543	0.12428	0.23763
107	7.4244	4.316	0.41343	1981.6	0.98874	1.5407	0.30208	0.62662	0.74214	0.43735	0.50232
108	6.7656	4.1715	0.14963	1917.9	3.6802	1.5234	0.8293	0.57726	0.96774	0.078148	0.29635
109	7.1081	3.9256	0.104	1812	2.9781	1.0732	0.22898	0.49888	0.36227	0.80137	0.026276
110	5.716	3.2754	0.30823	1873	3.3533	0.7781	0.5898	0.88117	0.18919	0.96142	0.73885
111	5.5159	1.9335	0.047852	1991.6	3.2485	1.0785	0.55213	0.70952	0.48706	0.97908	0.25633
112	6.1179	4.7172	0.070586	1904.1	1.4289	1.6676	0.033208	0.42755	0.76087	0.81213	0.74691
113	7.4123	5.639	0.29412	1923.5	1.018	1.7611	0.12009	0.49013	0.49325	0.067976	0.15316
114	16.09	6.1433	0.40963	2000	0.90369	0.77822	0.069784	0.93143	0.33687	0.70245	0.63608
115	5.7307	3.6202	0.82416	1923.8	0.90344	1.4409	0.013986	0.63208	0.57667	0.39511	0.51207
116	5.5766	3.8772	-0.05986	1892.8	1.4837	0.85576	0.87464	0.021304	0.83896	0.45149	0.21883
117	5.4557	3.4754	-0.055	1944.8	1.0634	0.77891	0.16343	0.15549	0.32769	0.80689	0.95205
118	10.416	6.8428	0.52583	1935.9	0.90322	2.7216	0.8338	0.60597	0.1746	0.60799	0.53258

Table B-1. Resampled Stochastic Parameter Values (Continued)

real. #	KDUVO	KDUAL	GWSPD	BULKDENSITY	CORAL	CORVO	SRC4Y	SRC4X	SRC3X	SRC2Y	SRC2X
119	7.7888	6.0854	0.59735	1803.9	0.90352	1.6841	0.25947	0.3505	0.13133	0.69187	0.46983
120	14.987	5.5024	-0.28378	1889.1	0.90351	2.1477	0.17971	0.01696	0.12417	0.65725	0.21304
121	6.5408	3.9942	0.25196	1933.7	0.90341	1.5891	0.3682	0.32693	0.14919	0.82472	0.49172
122	10.671	5.3934	0.80396	2022.8	0.90395	2.5036	0.26875	0.30965	0.53749	0.75493	0.63438
123	5.8361	4.5879	0.017479	2045.4	3.0164	2.7454	0.60795	0.21768	0.77931	0.20398	0.16495
124	7.1499	5.6726	0.34544	2019.8	2.4344	1.9289	0.18763	0.16686	0.20988	0.5691	0.58279
125	7.6797	8.1239	0.096832	1842.8	2.5249	1.5968	0.98125	0.76469	0.2517	0.3173	0.85904
126	5.932	3.5889	0.28785	1832.8	2.4076	1.5787	0.39829	0.95212	0.034587	0.52336	0.1135
127	6.7048	5.0797	0.17443	1981	1.2767	1.6157	0.056255	0.90495	0.98011	0.48855	0.91575
128	7.5849	5.2913	-0.12699	1835.2	1.5866	1.3035	0.87817	0.94688	0.25589	0.33424	0.20698
129	7.212	3.9432	0.1424	1798.4	1.7706	1.7714	0.47718	0.47024	0.19356	0.55568	0.55688
130	7.831	5.1913	-0.31069	1720.1	3.1815	2.2739	0.95338	0.39089	0.73424	0.72894	0.50726
131	8.0972	7.2211	0.64357	1965.9	0.90343	1.116	0.69971	0.58612	0.92169	0.67742	0.27223
132	7.6639	5.7891	-0.2927	1985.9	0.90305	1.5025	0.1319	0.56659	0.26685	0.90542	0.13879
133	8.0294	5.5701	0.36393	1938.8	1.3017	1.6536	0.90639	0.66534	0.7532	0.2594	0.31207
134	6.2922	3.5566	-0.18177	1961	3.4344	1.1616	0.24114	0.94237	0.65911	0.34417	0.28603
135	6.7919	4.9812	-0.11658	1859.2	0.90309	1.0038	0.042086	0.3139	0.012702	0.70527	0.89991
136	6.9603	4.733	0.67106	2061.5	0.90365	0.93824	0.43459	0.98723	0.17691	0.36239	0.39637
137	5.9763	4.7807	-0.0749	1892.1	1.4591	1.6802	0.8406	0.24623	0.24321	0.74055	0.34012
138	5.8133	4.1604	0.20124	1927.6	0.90399	2.8913	0.4496	0.73276	0.79884	0.86859	0.29014
139	7.209	3.3904	0.34952	1756	1.1114	2.2309	0.85058	0.013066	0.70983	0.98059	0.4625
140	10.967	6.066	-0.23887	2084.8	2.1687	1.4077	0.19363	0.91877	0.57169	0.062484	0.59253
141	6.5514	5.0181	0.28548	1915.2	2.1627	1.96	0.81428	0.213	0.23506	0.62553	0.8923
142	6.4987	3.5084	-0.21553	2033.8	1.5521	2.7681	0.28203	0.030125	0.99984	0.93706	0.43827
143	5.6205	2.9164	-1.4733	2007.2	0.90372	1.0108	0.78117	0.1124	0.90435	0.68037	0.00137
144	15.631	5.7692	0.13213	1920.1	0.90361	1.478	0.45778	0.62244	0.20289	0.1124	0.67711
145	6.5031	5.0007	-0.37782	1782.1	3.6308	1.3834	0.54002	0.83238	0.54177	0.059496	0.055209
146	7.3723	4.2696	-0.17206	1856.2	1.4484	1.7392	0.58368	0.82026	0.49892	0.93132	0.8671
147	5.9872	3.4647	0.46085	1874.5	2.7317	1.1979	0.28947	0.064219	0.008741	0.086082	0.042408
148	7.4014	5.6886	-0.32636	2010.9	2.048	1.5757	0.83873	0.18767	0.45303	0.24793	0.17381

Table B-1. Resampled Stochastic Parameter Values (Continued)

real. #	KDUVO	KDUAL	GWSPD	BULKDENSITY	CORAL	CORVO	SRC4Y	SRC4X	SRC3X	SRC2Y	SRC2X
149	5.9334	3.358	0.16814	1861	3.7102	1.4905	0.71606	0.45623	0.60712	0.106	0.8472
150	7.5823	4.8848	-0.36515	1955.4	0.90362	1.5925	0.772	0.25397	0.046208	0.35463	0.7418
151	7.765	6.2909	0.24095	1887.6	0.9033	1.0412	0.99159	0.37394	0.16138	0.8983	0.33576
152	6.8184	4.6906	-0.16259	1876	0.92863	1.8934	0.078416	0.26234	0.47477	0.41185	0.8627
153	10.24	6.0373	0.080839	1950.4	0.90306	0.95402	0.37664	0.16391	0.072875	0.20549	0.98379
154	0.55423	3.1138	-0.1468	1801.7	0.90376	1.3353	0.67507	0.85191	0.56233	0.91132	0.77248
155	5.3984	2.9881	-0.18609	1852.6	2.0553	1.7596	0.64711	0.24118	0.78982	0.14203	0.022912
156	7.4192	4.4159	0.23382	1946.4	0.90324	1.3632	0.29059	0.11742	0.16658	0.5841	0.33087
157	1.2752	3.9764	-0.34614	1932	3.2184	0.77879	0.21752	0.56409	0.37232	0.071179	0.086622
158	5.5865	3.9088	0.38434	1818.8	1.876	0.92785	0.40653	0.028803	0.093443	0.45984	0.90492
159	16.91	5.8988	-1.1077	1823.5	2.4529	1.8267	0.09683	0.8887	0.99051	0.28945	0.44384
160	5.3907	2.9297	0.29815	1921.2	3.3049	1.6886	0.77907	0.84141	0.82286	0.40239	0.14267
161	7.9461	5.8762	-0.39788	1805.6	1.0831	0.77834	0.94128	0.067398	0.59004	0.87679	0.1026
162	7.0477	3.1286	-0.47182	1748.7	1.8898	1.085	0.73848	0.27179	0.11254	0.033604	0.25055
163	6.6373	4.2243	-0.42075	1943.2	2.0836	0.77865	0.5124	0.090902	0.29907	0.78995	0.93382
164	5.7946	4.965	-0.27865	1979	2.3667	0.77856	0.65853	0.044761	0.71303	0.009268	0.13014
165	6.0033	3.2186	-0.21132	1975.6	3.1379	0.94558	0.42716	0.99581	0.93247	0.63505	0.79472
166	6.7439	5.457	-0.38635	1954	0.90328	1.5573	0.80914	0.14267	0.18078	0.46381	0.36175
167	7.0064	3.4989	-0.03073	1830.6	1.1302	1.6278	0.97148	0.19133	0.83382	0.54465	0.22192
168	6.3715	2.5263	-0.48095	1831.6	0.903	1.2828	0.86946	0.419	0.13968	0.55282	0.99942
169	6.2635	3.4	0.21954	1999.3	0.99714	0.8477	0.34431	0.073091	0.68898	0.89467	0.4245
170	14.659	8.659	0.45565	1814.2	2.6418	1.1898	0.68117	0.33547	0.40532	0.90013	0.91304
171	6.5549	4.4726	0.16509	1893.7	2.401	1.1109	0.70351	0.69854	0.72757	0.98757	0.75225
172	6.1013	5.7161	-0.15267	1983.3	1.2186	1.4499	0.81611	0.25826	0.61445	0.46792	0.90571
173	7.5434	5.527	0.20554	2050.5	2.6047	2.3379	0.76866	0.058454	0.21765	0.58804	0.3155
174	8.2794	4.0664	0.96462	1911.2	2.7415	0.89771	0.082041	0.40006	0.060625	0.38108	0.96639
175	7.9979	4.2885	0.31596	1894.7	0.90325	1.6091	0.91047	0.82838	0.88732	0.99868	0.18895
176	6.8041	6.0221	-1.2186	1776.4	3.2702	0.7785	0.66477	0.46953	0.042516	0.62485	0.48731
177	6.6767	4.7963	-0.09508	1855.9	2.0157	0.88506	0.96164	0.33283	0.29031	0.47929	0.60973
178	6.4386	2.255	-0.45186	1988.5	2.8606	0.77832	0.006732	0.52745	0.28427	0.74792	0.23012

Table B-1. Resampled Stochastic Parameter Values (Continued)

real. #	KDUVO	KDUAL	GWSPD	BULKDENSITY	CORAL	CORVO	SRC4Y	SRC4X	SRC3X	SRC2Y	SRC2X
179	7.141	5.5461	0.006338	1837.4	0.90374	0.77859	0.15811	0.55268	0.023901	0.18067	0.47559
180	7.8443	6.2661	0.37781	1899.1	2.8672	1.3971	0.62791	0.36613	0.37716	0.25127	0.19465
181	7.0736	4.9344	0.27154	1926.4	1.6385	0.77808	0.84643	0.60261	0.079115	0.17635	0.72495
182	6.7374	1.996	-0.39143	1880.1	1.822	2.081	0.53641	0.4478	0.35914	0.38798	0.014873
183	5.5053	3.436	0.47384	2052.7	2.5136	1.3331	0.43998	0.95684	0.41408	0.21347	0.83035
184	16.604	6.1784	0.70686	2016.2	0.90358	1.3131	0.82124	0.41314	0.95968	0.61257	0.39318
185	7.3825	6.1914	-0.94859	2028.7	0.90389	1.2114	0.14096	0.86368	0.87878	0.73015	0.824
186	6.3639	3.4209	0.3194	1970.8	1.8143	1.6253	0.17332	0.83925	0.42664	0.75893	0.18395
187	7.7803	5.8127	-0.42838	1853.7	1.1646	2.6512	0.29535	0.6393	0.2468	0.32991	0.2443
188	7.3968	5.3167	-0.40788	1889.8	1.2623	1.2132	0.62056	0.077406	0.27678	0.12604	0.51919
189	8.0923	5.8459	-0.0098	1878.8	0.90314	1.1667	0.27374	0.81653	0.73931	0.52789	0.26466
190	7.4329	5.2743	0.42213	1912.5	0.90346	0.77845	0.80183	0.10476	0.10591	0.85939	0.80646
191	6.1279	4.0069	-0.09548	1868.6	1.4057	1.3999	0.50392	0.80569	0.22811	0.023383	0.32794
192	6.3392	4.6196	-0.41476	2003.6	3.3367	1.791	0.64456	0.1335	0.21443	0.53591	0.66755
193	6.1161	4.8803	-1.3166	1866	0.90332	0.7784	0.73013	0.97535	0.38237	0.67251	0.69203
194	0.30637	2.8997	0.24466	1735.4	1.9855	1.6741	0.38362	0.34451	0.67767	0.42816	0.70837
195	5.4753	2.3675	-0.24962	1768.8	0.90341	1.6045	0.51658	0.77213	0.27475	0.48303	0.58716
196	7.3568	5.2147	-0.176	1795.8	1.3102	0.9639	0.35128	0.64598	0.11775	0.64953	0.3061
197	6.8571	4.5789	-0.33088	1836.8	0.90334	1.7525	0.56869	0.694	0.50191	0.4735	0.6721
198	7.1083	4.0231	0.77472	1951.9	1.152	0.99489	0.39476	0.72323	0.46947	0.57942	0.092109
199	6.6074	5.4246	0.25766	1885.4	2.2515	1.178	0.65197	0.18141	0.47965	0.65273	0.37658
200	6.1683	4.2044	0.19183	1910.7	3.1226	0.77824	0.046482	0.68272	0.80814	0.091389	0.15855

Table B-1. Resampled Stochastic Parameter Values (Continued)

real. #	SRC3Y	SRC1Y	SRC1X	HAVO	LDISP	KDRAVO	KDRAAL	KD_PU_VO	KD_PU_AL	KD_PU_C0L
1	0.92233	0.25505	0.74124	15.158	1.313	191.85	170.3	90.304	87.115	4.2804
2	0.95718	0.43026	0.82308	5.231	1.996	438.05	321.83	296.2	128.74	4.5635
3	0.39566	0.78442	0.12747	7.789	1.8919	315.77	508.4	96.723	102.66	4.6501
4	0.83861	0.26775	0.71883	8.064	1.8993	823.19	978.39	33.548	93.633	4.8718
5	0.52003	0.57509	0.094709	6.281	2.5643	875.12	769.2	55.826	102.81	3.7980
6	0.40076	0.96621	0.9459	9.449	2.1515	789.01	900.47	58.053	74.556	5.1715
7	0.094518	0.093636	0.46901	4.946	2.6278	786.48	844.16	100.7	111.5	4.5060
8	0.32186	0.17194	0.84957	5.365	1.8634	865.84	827.29	63.628	76.41	5.8273
9	0.30145	0.85606	0.16371	15.893	2.2814	364.19	527.36	120.34	112.2	5.5088
10	0.57727	0.11274	0.96106	7.689	1.4344	797.1	251.58	98.732	110.55	4.1104
11	0.74875	0.15598	0.086856	1.125	2.1713	322.86	935.95	108.93	141.46	3.9581
12	0.6884	0.20431	0.40849	9.047	1.3276	366.98	176.25	115.46	97.821	4.6365
13	0.11426	0.97927	0.80415	0.968	3.3988	237.1	459.82	125.54	115.14	5.0327
14	0.077847	0.038325	0.39857	4.660	1.8369	892.57	306.82	99.777	89.356	4.7745
15	0.47977	0.67091	0.53651	2.573	2.1315	342.82	722.33	47.92	94.597	4.9787
16	0.56804	0.91726	0.52864	5.602	2.5869	947.77	592.07	124.29	126.95	5.8763
17	0.97516	0.75352	0.96649	4.996	1.738	277.76	398.99	108.06	98.209	5.0810
18	0.22547	0.098027	0.27507	1.676	2.8558	181.8	804.65	109.59	83.384	3.7712
19	0.11894	0.90477	0.51826	1.077	1.7207	169.97	229.43	106.12	94.169	3.9250
20	0.44268	0.65648	0.4869	3.141	2.2336	382.72	520.65	109.97	87.421	3.6536
21	0.86671	0.87858	0.86223	3.002	1.8704	915.02	368.66	96.453	125.67	4.1820
22	0.37889	0.51061	0.8531	4.304	1.4624	483.89	143.12	169.19	103.75	5.6731
23	0.18952	0.45367	0.61803	4.741	0.83082	357.62	604.77	109.04	115.5	5.3456
24	0.77685	0.032638	0.93762	3.898	1.5078	839.57	137.68	95.04	101.48	5.6393
25	0.48162	0.79486	0.64681	3.671	1.8783	901.9	765.48	96.029	101.76	4.9227
26	0.67481	0.28202	0.28096	2.710	2.2218	749.18	638.22	124.09	116.2	4.1439
27	0.016023	0.91494	0.79437	15.809	0.67777	386.2	670.05	268.23	156.79	3.9292
28	0.48515	0.29132	0.2558	5.676	1.7298	728.67	595.11	48.879	87.909	4.7882
29	0.31677	0.86088	0.87083	1.401	3.1006	710.85	801.34	223.13	124.07	5.5724

Table B-1. Resampled Stochastic Parameter Values (Continued)

real. #	SRC3Y	SRC1Y	SRC1X	HAVO	LDISP	KDRAVO	KDRAAL	KD_PU_VO	KD_PU_AL	KD_PU_C0L
30	0.47158	0.95708	0.22766	9.231	1.3287	578.95	287.2	103.57	106.62	4.5271
31	0.87638	0.25117	0.35533	13.125	2.1624	600.92	550.08	95.733	92.572	4.4803
32	0.84049	0.75826	0.066926	4.410	1.385	205.98	336.68	44.124	82.144	4.3017
33	0.79945	0.36122	0.71376	4.877	2.6009	269.1	816.16	26.919	75.323	4.2503
34	0.087804	0.8988	0.88781	2.241	2.7057	525.12	994.94	89.955	77.693	3.8711
35	0.73521	0.77603	0.2629	1.957	2.0292	927.46	543.12	121.2	91.276	4.8427
36	0.28329	0.060343	0.24624	17.711	3.0503	172.61	355.55	70.693	76.655	4.9358
37	0.82935	0.82288	0.070104	2.402	1.9786	920.22	181.29	52.094	74.015	4.6561
38	0.042963	0.33111	0.15903	1.183	1.4821	829.07	374.93	117.73	93.13	4.5549
39	0.85708	0.73262	0.89719	3.329	1.9402	293.68	894.64	98.184	107.62	4.0871
40	0.60087	0.72999	0.42689	10.239	2.6368	906.51	560.1	129.16	105.03	3.2589
41	0.49271	0.10448	0.77958	2.445	2.3116	231.07	691.6	99.503	85.243	3.8497
42	0.64192	0.96389	0.50726	2.844	2.2754	944.28	158.05	100.71	95.463	5.5640
43	0.2041	0.71481	0.94157	7.315	2.1155	968.83	620.16	127.49	100.21	4.9771
44	0.18387	0.27955	0.6511	3.041	2.3907	152.04	292.65	104.9	84.399	5.5546
45	0.98648	0.43556	0.40458	0.417	2.7365	900.41	774.39	93.399	121.6	5.6584
46	0.23594	0.70606	0.097513	4.133	2.3716	724.12	192.57	123.5	105.44	4.6247
47	0.9144	0.46205	0.26876	1.828	2.0254	257.4	617.25	101.5	108.69	5.0652
48	0.63216	0.56861	0.30615	4.532	1.1684	696.14	654.18	108.09	121.87	5.4658
49	0.51583	0.8261	0.74634	1.277	2.1974	850.09	213.01	68.76	99.02	4.5905
50	0.8528	0.83683	0.2883	6.354	2.0765	249.14	868.01	120.19	90.383	4.4906
51	0.53245	0.42635	0.90682	18.841	2.7894	636.37	916.94	31.245	96.036	4.3295
52	0.3125	0.12124	0.18823	3.581	1.7479	228.58	660.12	119.08	108.23	5.5882
53	0.79448	0.99326	0.38079	0.862	2.1889	308.05	927.64	127.89	111.08	5.7803
54	0.2736	0.41402	0.75965	0.664	0.46339	756.15	726.75	121.96	80.495	4.9715
55	0.82136	0.94926	0.57277	3.463	0.97016	506.62	873.56	111.78	96.438	5.6818
56	0.24226	0.47853	0.65891	9.264	2.3606	799.26	884.41	123.18	87.709	4.9327
57	0.30565	0.31586	0.63843	13.715	1.6016	999.94	681.02	118.62	89.156	4.4186
58	0.87226	0.30481	0.23333	4.827	0.25367	431.79	571.3	92.604	97.251	4.3427
59	0.34771	0.81349	0.55574	2.905	2.5133	652.12	480.85	52.708	92.983	5.9321
60	0.53539	0.18244	0.43489	0.078	0.93803	966.49	813.06	108.88	96.181	4.9131

Table B-1. Resampled Stochastic Parameter Values (Continued)

real. #	SRC3Y	SRC1Y	SRC1X	HAVO	LDISP	KDRAVO	KDRAAL	KD_PU_VO	KD_PU_AL	KD_PU_C0L
61	0.69358	0.072783	0.20895	6.208	2.2049	327.18	326.07	113.29	109.16	4.9928
62	0.37424	0.005167	0.43543	3.770	2.1004	773.99	539.24	61.532	88.724	5.1110
63	0.80636	0.65482	0.62131	4.271	1.5823	802.08	319.46	93.79	70.915	5.6913
64	0.95066	0.54284	0.91978	12.312	2.4195	348.42	276.85	82.819	97.502	5.6667
65	0.94153	0.97469	0.057611	14.551	1.4013	765.3	746.99	64.415	83.784	5.6949
66	0.38226	0.048251	0.4617	13.256	3.199	105.66	821.22	96.256	89.718	5.4470
67	0.62941	0.61653	0.38797	8.296	1.7649	512.22	908.36	126.18	127.89	5.4320
68	0.56358	0.98803	0.62566	4.697	1.6497	597.5	255.95	113.55	99.808	5.3808
69	0.753	0.13847	0.19972	2.381	1.0524	411.65	757.85	47.151	102.43	4.5852
70	0.41038	0.61048	0.47687	3.750	4.5701	628.82	652.53	107.02	114.16	3.9909
71	0.50596	0.76298	0.75346	4.791	2.553	777.39	630.04	128.15	117.51	5.3169
72	0.35308	0.58728	0.83407	11.250	1.49	501.84	854.87	100.54	101.63	4.7010
73	0.72002	0.84202	0.17657	10.774	1.6344	806.66	134.47	101.57	109.6	4.7159
74	0.14626	0.68295	0.07776	4.085	1.619	813.08	740.3	105.18	104.64	4.2315
75	0.066744	0.38841	0.026305	12.916	1.7716	145.68	396.12	111.4	124.17	5.4556
76	0.40925	0.42092	0.041884	1.901	2.9928	912.04	342.71	126.98	113.06	4.6658
77	0.75816	0.63356	0.19002	0.972	2.0748	683.34	714.72	16.105	69.555	4.9426
78	0.17325	0.53555	0.79986	11.716	0.036259	271.18	756.88	127.94	103.52	4.6721
79	0.17749	0.08885	0.50064	0.735	1.2689	759.01	860.64	110.31	118.45	4.5498
80	0.65533	0.31436	0.13959	0.533	2.8701	372.36	364.79	16.123	81.2	4.3902
81	0.13682	0.5298	0.543	1.222	0.793	355.91	752.04	107.09	108.04	5.8997
82	0.34247	0.32268	0.29273	14.707	2.135	420.4	302.23	169.79	117.2	5.3603
83	0.8816	0.1638	0.004696	3.298	2.5754	477.61	687	115.38	138.11	4.8906
84	0.021631	0.93282	0.034844	0.496	1.6476	576.68	738.93	120.33	95.649	4.5763
85	0.36704	0.28987	0.33286	2.052	1.8058	215.64	664.61	111.45	100.39	5.5779
86	0.49834	0.98297	0.2155	2.143	2.2666	962.97	313.04	110.97	110.15	5.4691
87	0.26303	0.59693	0.14617	2.230	3.1643	137.62	695.13	299.14	109.9	5.3922
88	0.77494	0.5598	0.64268	13.897	3.326	343.39	381.16	117.26	73.277	5.6234
89	0.29397	0.38192	0.4223	3.828	3.2587	982.55	430.74	112.79	103.68	5.3744
90	0.89941	0.35616	0.44701	0.593	1.22	568.32	573.95	116.53	130.47	5.6770
91	0.76656	0.80189	0.45487	4.908	1.962	118.83	126.83	110.22	131.81	5.6881

Table B-1. Resampled Stochastic Parameter Values (Continued)

real. #	SRC3Y	SRC1Y	SRC1X	HAVO	LDISP	KDRAVO	KDRAAL	KD_PU_VO	KD_PU_AL	KD_PU_C0L
92	0.63929	0.74595	0.53056	2.347	1.3698	333.02	989.47	120.59	99.181	4.2700
93	0.86447	0.92068	0.66988	2.098	2.24	559.88	344.58	128.29	119.99	5.6460
94	0.9357	0.50364	0.31131	1.976	3.4595	424.79	512.48	81.96	98.194	4.9060
95	0.35996	0.37754	0.98715	12.749	1.7585	199.83	416.67	214.97	120.86	3.7339
96	0.99924	0.64932	0.6606	0.800	0.41495	134.12	114.86	237.13	110.95	3.5904
97	0.28863	0.35212	0.36658	2.730	1.6868	102.1	795.33	102.76	81.501	5.1375
98	0.99314	0.34661	0.10037	0.647	3.0595	318.89	309.2	99.114	93.699	4.4413
99	0.42653	0.23963	0.037187	7.917	1.417	873.02	402.88	90.315	85.688	5.8433
100	0.33084	0.79766	0.17138	7.995	1.2469	583.6	247.25	108.06	107.42	5.6115
101	0.42259	0.22354	0.7233	3.626	1.7033	713.27	211.67	53.206	85.996	4.8792
102	0.84776	0.62524	0.73714	4.336	2.6104	284.91	941.27	93.82	97.341	4.7655
103	0.057725	0.36634	0.76158	12.561	1.2976	633.5	464.4	69.486	105.78	4.8590
104	0.96879	0.47187	0.13328	1.373	0.89703	691.48	731.85	46.285	77.453	4.4407
105	0.7066	0.37193	0.57744	4.452	1.4986	679.35	502.4	103.07	90.736	3.9455
106	0.2104	0.71681	0.99385	9.661	1.93	718.95	370.31	92.207	106.78	5.9834
107	0.032139	0.30865	0.35219	0.770	2.4818	958.73	102	92.673	95.276	5.5449
108	0.78493	0.55127	0.23633	3.241	1.91	465.56	857.75	96.317	123.31	5.4404
109	0.54848	0.08343	0.68564	2.518	2.4269	618.97	536.05	99.752	113.53	4.9968
110	0.96153	0.89494	0.54785	6.785	0.337	854.01	921.47	100.86	107.96	5.7257
111	0.62488	0.044425	0.91427	3.854	1.6652	981.82	472.75	91.209	95.83	4.7466
112	0.69681	0.85203	0.92816	6.698	1.5314	165.82	830.4	124.37	114.99	4.8282
113	0.52809	0.86964	0.70423	1.461	2.0875	647.98	162.04	127.06	120.16	4.5992
114	0.61818	0.58153	0.80775	2.611	1.6168	519.13	930.53	108.83	84.747	5.6487
115	0.46203	0.41723	0.31862	3.167	1.123	937.13	195.45	99.599	96.639	3.8759
116	0.20919	0.33963	0.49977	10.959	1.8505	292.87	785.6	106.33	79.1	4.9638
117	0.39316	0.84877	0.86639	1.510	2.3377	221.66	466.18	96.406	94.934	4.7551
118	0.51324	0.69222	0.84208	10.391	2.0452	845.4	791.83	80.688	72.275	4.9250
119	0.50401	0.18607	0.37533	9.622	2.6881	730.58	236.97	58.767	79.498	5.8599
120	0.97274	0.72227	0.32996	8.551	2.0178	702.2	441.76	23.371	85.839	3.6388
121	0.90393	0.76623	0.69825	1.537	2.2099	124.07	120.97	129.61	115.89	5.9687
122	0.16682	0.90667	0.3208	2.812	1.1146	887.34	601.3	101.88	89.549	4.9881

Table B-1. Resampled Stochastic Parameter Values (Continued)

real. #	SRC3Y	SRC1Y	SRC1X	HAVO	LDISP	KDRAVO	KDRAAL	KD_PU_VO	KD_PU_AL	KD_PU_C0L
123	0.88685	0.78667	0.33837	3.377	1.8277	594.89	487.94	99.719	100.93	4.6396
124	0.93377	0.88469	0.049508	14.072	0.54525	389.24	983.39	96.849	102.08	5.2270
125	0.8012	0.49335	0.59546	3.433	2.979	480.65	433.28	97.548	81.699	4.8332
126	0.27749	0.078469	0.90494	8.195	1.963	547.81	265.01	111.24	112.29	3.7221
127	0.15151	0.11629	0.56557	5.101	2.4552	178.03	424.58	108.54	135.4	4.8871
128	0.23227	0.66062	0.60165	4.047	2.6825	264.86	331.56	127.96	108.46	5.4989
129	0.55875	0.88816	0.47306	16.849	2.1129	528.17	486.76	23.377	98.536	5.5355
130	0.2558	0.46514	0.20482	4.371	1.9442	862.28	297.69	119.44	112.74	5.5138
131	0.98325	0.44402	0.78375	1.879	2.0021	196.29	493.03	104.65	109.29	4.8069
132	0.70346	0.6861	0.51445	2.790	2.6619	933.76	608.58	106.59	86.628	5.2099
133	0.43036	0.74351	0.67275	2.993	2.3754	113.09	563.74	108.84	92.665	4.8474
134	0.59479	0.24391	0.18118	2.673	2.8191	611.49	703.65	17.447	92.329	3.4887
135	0.029181	0.54944	0.44236	7.478	3.5157	554.31	284.02	19.775	100.62	5.6529
136	0.29642	0.40806	0.16692	4.512	2.9033	660.81	166.35	91.784	87.352	3.8309
137	0.71369	0.59312	0.59332	3.694	3.0078	515.99	578.66	50.496	86.272	3.4490
138	0.91854	0.19074	0.63055	3.529	3.307	140.74	648.08	123.04	96.886	4.9556
139	0.45967	0.51566	0.95385	7.008	1.676	664.82	585.21	85.754	94.293	4.8637
140	0.25344	0.93944	0.52473	10.442	1.5508	336.3	476.3	112.83	116.62	4.9499
141	0.099923	0.80992	0.89486	3.231	1.1519	995.02	449.12	93.917	93.336	4.8208
142	0.24977	0.13496	0.98272	10.658	2.4377	394.86	674.88	118.52	132.7	5.7715
143	0.036624	0.20762	0.24422	4.612	3.5447	304.25	234.78	116.07	124.91	4.1553
144	0.051719	0.26209	0.006894	8.680	1.5218	879.45	947.05	119.99	113.85	5.3273
145	0.57483	0.63694	0.58037	9.901	2.1419	442.83	152.68	12.842	88.442	5.5179
146	0.41881	0.15465	0.36144	2.311	1.8391	410.47	719.9	101.76	93.923	5.9539
147	0.22244	0.14066	0.14225	7.603	2.0595	827.17	889.36	116.49	104.14	5.2782
148	0.68188	0.19518	0.10796	3.925	2.6459	300.53	634.47	118.02	91.116	3.9851
149	0.72764	0.10513	0.88462	1.599	2.5012	891.05	390.81	66.221	78.156	5.4854
150	0.43902	0.44513	0.11251	5.203	1.2316	241.1	546.37	105.69	110.49	4.8009
151	0.83171	0.60065	0.25367	4.160	2.3044	186.78	223.17	26.465	91.677	5.7046
152	0.21903	0.05082	0.99545	1.323	1.7878	624.78	842.01	104.69	98.913	5.4203
153	0.73195	0.12708	0.83865	1.791	2.8058	783.67	956.27	104.7	102.2	4.4565

Table B-1. Resampled Stochastic Parameter Values (Continued)

real. #	SRC3Y	SRC1Y	SRC1X	HAVO	LDISP	KDRAVO	KDRAAL	KD_PU_VO	KD_PU_AL	KD_PU_C0L
154	0.6762	0.029674	0.77487	6.511	1.1833	988.97	531.89	112.04	104.21	5.4115
155	0.15591	0.40127	0.2951	3.088	0.99647	454.6	912.9	118.23	84.029	5.5970
156	0.65336	0.16679	0.45652	16.213	1.0783	488.62	243.89	100.77	82.78	4.4704
157	0.78953	0.64082	0.81817	2.941	2.4897	815.64	679.99	100.08	103.24	4.6806
158	0.92559	0.17548	0.58945	16.672	2.3218	456.58	186.9	47.529	97.876	4.0638
159	0.6146	0.60552	0.56322	1.685	0.70349	212.34	996.89	40.481	84.26	5.8121
160	0.16497	0.000294	0.68255	12.220	1.5591	461.05	178.25	177.41	94.482	5.4813
161	0.59504	0.87101	0.019925	10.114	2.5235	563.58	882.73	122.08	111.91	4.5191
162	0.19052	0.39438	0.72575	5.808	1.697	738.55	847.2	99.741	101.24	4.3831
163	0.74153	0.34185	0.87858	15.300	2.0564	495.2	499.64	61.494	106.25	3.7808
164	0.083627	0.52435	0.34361	1.094	1.4214	534.17	808.26	127.98	88.797	3.9056
165	0.45195	0.81843	0.81288	0.701	2.3472	471.15	977.34	105.15	90.127	4.7870
166	0.81384	0.22875	0.97654	0.445	2.251	613.59	205.96	112.9	106.05	5.5267
167	0.2695	0.73651	0.30146	11.463	2.9584	858.45	589.16	96.349	99.705	4.6130
168	0.66599	0.29998	0.92251	2.185	1.2731	115.43	148.63	102.27	85.113	4.0060
169	0.1286	0.21367	0.73255	3.996	1.448	952.98	968.45	43.687	82.369	4.6983
170	0.90937	0.2454	0.34744	1.752	1.09	689.46	442.49	93.817	100.01	5.2650
171	0.001231	0.77299	0.11959	8.781	3.8606	554.82	261.49	127.63	106.41	3.1175
172	0.4656	0.83016	0.93346	13.446	3.1732	244.5	699	105.07	61.47	4.7295
173	0.19628	0.022893	0.76523	11.081	3.6345	500.05	780.29	105.03	90.458	5.6042
174	0.54137	0.23146	0.60978	0.367	1.8184	416.75	968.89	95.594	122.48	5.6344
175	0.36311	0.99983	0.053292	4.567	3.1094	707.24	953.45	119.63	95.041	5.1588
176	0.60953	0.70036	0.27276	2.534	2.7539	155.74	945.94	99.692	100.87	4.5358
177	0.064173	0.21845	0.15009	12.027	1.9175	654.72	623.42	104.98	118.15	4.3634
178	0.76396	0.92607	0.21335	6.586	2.4006	433.07	555.74	126.82	102.99	5.9885
179	0.10918	0.39894	0.41905	1.639	1.3675	740.08	105.31	109.7	104.85	5.2525
180	0.89186	0.018397	0.12176	4.221	1.9905	403.18	777.53	122.92	98.747	4.9020
181	0.13459	0.45851	0.67736	6.880	0.97985	131.08	877.56	31.075	78.69	5.5495
182	0.94536	0.066174	0.22481	1.313	2.8343	450.78	266.84	107.18	80.179	4.4101
183	0.074184	0.27323	0.063419	9.988	2.8894	259.14	358.23	105.52	80.941	4.6913
184	0.33522	0.56336	0.69415	6.146	1.5716	538.12	202.45	64.375	91.579	5.9230

Table B-1. Resampled Stochastic Parameter Values (Continued)

real. #	SRC3Y	SRC1Y	SRC1X	HAVO	LDISP	KDRAVO	KDRAAL	KD_PU_VO	KD_PU_AL	KD_PU_C0L
185	0.38501	0.57366	0.4949	3.517	0.89307	767.45	408.75	102.49	118.82	4.6171
186	0.64828	0.67742	0.78821	7.207	0.75759	543.77	423.04	120.39	114.51	4.2114
187	0.55432	0.3274	0.82971	2.035	1.3431	672.33	834.53	124.19	104.48	4.7366
188	0.58086	0.49706	0.48494	19.322	1.0364	641.42	130.4	275.32	113.4	5.3329
189	0.010006	0.95063	0.41403	0.843	1.591	929.22	413.17	90.251	83.199	3.3167
190	0.81791	0.48478	0.97384	4.037	2.9223	974.17	384.56	109.61	105.37	5.5808
191	0.10396	0.14898	0.95984	11.665	2.4702	743.93	640.94	117.27	96.809	5.0963
192	0.008292	0.48702	0.022384	0.289	2.7737	284.09	219.8	108.01	88.152	5.6072
193	0.66128	0.010403	0.85706	0.887	2.5306	587.59	453	109.69	107.23	5.2849
194	0.44669	0.056335	0.013682	8.833	1.7959	668.91	963.31	34.465	91.033	5.2949
195	0.58695	0.50667	0.080381	0.924	0.60612	162.67	903.2	37.662	92.086	5.6213
196	0.14264	0.66797	0.39326	5.436	2.2902	604.69	272.75	100.65	91.916	5.2178
197	0.71574	0.5321	0.55188	1.006	0.84056	837.67	112.33	45.028	89.853	5.0028
198	0.048634	0.62298	0.37462	5.964	2.7289	218.81	349.72	103.43	99.369	5.1921
199	0.12266	0.69669	0.61218	7.132	1.2041	398.88	514.47	118.09	119.54	5.4031
200	0.32612	0.9429	0.70614	5.875	2.4135	375.84	709.58	112.16	86.921	4.3237

Table B-1. Resampled Stochastic Parameter Values (Continued)

real. #	KD_AM_VO	KD_AM_AL	KD_AM_COL	KD_CS_VO	KD_CS_AL	KD_CS_COL	CONC_COL
1	6309.1	4730.4	6.5351	4824.9	617.72	3.8786	-4.572
2	5007.6	5342.1	5.4447	3283.2	560.12	3.4041	-5.7843
3	5589.4	8261.8	4.8395	5971.4	534.18	3.6749	-8.8173
4	7302.6	6245.2	6.6296	6323.1	827.68	3.9087	-8.0077
5	5992.9	6287	4.8973	3155	674.44	2.2705	-5.7211
6	5262.8	4788	6.7566	4040.3	690.22	2.8873	-6.7879
7	2893	8144.2	5.2392	4133.2	606.63	3.5717	-7.6456
8	3603.4	6889.1	4.5868	4957.6	306	2.5735	-8.5382
9	5643.8	7741.2	5.6826	4672.8	867.06	2.6883	-8.3826
10	3583.3	5909.9	5.7904	5535.5	750.13	3.5812	-7.8268
11	8540.9	5513.8	4.8169	3188.8	740.75	2.7641	-5.4308
12	5508.4	2825.5	6.6948	5720.5	770.37	3.4680	-7.4885
13	8724.2	7377.1	6.8118	3442.1	266.83	2.1051	-7.9463
14	5089.3	7061.1	6.3204	6041.6	657.5	2.3401	-5.3155
15	5808.5	5920.6	5.3310	3614.8	668.57	3.6235	-6.3063
16	4777.5	5522.6	5.8099	6539.7	965.15	3.5680	-6.038
17	4977.8	3305.5	5.5915	4220.7	389.36	2.6242	-8.9285
18	6542.9	2272	6.3937	3590.5	314.42	3.3368	-5.1203
19	4993	5558.6	6.3339	4950.8	931.04	2.7255	-5.015
20	6706.8	5120.3	5.7864	6480.9	748.94	2.5836	-8.6327
21	5726.8	5387.4	5.2634	6331.2	876.74	3.6523	-7.7092
22	6860.1	3553.6	5.0370	5142	910.33	2.8175	-6.4254
23	7545.6	2579	5.3519	6001	773.03	3.6354	-3.895
24	7054.6	3372.9	5.8597	5089.8	882.09	2.7515	-6.355
25	3854.7	6983.9	6.5554	3213.3	211.23	3.5346	-6.8006
26	6472.6	3036.3	5.8147	3001	396.27	3.2209	-7.9992
27	4620.5	5009.2	6.4296	5355.6	757.18	3.2262	-5.2569
28	5306.4	7479	5.1151	4520.6	677.06	3.6131	-8.3503
29	5660.7	7023	6.2314	6300.8	393.27	2.7444	-8.4815
30	4297.1	5867.5	6.0915	5966.3	887.33	3.5988	-8.7293
31	5051.6	4283	6.8673	4550.5	474.94	3.5616	-8.1127

Table B-1. Resampled Stochastic Parameter Values (Continued)

real. #	KD_AM_VO	KD_AM_AL	KD_AM_COL	KD_CS_VO	KD_CS_AL	KD_CS_COL	CONC_COL
32	6115.2	4876.6	4.1311	4318.2	714.81	2.6805	-5.0346
33	8317	5640.6	5.8788	5113.8	602.9	3.0525	-5.9699
34	2275.6	5746.9	5.3663	6611.1	803.33	2.5272	-8.3377
35	4908.8	4073.5	6.4875	4277.7	779.54	2.5392	-8.296
36	6693	5035	6.9595	4693.2	411.36	3.6880	-5.8621
37	4723.8	7013.3	4.8852	6499.2	705.79	2.1769	-7.9177
38	6277.4	5160.7	6.9065	6124.2	709.48	3.3973	-4.4364
39	5181.5	4893.3	5.5222	5800.6	720.07	2.8232	-7.2399
40	7778.2	4527.7	5.9593	3033	343.37	3.2912	-6.1793
41	5349.7	7316.6	4.9502	5821.6	777.99	2.9877	-8.9181
42	6431.5	6816.2	4.8666	4617.6	549.49	3.1674	-6.3317
43	2724.4	3759.5	4.9395	1221	796.79	2.9675	-7.5121
44	6243.5	5785.8	5.8712	6359.9	590.83	2.8696	-7.3863
45	5925.8	4714.3	6.1445	4464.6	243.19	2.7023	-8.425
46	1965	6376.5	6.6558	6440.8	894.15	2.9331	-7.8574
47	5037.4	6725.3	4.7309	2887.8	903.14	3.6463	-8.4126
48	7443	4304	5.7277	4745.8	538.95	2.8814	-6.7385
49	4462	5212.8	5.9290	6080.2	422.12	3.5294	-8.0285
50	4035.1	5657.4	5.7352	6162.7	509.71	2.8766	-6.7708
51	5554.9	6420.5	5.2172	5620.3	453.26	2.3533	-8.2752
52	8071.4	4949.3	6.4202	3665.8	228.18	2.8028	-8.5786
53	7348.9	5477.7	6.9912	4604.2	653.48	3.0161	-5.961
54	5461.1	5625.9	5.7499	4374.7	331.77	3.4751	-7.1264
55	7018.4	7145.9	4.9984	3269	110.95	3.6719	-5.6324
56	3837.1	4805	5.6154	5041.6	936.66	2.6705	-5.6515
57	6594.9	6131.6	6.7445	3732.9	524.79	2.6578	-8.6058
58	5954.2	3231.6	6.4616	5512.2	987.52	3.4315	-6.5611
59	5596.7	5326.9	4.7420	4582.7	763.5	3.6969	-4.6876
60	5418.1	4607.3	6.4741	6579.8	807.2	3.6680	-7.1741
61	5133.5	4100.7	6.5664	4294.6	520.07	2.4733	-6.8259
62	5157.4	4938.7	5.8312	6408.7	256.39	3.8385	-6.0998

Table B-1. Resampled Stochastic Parameter Values (Continued)

real. #	KD_AM_VO	KD_AM_AL	KD_AM_COL	KD_CS_VO	KD_CS_AL	KD_CS_COL	CONC_COL
63	4670.8	4844	6.5497	6558.7	292.95	3.3557	-5.5944
64	4867.2	5144	4.9779	6514.3	993.65	3.5556	-5.5647
65	3446.8	7923	6.3795	4354.9	382.29	2.8582	-4.9253
66	5491.3	8625.9	4.8559	5495	906.26	3.4896	-4.7857
67	6156.1	4018.3	5.9815	6404.6	790.76	3.2972	-6.6733
68	6385.1	4135.9	6.6414	3833.9	641.08	3.9440	-4.0582
69	7549.7	4323.1	5.9031	6780.7	857.31	3.4630	-7.6129
70	5771	3145.7	4.9035	5579.7	471.12	2.7098	-7.2777
71	7105.6	6195.3	5.2926	3406.9	834.26	2.2552	-4.6302
72	6982	4346.1	5.4560	5564.9	408.06	3.1792	-5.6844
73	4534.3	6800.1	4.6366	1895.6	489.25	3.1359	-5.2873
74	1379.9	6227.9	6.0219	141.19	756.85	3.0487	-7.0552
75	2698.3	5880.5	5.6957	3098.8	367.47	2.8960	-8.7995
76	5210.5	6572.4	6.7109	3475.8	134.04	2.1340	-5.8189
77	4280	1694.7	4.2831	4996.3	360.62	2.5599	-7.2497
78	3914.1	5389.7	5.6608	5933.4	853.07	3.5461	-6.2719
79	9002.5	4631.3	6.3418	4915	403.1	3.5942	-8.0875
80	6572.1	5364.9	5.1451	4057.6	477.94	3.7520	-8.6709
81	6921.6	2799.2	5.7018	4897.6	445.81	3.4561	-6.4535
82	4152.2	7436.8	4.9250	4190	683.38	2.2281	-6.5244
83	7164.9	4389.7	5.6492	3320.4	693.33	2.8429	-6.4857
84	2388.7	6013.4	5.7170	5696.7	163.8	2.6344	-4.3981
85	6874.5	3492.4	5.5117	5013.6	983.28	3.9624	-4.5272
86	3782.3	6217	5.9032	6214.5	461.19	2.6480	-7.4294
87	3630.1	7190.7	4.5803	6282	952.5	3.4821	-8.0503
88	4365.5	5547	6.8266	3923.8	925.98	3.6803	-4.5105
89	3683.3	4475	5.0791	5231.6	430.68	3.6910	-6.8462
90	6008.9	5068.9	6.4046	4138.7	249.24	3.3073	-7.9359
91	3750	9774.6	6.0279	3655.1	918.62	3.0975	-7.889
92	6233.9	6352.9	6.9300	5828.7	568.55	2.3213	-6.2493
93	3459.8	4572.1	6.3086	4889	825.23	2.6000	-7.4708

Table B-1. Resampled Stochastic Parameter Values (Continued)

real. #	KD_AM_VO	KD_AM_AL	KD_AM_COL	KD_CS_VO	KD_CS_AL	KD_CS_COL	CONC_COL
94	7865.3	5818.5	5.6892	3166	202.33	2.5084	-3.7317
95	4228.9	6409.7	6.2134	5202.8	836.23	3.4954	-5.393
96	5531.3	5697.5	6.1669	3971.1	872.68	3.6501	-5.5001
97	3939.6	8295.4	4.6709	3557.2	767.05	2.7793	-6.6074
98	5965.7	5955.8	5.3185	4487.9	651.73	2.5491	-8.3675
99	3738.6	3419.1	5.6059	5870.2	947.46	2.7711	-7.0308
100	4802.2	6453.6	6.5686	6737.4	615.38	2.8674	-7.7203
101	3334.5	6512.4	4.4403	3795.9	849.13	2.8082	-6.1279
102	8595.9	3630.2	5.4799	4640.8	784.32	2.7580	-8.0694
103	7182.9	6042.8	5.8660	3052.4	971.84	2.7981	-8.8338
104	4958.2	6673.9	6.5135	6648.8	496.73	3.2720	-7.0745
105	3082.9	6544.4	6.5400	6601.3	532.24	3.1580	-6.6485
106	3965.4	3727.4	4.3639	5069.1	582.39	2.9045	-5.4409
107	9913.3	5460.2	6.6081	5103.4	697.14	3.5093	-7.6354
108	4795.8	4668.7	5.5864	6681.4	153.12	2.9743	-7.6714
109	6304.8	4165.6	5.9615	3428.4	456.57	2.4158	-6.9696
110	4754.5	7780.4	4.7672	4500.4	374.42	3.2487	-4.9795
111	7603.7	8058.4	5.9161	3516	319.59	3.8641	-8.708
112	4583.3	6781.7	4.5036	6016.5	923.56	3.6818	-7.1837
113	4824.3	6329.4	6.3703	6695.2	648.33	3.1176	-7.1191
114	5680.8	6059.6	6.6830	3694.1	730.7	2.9181	-8.9704
115	5790.5	5772.9	6.4466	3566.9	858.66	2.4464	-7.5521
116	6135.5	5134.4	5.8476	6374.1	816.55	3.4484	-7.0902
117	6639.2	4002.7	4.6930	5443.8	611.58	2.3651	-7.7541
118	7935.2	6464.4	6.6406	4340.5	999.65	2.6193	-6.1412
119	6028.1	2417.6	5.9375	5657.6	624.34	3.5238	-8.158
120	5565.1	5717	6.2693	5849.5	119.59	2.4063	-8.9883
121	5245.4	5254.6	5.8866	5220.3	514.58	2.8493	-7.2082
122	4859.2	8446.5	4.5456	3622.5	722.78	2.9518	-6.9556
123	4938.5	4907.2	5.9711	5776.5	594.79	3.6188	-8.4713
124	4263.1	6587	5.6385	3357.1	742.58	3.5120	-5.9011

Table B-1. Resampled Stochastic Parameter Values (Continued)

real. #	KD_AM_VO	KD_AM_AL	KD_AM_COL	KD_CS_VO	KD_CS_AL	KD_CS_COL	CONC_COL
125	6522	4395.8	5.5446	5683.3	289.63	3.5772	-6.5865
126	6063.9	4229.3	6.8772	4852.6	347.87	2.7207	-7.7741
127	6655.9	5738.2	6.2526	2360.3	220.63	2.9231	-8.1362
128	5176.9	5850.1	6.5980	3398.7	279.91	3.5034	-6.0613
129	7281.7	6652.4	6.2753	3858.1	504.53	3.4137	-6.0073
130	5363.8	3970	5.9472	3952	545.05	2.9417	-8.2235
131	6036.8	5837.6	5.9920	5341.6	570.11	3.3768	-8.1668
132	5744.8	3624.1	5.4277	4555	812.12	2.9728	-7.3502
133	4693.1	4979.4	6.6769	3229.1	208.85	2.7330	-7.0104
134	5832.9	3820.4	6.6750	3531.8	957.43	2.8329	-6.6947
135	6088.4	6504	6.6494	4237.7	700.06	2.9378	-4.3359
136	4699.9	6627.1	6.7938	6200.4	822.84	2.1494	-5.7531
137	6505.9	4594.3	5.9507	3809.9	498.66	2.9847	-7.5684
138	4337.4	4680.7	6.3561	6640.2	192.87	2.4825	-5.3565
139	3542.1	4758.5	5.8380	3697.6	663.39	3.4455	-7.4479
140	5904.2	5223.5	5.6201	3766.7	254.42	3.3204	-6.7548
141	6444.3	5584.3	5.6273	4406.8	939.57	3.5486	-6.9388
142	4544.6	7527.3	5.7533	3312.6	733.53	2.6092	-6.1196
143	4605.5	7679.4	6.5916	6234.3	916.07	2.9248	-6.7004
144	5897.9	5606.4	5.8254	4030.4	620.29	3.6389	-7.371
145	3214.5	7092.3	5.1766	5281.3	944.22	3.4867	-6.5065
146	7462.2	7369.8	5.3910	4257.1	435.09	3.3861	-6.4789
147	5103.6	6925.5	4.3864	3061.2	840.62	3.0916	-7.2809
148	6768.2	5482.9	6.5755	6759.3	814.05	3.0240	-7.8089
149	4003.2	7607.4	5.0107	5456.8	440.8	3.6597	-5.0888
150	8022.6	6688.6	6.1236	5386.6	280.49	3.1915	-5.1417
151	7385	5990.2	6.5229	4207.8	528.33	2.8321	-8.2405
152	5476.4	6935.5	6.6920	5163.7	232.73	3.7372	-7.6861
153	7657.2	3914.4	5.5505	4656	482.77	3.6637	-4.374
154	6613.2	4824.2	5.4669	3989.2	188.78	2.0249	-8.8522
155	4174.4	5260.6	6.0568	4797.1	637.17	3.6560	-6.1817

Table B-1. Resampled Stochastic Parameter Values (Continued)

real. #	KD_AM_VO	KD_AM_AL	KD_AM_COL	KD_CS_VO	KD_CS_AL	KD_CS_COL	CONC_COL
156	4384.3	4742	5.5270	541.24	681.73	3.5181	-7.5344
157	6401.8	3705	6.4784	4716.4	737.32	3.3493	-8.6836
158	4075.5	4987.3	6.8507	6061.8	447.66	3.5606	-6.3775
159	4126.3	9063.8	6.6274	5601.3	954.54	3.5888	-7.4084
160	3047.5	4545.2	5.9215	2606.8	553.13	2.9480	-8.8816
161	5317.5	5310.4	5.2054	4788.7	800.32	3.6927	-8.2007
162	4044.6	4444.7	6.4576	4100.6	981.31	3.3876	-4.2662
163	5855.3	3867.3	6.9439	3898.7	899.82	3.3137	-7.3117
164	6833.2	4440.7	4.7797	4979.9	644.04	2.9990	-6.9054
165	5281.1	7158.9	5.4064	3128.2	628.51	2.4957	-7.598
166	2947.2	1920	5.2725	4441.5	879.62	3.2435	-5.2248
167	6202.2	3271	5.9978	5412	579.7	3.1305	-4.7488
168	4188.8	3107.8	5.7779	6704.9	353.62	3.7884	-4.8991
169	5070.1	6842.6	5.7652	5478.8	297.66	2.9944	-6.2265
170	4399.1	5674.1	5.5660	5742.2	891.97	2.4558	-6.8629
171	5627.1	6268.8	6.6095	3374.3	426.2	3.2084	-6.4087
172	6748.7	7287.1	6.6205	4159.3	703.3	2.9821	-6.3856
173	6787.9	7970.3	6.1174	5260.7	268.5	3.5398	-5.1919
174	6186.4	7869.5	6.6647	3748.4	340.47	3.4275	-6.0434
175	5228.2	5434.1	5.6690	1418.7	180.84	3.6291	-7.3288
176	7144.7	5181.5	4.9585	6180	327.57	3.0748	-8.9459
177	3394.1	7560.4	5.9763	5305.7	843.16	2.9581	-5.8791
178	7724.3	6023.7	6.5819	3251.3	313.53	3.6042	-7.157
179	4440.5	6145.1	4.7188	6453.4	977.55	2.6958	-8.7779
180	6999.5	5277.7	6.1857	5320.7	418.41	3.5930	-6.5596
181	5711	6168.9	5.9346	4842.2	511.78	3.4179	-8.5473
182	5402.8	4243.5	5.5720	5188.1	167.1	3.3708	-5.4973
183	5866.1	2595.4	5.4095	700.81	861.91	3.6422	-8.1846
184	7249	2974.5	5.4930	3851.2	141.38	3.4392	-6.2812
185	4647.9	4503.3	6.5013	4093.8	365.62	2.9097	-8.5817
186	3142.8	6104.4	6.2958	5925.6	562.62	3.2596	-8.6539

Table B-1. Resampled Stochastic Parameter Values (Continued)

real. #	KD_AM_VO	KD_AM_AL	KD_AM_COL	KD_CS_VO	KD_CS_AL	KD_CS_COL	CONC_COL
187	6954.6	6746.3	6.5090	4764.7	788.4	2.2855	-7.8687
188	8147.1	8715.9	5.9861	5888.5	667.15	3.3601	-6.6348
189	5368.6	3526.3	6.9769	4424.9	967.31	3.3299	-6.9914
190	6359	3945.3	4.8049	6246.1	555.85	2.0420	-7.787
191	6330	4117	4.9715	5631.4	587.59	3.6088	-8.7485
192	4483.9	6078.1	6.6680	3896.4	378.1	3.2772	-4.8491
193	3289.1	5088.1	4.0572	4001.4	600.52	3.9912	-6.895
194	2548.5	3789.7	6.2105	3110.5	102.37	2.8567	-7.9751
195	8255.2	5962.6	5.6564	5763.1	631.46	2.7879	-4.7318
196	6161.5	7222.2	6.9137	6135	576.05	3.1997	-8.4518
197	4506.1	5051	5.7987	3483.6	486.68	3.6209	-8.5185
198	5427.5	4202.9	6.4161	1670.4	463.56	2.9615	-8.3199
199	4889	5419	5.8950	6096.5	147.01	2.9019	-8.8695
200	5703.4	6314.5	4.2159	5402.6	724.4	2.3891	-6.2063

Output DTN: SN0407T0502103.013.

Table B-2. Comparison of Simulated Median Transport Times for the Re-Sampled Parameters and the Base Case at Three Levels of Cumulative Probability

	5th Percentile Transport Time (years)	**Median Transport Time (years)**	**95th Percentile Transport Time (years)**
Carbon, Technetium, Iodine (Re-Sampling)	70	620	15570
Carbon, Technetium, Iodine (Base-Case)	90	640	13100
% Difference	22.2	3.1	18.9
Americium, Thorium, Protactinium (Re-Sampling)	>100000	>100000	>100000
Americium, Thorium, Protactinium (Base Case)	>100000	>100000	>100000
% Difference	0.0	0.0	0.0
Cesium (Re-Sampling)	>100000	>100000	>100000
Cesium (Base Case)	>100000	>100000	>100000
% Difference	0.0	0.0	0.0
Plutonium (Re-Sampling)	16000	>100000	>100000
Plutonium (Base Case)	25000	>100000	>100000
% Difference	36.0	0.0	0.0
Neptunium (Re-Sampling)	2090	16450	>100000
Neptunium (Base Case)	2300	18200	>100000
% Difference	9.1	9.6	0.0
Plutonium and Americium – Irreversible Colloids (Re-Sampling)	820	22130	>100000
Plutonium and Americium – Irreversible Colloids (Base Case)	900	18500	>100000
% Difference	8.9	20.	0.0
Radium (Re-Sampling)	>100000	>100000	>100000
Radium (Base Case)	>100000	>100000	>100000
% Difference	0.0	0.0	0.0
Strontium (Re-Sampling)	42100	>100000	>100000
Strontium (Base Case)	86700	>100000	>100000
% Difference	51.4	0.0	0.0
Uranium (Re-Sampling)	1850	23360	>100000
Uranium (Base Case)	2400	24300	>100000
% Difference	22.9	3.9	0.0
Plutonium and Americium – Irreversible Colloids – Fast Fraction (Re-Sampling)	50	330	3570
Plutonium and Americium – Irreversible Colloids – Fast Fraction (Base Case)	70	310	2340
% Difference	29.	6.5	53.
Output DTN: SN0407T0502103.013			

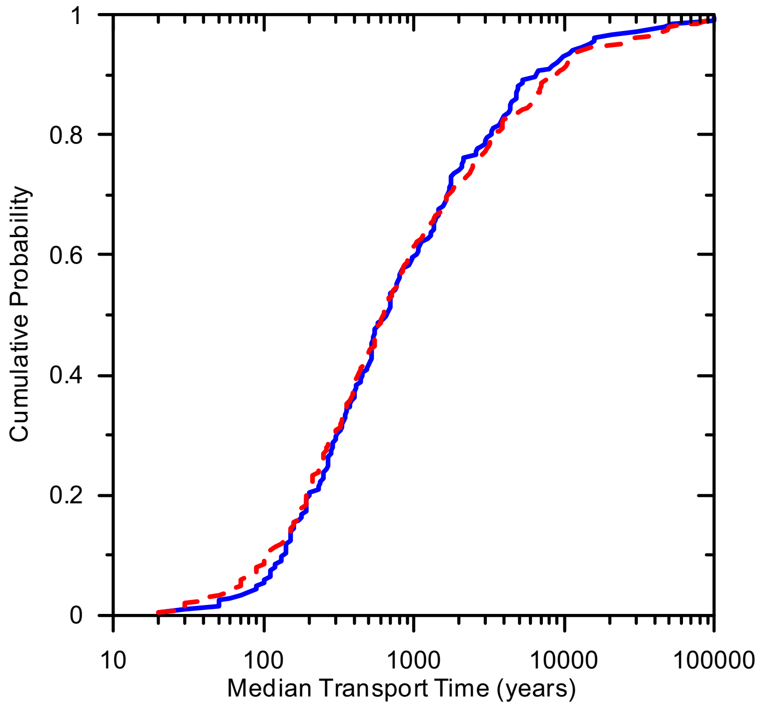

Output DTN: SN0407T0502103.013

Figure B-1. CDF of Median Simulated Transport Time of Nonsorbing Species (Carbon, Technetium, and Iodine) for the Base Case (Solid Blue Line) and the Re-Sampled Parameters (Dashed Red Line)

INTENTIONALLY LEFT BLANK

APPENDIX C

QUALIFICATION OF UNQUALIFIED GROSS ALPHA CONCENTRATION DATA

The analysis of the gross alpha concentrations in groundwater presented in Section 6.8 used some data as direct input obtained either unqualified data generated by the YMP or outside sources. These data were the results of measurements of ambient gross alpha activity in groundwater in the Yucca Mountain region or near the Nevada Test Site. The data are used in this report to assess the natural background concentrations in groundwater. Due to the random nature of radioactive decay and the relatively low concentrations of alpha emitting radionuclides in natural groundwater, there are fluctuations in measured values of the gross alpha concentrations as well as negative concentration values reported. Although a negative value for gross alpha activity is physically unrealistic, such negative estimates are an expected outcome for measurements of low-activity samples, and are retained in statistical analysis for consistency (see discussion in Section 6.8.2.2).

The unqualified data are demonstrated in this appendix to be suitable for intended use within this report, in accordance with LP-SIII.2Q-BSC, *Qualification of Unqualified Data*, and LP-SIII-10Q-BSC, *Models*.

C1. DATA FOR QUALIFICATION

The following five data sets are cited as direct inputs (see Table 4-1) and to be qualified for intended use in this report:

#1 Table E-1 of *Yucca Mountain Site Characterization Project Radiological Programs, Radioactivity in FY 1997 Groundwater Samples from Wells and Springs Near Yucca Mountain* (CRWMS M&O 1998 [DIRS 104963])

#2 Table 8.3 of *Nevada Test Site Annual Site Environmental Report for Calendar Year 2000* (Townsend and Grossman [DIRS 156604])

#3 Table 8.3 of *Nevada Test Site Annual Site Environmental Report for Calendar Year 2001* (Townsend and Grossman [DIRS 173960])

#4 Table 8.3 of *Nevada Test Site Annual Site Environmental Report for Calendar Year 2002* (Townsend and Grossman [DIRS 168841])

#5 Tables 3-1, 3-2, and 3-3 of *Nevada Test Site Environmental Report 2003* (Wills 2004 [DIRS 173956])

C2. QUALIFICATION METHOD AND RATIONALE FOR SELECTION

The data qualification was performed in accordance with the data qualification plan, as shown in Figure C-1. This plan was developed according to LP-SIII.2Q-BSC. The selected methods for use were the Corroborating Data method and the Technical Assessment method. The rationales for selecting these methods are as follows:

- Existing qualified and unqualified data are available for use to corroborate the unqualified data sets.

- Data collection procedures are unavailable for review. Therefore, evaluation of the data acquisition and subsequent data development discussed in source documentation is required to have sufficient confidence in reliability and correctness of the data for their intended use.

C3. EVALUATION CRITERIA

The evaluation criterion used to qualify the unqualified data sets #1 through #5, as identified in Section C.1, is as follows, per LP-SIII.2Q-BSC, Attachments 3 and 4:

- The data must demonstrate the properties of interest.

- The quality and reliability of the measurement control program under which the data were generated must demonstrate acceptable scientific and administrative practices or process.

- Available corroborating data must substantiate or confirm parameter values of unqualified data.

C4. EVALUATION RESULTS

The results of evaluation are summarized as follows:

- Data of Interest in This Report

The data from data sets #1 through #5 represent the measurements of gross alpha radioactivity in groundwater samples from wells and springs near Yucca Mountain in different fiscal years. They are the properties of interest in this report (see Section 6.8), and used to support the assessment of natural background concentrations in groundwater under future climatic conditions.

- Technical Assessment

Data Set #1

These data were the results of well and spring water monitoring activities performed during FY 1997 for the YMP. The water samples were collected by USGS personnel from eight locations near the Yucca Mountain. Although water sampling for this data set was a conventional quality activity, all samples were collected, using sampling procedure YMP-USGA-HP-298, *Method Used to Collect Ground-Water Samples for Radiochemical Analysis* (CRWMS M&O 1998 [DIRS 104963], Section 2.2). Water samples were analyzed by a contract laboratory (Teledyne Brown Engineering) that is experienced in conducting laboratory water sample analysis. The QA program of Teledyne Brown Engineering was subsequently audited by the Office of Quality Assurance of YMP in 1998, and accepted (CRWMS M&O 1998 [DIRS 174521]). Analysis results from the laboratory were validated in accordance with the data validation procedure (CRWMS M&O 1998 [DIRS 104963], Section 2.4). The full set of documentation related to data analysis, validation, and evaluation of laboratory QA program is available in the YMP records package MOY-980505-03-01.

In conclusion, the data presented in this data set were generated using acceptable scientific practices, and met applicable requirements.

Data Sets #2 through #5

These data were the results of groundwater monitoring activities performed during fiscal years 2000 to 2003 near the Nevada Test Site (NTS). They were associated with the water samples from four wells, selected out of those collected from over 60 wells (Townsend and Grossman 2001 [DIRS 156604], Table 8.3; Townsend and Grossman 2002 [DIRS 156604], Table 8.3; Townsend and Grossman 2003 [DIRS 156604], Table 8.3; and Wills 2004 [DIRS 173956], Tables 3-1 to 3-3). The water sampling activities were administrated by Bechtel Nevada, with the sample analysis performed by offsite analytical laboratories.

QA program developed in accordance with DOE Order 414.1A was used in collection and analysis of the water samples to ensure that data produced by the Bechtel Nevada in-house Analytical Services Laboratory and subcontracted radiochemistry laboratory met customer- and regulatory-defined requirements (Townsend and Grossman 2001 [DIRS 156604]), Section 9.0; Wills 2004 [DIRS 173956], Section 17.0). The QA program used included elements of data and measurement quality objectives, sampling plan, laboratory sample analyses, data management procedures, and data review and systematic assessments. These elements ensured that (1) data collection, analyses, and projected data use had clear goals and objectives; (2) analysis of samples for required parameters met Bechtel Nevada, DOE, and regulatory-defined requirements, in addition to those of published standard practices with respect to measurement precision and accuracy, and data checking, verification, and validation; and (3) analytical data were reliable and of high quality.

In addition, DOE also tasked the Desert Research Institute to provide independent verification of the level of radioactivity within some of the groundwater wells (Townsend and Grossman [DIRS 156604]), Section 8.5). These oversight activities provided a direct comparison to the results obtained by the Bechtel Nevada and its subcontractors, and additional confidence in the reliability and quality of the results.

It can be concluded that the data presented in these data sets were produced using acceptable scientific practices, and met applicable requirements.

- Corroborating Data

The gross alpha concentration data set presented in Section 6.8.1 (DTN: MO9904RWSJJS98.000 [DIRS 165866]) is qualified. These data were the results of a groundwater-testing program conducted in fiscal year 1998 (see Section 6.8.1). Groundwater samples were collected from six wells and two springs. Some groundwater samples collected for data sets #1 through #5 were from the same wells that provided samples for generating the qualified data. Therefore, the qualified data (DTN: MO9904RWSJJS98.000 [DIRS 165866]) are used to corroborate the data sets #1 through #5. In addition, five sets of unqualified data are also compared with each other for general consistency. The latter approach may serve as a further confirmation of the reliability and correctness of unqualified data. It should be indicated that additional data collected at the

Nevada Test Site in 1990s by DOE are also available (CRWMS M&O 1998 [DIRS 104963], Table 8) for corroborating purposes, and are not used in this report.

Data generated from groundwater samples collected from two wells, UE-25 J-12 and UE-25-13, are selected for comparison purposes, because data from these two wells are available in all six data sets used in this report (see Table 6-19). Histograms of the estimated gross alpha concentration data from UE-25 J-12 and UE-25 J-13 wells are compared in Figure C-2 for six sets of data provided in Table 6-19. It appears that the unqualified data (identified as UnQ#1 to UnQ#5 in Figure C-2) are in general consistent with the qualified data. Owing to a limited number of samples from qualified source, the range of parameter values from the unqualified data is greater than that from the qualified data. However, a general consistency is clearly indicated when comparing these five sets of unqualified data with each other, with some degree of scattering in the range of parameter values. Similar comparisons can be made with data from different wells or springs.

It appears that uncertainties associated with the data collected, including both qualified and unqualified, are relatively great (see Table 6-19). Some of the data values reported were below the detectable limit of measuring devices (Townsend and Grossman 2002 [DIRS 173960], footnote of Figure 8.3). Statistical variations associated with the radioactive decay process and the relatively low concentrations of alpha emitting radionuclides in natural groundwater, as explained in Section 6.8.2, were considered the primary causes of the uncertainties associated with the data collection. When these detection limits and uncertainty values are considered, outlying values are found to overlap with most other values in the data sets. Therefore, the reliability of these data should be evaluated based on their general consistency with each other, which was indicated from the data comparison discussed above.

C5. CONCLUSION

The evaluation found that the data sets #1 through #5 were generated by the USGS and Bechtel Nevada based on acceptable scientific practices and requirements, and were reliable and correct. It is concluded, therefore, that these data are acceptable for their intended use as direct input within this model report.

BSC	**Data Qualification Plan** *Complete only applicable items.*	QA: QA Page 1 of 1

Section I. Organizational Information		
Qualification Title Qualification of Gross Alpha Concentration Data		
Requesting Organization BSC Postclosure Activities/Natural Systems		
Section II. Process Planning Requirements		
1. List of Unqualified Data to be Evaluated (1) CRWMS M&O 1998. Yucca Mountain Site Characterization Project Radiological Programs, Radioactivity in FY 1997 Groundwater Samples from Wells and Springs Near Yucca Mountain. Rev. 00. Las Vegas, Nevada: CRWMS M&O. ACC: MOL.19990218.0213. (DIRS 104963), Table E-1 (2) Townsend, Y.E. and Grossman, R.F., eds. 2001. Nevada Test Site Annual Site Environmental Report for Calendar Year 2000. DOE/NV/11718-605. Las Vegas, Nevada: U.S. Department of Energy, Nevada Operations Office. TIC: 251545. (DIRS 156604), Table 8.3 (3) Townsend, Y.E. and Grossman, R.F., eds. 2003. Nevada Test Site Annual Site Environmental Report for Calendar Year 2002. DOE/NV/11718-842. Las Vegas, Nevada: U.S. Department of Energy, National Nuclear Security Administration, Nevada Site Office. ACC: MOL.20040413.0146. (DIRS 173960), Table 8.3 (4) Townsend, Y.E. and Grossman, R.F., eds. 2003. Nevada Test Site Annual Site Environmental Report for Calendar Year 2002. DOE/NV/11718-842. Las Vegas, Nevada: U.S. Department of Energy, Nevada Operations Office. (DIRS 168841), Table 8.3 (5) Wills, C.A., senior author. 2004. Nevada Test Site Environmental Report 2003. DOE/NV/11718-971. Las Vegas, Nevada: U.S. Department of Energy, Nevada Operations Office. (DIRS 173956), Tables 3-1, 3-2, and 3-3		
2. Type of Data Qualification Method(s) [including rationale for selection of method(s) (Attachment 3) and qualification attributes (Attachment 4)] Corroborating Data and Technical Assessment shall be the qualification methods used. Rationales for selection of methods are as follows: (1) Existing qualified and unqualified data are available for use to corroborate the unqualified data sets; and (2) Data collection procedures are unavailable for review. Therefore, evaluation of the data acquisition and subsequent data development discussed in source documentation is required to have sufficient confidence in reliability and correctness of the data for their intended use. Qualification attributes to be examined may include items 3, 5, and 10, based on LP-SIII.2Q-BSC, Attachment 4.		
3. Data Qualification Team and Additional Support Staff Required Bill Arnold (chair), Terry Grant, and Yiming Sun		
4. Data Evaluation Criteria (1) The data must demonstrate the properties of interest; (2) The quality and reliability of the measurement control program under which the data were generated must demonstrate acceptable scientific and administrative practices or process; and (3) Corroborating data must substantiate or confirm values of unqualified data.		
5. Identification of Procedures Used LP-SIII.2Q-BSC Rev. 0, ICN 0, Qualification of Unqualified Data LP-SIII.10Q-BSC, Rev. 0, ICN 1, Models		
Section III. Approval		
Qualification Chairperson Printed Name Bill Arnold	Qualification Chairperson Signature Bill W. Arnold	Date 07/22/2005
Responsible Manager Printed Name Ming Zhu	Responsible Manager Signature [signature] for Ming Zhu	Date 07/22/2005

LP-SIII.2Q-BSC FORM NO. LSIII2-1 (Rev. 01/19/2005)

Figure C-1. Data Qualification Plan

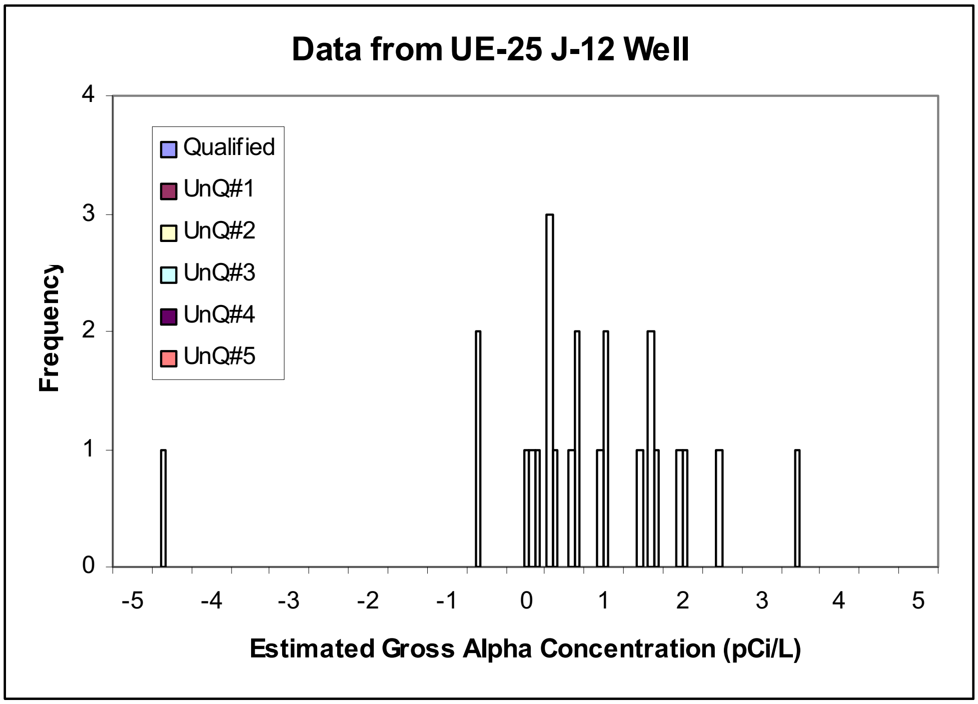

(a)

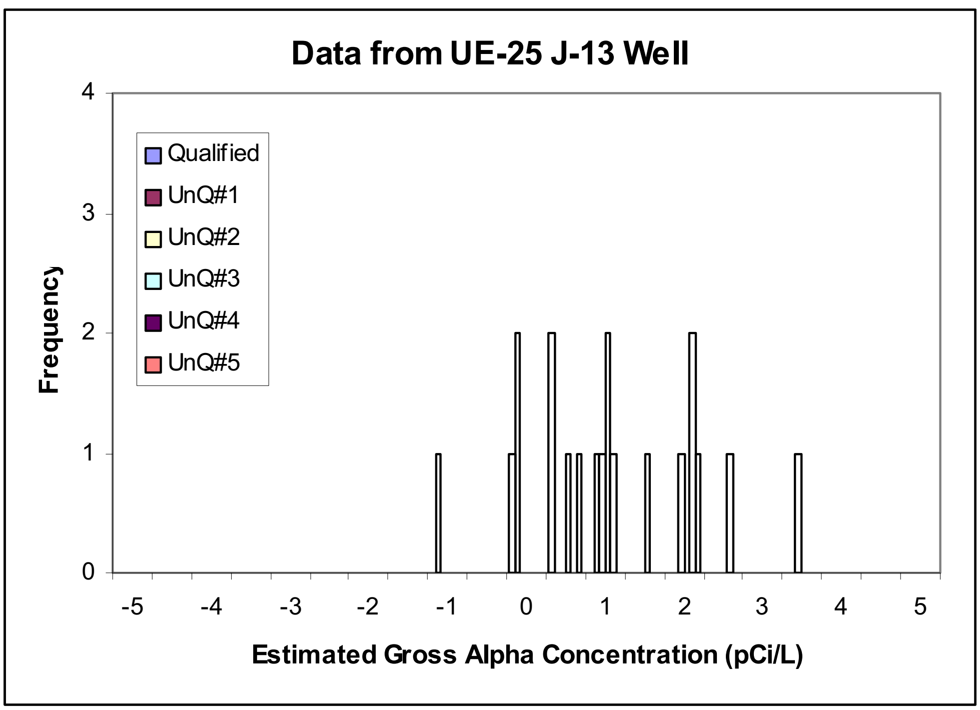

(b)

Source: DTN: MO9904RWSJJS98.000 [DIRS 165866]; CRWMS M&O 1998 [DIRS 104963], Table E-1; Townsend and Grossman 2001 [DIRS 156604], Table 8.3; Townsend and Grossman 2002 [DIRS 173960], Table 8.3; Townsend and Grossman 2003 [DIRS 168841], Table 8.3; Wills 2004 [DIRS 173956], Table 3-3.

Figure C-2. Comparison of Estimated Gross Alpha Concentration from Different Sources